MODELING, EXPERIMENTAL INVESTIGATION AND OPTIMIZATION OF MACHINING PARAMETERS IN CNC END MILLING OF AN AEROSPACE MATERIAL: A NOVEL APPROACH

Thesis

Submitted in partial fulfilment of the requirements for the Degree of

DOCTOR OF PHILOSOPHY

by

B. SRINIVASA RAO

Reg.No. 155134 ME15P04

DEPARTMENT OF MECHANICAL ENGINEERING

NATIONAL INSTITUTE OF TECHNOLOGY KARNATAKA

SURATHKAL, MANGALORE – 575025

APRIL -2024

DECLARATION

I hereby declare that the Research Thesis entitled "**MODELING, EXPERIMENTAL INVESTIGATION AND OPTIMIZATION OF MACHINING PARAMETERS IN CNC END MILLING OF AN AEROSPACE MATERIAL: A NOVEL APPROACH**" which is being submitted to the **National Institute of Technology Karnataka, Surathkal** in partial fulfillment of the award of the degree of **Doctor of Philosophy in Mechanical Engineering** is *a bonafide report of the research work carried out by me*. The material contained in this Research Thesis has not been submitted to any other Universities or Institutes for the award of any degree.

Register Number: **155134ME15P04**

Name of Research Scholar: **B. Srinivasa Rao**

Signature of the Research Scholar: B. Srinivasa Rao

Department of Mechanical Engineering

Place: NITK-Surathkal

Date: 06/04/2024

CERTIFICATE

This is to certify that the Research Thesis entitled "**MODELING, EXPERIMENTAL INVESTIGATION AND OPTIMIZATION OF MACHINING PARAMETERS IN CNC END MILLING OF AN AEROSPACE MATERIAL: A NOVEL APPROACH**" submitted by **Mr. B. Srinivasa Rao (Register Number: 155134 ME15P04)** as the record of the research work carried out by him, *is accepted as the Research Thesis submission* in partial fulfillment of the requirements for the award of the degree of **Doctor of Philosophy.**

Research Guides

H-S-Nayaka

Dr. ShivanandaNayaka H
Professor
Department of Mechanical Engineering
Date: 09/04/2024

Ch Babu

Dr. Ch. KannaBabu
DGM (Design)
AERDC, HAL (DC)
Date: 06.04.2024

Chairman-DRPC
Department of Mechanical Engineering
National Institute of Technology Karnataka, Surathkal
Date: 9/4/2024

राष्ट्रीय प्रौद्योगिकी संस्थान, कर्नाटक
यांत्रिकी अभियांत्रिकी विभाग
Dept. of Mechanical Engineering
National Institute of Technology

Dedicated to*……*

My beloved parents and family members…

&

All my teachers and colleagues who taught and encouraged me with positive thoughts

ACKNOWLEDGEMENT

This thesis exemplifies the results of the last few years' of my doctoral work whereby i have been accompanied and supported by many people. It is an honor and a very pleasant opportunity to be able to express my gratitude to all of them.

I am indebted to my supervisors **Dr. Shivananda Nayaka H,** Professor, Department of Mechanical Engineering, National Institute of Technology Karnataka, Surathkal, and **Dr. Ch. Kanna Babu,** DGM (Design), AERDC, Hindustan Aeronautics Ltd, Bangalore for their excellent guidance and support throughout my research work. Their experience, passion, dedication and kindness have inspired me to challenge myself and develop as a person as well as improve my technical abilities. Their constant encouragement, help and review of my research work during entire course are invaluable. I also take this opportunity to thank the Director, NITK Surathkal and Head of Mechanical Engineering Department, NITK Surathkal for allowing me to carry out my doctoral studies.

I wish to express my sincere gratitude to Research Progress Assessment Committee members **Dr. Shashibhushan Arya**, Associate Professor, Department of Metallurgical and Materials Engineering and **Dr. Mrityunjay Doddamani,** Associate Professor, Department of Mechanical Engineering for their unbiased appreciation and criticism all through this research work.

I wish to express my sincere thanks to **Dr. M. R. Ramesh**, Professor, and Department of Mechanical Engineering for his valuable suggestions and encouragement at the beginning of my doctoral research work and during my course work.

I would like to thank all the teaching and non-teaching staff members of the Department of Mechanical Engineering, NITK Surathkal for their continuous help and support throughout the research work.

I wish to express my thanks to Prof. **K. Narayan Prabhu**, Professor of Department of Metallurgical and Materials Engineering for permitting me to use the Scanning Electron Microscope for characterization of specimen and I also express my gratitude to **Dr. Uday Bhat**, Associate Professor, Department of Metallurgical and Materials Engineering for allowing me to use optical microscope instrument. I also thank **Ms.**

Rashmi Banjan of Department of Metallurgical and Materials Engineering for her support in connection with the use of Scanning Electron Microscope.

I would like to thank **Sri. Balaji Singh**, Senior Manager, Foundry and Forge Division, Hindustan Aeronautics Ltd, for his continuous encouragement, valid suggestions and support in conducting trial experiments at TTI. I would like to thank **Sri. Chikappa**, Manager, CAD/CAM lab and **Sri. K Srinivas** sir retired DGM (Tooling) LCA Tejas Division, Hindustan Aeronautics Ltd, Bangalore for their support and valuable suggestions in framing the required progressive feed drawings. I also would like to thank **Mr. Avinash**, CNC machinist at TTI, Hindustan Aeronautics Ltd, for his support in conducting the trial experiments.

I would like to thank my dear friend and classmate **Dr. M Srinivasa Rao**, HOD, Govt Polytechnic College, Ongole for allowing me to conduct end milling experiments in their college machine shop.

I would like to thank **Dr. M. Pradeep Kumar**, Associate Professor, Department of Mechanical Engineering, Anna University, Chennai for allowing me to conduct trail experiments on end milling machining at the beginning of my research work.

I am indented to all my friends of Department of Mechanical Engineering and other Departments of NITK Surathkal for their constant help and encouragement during my entire research work.

I would like to share one of the happiest moment of my life with my better half, my loving daughter and my dear son. I feel happy to express my sincere appreciation to all my family members for their understanding, care, continuous support and encouragement during this period.

I would like to pay a special thanks to my dear friends **Dr. M Srinivasa Rao**, **Mr. B.P. Reddy, Mr. Suman, Mr. Ramakrishna, Mr. Chickappa, Mr. Ajay and Mr. Manish Kotari** with whom i shared many laughs and tears. They have been supportive at any time of the day and night during all my ups and downs and for their timely help and moral support.

The list goes on and there are many others i should mention. There are people who have helped me all the way and provided me support when i didn't even realize i needed it, or needed it now or needed it constantly. Listing all of them would fill a book itself. So, i merely will have to limit myself to a few words; I THANK YOU ALL……!

B Srinivasa Rao

ABSTRACT

Machining of aerospace materials is a challenging task, as it involves high strength; huge variety of materials, requirement of complex geometric shapes with very close tolerances. Especially machined components assembled in fighter aircraft structures such as: longerons, spars, central frames, side frames, shear walls, trouser ducts, integral fuel walls and various supporting ribs of the fuselage etc., will be subjected to high level of fatigue loads during maneuvering. In case of these structural components surface finish as well as dimensional accuracy of the fabricated parts plays an important role in their fatigue life and in-turn durability of fighter aircraft. Therefore, it is very important to fabricate a component with good surface finish to enhance the life of each structural detail component and in-turn life of an aircraft.

Machining process is the removal of unwanted material from workpiece, so as to obtain an end product of desired size and shape with required surface quality. End milling process is a multipoint, uninterrupted cutting process, in which contact between cutting tool edge and workpiece is not continuous. Underutilization of the high-cost CNC machine tools to its full capacity is the major drawback in the manufacturing domain and it is limiting the efficient usage of machine tools, as it is being continuously run at sub-optimal conditions since many years. At the same time demand for better quality fabricated products has encouraged the metal cutting industry to continuously enhance the quality of machined products through various machining processes. Out of several types of available machining processes, end milling is one of the most fundamental metal removal process occupying the center of manufacturing industries. It is affected by controlled and uncontrolled parameters like: input machining process parameters, ambient conditions, type of coolant being used, tool geometric parameters, tool and workpiece material combination etc.

The present research work has been carried out in three phases while machining of BS L168 aluminum alloy using carbide solid end mills under two different kinds of machining environments called constant feed machining (CFM)and progressive feed machining (PFM).In the first phase a new approach of controlling the machining feed rate called progressive feed machining has been adopted through part programming then experimentally studied and analyzedits merits and demerits over the traditional constant feed machining, by mainly focusing on the measurement, prediction and analysis of

output performance characteristics such as: average surface roughness (R_a), cutting tool tip temperature (T), material removal rate (MRR), surface topography and chip morphology through end milling experiments on the said aluminum alloy work material. Further, it is investigated, the influence of cutting parameters on above said performance characteristics in PFM over CFM through predictive modelling by response surface methodology (RSM) and Analysis of variance (ANOVA) techniques. Three level variations of cutting process parameters were considered with CFM and PFM machining environments for modelling and optimization purpose by keeping nose radius and rake angle constant at 0.8mm and 16^0 respectively. Feed rate (*f*), cutting speed (*s*) and depth of cut (*d*) are the cutting parameters considered as significant factors here. Cutting speed(*s*) varies from 2.09m/sec(2000rpm) to 4.188m/sec(4000rpm), feed rate(*f*) varies from 0.1mm/rev(200mm/min) to 0.15mm/rev (600mm/min) and depth of cut(*d*), varies from 0.75mm to 2.25mm.

Taguchi's Design of Experiment (DoE) has been followed to perform the end milling experiments and to analyze machining process parameters. Later, regression mathematical models were developed for the experimental values of surface roughness (R_a), cutting tool tip temperature rise (T) and material removal rate (MRR) using response surface methodology (RSM) technique. The predicted values of performance characteristics are compared against respective experimental results and were found in close agreement. Further, signal to noise (S/N) ratio analysis was carried out using 'lower-the-better' quality characteristics for surface roughness and cutting tool tip temperature rise, since these performance characteristics are to be minimized for betterment of the machining process. At the same time 'higher-the-better' quality characteristic has been chosen for material removal rate, since higher MRR is always recommended and it is required for quick machining. Later on, ANOVA was applied to further analyze the data in order to check not only the adequacy of developed regression models but also to find the influence of individual input cutting parameters on the output performance responses. Furthermore, correlation plots, model fitness check plots, main effect plots, interaction plots, 3D surface plots and lastly contour plots have been established for all the circumstances of machining conditions with CFM and PFM for further analysis.Detailed comparative study and experimental investigation between proposed PFM and traditional CFM characteristics on work material using end milling process have been established.

In the second phase, further experimentation has been carried out according to One Factor at A Time (OFAT) approach. For this experimental study, five level variation of cutting parameters were considered: cutting speed(*s*) varies from 2.09m/sec (2000rpm) to 6.28m/sec (6000rpm), feed rate (*f*) varies from 0.1mm/rev (200mm/min) to 0.167mm/rev (1000mm/min) and depth of cut (*d*) varies from 0.75mm to 3.75mm respectively,in-order to obtain smooth and extended form of two-dimensional plots. Besides that, nose radius (NR) and rake angle are the tool geometric features have been taken into consideration. Therefore, better understanding of the influence of individual cutting parameters on performance characteristics is possible. Tungsten carbide solid end mills with different nose radii of 0.4mm, 0.8mm and 1.2mm with a rake angle of 16^0 and tool diameter of 20mm have been used for this OFAT experimentation on the above-mentioned CNC milling machining center. Combined effect of variation in nose radius and cutting parameters have been analyzed with the help of established graphs on surface roughness, cutting tool tip temperature and material removal rate. Furthermore, effect of nose radius on surface topography has been carried out by means of optical microscopic study.

From the experimental results and established two dimensional plots, it is observed that lower surface roughness and minimum MRR and maximum cutting tool tip temperature were obtained with 1.2mm nose radius. Whereas higher surface roughness, maximum material removal rate and lower cutting tool tip temperature rise were observed with 0.4mm nose radius. An increase in nose radius of end mills from 0.4mm to 1.2mm, resulted in decrease of material removal rate as well as decrease of surface roughness, but an increase in cutting tool tip temperature within the selected range of process parameters was noticed.

In the third phase, Taguchi's single-objective optimization further multi-objective optimization of end milling process parameters have been carried out by means of multi-objective optimization techniques such as: Taguchi based Grey Relational Analysis (T-GRA) and Taguchi coupled 'Technique of Order Preference Similarity to the Ideal Solution' (T-TOPSIS). Experimental outcomes have proved that the output responses in end milling process can be enhanced efficiently through T-GRA approach. Comparative analysis between T-GRA and T-TOPSIS has been carried out, which revealed that T-GRA is giving a better output result over T-TOPSIS and hence it is more suitable technique for multi-characteristic optimization of end milling process.

Experimental results were further analyzed using ANOVA and S/N Ratio techniques. Then, to validate the test results obtained through optimized conditions, confirmation tests were performed.Finally, it has been investigated that, proposed PFM along with the chosen multi-objective optimization techniques has yielded better results.

The investigation reveals that surface roughness (R_a) is predominantly affected by feed rate and the proposed PFM yields better surface finish over the existing CFM with both coated (TiAlN) and un-coated cutting tools. Depth of cut was identified as the most influencing parameter affecting the cutting tool tip temperature followed by feed rate and cutting speed is having least effect over it. However, progressive feed machining had yielded lower values of cutting tool tip temperature over existing constant feed machining with both coated (TiAlN) and uncoated cutting tools. Coated cutting tool has given a better result in case of surface roughness and cutting tool tip temperature. However, there is no much difference was found in material removal rate between coated and uncoated tools.

KEYWORDS

RSM, ANOVA, S/N ratio, End milling, Progressive feed machining, Surface roughness, Taguchi, Regression, T-GRA, TOPSIS, MRR, Nose radius, Cutting tool tip temperature, OFAT

CONTENTS

LIST OF FIGURES

LIST OF TABLES

Nomenclature

LIST OF ABBREVIATIONS

Al	: Aluminum
ANN	: Artificial neural network
ANOVA	: Analysis of variance
ANOM	: Analysis of mean
Btu	: British thermal unit
CAM	: Computer Aided Manufacturing
CNC	: Computer numerical control
CFM	: Constant feed machining
CFM	: Constant feed machining
CVD	: Chemical Vapor Deposition
DF	: Degree of freedom
DFA	: Desirability function analysis
DoE	: Design of Experiment
DF	: Degree of freedom
DFA	: Desirability function analysis
Eqn	: Equation
Exp	: Experimental
Exp.Value	: Experimental Value
FEA	: Finite Element Analysis
F-Value	: Value of F distribution
F-Value	: Value of F distribution
GA	: Genetic algorithm
GRA:	: Grey Relational Analysis
GRC:	: Grey Relational Coefficient
GRG:	: Grey relational grade
HB	: Higher-the-better
MAM	: Modulation-assisted machining
MB	: Medium-the-better
MMBtu	: One million (One thousand) Btu
MOGA	: Multi objective genetic algorithm
MRR	: Material removal rate
NR	: Nose Radius
OA	: Orthogonal Array

OFTA	: One Factor At a Time
P-value	: Probability value
PCR	: Percentage Contribution Ratio
PFM	: Progressive Feed Machining
PVD	: Physical Vapor Deposition
Pred	: Predicted
RA	: Regression Analysis
RE	: Residual Error
RSM	: Response Surface Methodology
SB	: Smaller-the-better
SEM	: Scanning Electron Microscopy
SSt	: Sum of squared deviations
SSd	: Squared deviations
SSe	: Squared error
TEM	: Transmission Electron Microscopy
TLBO	: Teaching–learning-based optimization
TOPSIS:	: Technique of Order Preference Similarity to the Ideal Solution
VMC	: Vertical milling center
w.r.t	: With respect to

LIST OF SYMBOLS

D	: End mill diameter
d	: Depth of cut
d_c	: Depth of cut in CFM
d_p	: Depth of cut in PFM
F	: Fitness value
f	: Feed rate = Intended feed rate = fc
f_s	: Increase in feed rate per step
f_o	: Starting feed rate (feed rate for step-1)
f_c	: Feed rate in CFM
f_p	: Feed rate in PFM
f_s	: Increase in feed rate per step
f_o	: Starting feed rate
l	: Step distance
n	: Number of steps chosen
P	: P-value / Probability value

R_a	: Average surface roughness
s	: Cutting speed
s_c	: Cutting speed in CFM
s_c	: Cutting speed in PFM
d	: Depth of cut
D	: Depth of milling cut
W	: Width of milled slot
L	: Length of milling cut
t	: Time taken to form a milling slot
T	: Cutting tool tip temperature rise
T_{CU}	: Cutting tool tip temperature rise in CFM with uncoated tool
T_{CC}	: Cutting tool tip temperature rise in CFM with coated tool
T_{PU}	: Cutting tool tip temperature rise in PFM with uncoated tool
T_{PC}	: Cutting tool tip temperature rise in PFM with coated tool
Vs or vs	: Versus
x	: Percentage of starting feed rate ($f=fc$) in PFM
Y	: % of improvement in average surface finishing
W	: Width of milling cut

SUBSCRIPTS

a	: Average
z	: Force acting along Z-direction
x	: Force acting along X-direction

CHAPTER 1

INTRODUCTION

1.1 BACKGROUND OF STUDY

Manufacturing is the backbone of any industrialized country in the present scenario. Among various manufacturing processes, material removal is one of the oldest and most indispensable processes for shaping components to the required size and shape. Removing of unwanted segments of material from workpieces in the form of chips so as to obtain a finished final product of required shape and size with required surface quality is called as machining (Subramanian et al. 2013). In machining, considerable amount of material will be removed from the work sample in the form of chips, to bring it to the required shape and size (Kant and Sangwan 2014). Machining process with its intrinsic versatility and associated precision machine tools, capable of being driven by computers has been responsible for recent industrial advancements. The growth of any manufacturing industry is largely depending upon development of various kinds of machining facilities it comprises. The driving force behind this development is the ability to make parts with high quality and accuracy, both at faster rate and at lower cost. In view of its economic importance, complexity of process and to develop new machine tools, cutting equipment, techniques and processes researchers have continuously expressed their desire in understanding the principles of cutting mechanisms.

The primary objective of any machining process is to manufacture a product of required size and shape, with a specified quality. Product superiority comes from a rigorous design of three factors: 1) Manufacturing process, 2) Type of product and 3) Materials used. Proper design of manufacturing process ensures not only product quality, but also its performance capability and efficiency in manufacturing cost (Fukuo et al. 2016). In order to get a good dimensional accuracy, good surface finish, and complex geometrical shapes at a faster rate of production, high strength materials are generally processed on high value and high precision CNC machines. But, metal removal with CNC machining process is more expensive, when

compared to other manufacturing processes such as forging, casting, due to high capital investment and high maintenance as well as running costs. Hence, there is a need to operate these high-cost machines as effectively as possible to get best out of them (Landau and Lifschitz 1966; Suresh and Baskar 2012).

Many researchers have employed various optimization techniques for solving machining processes. Proper machining parameters were selected by using different types of optimization techniques available based on the suitability of particular application. The confront of contemporary manufacturing industry is primarily focused on the production of high-quality products, in terms of achieving surface finish, dimensional accuracy and also concentrates on minimum tool wear, cost economy of machining with high production rate as well as increase of performance of the product (Patel et al. 2012; Durga Prasad et al. 2015). Numerous mathematical models have been projected to focus on this, with a wider purpose. Underutilization of machine tool to its full capacity is the major drawback for any manufacturing-based industry and hence it has been addressed in the present research work.

1.2 END MILLING

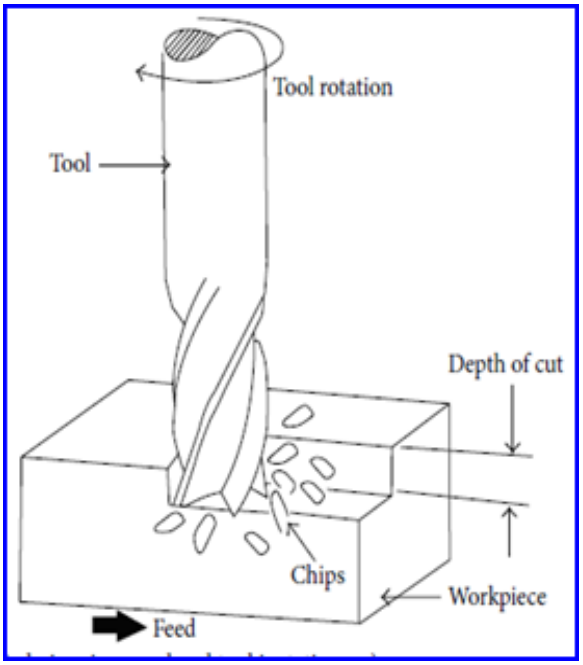

Figure 1.1 Illustration of end milling operation
(Tugrul Ozel and Taylan Altan, 2000)

Milling is the most commonly used machining process in manufacturing setups. It is a machining process of removing material by positioning a job below a revolving tool of several teeth. And that tool is referred to as a milling cutter. The multiple teeth present in the milling cutter enable milling process to be a faster method of machining (Siva et al. 2015). End milling process is a very common and important machining process not only due to its easy of machining but also due to its versatility, availability of various cutter profiles and curved surfaces (Singh et al. 2019). It is the most generally used metal cutting practise occupying in centre of manufacturing industries like aerospace, defence, automotive, marine and other fields. The ability to control the machining process for better quality final product is of paramount importance (Kannan et al. 2015).

1.3 MACHINING OF AEROSPACE MATERIALS

Machining of aerospace materials is a challenging task, as it involves high strength; huge variety of materials, requirement of complex geometric shapes with much closed tolerances. Especially machined components assembled in spacecraft / fighter aircraft structures such as: spars, longerons, central frames, shear walls, side frames, integral fuel walls, trouser ducts and various supporting ribs of the fuselage will be subjected to fatigue loads during manoeuvring. In these structural components surface finish as well as dimensional accuracy of the fabricated parts plays an important role in their fatigue life and in-turn permanence of fighter aircraft. Therefore, it is very significant to manufacture a part with good surface finish to improve the life of each structural component and in-turn life of an aircraft.

In the present research work, one of the most frequently used raw material for aerospace applications: BS L168 aluminium alloy has been chosen as the experimental material due to its better technical merits. It is a high strength material used for critical applications in the aerospace industry. And it is one of the most widely used aluminium alloy used for making spacecraft/fighter aircraft structural parts subjected to high range of fatigue loads, compressive loads due to high level of vibrations an aircraft usually subjected to. It has very good machinability and is thus used for production of complex and intricate shaped components of the fighter aircraft structures.

1.4 PROPOSED STUDY OUTCOME

The present research work is an outcome, to develop regression mathematical models using RSM technique, to establish an association between machining process parameters and corresponding performance responses, through which we can predict the performance characteristics of end milling process. After that, the predictions are made by RSM models were authenticated by performing validation experiments. The predictions obtained through the developed regression equations are then examined further w.r.t training and validation data to measure the fittingness of developed models to chosen material by end milling process.

Experiments have been conducted on the work material test specimens by means of both traditional CFM and PFM. Later on, regression models have been separately developed for each of the cutting tools: coated (TiAlN) and un-coated solid end mills against each machining type. The developed regression models will ascertain and foresee the common best machining parameters that hold good for other type of material also.

The present research work demarcates a new inclusive method for choosing optimum machining parameters to do end milling on BS L168 aluminium alloy on a chosen milling machine. This methodology is based on a perfect modelling and optimization methods such as OFAT, RSM, ANOVA, Taguchi's single objective optimisation techniques and multi-objective optimisation techniques like: T-GRA and T-TOPSIS. Firstly, development of these models simulates the association of end milling parameters and their effect on performance characteristics considered for study such as: cutting tool tip temperature, surface roughness, material removal rate, surface topography and chip morphology. The developed regression mathematical models are used on the above-mentioned material so as to verify their general idea. Further, this study was concentrated in not only developing a model that behaves and performs in a better way but also provides the desired output.

So far, no article was found from the literature to study on the effect of proposed PFM of end milling process responses such as: Cutting tool tip temperature, Surface roughness, MRR,

Surface topography and chip morphology. The present research work made an attempt to study the feasibility and effect of proposed progressive feed machining approach for machining of selected aerospace material BS L168 aluminium alloy. It is anticipated that proposed progressive feed machining produces the aircraft structural components with high surface quality, closed dimensional accuracy and in turn with high fatigue strength for improving the product life. Results attained presented the reliability of Taguchi's method for reduction of cutting tool tip temperature, reduction of surface roughness and enhancing of MRR during end milling of BS L168 aluminium alloy. These results may be useful for academic exploration as well as industrial applications.

1.5 NEED FOR OPTIMISATION

Optimization may be demarcated as the procedure to find the best level of controlling parameters that give desired value for objective function. In other words, it is an act of obtaining the best results under given circumstances. The objective function, variables and constraints are the three basic ingredients of optimization problems. In any engineering system, engineers and designers have taken many technological and executive decisions either to minimize the effort required or to maximize the desired output.

In general, any machine tool manufacturer suggests a range of cutting process parameters for various machining activities in the form of maximum and minimum values. But in actual practice exact values of optimum cutting parameters are required to prepare the process plan as well as CNC part program and therefore to get best possible output responses with available resources. So, modelling of regression mathematical equations and optimization of machining parameters are of great concern in manufacturing environments. The economical production of components plays an important role in competing with the present market. The optimal values are determined even before the raw material is put on to the machine tool for fabrication. Many researchers have employed various optimization techniques to optimize different machining processes. It has been recognized that cutting conditions such as feed rate, spindle speed and depth of cut in machining operation should be selected to optimize the economics of machining as assembled by productivity, total manufacturing cost per

component or some other suitable criteria (Gilberth, 1950).

Finding the combination of input process parameters at which optimum output process responses will be obtained is an utmost important activity for operating predominantly high-cost CNC machine tools. Particularly, use of these sophisticated high-cost CNC machine tools coupled with high labour costs, optimum machining parameters are essential for producing the components economically. It is essential to systematically investigate the process or product variables that influence the product quality. After identifying influential parameters, one can achieve improvement in order to enhance the product manufacturability, reliability, quality and field performance etc.

Effective machining mainly depends upon proper selection of cutting parameters. Therefore, many researchers have employed various optimization techniques to study the machining processes. Machining variables were selected properly by using different optimization techniques available based on the suitability of a particular application. Some of the optimization techniques frequently used in optimization of machining parameters is listed here. ANN, PSO, GA, RSM, T-GRA, TOPSIS, Fuzzy logic etc,

It is very challenging to ascertain or to select the exact machining factors to attain desired process performance characteristics by means performing experiments. Hence to overcome this, statistical modelling techniques such as: Taguchi's Orthogonal Array (OA), RSM, OFAT experimental approach, ANOVA and S/N ratio analysis have been employed in the present research work. Further optimization techniques such as: Taguchi's single-objective optimization technique; multi-objective optimization techniques like: T-GRA and T-TOPSIS was employed in the present research work in order to enhance the machining process for better output. Since, the main objective of a particular processing system is to optimize the multiple responses of the process. The present research work mainly focuses on multi-response optimization of performance characteristics of end milling process. Due to involvement of huge number of performance futures and process variables, optimization of end milling process has become a combinatorial task.

1.6 CONSTANT FEED vs PROGRESSIVE FEED MACHINING

In general, a constant feed rate will be selected for a given cut section while preparing CNC part program. That means feed rate is constant from start to end of the milling cut segment to be made as shown in Figure 1.2. When the controller of the machine tool executes part program one block at a time or block by block, there exists a time delay between executions of two successive blocks. This leads to stop and go fashion of tool movement while cutting the workpiece. Due to this at the start of every cut segment and where there is a change in cut direction, tool starts from a stationary position with a feed rate of ZERO mm/min and accelerates to the intended feed rate instantly. This may lead to sudden impact of cutting tool with the workpiece, which leads to increase in cutting force and induced residual stresses. Rubbing of cutting tool with workpiece causes rise in cutting temperature and chattering, which in turn leads to high tool wear and reduction in tool life, causes more spindle and tool deflections, finally causes poor surface finish and product quality etc.

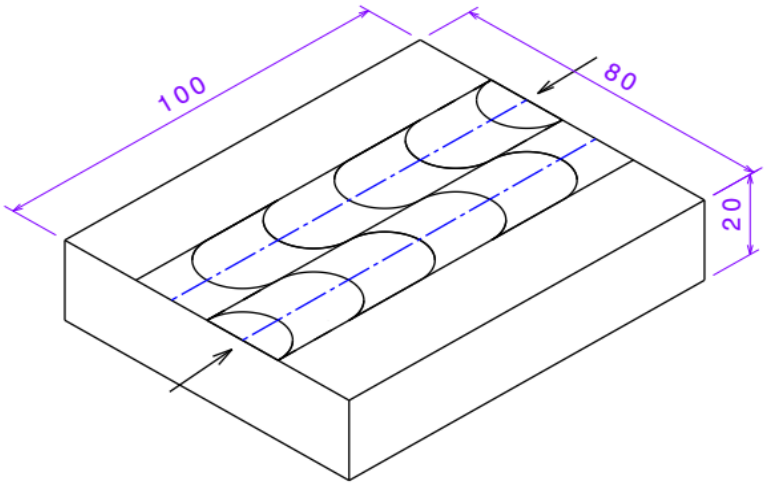

Figure 1.2 Constant feed machining

To overcome this kind of ill effects of machining, a novel technique called progressive feed machining has been proposed, studied and analysed in detail in the present research work. An existing solution for this problem is an ‘Adoptive Control’ system which is an online

optimization control technique. In the case of 'Adoptive Control', with the help of sensors, parameters are changed dynamically thereby maintaining constant cutting force. But the cost of 'Adoptive Control' is much higher and can't be installed or not even feasible to install on all the CNC machines.

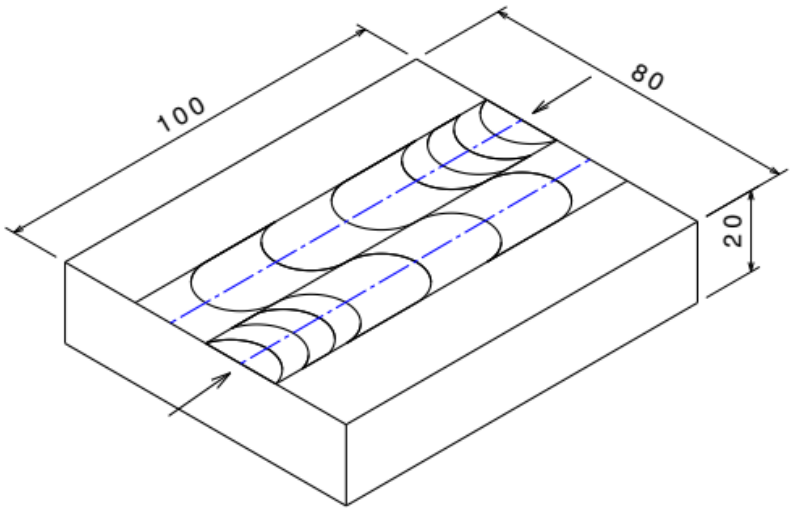

Figure 1.3 Feed steps in progressive feed machining

Hence, an offline optimization technique called, progressive feed machining has been adopted in this research work. This is a novel technique, cost effective and requires no additional equipment. In this type of machining, feed rate increases progressively from ZERO to intended feed rate step by step as shown in Figure 1.3. Once it reaches the targeted feed rate, it will be constant for rest of the cut. This concept of progressive feed machining eliminates the sudden acceleration of the tool at beginning and thus reduces the ill effects discussed above. The proposed progressive feed machining will be a better solution and it can be incorporated in the part program itself and hence it is a zero-cost approach. A brief comparative analysis between existing constant feed machining and proposed progressive feed machining has been made besides finding the influence of cutting parameters on output responses through predictive modelling and further optimization of end milling process. This concept of progressive feed machining along with optimization will yield better results in machining.

1.6.1 Anticipated benefits due to progressive feed machining

1. An improvement in surface finish which in turn will reduce or eliminate the secondary finishing operations.
2. Reduction in cutting temperature obviously leads to low cutting tool tip temperature, which in turn leads to reduction in tool wear.
3. Tool life will increase since there is a decrease in initial cutting forces and in turn tool wear.
4. As the tool life increases, number of setups will come down and therefore reduction in setup time in turn cycle time.
5. Once there is a reduction in cycle time, total machining cost will come down.
6. When tool life increases, tooling cost will come down and hence reduction in overall production cost and in turn 'product cost'.
7. Even an increase in machine tool life due to reduced cutting forces and machine tool vibrations will be anticipated.

1.7 ORGANIZATION OF THE THESIS

In the present research work, a systematic study and detailed analysis has been conceded out to explicate the end milling performance on BS L168aluminium alloy through existing CFM and proposed PFM. In addition to that, study and analysis of performance responses through the experimentation based on Taguchi's Orthogonal Array (OA), One Factor at A Time (OFAT) approach has been done. Later on, development of the regression mathematical models by response surface methodology (RSM) and further analysis with ANOVA and S/N ration techniques was carried out. Further on, single objective optimization using Taguchi's optimisation technique, and then multi-response optimization of end milling process using Taguchi based GRA and Taguchi coupled TOPSIS techniques have been carried out. Various stages of research work which have been carried out are summarized in detail in the following chapters.

Chapter 1 entitled 'Introduction' presents past and present contextual challenges of end

milling process and inspiration to take up the present research work. Details about machining of aerospace materials, merits and demerits of BS L168 aluminium alloy as a work material. The need for optimization of machining parameters is brought out in detail. Further, briefs about proposed PFM. Overview of the entire proposed research work is enlightened in this chapter under the organisation of the thesis title.

Chapter 2 presents an inclusive survey of literature on end milling process and the impact of cutting parameters on end milling performance characteristics. This chapter also discusses about the literature on current knowledge in the area of Response Surface Methodology (RSM), application of Taguchi's DoE, ANOVA, S/N ratio analysis, Multi objective optimization techniques such as: Taguchi based GRA and Taguchi coupled TOPSIS and then OFAT approach of experimentation. Further, summery of literature review, problem statement, scope and plan of research were discussed here. Furthermore, presents the objectives and aim of present thesis which were derived on the basis of gaps identified through the literature review.

Chapter 3 entitled 'Theory and Experimentation' explains about theory, concept and describes about the proposed progressive feed machining (PFM) of end milling process in detail. How to implement PFM through part programming and calculation of progressive feed rate steps has been explained in detail with the help of illustrations, equations and tables. And also, it is explained about selection of various experimental requisites for performing experiments and different kind of measuring instruments used to measure the performance characteristics. Different types of experimental setups, equipment's used for conducting the machining experiments and instruments essential to measure material removal rate, cutting tool tip temperature, surface roughness and surface topography have been explained with corresponding illustrations in detail. What are the levels of cutting parameters considered how their range has been finalised for existing CFM as well as PFM is explained.

Chapter 4 discusses about Taguchi's parametric design, which has been amalgamated to ascertain the number of experiments required to be performed. Modelling of end milling machining process using RSM has been done and ANOVA was performed to check the

validity of established mathematical regression models for existing constant feed machining and proposed progressive feed matching as well, and to find most influenced cutting factors in both the types of machining. Deliberates about the formulation of prediction regression mathematical models against each response in both the cases of machining environments using RSM and also explains about confirmation or validation tests conducted to further evaluate the competence of the established regression models.

Chapter 5 presents about OFAT method of experimentation and analyses the effect of cutting process parameters along with the effect of variation in nose radius (NR) of the end mills on performance characteristics. It also explains about consideration of five level increase of cutting parameters, how to vary one cutting factor at a time by keeping other cutting parameters constant at their mean levels. Also presents about the effect of cutting parameters on the considered performance characteristics by means of established two dimensional plots. Further presented the microscopic analysis carried out to explain about the influence of nose radii of end mills on surface topography.

Chapter 6 discusses about the construction of optimization models and to ascertain the optimal levels of machining parameters in order to obtain the anticipated responses. It has been explained, analysed and proved about the importance of multi-response optimization over single response optimization.

- Development of multi-response optimization models using Taguchi based Grey Relational Analysis (T-GRA).
- Development of multi-response optimization models using Taguchi coupled TOPSIS technique.
- Validation of developed and performed optimization processes by means of confirmation experiments.
- Comparison between T-GRA and T-TOPSIS techniques.
- Addresses the percentage of effect of each input cutting factor on the output performance characteristics.

Overall, it describes in detail about the concept of T-GRA and T-TOPSIS procedures.

Chapter 7 entitled ‘Conclusion’ presents the overall summery of research work carried out and the objective conclusions drawn. Further direction and future scope and limitations of research work is also stated in this chapter.

CHAPTER 2

LITERATURE REVIEW

2.1 INTRODUCTION

This chapter furnishes about the research work carried out by leading researchers in the area of end milling process on different materials, effect of cutting process parameters on various performance responses and optimization of end milling process on the same in the past. It mainly addresses the literature available on the following topics.

(i) Importance of end milling process, influence of process parameters such as: feed rate, spindle speed, DoC and nose radius (NR) on the considered output responses.

(ii) Machining of aluminium alloys on end milling machines and optimization of the same for better outputs.

(iii) Influence of tool NR at constant tool diameter and rake angle on the performance responses.

(iv) Importance of surface roughness, temperature rise in machining, surface topography, cutting tool tip temperature, chip morphology and MRR.

(v) Various experimental and modelling techniques such as: Taguchi's DoE, Response surface methodology, ANOVA, S/N ratio and OFAT approach of experimentation etc.

(vi) Single and Multi-objective optimization techniques: Taguchi's single objective optimisation technique, multi-objective optimisation techniques such as: Taguchi based GRA and Taguchi coupled TOPSIS.

Based on the literature review, what is the research scope, what are the research gaps and motivations to the present research work have been established.

Then important research objectives were extracted and then scheme of present research was framed.

2.2 OPTIMIZATION OF END MILLING PROCESS

While doing machining, selection of appropriate cutting conditions is very much significant in-order to get the better output performance with minimum efforts and available resources. Attainment of optimum cutting conditions is a challenging task in any kind of machining processes. Especially optimization of end milling is a combinatorial task due to the association of a bulky number of process variables and performance features. (Ghosh et al. 2020). Numerous statistical methods, including Taguchi's approach, can be used to optimize process parameters in order to improve the quality of machined components. It is clear that process parameter values cannot be determined just like that for a certain process; optimization techniques must be utilized in order to find optimal values to certify optimum utilization of attributers' (Rao and Kalyankar 2014). For this reason, various mathematical approaches are used, such as GRA, Fuzzy Logic, PSO, SAW, TOPSIS, etc. Optimized the machining characteristics with an approach of Taguchi-Grey for machining of SS316L with HSS tool and suggested better performance in the grey theory Sharma et al. (2021).

2.2.1 Taguchi' single objective optimization technique

Taguchi's single-objective optimization technique is one of the most robust designs available to find out optimum cutting conditions when there is a single response to be optimised. Taguchi method was used to obtain optimum machining parameters in milling (Gürcan, 2016). Taguchi's method uses a special kind of OAs to learn the entire parametric space with a minimum number of experiments (Lande et al. 2016). Milling experiments were performed on Al6061, according to Taguchi's orthogonal array (L_{16}) for different combinations of controllable parameters viz: cutting speed, feed and DoC. Against each experimental run surface roughness value has been recorded and further analysed using S/N ratios and then optimum combination of machining parameters have been identified (Sukumar et al. 2014).

Harne et al. (2015) employed Taguchi optimization methodology to optimize the machining parameters in end milling of die steel. An OA, S/N ratio and ANOVA were employed to analyse the effect of input process parameters on the output responses. Regression

mathematical models were developed to predict the performance responses.

2.2.2 Multi objective optimization using T-GRA and T-TOPSIS

Simultaneously obtaining better multiple output performance responses from a machining process is an important objective for any manufacturing industry in order to attain the better finished components in terms of quality and quantity. Finding of optimum combination of machining conditions by multi-objective optimization is comparatively a complicated procedure than the selections of optimum cutting conditions by single objective optimization (Aggarwal et al. 2008). In the present scenario the industrial requirements are keep on increasing and multiple responses are to be optimized concurrently to compete with the existing market demand.

Tsao et al. (2009) employed GRA multi-objective optimization technique on end milling parameters while machining Al6061alloy. Optimum parametric combination found by GRA has successfully decreased the performance response (R_a) from 0.44µm to 0. 24µm. Based on L_{27}orthogonal array design, considering constant tool diameter, feed rate, spindle speed and DoC as input machining parameters milling experiments were conducted.

The main benefit of Taguchi's philosophy is that, it predicts the optimal parametric combination a discrete domain. But its main constraint is, when solving multi-objective problems, it despondently fails there (Gopal et al. 2018). In order to eliminate this drawback, grey relation theory (Rathodet al. 2017), TOPSIS (Parthiban et al. 2018), MOORA (Majumder et al. 2018) etc, were integrated with the Taguchi's philosophy.

Sivaiah and Chakradhar (2019) worked on T-TOPSIS and T-GRA with cryogenic cooling coolant on turning of 17-4 PH SS material. Surface roughness, flank wear and MRR are the performance responses and spindle speed, DoC & feed rate are the controllable factors. Liquid nitrogen was used as a cryogenic coolant. They found that, T-GRA is yielded better results over T-TOPSIS technique.

2.3 MODELING OF END MILLING PROCESS USING RSM

RSM is a combination of statistical and mathematical tools for designing, enhancing and optimizing processes (Myers et al. 2016). It is a collection of experimental strategies, mathematical models, and statistical inferences that enable an experimenter to make an efficient empirical exploration of the system of interest (Campatelli et al. 2014). The developed mathematical models by employing RSM can be used to predict the output responses for a machining process considered. RSM can be used in the following areas successfully.

- To find the optimum combination of cutting parameters that yields a required output response and describes that response near to the optimum.
- To determine how a specific response is affected by changes in the level of factors over the specified levels of interest.
- To achieve a quantitative understanding of the system behaviour over the region tested.
- To predict product properties throughout the region, even for a factor combination that is not actually run.
- To find the conditions necessary for process stability.

Here, the well-known regression analysis is employed for fitting the models. All the regression model-building methods and tools for checking the adequacies of model are therefore appropriate in the RSM.

Mithilesh et al. (2014) studied the effect of cutting parameters such as: spindle speed, feed per tooth, axial and radial depth of cuts during ball-end milling of Al2014-T6 under dry condition. The experiments were conducted based on face cantered, rotary central composite design (RCCD). Three cutting force components i.e., tangential, radial and axial forces were measured and then ANOVA is performed. They found that the quadratic model is best fitted for prediction of the force components. The analysis of result shows that the cutting forces increases with the increase in feed per tooth and axial depth of cut, but it decreases with

increase in cutting speed. Radial depth of cut has significant effect on the cutting force components.

Daniyan et al. (2021) developed the prediction model based on a combination of central composite design and RSM for MRR in end-milling operation of aluminium alloy AA6063-T6. The cutting parameters were also optimized using the composite desirability function. They found that, feed rate, depth of cut and cutting speed were the key contributing parameters towards MRR.

Mia Mozammel et al. (2018) conducted end milling experiments with MQL based on Taguchi and RSM techniques. Lubricant flow rate, feed and spindle speed are the parameters considered. ANOVA was used to find the influence of variables and then a comprehensive statistical analysis was performed by the interaction effects, perturbation plots and 3D surface plots.

Selaimia et al. (2017) followed Desirability approach and RSM to develop model and to optimise the machining conditions that will maximise MRR and minimise R_a simultaneously.

2.4 ANALYSIS OF VARIANCE

ANOVA can be useful for interpreting input data and test results in a controlled way after a series of trials (Shaw, 1984). It was applied to analyse the impact of the developed model and effect of cutting parameters on the performance characteristics. It is a collection of statistical models and their connected evaluation procedures used to analyse the differences among group means in a sample (Myers et al. 2016; Uma et al. 2016).

ANOVA was developed by statistician and evolutionary biologist Ronald Fisher. In the ANOVA setting, the observed variance in a particular variable is partitioned into components attributable to various sources of variation. ANOVA provides a statistical test of whether the population means of several groups are equal or not and therefore generalizes the *t*-test to more than two groups. ANOVA is useful for comparing three or more group means

for statistical significance. It is conceptually similar to multiple two-sample t-tests, but is more conservative, resulting in fewer type-i errors, and is therefore suited to a wide range of practical problems.

2.5 OFAT EXPERIMENTATION

OFAT experimental design is also known as One-Variable-at-A-Time experimental methodology. It is an approach of experimentation and graphical representation of the influence of cutting parameters on performance responses. It is a kind of experimental procedure, in which each individual control factor varies at one time by keeping other process parameters kept constant at their respective average levels.

Vasu and Shivananda (2018) performed turning experiments on EN47 spring steel samples with different nose radii carbide tools, and then obtained results were compared with each other. Experiments were conducted based on OFAT approach of experimentation. Cutting speed, feed rate and depth of cut are the input process parameters and cutting force; surface roughness and cutting tool tip temperature are the corresponding performance responses considered for this study. Their result revealed that the lower cutting force and better surface roughness were obtained with 1.2mm nose radius. Similarly minimum cutting tool tip temperature was obtained with 0.8 mm nose radius.

In the past, many researchers from machining area have used OFAT approach of experimentation (Manna 2013; Sharma et al. 2015; Manjaiah et al. 2016). This method of experimentation consists of selecting a baseline set of levels for each factor, and then successively varying each factor over its range by keeping other factors held constant at the baseline level. 2D plots will be established to show the variation of response variables against variation of one input factor by keeping other input factors constant at their mean levels (Montgomery 2017).

2.6 CUTTING TOOL TIP TEMPEARTURE

Temperature while doing machining is an important process condition in the study and nurturing of the effects of a metal cutting process. During machining process, heat gets

generated as a result of plastic deformation of metal and friction along the tool–chip and tool–workpiece interfaces. This heat generation, rises the temperature of the cutting tool as well as workpiece and causes various thermal damages like: thermal enlargement, degradation of dimensional tolerance, surface damage, increase of cutting force and tool wear. In order to avoid these ill effects and to choose suitable machining conditions, it is necessary to acquire precise statistics about milling temperatures. Some of the main factors influencing the cutting temperature are: workpiece material, cutting tool material, range of process parameters chosen, tool geometry, cutting coolant, and ambient temperature in the machine tool cabin etc.

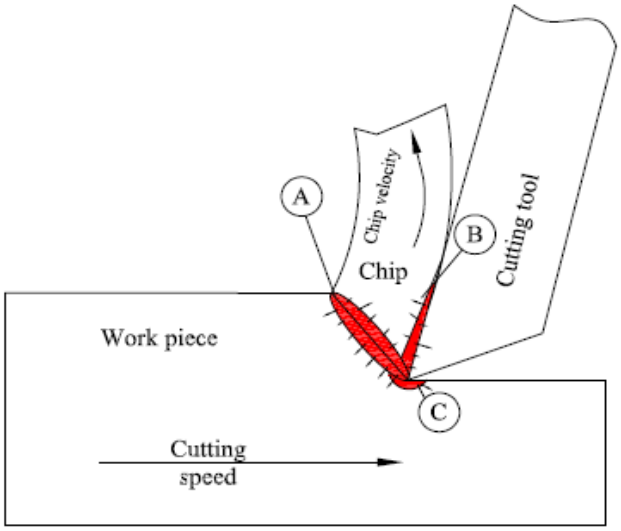

Figure 2.1 Sources of heat generation in orthogonal cutting process

Heat gets generated (Figure 2.1) mainly along the shear plane due to plastic deformation of the material. This zone is normally referred as primary deformation zone (A). The zone where heat gets generated due to friction at interface between tool and workpiece is called as secondary deformation zone (B). Also, due to flank friction, heat gets generated in the tertiary zone (C) (Norouzifard and Hamedi 2014). The generation of heat puts a limit on cutting speed, thus reducing the production rates. The high cutting temperature generated during machining may also result in tool deformation, fracturing and formation of built-up edge and also results in less dimensional accuracy of the product, damage to the workpiece surface and development of micro cracks at the surface (Bhirud and Gawande 2017).

Cutter edge temperature in milling is an important factor to cutter life. With high cutting speed and feed rate the cutting efficiency is high. But this high cutter edge temperature shortens the cutter life. Therefore, it is necessary to know the cutter edge temperature in milling. Deng et al. (2020) studied the cutter edge temperature in trochoidal milling based on the engagement between cutter and workpiece. A temperature comparison was made between trochoidal and side milling based on the analytical approach, and the reasons that trochoidal machining could extend the cutter life were found.

Muhammad and Adesta (2016) conducted experiments with a tool path method of contour in. Results presented by them indicated that by increasing cutting speed the cutting temperature is lower than the same with low cutting speed. However, by decreasing feed rate leads to cutting temperature low. Kai et al. (2011) investigated the temperature distribution of the micro-cutter in the micro-end-milling process by numerical simulations and experimental approach. Experimental verification of the simulation model is carried out on a micro-end-milling process of aluminum alloy 2024-T6 with a high-precision infrared camera. Their results showed that with increase of tool edge radius the mean cutting temperature and effective stress decreases, while cutting force increases. The tool edge radius has been found to be the major factor affecting micro-cutter temperature distribution.

Vasu and Shivananda (2019) conducted turning experiments on EN47 spring steel samples using coated and uncoated tungsten carbide tools. Coated tool inserts exhibit 1.27- and 1.29-times better outputs than the uncoated tool insert for tool tip temperature and surface roughness respectively. In wet machining Ra and tool tip temperature (T) is reduced by 22.59% and 21.29% respectively than the dry machining. Mahesh (2020) conducted turning experimentation on Aluminum6061 workpiece material using Al_2O_3 coated carbide tool and found that, spindle speed is the greatest influencing parameter for temperature. It is minimal between 91m/min to 98m/min cutting speed. Best minimum temperature values were obtained between 0.6mm to 0.8mm of nose radius of the cutting tool.

Ajith et al. (2019) worked on optimization of input factors: mass fraction and particle size of SiC, DoC, feed rate and spindle speed in the milling of Al5059/SiC/MoS2.The result shows

that an addition of weight percentage of the reinforcement's results in higher surface roughness, temperature, cutting forces but lowering the MRR.

Yuan et al. (2017) proposed an analytical model for predicting the transient tool temperature in Modulation-assisted machining (MAM). It takes into account the variation of unreformed chip thickness during MAM. The developed analytical model is consistent with FEM results. A set of cylindrical turning experiments is carried out with and without modulation, showing that MAM can effectively reduce the average tool temperature by 30% approximately compared to conventional machining.

Yinfei et al. (2020) machined pure Iron with Different Grain Sizes on a turning machine. The results showed that the cutting temperature of fine-grain was smaller by 50°C than the coarse grain. This indicates that fine grain of pure iron in finishing can get smaller cutting temperature. The cutting temperature and residual stress of machining fine-grain iron were much smaller than the coarse grain at all levels of cutting parameters.

Satish et al. (2020) in their research work emphasizes on the impact of cutting speed, feed rate, and depth of cut and step-over on the work-piece temperature during 2.5D milling of Inconel625 under dry condition. The temperature of the work-piece has been estimated with the help of pyrometer type thermometer. The prognostic model in this study is generating values of the work-piece temperature which is close to those readings recorded experimentally.

Kadirgama et al. (2009) have used RSM and developed first-order temperature model while machining HASTELLOY C-22HS with carbide coated cutting tool. Finite element analysis (FEA) was employed for confirmation of the temperature distribution on cutting tool. Feed rate was found to be the most dominating parameter affecting the cutting temperature, followed by the axial depth and cutting speed.

Noor et al. (2018) conducted experiments on Al 6061-T6 by using a high-speed steel (HSS) end cutter based on the central composite design of RSM. Multi objective genetic algorithm

(MOGA) has been applied to optimize the machining parameters that simultaneously minimize temperature and surface roughness. Milling, as a process, has evolved with new machines and methods being employed in order to obtain the best results consistently. Milling tools have also seen quite an evolution from the uncoated high-speed steel (HSS) tool, to the now vastly used coated tools. Multilayer coatings achieve overall better results in most of the applications when compared to mono layered and uncoated tools. With these coatings there is a significant improvement on tools' life and machining quality.

The deposition process is also an important factor, when choosing a coating for a milling application Savkovic et al. (2020). PVD and CVD processes achieve different types of coatings. In coatings applied to tools, generally nitrides, carbides, borides and oxides of transition metals are used. Nitrides used as coatings for cutting tools are TiN, TiAlN, CrN, ZrN, TiSiN, TiAlSiN, CrAlN, TiAlCrN and cBN and Carbides for coatings are TiC, CrC and WC. For boride coatings, TiB2 is used due to its chemical inertness, high hardness and good wear resistance (Swain et al. 2017; Masooth et al. 2020). In the study carried out by Skordaris et al. (2016) the influence of the film thickness of a nano structured multilayer coating on mechanical properties and milling performance is analyzed.

PVD coatings are usually used for finishing operations due to their overall thickness, these being thinner than their CVD counterpart. PVD is often used for applications requiring a better surface finish on the workpiece (Fernández et al. 2013). PVD consists of different methods, such as: evaporation, sputtering and molecular beam epitaxial, where direct current magnetron sputtering is being the most used technique. The PVD process, when compared to CVD, runs at a lower temperature (under 500^0C), and is more environmentally safe due to the type of materials that CVD uses (Caliskan et al. 2017, Baptista et al. (2018a & 2018b)). Lot of research has been observed through literature on conventional constant feed machining with coated and uncoated tools to minimize cutting tool tip temperature. But there are very few articles (Badrinadhan and karunamurthy 2014a & 2014b) available on progressive feed machining. However, to the best of author's knowledge there is no literature observed on minimizing of cutting tool tip temperature through progressive feed machining in end milling.

2.7 SURFACE ROUGHNESS

The challenge of contemporary machining industries is mainly interested in the achievement of high-quality products in terms of surface finish, dimensional exactness in a stipulated time. It demands a lot of manual bench work to bring certain areas of end milled part surface finish to the desired level. This consumes a considerable amount of time and separate tooling and other resources. Quality of machined surface is one of the most important concerns which affects the functionality of machined component and in-turn its life and durability. Machined components used for aerospace applications subject to rigorous surface analysis to detect surface damages that will be detrimental to the highly expensive machined components. Surface finish is an important factor for surface sensitive parts subjected to fatigue loads. Hence, understanding of surface finish provides many opportunities to avoid failures and to enhance component integrity as well as to reduce production cost.

Especially machined detail components, assembled in fighter aircraft structures, like: longerons, spars, central frames, side frames, shear walls, trouser ducts, integral fuel walls and various supporting ribs of the aircraft fuselage, will be subjected to high level of fatigue loads during manoeuvring. In the case of these parts surface finish plays a crucial role and it is great concerned in their fatigue life and therefore durability of the aircraft. Hence, it is very important to fabricate a component with best possible surface finish to enhance the life of these detail components and in turn life of aircraft. The chosen material for this research work is widely used for high technology applications like aerospace, defence, marine and automotive machined components due to its high level of technical merits. A good quality milled surface significantly improves not only fatigue life but also corrosion resistance and creep life. Some of the fighter aircraft detail parts are very intricate in shape and needs extensive scooping of material by end milling processes to realize the final component with an acceptable surface finish.

Ability to control the machining process by setting proper input factors for a better surface finish and in turn a good quality product is of vital importance. Researchers have concentrated on various optimization and predictive modelling techniques to determine the optimal input parameters, and to achieve the better surface finish. Lot of research has been

observed through the literature on conventional constant feed machining of end milling process and minimizing the surface roughness using different statistical and optimization techniques. But only few research articles (Badrinadhan and Karunamoorthy (2014a & 2014b) are available on progressive feed machining, wherein the feed is applied progressively rather than instantly in order to minimize cutting force, tool wear, chattering and tool vibration. However, to the best of author's knowledge there is no literature observed on minimizing surface roughness through proposed progressive feed machining in end milling process.

Surface finish is one of the major significant requirements in machining process. In a CNC milling process, proper setting of cutting parameters is vital to obtain better surface finish. Surface roughness is also an important measure of the technical quality of a machined component and it is a factor greatly influences the manufacturing cost. The quality of the surface of a product plays an important role in its performance. A good quality milled surface significantly improves fatigue life, corrosion resistance and creep life. In addition, it also affects surface friction, light reflection, ability of holding a lubricant, electrical and thermal contact resistance. The desired surface roughness value is usually specified for an individual part, and specific processes are selected in order to achieve the specified finish. Surface specification can also be a good reference in determining the stability of a machining process. Since, the stability of a machine tool is contingent with the quality of the machined part (Ramesh et al. 2012).

Dutta et al. (2013) studied the correlation between tool flank wear and surface texture in end milling process. Micro and nano-particles are being widely applied in industrial applications. In such cases the particle size plays a major role. In this work condition monitoring of HSS mills and coated carbide milling inserts has been performed by analysing the resulting end-milled surface images using image texture analyses. Texture descriptors obtained have been highly correlated with the trend of flank wear.

Reddy (2013) used Taguchi's DoE to investigate the machining characteristics of GFRP. From ANOVA results, it is understood that spindle speed and DoC are the most significant factors affecting the responses, their contribution in an order of 26.84% and 40.44%

respectively. Finally, by applying artificial neural network (ANN) he compared the predicted values from the developed model with the experimental values.

Rodygina et al. (2014) analysed the conditions of rigid technological system and an unworn tool the strain constituent of micro irregularity height has the largest value. His work suggests a research method for forming strain constituents of roughness when cutting surfaces with the use of FEM. Based on the described model the basic regularities of the strain component formation depending on some machining parameters are identified.

Surface roughness is a widely used index of product quality as well as environmental impact. Quality features include parameters such as aesthetics, tribological consideration, fatigue life enhancement, corrosion resistance, and precision fit of significant mating surfaces, subsequent processing advantages (Kant et al. 2013). Surface roughness also denotes the amount of energy and other resources consumed during machining; good surface finish can also help to reduce the life cycle environmental impacts of spur gears in automotive drive train components. Improved surface finish of one spur gear has been found to decrease life cycle primary energy consumption by 1MMBtu, which represents approximately 17% of the energy usually required to manufacture an automobile (Kannan et al. 2015a).

Poor surface quality of a machined component requires further finishing operations like Polishing, Lapping, Honing, Buffing and other finishing operations. Which means that more machining time, high machining cost, high tooling cost, high lead-time and finally higher product cost? On the other hand, poor surface finish finally leads to poor product quality. When conservative cutting parameters were chosen in order to avoid high surface roughness, the productivity will come down. High conventional feed rate, in addition to damage the cutting tool and workpiece, will also create unwanted vibrations in machine tool and may cause chatter and finally high surface roughness (Kannan et al. 2014). Most of the machining operators will go with ‘trial and error’ method of setting of input cutting parameters to obtain better output responses like surface roughness, power consumption, cutting force, tool life etc. Which is not an effective way of machining method and it is more time consuming and of course not a cost-effective process. Thus, a mathematical model using statistical method of

evaluation provides a better solution (Patel et al. 2012).

Sourabh et al. (2015) in their work the effect of machining parameters speed, feed, and depth of cut are studied on surface roughness for milling operation. For surface roughness, our observation is based on 'smaller-is-better' quality characteristic of S/N ratio. Cutting speed has optimization of milling process parameter for surface roughness of Inconel718 by using Taguchi method. The lowest surface roughness (Ra) of 0.80mwas achieved corresponding to: f: 0.12mm/rev, Vc: 55m/min. and d: 1.6 mm. Taguchi robust design is suitable for modelling surface finish in CNC milling.

Mohamad (2014) proposed several architectures of single and multi-layer back propagation neural network methods, to predict tool wear progression within the end milling process of Inconel718. The end milling process was carried out in a cryogenic environment, with cutting parameters of cutting speed, Vc (140 - 170 mm/min), feed rate, Fz (0.05 - 0.1 mm/tooth), axial depth of cut, ap (0.3 - 0.5 mm), and radial depth of cut, ae (0.2 - 1 mm). A coated carbide end ball nose, with a diameter of 5 mm, was used as a cutting tool. The cutting forces exerted during the milling process were measured using a strain gauge-based dynamometer in x, y, and z directions. In order to apply a feed forward back propagation neural network method to predict tool wear; Vc, Fz, ap, ae, and the resultant force (FR), were taken as inputs, and tool wear was obtained as an output.

Chockalingam (2012) research deals with the effect of different coolant conditions on milling of AISI 304 stainless steel. In this investigation cooling methods used were flooding of synthetic oil, water-based emulsion, and compressed cold air. Cutting forces and the surface roughness were studied and tool flank wears observed. Comparison between different coolants' effect to the milling of AISI 304 stainless steel is done and the results from the study can provide very useful information in manufacturing field. The experiment results showed that water-based emulsion gave better surface finish and lower cutting force followed by synthetic oil and compressed cold air. Different cooling conditions are required different parameters in order to obtain lower surface roughness and cutting force. Chipping was the initial wear mode in the milling of AISI 304 stainless steel.

2.8 MATERIAL REMOVAL RATE

In end milling process, material removal rate (MRR) is measured as a significant productivity factor and it is the best predictor of the machining performance in metal cutting process. The principal objective of present manufacturing industries is to make ease, high quality products with highest possible productivity in a short interval of time. Therefore, material removal rate is considered to be an important technical requirement in any kind of machining process. MRR in end milling process demonstrates the amount of metal expelled from the workpiece in a given period of time.

The productivity of any machining process is measured by material removal rate. Thus, productivity can be increased by removing the higher volume of material in the form of chips in metal cutting process. In order to improve the productivity, an accurate prediction of the material removal rate is required for reducing machining cost in production (Liuetal 2016). The cutting process, type of cutting tool, cutting parameters and workpiece material are some of the things, which decides the ability of a manufacturing process to be proceeded to produce the desired surface finish will depend (Deshpande et al. 2017).

Natarajan et al. (2011) adopted RSM methodology to achieving maximum MRR and minimum surface roughness for the multi-response optimizations in micro end milling operation. Second order quadratic models were developed for MRR and R_a. Desirability function approach has been used to develop the models for determining the optimum machining parameters. Finally, it was observed that the experimental response value was in good agreement with the predicted values. MRR was calculated by using the following equation 2.1.

$$MRR = (I_w - F_w) / (\rho \times t) \text{ cc/min} \quad \ldots\ldots\ldots\ldots\ldots \quad (2.1)$$

Where, I_w is initial weight of work coupon,

F_w is final weight of work coupon,

ρ is density of workpiece material and

t is time taken to cut the material for one pass in min.

The MRR for the end milling operation can also be calculated against each experiment by using the following equation 2.2 (Li, C et al. 2016).

$$MRR = \frac{W*D*L}{t} \text{ mm}^3/\text{min} \text{ ……..(2.2)}$$

Where, W: is the width of milling cut in mm,

D: is the depth of cut in mm,

L: is the length of slot in mm and

t: is the time taken to form a cutting slot as shown in Figure 1.2 and Figure 1.3, with an end mill of 20mm diameter in min.

2.9 SURFACE TOPOGRAPHY

Li, W and Y.B. Guo (2014) in their work, the influence of cutting tool wear on surface integrity and its impact on fatigue performance of Inconel718 alloy (45 ± 1 HRC) by end milling process using PVD coated cutting tools are studied. The evolutions of surface integrity including surface roughness, microstructure, and micro hardness were characterized at three levels of tool flank wear (VB=0mm, 0.1mm, 0.2mm). At each level of tool flank wear, the effects of spindle speed, feed rate, and radial depth-of-cut on surface integrity were investigated. End milling can produce surface finish between 0.1 micron and 0.3 micron under most of the conditions. They also found that, surface roughness obtained is higher in step-over direction over the feed direction.

Masmiati et al. (2015) used Taguchi's optimization method in order to identify the main factors that will cause the greatest variation and also to find the controllable parameters in the least unpredictability.

Data analysis was performed using S/N ratio response analysis and ANOVA. The results obtained at optimum cutting condition through this analysis showed improvements in residual stress as well as micro hardness in inclined end milling process.

2.10 CHIP MORPHOLOGY

Increase in DoC causes increase in shearing area of the material, resulting in increased chip thickness, higher cutting forces, and thermal stresses. The quality of workpiece machined surface, cutting forces, and tool wear for different set of process variables can be compared using the chip morphology (Nurhaniza et al. 2016). In dry milling experiments conducted by (Rajender et al. 2022), at the low value of TRS, FR, and DoC, continuous chips of small thickness are obtained. Whereas, at higher value of TRS, FR, and DoC, strain hardening occurs, resulting in discontinued brittle chips. Higher chip thickness corresponds to the higher temperature generation resulting in a higher possibility of reduced tool life. The SR is greatly influenced by the cutting parameters, material composition, and machining environment (Sarkar and Datta 2021).

2.11 CUTTING TOOL

During machining of a workpiece material, cutting tool is subjected to thermal and mechanical stresses, which is an important aspect to be addressed for any manufacturing industry in order to decrease machining time as well as machining cost without compromising product quality. This tendency places more prominence on the cutting tool manufactures to produce tools with high wear resistance, toughness and hardness at high temperatures. Sintered carbide tools are produced by powder metallurgy (P/M) technique and have rich machining properties for machining hard materials generally used in aircraft and marine gas turbines, like high red hardness (of about 1000^0C), high wear resistance, high modulus of elasticity, low thermal expansion and high thermal conductivity. The property of carbide tool depends upon.

i. Method of manufacturing.
ii. Chemical composition.
iii. Micro structure of the tool material etc.

According to ISO, carbide tools have been grouped under three series.

i. Tools used for cutting cast iron and non-ferrous metals are designated from: K_{01} to K_{40}.

ii. Tools used for machining steel are designated as: P_{01} to P_{60}

iii. Tools used for general purpose applications are designated: M_{10} to M_{30}.

Figure 2.2 Different types of carbide inserts.
(https://www.indiamart.com/proddetail/carbide-insert-4672327130.html)

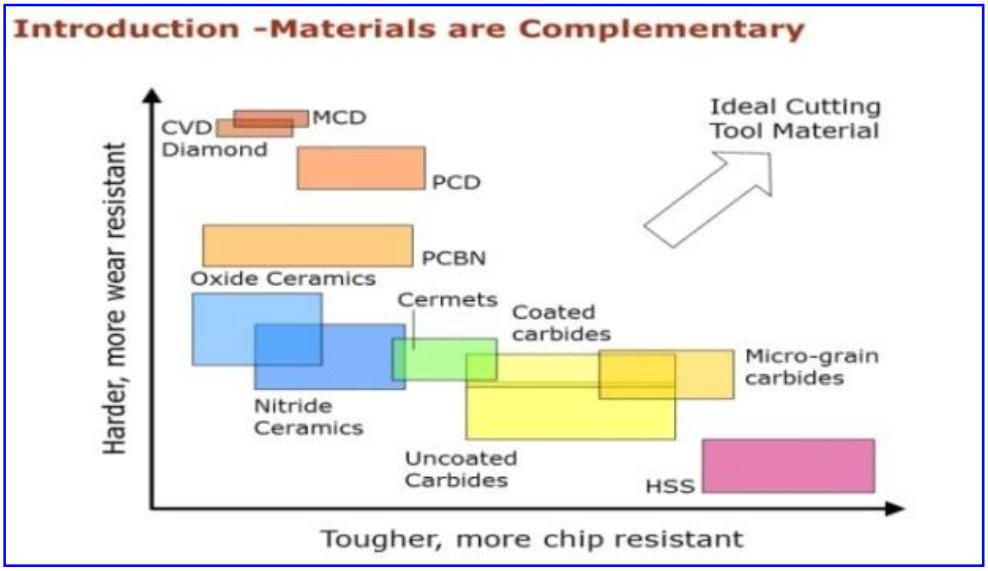

Figure 2.3 Different types of carbide inserts and their working range.
(http://www.hm-dia.com/Product/034159654.html)

Different types of carbide inserts have been shown in Figure 2.2 and the working range of carbide tools are shown in Figure 2.3. And Figure 2.4 illustrate the end milling cutter

nomenclature.

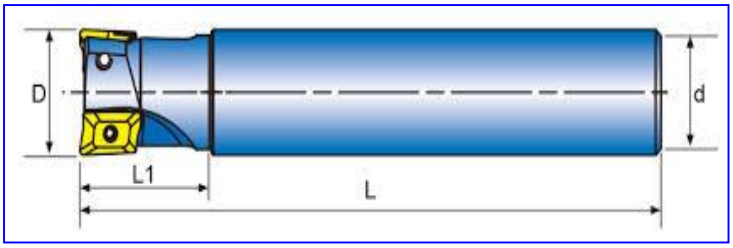

Figure 2.4 End milling cutter nomenclature
(www.widia.com)

Where,
d - Shank diameter
D - Effective cutting diameter
L - Overall length
L_1- Head length

In general,

i. Higher the cutting-edge angle, higher is the cutting-edge strength.
ii. Power requirement is proportional to edge angle.
iii. Tendency to vibrations increases with the increase of cutting-edge angle.
iv. Versatility and accessibility increase as the cutting-edge angle decreases.

2.12 GREY RELATIONAL ANALYSIS

GRA has been broadly applied in evaluating the performance of a complex project with meagre information. However, the data to be used in GRA must be pre-processed into quantitative indices for normalizing raw data for another analysis. In the present work, GRS has been used to optimize the machining parameters during machining of BS L168 aluminium alloy work specimens.

Optimization of end milling process is a combinatorial task due to the involvement of a bulky number of process variables and performance features. Process-specific numerical models or mathematical functions are required for the evaluation of parametric combinations in order to get the better quality of machined parts and machining time (Ghosh et al. 2020). It has been found from the literature that Taguchi method has been utilized largely for parametric

optimization since this method adopted an Orthogonal Array design of experiment, utilizing a minimum number of experimental runs with less experimentation cost and time. The advantage of Taguchi's philosophy (Pandey et al. 2017; Gopal and Soorya 2018; Kant and Sangwan 2014) is that the method predicts the optimal combination of process parameters within a discrete domain. However, when the issue of solving multi-response problem, appears, it miserably fails there. To eliminate this drawback, grey relation theory (Rathod et al. 2017; Kant and Sangwan 2014) desirability function (Singh et al. 2013), TOPSIS (Parthiban et al. 2018), utility concept (Kumar and Singh 2014), MOORA (Majumder and Maity 2018) have been integrated with Taguchi's philosophy. Sivaiah and Chakradhar et al. (2019) worked on a combined Taguchi coupled TOPSIS and Taguchi based Grey Relational Analysis (T-GRA) for optimization of three responses: Surface roughness, flank wear and material removal rate in turning of 17–4 PH SS material. TiAlN coated KC5010 carbide inserts were used in cryogenic environment for machining the test sample. Liquid nitrogen was used as a cryogenic coolant and cutting speed, feed rate and depth of cut as controllable process parameters. They found that, the results were improved by T-GRA compared to results by T-TOPSIS.

Emel and Ozcelik (2013) exposed that the feed force increases with increase in spindle speed, feed rate and depth of cut while the radial force is also increased with increase in depth of cut during milling process. On the other hand, an increase in cutting force leads to machine vibration and tool chattering, which diminishes the quality of machined surface of the end product. Shrivastava and Singh (2018a, 2018b) used pre-processed signals to evaluate anew output parameter: chatter index in high-speed machining. Ensemble empirical mode decomposition technique has been used to rectify the signals recorded by using sensors contaminated by background noise. For estimating the dependence of output responses on input cutting parameters, mathematical models have been developed using RSM. Optimal cutting zone has been predicted using the artificial neural network and multi-objective genetic algorithm. Machining in the obtained optimal zone had improved the productivity, by decreasing tool chatter and increasing MRR simultaneously.

Sivasakthivel and Sudhakaran (2013) reported that increase in spindle speed results in

increased temperature during end milling of Al6063 alloy and also states that formation of built-up edge occurs due to temperature, which results to minimal surface finish. Also, this increase in cutting temperature leads to deformation in the workpiece and in turn to poor machining accuracy (Liao and Lin 2007). Tsao et al. (2009) performed the multi-objective optimization on end milling parameters while machining Al6061PT651alloy through GRA technique. The grey relational optimal combination effectively decreased the surface roughness from0.44 micron to 0.24 micron. Further, GRA is an uncomplicated tool which does not require complex formulations for multi-objective optimization; and hence the results can be obtained in a short period of time. So, GRA technique can be used for solving the multi-response problems effectively. The multiple objective optimizations were carried out using grey relational analysis and desirability function analysis, for simultaneous evaluation of process parameters for milling of AISI 304 stainless steel, as a dynamic approach Naresh and Rajasekhar (2016). They found, the optimum setting of cutting speed, feed rate, and depth of cut for minimization of surface roughness and maximization of material removal rate.

A multiple-objective optimization methodology (Murthy and Rajendran 2012) by using principal component analysis, grey relational analysis and Taguchi method has been proposed to optimize the machining parameters. Three different levels of input parameters were planned as per Taguchi's L_9orthogonal array. The parameters were optimized from analysis of mean (ANOM) and Analysis of variance (ANOVA) was employed to investigate the effect of machining parameters on the variables (Shihab and Mohamed 2016). Results of this study indicated that, the depth of cut has the most significant influence on the response Ra, with highest percentage of contribution followed by feed rate and cutting speeds having least percentage of influence.

Optimum condition of various input parameters is determined by deploying grey relational analysis to obtain the best quality characteristics (Gupta and Kumar 2013; Wang et al. 2013; Ramanujam et al. 2011; Senthilkumar et al. 2014). The first step involved in grey relational analysis is normalizing the experimental data according to the type of performance response to avoid different units and to reduce the variability. A suitable value is derived from the

original value to make the array between '0'and '1' and this procedure is called data processing. It is a method of converting the original data to a comparable data. If the response is to be minimized 'smaller-the-better' characteristic is envisioned for normalization to scale it into an acceptable range. In the present work, the surface roughness and cutting tool tip temperature are to be minimized, hence 'Smaller-the-better' (SB) is the form we obtained as the original sequence, then this original sequence can be normalized as follows (Umamaheswar rao et al. 2018) equation 2.3.

$$x_i^*(k) = \frac{max\left(x_i^o(k)\right) - x_i^o(k)}{max\left(x_i^o(k)\right) - min\left(x_i^o(k)\right)} \quad \text{..... (2.3)}$$

Similarly material removal rate is the performance response is to be maximised for process betterment. Therefore, 'Higher-the-better' is the form we have chosen as an original sequence. This original sequence can be normalised using the equation 2.4

$$x_i^*(k) = \frac{x_i^o(k) - min\left(x_i^o(k)\right)}{max\left(x_i^o(k)\right) - min\left(x_i^o(k)\right)} \quad \text{..... (2.4)}$$

Where, i=1,….,m; k=1,….,n., and 'm' is the number of experimental data, 'n' is the number of responses, $x_i^o(k)$ denotes the original sequence, $x_i^*(k)$denotes the sequence after data processing, $max\left(x_i^0(k)\right)$denotes the largest value of $x_i^0(k)$, $min\left(x_i^o(k)\right)$ denotes the smallest value of $x_i^o(k)$, and x is the desired value (Tosun and Pihtili 2010). If larger the grey relational grade better is the multiple performance characteristics. However, the relative importance among the parameters for the multi- performance characteristics will still need to be identified, so that the optimal combinations of the process control parameter levels can be determined more accurately (Mukhopadhyay et al. 2016).

2.13 MOTIVATION FOR PROPOSED RESEARCH WORK

Machining is one of the most critical fields and it is still an open ground for the researchers after more than TEN decades of exploration, mainly because of continuous developments and up gradations in the machining technology, materials and advancements in the computational, modelling and optimization techniques. In general, machine tool

manufacturers suggest a range of cutting parameters for various machining processes in the form of maximum and minimum values (Baskar et al. 2005). But in actual practice exact values of optimum cutting parameters are required to prepare the process plan, part program and thus to get the required output responses with minimum possible inputs. But in most of the cases, machine tools are not utilized to their full capacity. This limitation is mainly due to failure in running the machine tools at their optimum operating conditions. Problem of arriving at the optimum levels of the cutting parameters has attracted the attention of many researchers and production engineers for a longer time.

Literature survey on milling machining reveals that most of the researchers have tried to vary the machining parameters such as cutting speed, feed rate and depth of cut for machining different kind of work materials with diverse cutting tools (Barathiraja et al. 2012). In CNC machining 'Offline Optimization' of cutting parameters is possible, which when implemented will avoid catastrophic failures during machining.

Recent developments in "Virtual Machining" have enabled this very much. However, so far very little research has been observed on varying the feed rate progressively along a cut segment; therefore, the ill effects of sudden acceleration and therefore sudden impact of cutting tool with workpiece can be minimized to safer levels. And also, it is essential to optimize cutting parameters in order to improve the material removal rate, surface finish and at the same time to reduce the cutting tool tip temperature and in turn induced residual stresses etc.., for qualitative and economical machining. Multi-objective optimization will give an overall improved machining and therefore it has been chosen for optimizing machining processes. Proposed progressive feed machining combined with optimized machining conditions obtained through multi-objective optimization, will help the manufacturing community to achieve better quality products.

Modelling of regression mathematical equations and optimization of machining parameters are of great concern in manufacturing environments (Patel and Hiren 2012). The economical production of components plays an important role in competing with the present market. The optimal values are determined even before the raw material is put into production. It has been

observed that cutting conditions such as feed rate, spindle speed, DoC and performance responses like MRR in any machining operation should be selected to optimize the economics of machining as well as productivity, manufacturing cost per component or some other suitable criteria (Gilberth. 1950).

Optimization of cutting parameters is an important activity for operating predominantly high-cost CNC machine tools. With the use of theses sophisticated and high-cost CNC machines, coupled with high labour costs, optimum machining parameters are essential for producing the parts economically. It is essential to systematically investigate the process or product variables that influence the product quality. After identifying the influential variables one can achieve improved machining process in order to enhance the product manufacturability, reliability, quality and field of performance. Machine tool manufacturers suggest cutting parameters for various kinds of machining processes in the form of limits of minimum and maximum values. But in actual practice optimised exact values are required to obtain the better outputs.

2.14 OBJECTIVES OF RESEARCH WORK

Objectives of present research work are derived based on extensive literature review on machining of aerospace materials and the scope of implementing progressive feed machining for end milling process to improve the quality of output performance responses. Proposed progressive feed machining combined with optimized machining conditions obtained through multi-objective optimization techniques, will help the manufacturing community to achieve better quality products.

1. The primary objective of present research work is to adopt the concept of progressive feed machining (PFM) in end milling of BS L168 aluminium alloy through CNC part programme for better product quality. Further, to study and investigate the effects of PFM on end milling performance responses.

2. To investigate the effect of increasing machining feed rate progressively along the start of each cut segment and where there is a change in cut direction on the considered output performance responses like:
    a. Cutting tool tip temperature (T)
    b. Material removal rate (MRR)
    c. Surface roughness (R_a)
    d. Surface topography

3. To make a comparative experimental analysis between existing constant feed machining and proposed progressive feed machining and then to find the merits of PFM over CFM through the established 2D and 3D plots.

4. Modelling and parametric analysis of end milling process by RSM, with CFM and PFM environments by means of two statistical approaches:
   (i) Correlations between the parameters by multiple linear regression analysis and
   (ii) Analysis of Variance (ANOVA).

- To find the most influential input process parameter on the output performance response and to identify the significance of each individual input process parameter on machining performance characteristics by employing ANOVA technique. Then to validate the developed regression models for: cutting tool tip temperature, surface roughness and material removal rate.

- Correlation of experimental values of output responses with the predicted values obtained through the developed regression mathematical equations for both existing constant feed machining and proposed progressive feed machining and to find the level of agreement or level of fit between predicted values and experimental values

- To establish model fitness plots in order to find the adequacy, model fitness and to validate the developed regression models against each performance characteristics.

5. Further, experimental investigation and comparative analysis of cutting tool tip temperature, surface roughness and material removal rate with coated (TiAlN) and un-coated end mills both with constant feed machining and progressive feed machining. To check the merits of progressive feed machining with coated cutting tools over constant feed machining with coated and un-coated cutting tools.

6. To find single-objective optimization of machining parameters for end milling process by Taguchi's single objective optimisation technique. Further, to find the multi-objective optimisation of performance characteristics by employing T-GRA and T- TOPSIS techniques. To find the most suitable technique for the present research problem from these two. Further, to study and analyse the combined benefit of proposed progressive feed machining with optimized machining conditions attained by means of multi-objective optimization techniques. This will help the manufacturing community to achieve better quality products.

7. To analyse the effect of cutting tool nose radius (NR) on milling performance characteristics like: Cutting tool tip temperature, Surface roughness, Material removal rate by means of established 2D plots. Then, to find the effect of nose radius on surface topography by means of optical microscopic study.

To fulfil the above-mentioned objectives, experiments were conducted based on Taguchi's design of experiments L_{27} & L_9 Orthogonal Arrays and then according to One Factor at A Time approach of experimentation, on a three axis CNC vertical milling machining centre. BS L168 aluminium alloy test specimens are machined through existing CFM and proposed PFM using Ø20mm coated and un-coated carbide solid end milling cutters with two flutes and rake angle of 16^0.

2.15 RESEARCH SCOPE

Machine tool industry has made an exponential growth in its manufacturing capabilities in the past two decades. But in most of the cases, machine tools are not being utilized to their maximum capacity or to their full potential. It is one of the main drawbacks confronted by

present manufacturing industry. This limitation is mainly due to failure in operating the machine tools at their optimum operating conditions. Hence, the problem of arriving at optimum levels of cutting parameters has attracted the attention of many researchers and production engineers for a long time.

Literature survey on machining reveals that most of the researchers have tried to vary the cutting parameters such as cutting speed, feed rate and depth of cut for machining diverse materials with different cutting tools on various types of machine tools. In CNC machining 'offline optimization' of cutting parameters is possible, which when implemented will avoid catastrophic failures during machining.

Since, only inadequate research has been observed in the literature focusing on the PFM, research in this area gains a significant importance. Also, it is necessary to optimize the machining parameters in order to improve the material removal rate, surface finish at the same time to reduce the cutting tool tip temperature which in turn to reduce the induced residual stresses on workpiece surface as well as will increase the tool life. Multi-objective optimization is the better option when there are multiple responses needs to be optimized simultaneously rather a single response one at a time by means of single-objective optimization.

Based on extensive literature study it is understood that, multi-response optimization techniques like Taguchi based GRA and Taguchi coupled TOPSIS have yielded an overall improved machining performance and hence it has been chosen for optimizing machining process in the present research work. With the expectation of better machining results by means of progressive feed machining along with optimised machining conditions in the manufacturing domain this research work has been started.

2.16 CLOSURE

In the past few decades, magnanimous experimental research work has been carried out by the researchers to develop association between input process parameters and output

machining performance characteristics for fabrication of detail components with desired quality.

Lot of research articles are available on modelling and finding optimal machining conditions using some of the evolutionary techniques such as GA, Fuzzy Logic, RSM, and Taguchi based GRA, Taguchi coupled TOPSIS. Most of the researchers concentrated on ANN, GA and PSO to predict the optimal cutting parameters in the literature. Machinability investigations using optimization techniques such as single-objective optimization and multi-objective optimization are some of the areas where several papers have been published.

In the present research work, discussion has been done on the areas such as: surface roughness, cutting tool tip temperature and material removal rate in CNC end milling process of BS L168 aluminium alloy. Following are the list of summary points made based on literature review carried out about cutting tool tip temperature, surface roughness, MRR, response surface methodology (RSM), ANOVA, Taguchi's single-objective optimization, Taguchi based GRA, Taguchi coupled TOPSIS.

From the literature review it can be inferred that:

1. Numerous works have been carried out on modelling of CNC end milling process performance characteristics such as: cutting temperature, surface roughness, cutting force, power consumption and MRR for various aluminium alloys. But there is no significant work has been reported for the prediction and optimization of cutting tool tip temperature, average surface roughness, material removal rate, surface topography and chip morphology in case of BS L168 aluminium metal composite.

2. Further, to the best of author's knowledge no literature available on progressive feed machining of end milling process on BS L168 aluminium alloy to evaluate above mentioned performance responses. The researchers developed the models to predict different output responses based on various combinations of cutting parameters. But

very little literature available on machining of aerospace material with proposed progressive feed machining.

3. The present research work focuses on the development of regression mathematical models through RSM techniques and optimization of the same for both CFM and proposed PFM.

4. Prediction of T, R_a and MRR for various materials like EN24 grade steel, EN-31 steel, AISI H13 steel, AISI 52100 bearing steel, Titanium alloy Ti-6Al-4V, Inconel718, AL6351-T6, Composite Al/SiCp MMC and aluminium alloys (AA6061-T6) etc., in different milling processes have been attempted by many researchers.

5. Experiential models have been developed and optimizations of cutting parameters have been done to predict T, R_a, F, TW and MRR by several researchers in the past.

6. Many researchers have developed regression mathematical models to study and analyse the effect of cutting parameters on performance characteristics. They have employed ample number of statistical techniques like factorial design, single objective optimization and different multi-objective optimization techniques to determine optimum cutting conditions.

7. Cutting process parameters that influence the performance characteristics of end milling process are tool geometry, tool material, feed rate, cutting speed, and depth of cut, cooling fluid, process kinematics, workpiece dimension, workpiece hardness, and variation in cutting force, friction in cutting zone, chip formation and accelerations of the cutting tool etc.

8. RSM technique has been successfully used by various researchers for developing regression models for prediction of T, R_a, and MRR etc. Multi-objective optimization techniques like T-GRA and T-TOPSIS and Taguchi's single objective optimization techniques have been applied by many researchers in receipt of optimized cutting process parameters in order to obtain better output responses like: T, R_a, and MRR in various end milling processes.

9. Ample works have been seen in literature on T, R_a and MRR for end milling process of various types of aluminium alloys, but no work has been reported for predicting T, R_a and MRR in BS L168 aluminium alloy to the best of author's knowledge. It has been extensively used for components subjected to highly stressed and fluctuating loads such as: aircraft fuselage parts, aircrafts fittings, missile parts and various other aerospace, defence applications. Hence prediction of T, R_a and MRR for this grade is also vital.

10. The empirical models and regression models were developed for CNC end milling process, but no models were noticed for predicting R_a, T and MRR in progressive feed end milling process of BS L168 aluminium alloy.

CHAPTER 3

THEORY AND EXPERIMENTATION

3.1 INTRODUCTION

This chapter explains about how the progressive feed machining works in end milling of BS L168 work material. Further it offers the particulars about experimental arrangements used to perform the machining experiments on test specimens, experimental procedures and details considered for the present research work. Different kinds of measuring equipment used for measuring or calculating various end milling performance characteristics and their procedures have been explained. The output responses measured are MRR, surface roughness, cutting tool tip temperature, surface topography and chip morphology.

3.2. CONSTANT FEED MACHINING

The machining feed is a cutting velocity, at which the cutter was fed against the work sample material. Range of feed rate generally will be decided based on the type of machine tool and cutting tools used, surface finish desired, power available at the spindle, tool setup, rigidity of the machine tool, material strength and machinability of workpiece material (Ojolo et al. 2015). Feed rate was considered to be an important cutting parameter which will have more influence on the output process performance characteristics such as: surface finish of the machined components, cutting temperature, cutting tool tip temperature, MRR, surface topography and chip morphology etc.

For a milling machine where multi fluted cutting tools are involved, the desirable feed rate becomes dependent on the number of cutting teeth of the cutter in addition to amount of material to be removed per tooth per cut. Greater the number of cutting edges, higher is the feed rate permissible as it will remove more and more material effectively rather than to rub. Rubbing of tool over the workpiece may cause larger heat generation, chattering and

consequences are bad surface finish, less tool life due to excess temperature on the cutting tool tip, tool wear and finally poor product quality.

3.2.1 Cutting parameters for constant feed machining

Range of cutting parameters, their symbols and values for constant feed machining (CFM) are displayed in Table 3.1. The range of cutting parameters were chosen by considering the machine tool capacity as well as limiting conditions of the machine tool like maximum spindle speed and feed rate. Range of parametric values considered by the researchers in the literature and machine tool manufactures catalogue data. Finally, by performing trial experiments on BS L168 work material within the aforesaid range of cutting factors as depicted in Table 3.1.

Table 3.1 Machining parameters for constant feed machining

Cutting Parameter	**Symbol**	**Unit**	**Level 1**	**Level 2**	**Level 3**
Cutting speed	s_c	RPM	2000	3000	4000
Feed rate	f_c	mm/min	200	400	600
Depth of cut	d_c	mm	0.75	1.5	2.25

3.3. PROGRESSIVE FEED MACHINING

An attempt has been made to adopt a novel concept called progressive feed machining (PFM) in the present research work. Usually, when we are writing CNC part program a constant feed rate will be chosen for a given cut-segment. When the machine tool controller executes part program one block at a time or block by block, there exists a time delay between executions of two successive blocks. This leads to stop and go fashion of tool movement while machining. Due to this nature of cutting tool movement, at the start of every cut-segment and where there is a change in cut direction the tool starts from stationary position with a feed rate of ZERO mm/min and accelerates to the intended feed rate (f) instantly. This might lead to sudden increase in cutting force due to sudden impact of cutting tool with the

workpiece; consequences are sudden impact of cutting tool with workpiece, high cutting force, high cutting temperature, high cutting tool tip temperature in-turn high tool wear, high surface roughness and finally poor product quality.

Instead of that, if the feed rate increases progressively to the intended feed rate (*f*) at the start and where there is a change in the cut direction, these ill effects can be minimized to the safe level and/or can be eliminated to the maximum extent. In progressive feed type of machining, feed rate increases step by step until cutting tool travels through a distance equal to its diameter, after that it travels with an intended predetermined feed rate (*f*).

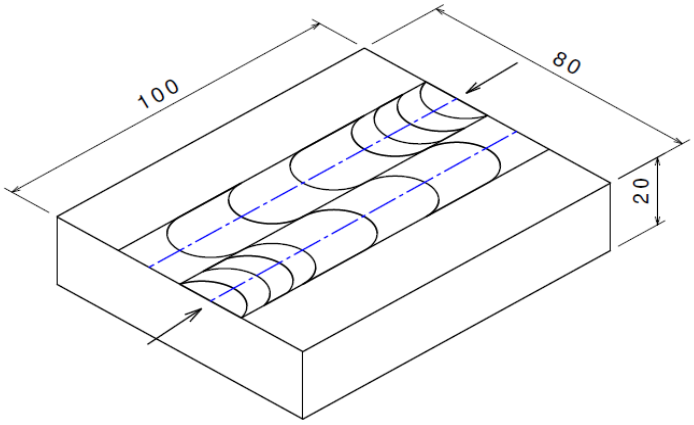

Figure 3.1 Concept of progressive feed rate with three steps

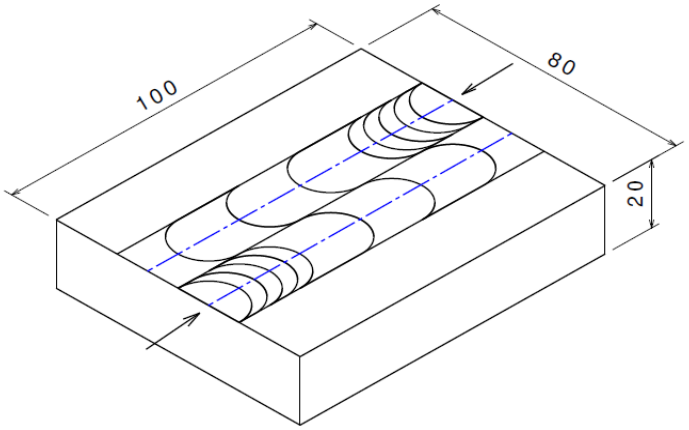

Figure 3.2 Concept of progressive feed rate with four steps

The idea of PFM with three steps and four steps was illustrated diagrammatically at Figure

3.1 and Figure 3.2 for milling and at Figure 3.3 and Figure 3.4 for turning operations respectively. In the present research work, author had considered and adopted progressive feed machining for machining through end milling operation on BS L168 aluminium alloy.

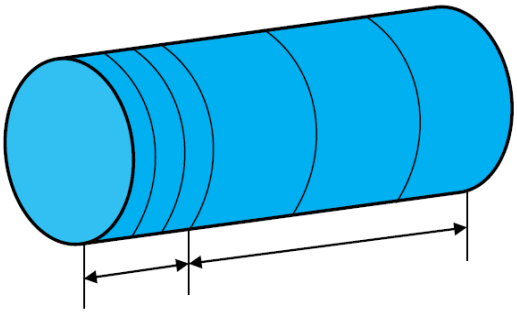

Figure 3.3 Concept of progressive feed rate with three steps (Turning)

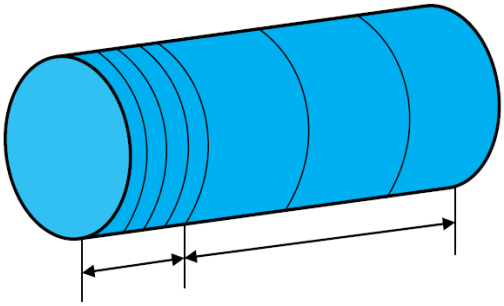

Figure 3.4 Concept of progressive feed rate with four steps (Turning)

3.3.1 Calculation of 'Step Distance' for progressive feed machining

The following equation 3.1 will be used for calculating step distance (l). It is equal to diameter of the end mill divided by number of steps chosen based on desired smooth start of the cut. If a greater number of steps considered more smooth start is possible.

$$l = \frac{D}{n} \quad \ldots\ldots\ldots\ldots \quad (3.1)$$

Where, l = Step distance, D = Cutter diameter, n = Number of steps through which feed rate is to be increased to reach the stipulated intended feed rate (f).

20mm diameter carbide solid end mills with two flutes have been chosen for this study with a nose radius of 0.8mm and rake angle of 16^0. Once the tool starts moving from its stationary position and after reaching a distance equal to its diameter (i.e 20mm), it will be fully engaged with the workpiece and hence there exists a firm support between tool and workpiece. Therefore, tool will be allowed to move with an intended feed rate of fmm/min and this 20mm would be considered as progressive feed zone. That means feed rate will be increased step by step through this distance of 20mm in a pre-determined number of steps (Eg: three, four or even more/less based on the requirement), thereafter it will travel with an intended feed rate of fmm/min. In the current research work, author has considered a four-step increase of feed rate (Table 3.2) with 30% of starting feed rate at level one, with 25% of starting feed rate at level two and with 20% of starting feed rate at level three as a case study.

Table 3.2 Machining parameters for progressive feed rate

Cutting Parameters	**Symbols**	**Units**	**Levels**		
Spindle speed	s_p	RPM	2000	3000	4000
Depth of cut	d_p	mm	0.75	1.5	2.25
Progressive feed rate	f_p	mm/min	200	400	600
Starting % of feed rate ($f = f_c$)	x	mm/min	30%	25%	20%

3.3.2 Calculation of increase in feed rate per 'step'.

The following equation 3.2; is intended to be used to determine increase in feed rate per step for proposed progressive feed machining.

$$f_s = \frac{f - f_0}{n} \text{mm/min} \quad \ldots\ldots\ldots\ldots\ldots\ldots (3.2)$$

Where, f_s = Increase in feed rate per step, f= Intended feed, f_0= Starting feed rate, $\boldsymbol{x}$ =starting % of feed rate ($\boldsymbol{x}$ = 30% of f or 25% of f, or 20% of f, at level one, level two and

level three respectively) and n = number of steps (four in this case). For example, when the intended feed rate is 200mm/min as in level one (Table 3.3), 'x' is 30% of 200mm/min, which is 60mm/min; this value will be taken as starting feed rate. The balance 140(200-60) mm/min is divided into four steps, with an equal step increase of 35mm/min (140/4), which gives the values of 60, 95,130,165 and then reaches the indented pre-set feed rate of 200mm/min. That means, feed rate increases progressively from '0' to '60'mm/min, '60' to '95'mm/min, '95' to '130'mm/min, '130' to '165'mm/min and finally from '165' to '200'mm/min step by step.

If the starting feed rate taken as 20% of intended feed (200mm/min) as in Table 3.4, it will be 40mm/min (20% of 200). The balance 160(200-40) mm/min is divided into four steps with an equal step distance of 40mm/min (160/4), which gives the values of 40, 80, 120, 160 and then reaches the intended feed rate of 200mm/min. In the same way for all the feed levels, percentage of starting feed rate and corresponding step values of feed rate have been calculated and tabulated in Table 3.3 and Table 3.4.

Even more combinations of percentage of starting feed rates can be considered as shown from Table 3.5 to Table3.10 based on the cutting tool and workpiece material combinations. Progressive feed rate steps calculated using equation 3.1 and equation 3.2 have been depicted from Table 3.3 to Table 3.10.

Table 3.3 Feed rate steps for PFM with four steps & 30%, 25%, 20% of starting feed rate *f*

Levels	**Feed rate (f_p) mm/min**					
	Starting % of feed rate	**Step 1**	**Step 2**	**Step 3**	**Step 4**	**Beyond Steps**
Level 1	30% of 200	60	95	130	165	200
Level 2	25% of 400	100	175	250	325	400
Level 3	20% of 600	120	240	360	480	600

Table 3.4 Feed rate steps for PFM with four steps & 20%, 25%, 30% of starting feed rate *f*

Levels	Feed rate (f_p) mm/min					
	Starting % of feed rate	**Step 1**	**Step 2**	**Step 3**	**Step 4**	**Beyond Steps**
Level 1	20% of 200	40	80	120	160	200
Level 2	25% of 400	100	175	250	325	400
Level 3	30% of 600	180	285	390	495	600

Table3.5 Feed rate steps for PFM with four steps & 25%, 20%, 15% of starting feed rate *f*

Levels	Feed rate (f_p) mm/min					
	Starting % of feed rate	**Step 1**	**Step 2**	**Step 3**	**Step 4**	**Beyond Steps**
Level 1	25% of 200	50	87.5	125	162.5	200
Level 2	20% of 400	80	160	240	320	400
Level 3	15% of 600	90	217.5	345	472.5	600

Table 3.6 Feed rate steps for PFM with four steps & 15%, 20%, 25% of starting feed rate *f*

Levels	Feed rate (f_p) mm/min					
	Starting % of feed rate	**Step 1**	**Step 2**	**Step 3**	**Step 4**	**Beyond Steps**
Level 1	15% of 200	30	72.5	115	157.5	200
Level 2	20% of 400	80	160	240	320	400
Level 3	25% of 600	150	262.5	375	487.5	600

Table 3.7 Feed rate steps for PFM with three steps & 30%, 25%, 20% of starting feed rate *f*

Levels	Feed rate (f_p) mm/min				
	Starting % of feed rate	**Step 1**	**Step 2**	**Step 3**	**Beyond Steps**
Level 1	30% of 200	60	106.67	153.34	200
Level 2	25% of 400	100	200	300	400
Level 3	20% of 600	120	213.34	306.68	600

Table 3.8 Feed rate steps for PFM with three steps & 20%, 25%, 30% of starting feed rate *f*

Levels	Feed rate (f_p) mm/min				
	Starting % of feed rate	Step 1	Step 2	Step 3	Beyond Steps
Level 1	20% of 200	40	93.33	146.67	200
Level 2	25% of 400	100	200	300	400
Level 3	30% of 600	180	320	460	600

Table 3.9 Feed rate steps for PFM with three steps & 25%, 20%, 15% of starting feed rate *f*

Levels	Feed rate (f_p) mm/min				
	Starting % of feed rate	Step1	Step 2	Step 3	Beyond Steps
Level 1	25% of 200	50	100	150	200
Level 2	20% of 400	80	186.67	293.34	400
Level 3	15% of 600	90	260	430	600

Table 3.10 Feed rate steps for PFM with three steps & 15%, 20%, 25% of starting feed rate *f*

Levels	Feed rate (f_p) mm/min				
	Starting % of feed rate	Step 1	Step 2	Step 3	Beyond Steps
Level 1	15% of 200	30	86.67	134.34	200
Level 2	20% of 400	80	186.67	293.34	400
Level 3	25% of 600	150	300	450	600

3.4 WORK MATERIAL DETAILS

BS L168 aluminium alloy is an extensively used material in high technology applications like aerospace, defence and automotive fields due to its excellent mechanical properties like high mechanical strength with good machinability. It is especially suitable for production of difficult, complicated& intricate shaped machining components used in aerospace and defence applications, especially in fighter aircrafts fuselage and wing parts. It is used for

critical applications and is commonly used in spacecraft or fighter aircraft structural components subject to high range of fatigue loads, high level of tensile and compressive loads, subjected vibrations. It has very good machinability and thus used for fabrication of intricate and multi-faceted parts by means of CNC machining. But corrosion resistance of this alloy is poor, particularly when exposed to water or salt.

Size of work samples (Figure 3.5) considered for conducting the experiments are: 100mm x80mm x20mm. Test samples have been prepared from a single billet of BS L168 aluminium alloy to have alike property all over the test coupon. The chemical configuration of the work sample materials is shown in Table3.11, were confirmed by spectroscopy. Mechanical and physical properties of the material are given in Table 3.12. Work sample after performing machining have been depicted in Figure 3.6.

Table 3.11 Chemical composition of BS L168

Major Elements	**Cu**	**Mn**	**Si**	**Mg**	**Fe**	**Zn**	**Ti+Zr**	**Ti**	**Cr**	**Ni**	**Al**	**Others**
Min	3.9	0.4	0.5	0.2	0	0	0	0	0	0	Balance	0
Max	5	1.2	0.9	0.8	0.5	0.25	0.2	0.15	0.1	0.1		0.15

Table 3.12 Physical properties of BS L168 aluminium alloy

Property	**Value**
Density	2.80 g/cm^3
Melting Point	640 ^{0}C
Thermal Expansion	22.8 X 10^{-6} /K
Modulus of Elasticity	73 GPa
Thermal Conductivity	155 W/m.K
Electrical Resistivity	40 % IACS

Figure 3.5 Work samples used for machining before machining

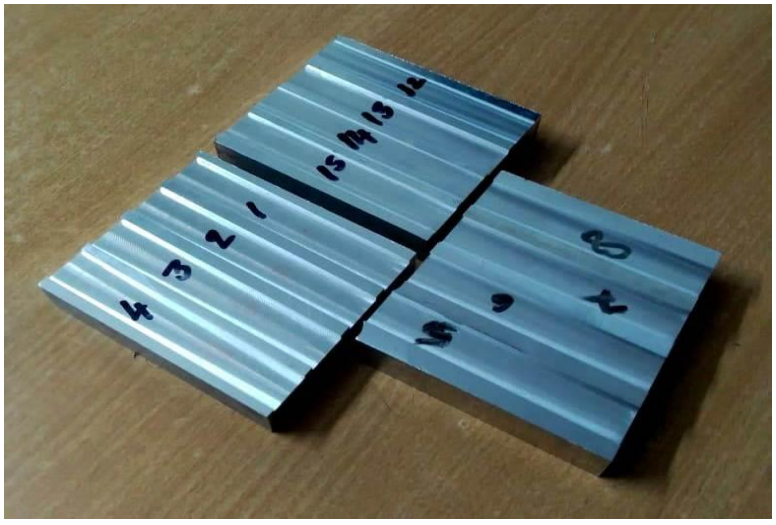

Figure 3.6 Work samples after machining

3.5 CUTTING TOOL DETAILS

X-PM16807-2000 carbide solid end mill cutter of 20mm diameter, with two flutes made by Precision measuring instruments Co., have been used for this purpose (Figure3.7). Two types of tungsten carbide end mills: coated (TiAlN), and uncoated with two flutes are used. The coating on the tool is made with PVD technique and had a thickness of 2.5 to 3μm. For OFAT experimentation three numbers of different radii end mills with 0.4mm, 0.8mm and 1.2mm with a constant rake angle of 16^0.

Figure 3.7 Solid carbide end mill cutter with two flutes

3.6 MACHINE TOOL DETAILS

Figure 3.8 AMS MCV–450 Vertical milling machine

AMS make MCV-450 model, three axes CNC vertical machining centre shown in Figure 3.8, used for conducting experiments. It is a three axes CNC vertical milling centre. Major specifications of the machine tool are as follows: Axis travel: X-800mm, Y-450mm, Z-500mm, Maximum spindle speed-6000rpm; Maximum feed rate-10m/min; Basic power supply-18kVA, Positional accuracy-0.015mm, Repeatability ±0.005mm. Dry machining condition (Figure 3.9) has been chosen in order to understand the clear-cut effect of input

cutting parameters on the performance characteristics.

Figure 3.9 Dry machining condition

3.7 MEASURING INSTRUMNETS

3.7.1 Surface roughness measuring instrument

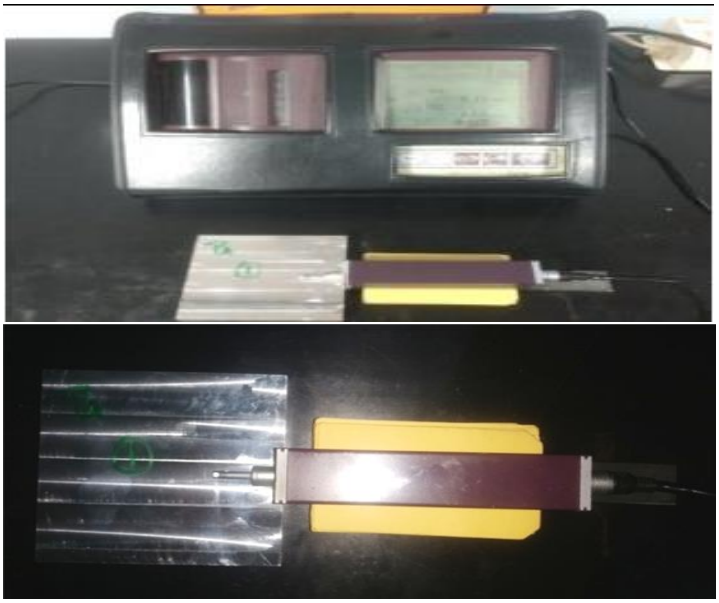

Figure 3.10 Mitutoyo Surftest SJ-301surface roughness tester

Mitutoyo Surftest SJ-301surface roughness tester (Figure 3.10) has been used to measure surface roughness by taking average of three readings, taken at three different locations on the machined surface of test specimens after each experimental run. It measures surface roughness with high accuracy and a wide range of 300µm.

3.7.2 Cutting tool tip temperature measuring instrument

Figure 3.11 Contactless industrial infrared digital thermometers

Figure 3.12 Cutting tool tip temperature measurement

HTC make industrial infrared digital non-contact thermometer (Figure 3.11) was used to measure the cutting tool tip temperature against each experimental run. Its temperature measuring range is -50^0C to $+550^0$C, accuracy is $\pm1^0$C and its response time is <500ms. Figure 3.12 shows the measurement of cutting tool tip temperature using industrial infrared

digital thermometer while conducting the experiments. Three reading have been taken from three different directions by focusing the laser on the tip of cutting tool. Then average of these three readings calculated and depicted in Table 4.3 of the chapter -4, for further analysis in the upcoming chapters.

3.7.3 Material removal rate measuring instrument

Essae DS-852 model digital weighing scale (Figure 3.13) has been used for measuring weight of the test pieces before and after machining. It is an ESSAE brand table top digital controller DS-852 model with weighing capacity of 5Kg maximum having an accuracy of 0.001gram. Each specimen has been weighted using afore said digital weighing machine before and after each experimental run of slot cutting.

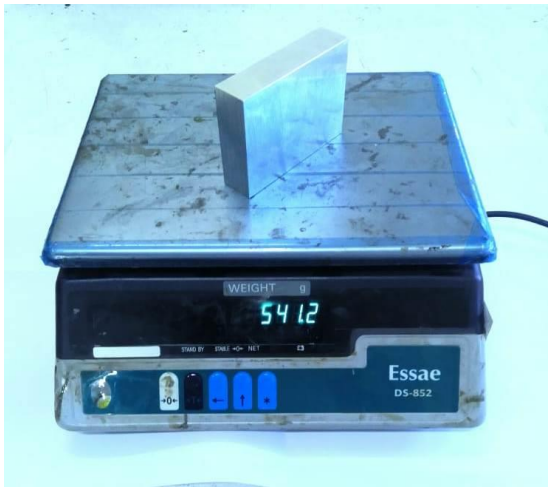

Figure 3.13 Weighing machine

MRR after each machining run has been calculated using weight loss method and computed from equation 3.3.

$$MRR = \frac{W_i - W_f}{t} \quad \text{..... (3.3)}$$

Where, W_i = Initial weight of the workpiece before machining (gm)

W_f = Final weight of the workpiece after machining (gm)

t = Total machining time (min)

3.8 METHODOLOGY AND EXPERIMENTAL DESIGN

3.8.1 Flow chart of research methodology

Methodology followed for the entire research work was briefly illustrated in the following flowchart (Figure 3.14).

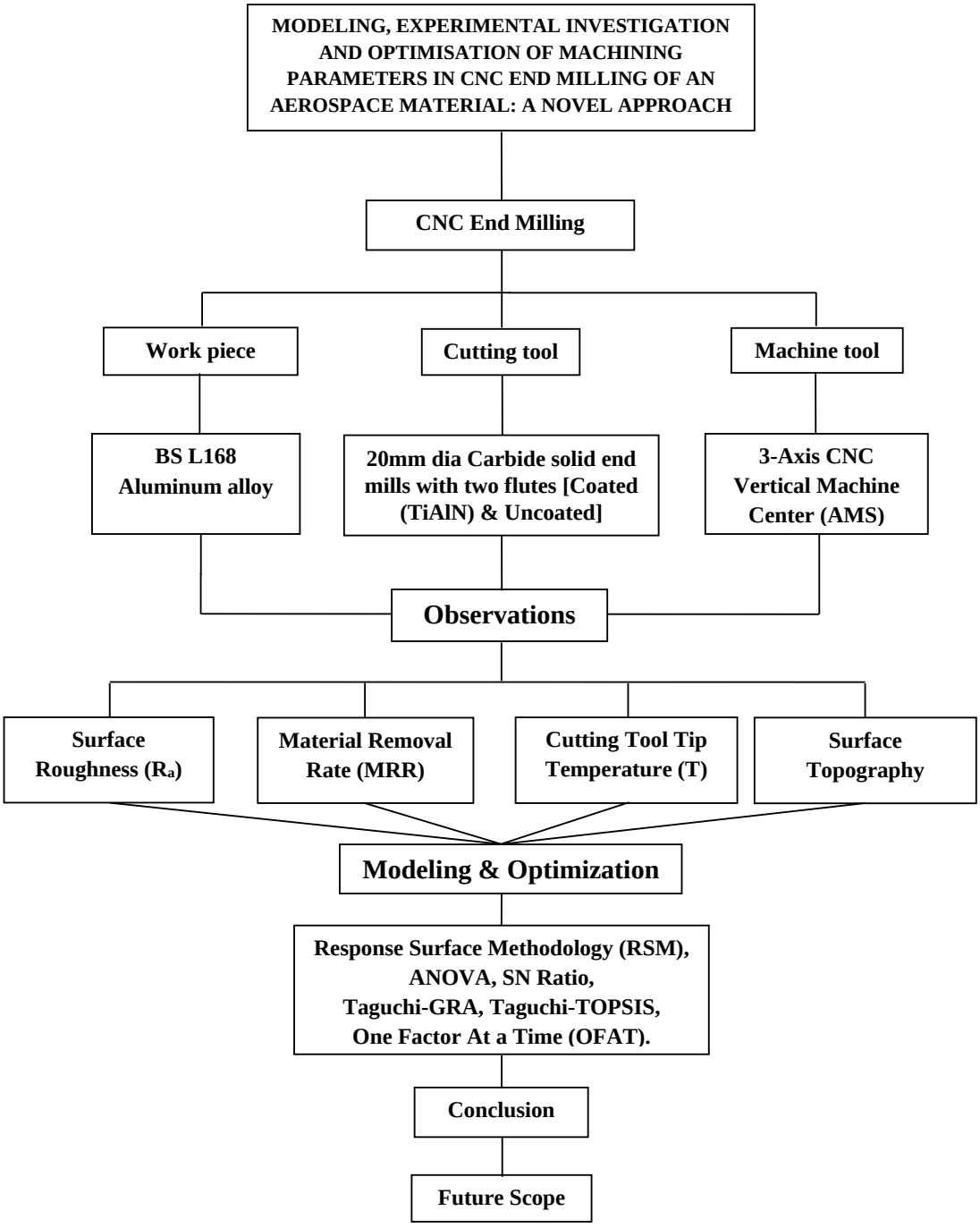

Figure 3.14 Flow chart for scheme of research work

Experiments were conducted according to L_9 orthogonal array for single-objective and multi-response optimization of performance characteristics. Single-objective optimisation was carried out through Taguchi's optimization technique and multi-objective optimisation by T-GRA, TOPSIS techniques. L_{27} orthogonal array has been followed for conducting the experiments for RSM based predictive modelling and design analysis. Further, fifteen number of experiments were conducted based on L_{15} table of One Factor at A Time (OFAT) approach to know the effect of each individual cutting process parameter on different end milling performance characteristics. Table 3.13 gives brief summary of experimental conditions used for this research work.

Table 3.13 Experimental conditions

Workpiece material and dimensions	BS L168 AL Alloy blocks, 100x80x20mm
Workpiece material chemical composition	Cu-4.21%, Mn-0.93%, Si-0.67%, Mg-7.76%, Fe-0.364%, Zn-0.298%, Ti-0.11% Cr-0.08%, Ni-0.78% and AL-Balance
Cutting tools used	TiAlN PVD coated KC5010 tungsten carbide end mills (An ISO designation of SNMG120408 MP), Kennametal made.
Machining environments	Dry (No coolant), Constant Feed Machining and Progressive Feed Machining
Cutting tool nose radii used	0.4mm, 0.8mm and 1.2mm
Machine tool used	AMS MCV-450 model, three axes CNC vertical milling machining centre

3.8.2 Experimental Designs

3.8.2.1 Taguchi L_9 Orthogonal Array (OA) design for optimization

Experiments have been conducted as per Taguchi's L_{27} orthogonal array (OA) design for modelling of the machining process parameters. And Taguchi's L_9 orthogonal array has been followed for multi-objective optimization studies of performance characteristics through T-

GRA and T-TOPSIS techniques. Since, it minimizes the number of experiments required, and with that the reduction in experimental cost and effort (Montgomery, 1987). The minimum number of experiments required to be conducted through Taguchi's OA given by the following equation -3.4.

$$(N_{min}) = (L-1) * F + 1 \quad \ldots\ldots\ldots\ldots\ldots \quad (3.4)$$

Where, N_{min}= minimum number of experiments required to be conducted.

F = number of controllable factors.

L = number of levels taken for each controllable factor.

Table 3.14 Taguchi L_9 Orthogonal Array design

Exp run	**Controllable process parameters**		
	Cutting speed (*s*)RPM	**Cutting feed (*f*)mm/min**	**Depth of cut (*d*)mm**
1	*s1*	*f1*	*d1*
2	*s1*	*f2*	*d2*
3	*s1*	*f3*	*d3*
4	*s2*	*f1*	*d2*
5	*s2*	*f2*	*d3*
6	*s2*	*f3*	*d1*
7	*s3*	*f1*	*d3*
8	*s3*	*f2*	*d1*
9	*s3*	*f3*	*d2*

As per Taguchi's design concept L_9orthogonal array (Table 3.14) has been designated for studying ANOVA and multi-objective optimization problem using optimization techniques like Taguchi based GRA and Taguchi coupled TOPSIS. Means of mean plots, ANOVA results and means of S/N ratio plots were obtained with the help of Minitab-18 statistical analysis software. And have been presented for both traditional CFM as well as proposed PFM in the forthcoming discussions.

3.8.2.2 Experimental plan of OFAT approach

Table 3.15 One Factor at A Time (OFAT) experimental design

Exp. run	Controllable process parameters		
	Cutting speed (*s*) RPM	**Feed rate (*f*) mm/min**	**Depth of cut (*d*) mm**
1	***s1***	*f3*	*d3*
2	***s2***	*f3*	*d3*
3	***s3***	*f3*	*d3*
4	***s4***	*f3*	*d3*
5	***s5***	*f3*	*d3*
6	*s3*	***f1***	*d3*
7	*s3*	***f2***	*d3*
8	*s3*	***f3***	*d3*
9	*s3*	***f4***	*d3*
10	*s3*	***f5***	*d3*
11	*s3*	*f3*	***d1***
12	*s3*	*f3*	***d2***
13	*s3*	*f3*	***d3***
14	*s3*	*f3*	***d4***
15	*s3*	*f3*	***d5***

OFAT approach of experimentation will be used to analyse the influence of each individual cutting process parameter on the machining performance characteristics. In this approach of machining one controllable factor will be varied keeping other controllable factors as constant at their respective mean levels. The controllable process parameters and their levels considered for performing experiments are shown in Table 3.15. In the literature, several researchers have considered and used this OFAT approach of experimental design in their works (Sharma et al. 2015; Manjaiah et al. 2016; Manna 2013).

Table 3.16 Milling process parameters and their levels for OFAT experimentation

Process Parameters	**Symbol**	**Unit**	**Level 1**	**Level 2**	**Level 3**	**Level 4**	**Level 5**
Cutting speed	*s*	rpm	2000	2500	3000	3500	4000
Cutting speed	*s*	m/sec	2.093	2.617	3.14	3.663	4.187
Cutting speed	*s*	m/min	125.6	157	188.4	219.8	251.2
Feed rate	*f*	mm/min	200	300	400	500	600
Feed rate	*f*	mm/rev	0.1	0.12	0.1333	0.143	0.15
Feed rate (Two tooth)	*f*	mm/tooth	0.05	0.06	0.067	0.0714	0.075
Feed rate	*f*	mm/sec	3.333	5	6.667	8.333	10
Depth of cut	*d*	mm	0.75	1.125	1.5	1.875	2.25

Table 3.15 depicts the OFAT design of experimentation indicating *s3, f3* and *d3* as mean levels of the feed rate (*f*) cutting speed (*s*), and depth of cut (*d*) respectively. Five experiments (from experiment ONE to experiment FIVE) will be conducted by varying the cutting speed (*s*) from '*s1'* to '*s5'* keeping other two cutting parameters: feed rate(*f*) and depth of cut(*d*) constant at their mean levels '*f3*' and '*d3*' respectively. Next five experiments (from experiment SIX to experiment TEN) will be conducted by varying the feed rate (*f*) from '*f1'* to '*f5'* by keeping other two cutting parameters: cutting speed (*s*) and depth of cut(*d*) constant at their mean levels '*s3*' and '*d3*' respectively. Similarly, five more experiments (from experiment ELEVEN to experiment FIFTEEN) will be conducted by varying the depth of cut (*d*) from '*d1'* to '*d5'* by keeping other two cutting parameters: feed rate (*f*) and cutting speed (*s*) constant at their mean levels '*s3*' and '*f3*' respectively.

Three types of solid end milling cutters with nose radii of 0.4mm, 0.8mm and 1.2mm have been used for this purpose. The range of cutting process parameters and their levels for

OFAT approach of experimentation was finalized based on the tool manuals, available literature and by conducting multiple number of preliminary trial experimental runs. End milling experiments were performed on BS L168 aluminium alloy of size 100mm x80mm x20mm test specimens.

The investigative machinability characteristics considered for the analysis through these experiments are: cutting tool tip temperature, surface roughness and material removal rate. In order to get smooth graphs and better illustration of variation of performance characteristics five levels of cutting process parameters were considered as depicted in the Table 3.16. The various machining process parameters in five levels is as follows: cutting speed varies from 2000rpm (2.094m/sec) to 4000rpm (4.188m/sec) feed rate varies from 200mm/min (0.1mm/rev) to 400mm/min (0.15mm/rev) and depth of cut varies from 0.75mm to 2.25mm.

3.8.2.3 Experimental plan through L_{27} Orthogonal Array (OA) for RSM

In the present work of experimental plan of RSM, L_{27} orthogonal array (OA) was employed by taking into account of three factors: cutting speed (*s*), feed rate (*f*) and depth of cut (*d*) at three levels of each factor as shown in Table 3.17. Second order polynomial model is the most widely used in RSM model due to its flexibility and easiness in estimating the process parameters.

Here also, the range of cutting process parameters and their levels for experimentation as per Taguchi's orthogonal array (OA) were finalized based on the tool manuals, literature available and by conducting preliminary trial experimental runs. Total twenty-seven numbers of experiments were conducted with different combinations of cutting process parameters, and against each experimental run performance characteristics were measured and then analysed further in the forthcoming chapters.

Table 3.17 RSM based L_{27} orthogonal array

Exp run	**Taguchi L_{27} orthogonal array**												
	A	**B**	**C**	**D**	**E**	**F**	**G**	**H**	**J**	**K**	**L**	**M**	**N**
1	1	1	1	1	1	1	1	1	1	1	1	1	1
2	1	1	1	1	2	2	2	2	2	2	2	2	2
3	1	1	1	1	3	3	3	3	3	3	3	3	3
4	1	2	2	2	1	1	1	2	2	2	3	3	3
5	1	2	2	2	2	2	2	3	3	3	1	1	1
6	1	2	2	2	3	3	3	1	1	1	2	2	2
7	1	3	3	3	1	1	1	3	3	3	2	2	2
8	1	3	3	3	2	2	2	1	1	1	3	3	3
9	1	3	3	3	3	3	3	2	2	2	1	1	1
10	2	1	2	3	1	2	3	1	2	3	1	2	3
11	2	1	2	3	2	3	1	2	3	1	2	3	1
12	2	1	2	3	3	1	2	3	1	2	3	1	2
13	2	2	3	1	1	2	3	2	3	1	3	1	2
14	2	2	3	1	2	3	1	3	1	2	1	2	3
15	2	2	3	1	3	1	2	1	2	3	2	3	1
16	2	3	1	2	1	2	3	3	1	2	2	3	1
17	2	3	1	2	2	3	1	1	2	3	3	1	2
18	2	3	1	2	3	1	2	2	3	1	1	2	3
19	3	1	3	2	1	3	2	1	3	2	1	3	2
20	3	1	3	2	2	1	3	2	1	3	2	1	3
21	3	1	3	2	3	2	1	3	2	1	3	2	1
22	3	2	1	3	1	3	2	2	1	3	3	2	1
23	3	2	1	3	2	1	3	3	2	1	1	3	2
24	3	2	1	3	3	2	1	1	3	2	2	1	3
25	3	3	2	1	1	3	2	3	2	1	2	1	3
26	3	3	2	1	2	1	3	1	3	2	3	2	1
27	3	3	2	1	3	2	1	2	1	3	1	3	2

3.9 CLOSURE

This chapter gives details about workpiece material (BS L168 aluminium alloy) chemical composition and physical properties. It is explained about two types machining CFM and proposed PFM on end milling machines. It also explains about how to implement proposed PFM through part programming in detail through illustrations. Different equipment's and their speculations used for conducting the experiments as well as different instruments used for measuring output performance characteristics of end milling with their measuring procedures are explained with corresponding photographs. Different types of experimental designs and procedures followed to conduct the experimentation like Taguchi's orthogonal arrays like L_9 and L_{27} and L_{15}table formats used for optimisation, modelling and OFAT approach of experimentation respectively have been given. Further, explains about experimental methodology and design with the help of a flow chart.

CHAPTER 4

MODELLING OF END MILLING PROCESS

4.1 INTRODUCTION

RSM has been discussed and used for modelling and analysis of machining performance characteristics in the present chapter. It is divided into two stages while doing end milling process on BS L168 aluminium alloy with proposed PFM and existing CFM. In the first stage, correlation models have been established between the input process parameters and output machining performance characteristics and then these models were validated by means of ANOVA and model fitness plots. Whereas, in the second stage, the direct and interaction effects of process parameters on end milling performance responses was studied and analysed with the help of established two dimensional and three-dimensional plots by means of Minitab-18 interface.

In any machining process there will be two or more process variables that are inherently related and it is necessary to explore the nature of their relationship. When user wants to find the set of input machining process parameters for a desired output, say for a particular value of surface roughness, it is difficult to directly interpret from the raw data obtained through experimentation without further processing. Therefore, to enable this, predictive models have been proposed and developed related to process parameters with the output response. Such a model developed can be used to predict the values of input cutting parameters at which we will achieve the desired output response. It is possible to control the process as per requirement and also it is possible to optimize the process for better output results.

4.2 EXPERIMENTATION

Process parameters and their levels considered for the present experimental work have been shown in Table 4.1 and Table 4.2, both for CFM and PFM respectively. Experiments were accomplished according to L_{27} orthogonal array-based face centred central composite design

and analysis was performed using Minitab -18 statistical analysis software based on RSM. Experimental results of performance characteristics obtained from the performed experiments are show in Table 4.3 for further analysis in the forthcoming sections.

Table 4.1 Control factors and their levels

Cutting parameters	Unit	Level 1	Level 2	Level 3
Cutting speed (s)	rpm	2000	3000	4000
Depth of cut (d)	mm	0.75	1.5	2.25
Feed rate (f)	mm/ min	200	400	600
Starting % of (f) in PF machining (X)	mm/ min	30% (60)	25% (100)	20% (120)

Table 4.2 Feed rate steps for progressive feed machining

Levels	Feed rate mm/min					
	Starting % of feed mm/min	Step 1	Step 2	Step 3	Step 4	Beyond Steps
1	30% of 200	60	95	130	165	200
2	25% of 400	100	175	250	325	400
3	20% of 600	120	240	360	480	600

4.3 RESPONSE SURFACE METHODOLOGY

RSM develops the regression mathematical equations using a statistical analysis for predicting the relationship between the independent input process variables and dependent output performance characteristics (Montgomery, 1987). It also explains the direct and interaction effect of process parameters on machining performance responses. Equation 4.1 gives the relation between independent input variables and dependent output variables.

$$y = f(X, Y, Z) \quad \ldots\ldots\ldots\ldots\ldots \quad (4.1)$$

Table 4.3 Experimental results from constant feed and progressive feed machining with coated and uncoated cutting tools

Exp Run No	*Depth of cut*	*Cutting speed*	*Feed rate*	*% of SFR*	*Constant feed machining (CFM)*						*Progressive feed machining (PFM)*					
	mm	*rpm*	*mm/ min*	%	Uncoated cutting tool			Coated cutting tool			Uncoated cutting tool			Coated cutting tool		
	D/d	*V/S/v/s*	*F/f*	*X*	T_{CU} ^{o}C	*Racu µm*	*MRRacu mm3/sec*	T_{CC} ^{o}C	*Racc µm*	*MRRacc mm3/sec*	T_{PU} ^{o}C	*Rapu µm*	*MRRapu mm3/sec*	T_{PC} ^{o}C	*Rapc µm*	*MRRapc mm3/sec*
1	0.75	2000	200	30	42.6	0.64	47.49	38.1	0.57	47.48	39.5	0.50	43.65	35.2	0.43	44.64
2	0.75	2000	400	25	44.3	0.83	92.19	39.9	0.71	92.20	41.8	0.68	84.82	37.8	0.57	84.66
3	0.75	2000	600	20	51.8	1.01	145.69	46.3	0.84	145.68	48.2	0.90	134.22	43.9	0.79	135.21
4	0.75	3000	200	30	43.3	0.51	49.75	37.5	0.43	49.70	39.4	0.40	45.87	34.4	0.32	46.27
5	0.75	3000	400	25	49.7	0.75	94.27	45.0	0.67	94.76	46.7	0.59	86.87	41.7	0.51	87.45
6	0.75	3000	600	20	59.2	0.92	147.40	54.1	0.83	147.63	56.3	0.78	135.84	50.8	0.66	136.40
7	0.75	4000	200	30	46.2	0.41	50.17	41.6	0.37	50.36	42.6	0.33	46.19	36.5	0.29	45.87
8	0.75	4000	400	25	52.7	0.67	96.72	48.2	0.56	96.57	49.1	0.53	88.98	45.1	0.45	89.24
9	0.75	4000	600	20	59.4	0.83	150.87	55.4	0.74	150.74	55.9	0.68	138.72	51.6	0.59	139.46
10	1.50	2000	200	30	51.3	0.57	93.13	45.9	0.49	93.33	46.7	0.46	85.63	43.3	0.42	85.87
11	1.50	2000	400	25	58.7	0.76	193.13	53.8	0.66	192.99	54.8	0.62	177.79	51.2	0.53	178.45
12	1.50	2000	600	20	63.6	0.95	289.78	59.2	0.84	289.54	59.7	0.78	265.87	56.7	0.67	267.78
13	1.50	3000	200	30	53.5	0.52	95.41	48.5	0.47	95.28	50.3	0.42	87.54	46.5	0.34	88.61
14	1.50	3000	400	25	58.6	0.67	195.32	54.7	0.59	195.54	55.0	0.52	178.52	50.7	0.49	180.47
15	1.50	3000	600	20	64.3	0.86	292.41	60.1	0.75	292.72	60.7	0.72	268.42	56.8	0.65	270.49
16	1.50	4000	200	30	54.7	0.42	97.98	51.2	0.36	97.62	50.8	0.34	89.78	46.2	0.28	90.78
17	1.50	4000	400	25	60.1	0.58	197.52	55.8	0.52	197.69	56.9	0.47	181.65	52.8	0.43	182.34
18	1.50	4000	600	20	69.1	0.76	294.52	63.2	0.67	294.18	65.7	0.61	270.25	61.2	0.54	272.48
19	2.25	2000	200	30	64.9	0.51	131.27	59.6	0.43	131.56	61.2	0.42	120.77	56.6	0.35	121.78
20	2.25	2000	400	25	74.5	0.71	282.43	70.2	0.64	282.68	71.5	0.57	260.47	66.7	0.48	261.57
21	2.25	2000	600	20	81.2	0.90	441.21	77.3	0.78	441.52	77.8	0.71	406.98	73.3	0.63	407.89
22	2.25	3000	200	30	66.4	0.43	133.52	61.9	0.36	133.47	62.4	0.36	123.76	58.5	0.32	124.12
23	2.25	3000	400	25	75.6	0.60	289.75	70.7	0.51	289.44	72.6	0.47	265.32	68.2	0.43	267.97
24	2.25	3000	600	20	82.3	0.82	444.62	77.2	0.72	444.42	78.9	0.64	411.76	74.5	0.55	412.06
25	2.25	4000	200	30	69.8	0.34	135.25	64.8	0.31	135.72	66.1	0.28	123.84	61.3	0.25	124.54
26	2.25	4000	400	25	78.7	0.54	297.23	73.6	0.47	297.43	75.8	0.42	272.86	71.8	0.36	272.16
27	2.25	4000	600	20	87.2	0.74	447.29	83.1	0.64	447.75	83.7	0.58	411.63	79.7	0.54	412.83

Where, ‘y’ is the desired output response. It is a function (*f*) of some independent variables X, Y and Z. Function (*f*) was fitted according to second-order polynomial regression equation / model and it is also termed as quadratic model. It is represented by the following equation 4.2.

$$y = \alpha_0 + \sum_{i=1}^{3} \alpha_i x_i + \sum_{i=1}^{3} \alpha_{ii} x_i^2 + \sum_{i<j}^{3} \alpha_{ij} x_i x_j \ldots\ldots\ldots \quad (4.2)$$

Where,α_0:Indicates an interceptor constant, andα_i,α_{ii} and $\alpha_{ij}$are the correspondingcoefficients oflinear, quadratic and cross-product terms in the regression equation 4.2 respectively. Here, $x_i$denotes the coded variables that correspond to the cutting parameters considered in the present study. Equations (4.3), (4.4) and (4.5) are used to transform the considered cutting parameters into coded variables x_i= 1, 2, 3.

$$x_1 = \frac{A - A_0}{\Delta A} \quad \ldots\ldots\ldots\ldots\ldots (4.3)$$

$$x_2 = \frac{B - B_0}{\Delta B} \quad \ldots\ldots\ldots\ldots\ldots (4.4)$$

$$x_3 = \frac{C - C_0}{\Delta C} \ldots\ldots\ldots\ldots\ldots\ldots (4.5)$$

Where, the resultant coded values of cutting parameters A, B and C are: x_1, x_2 and x_3 respectively. And respective zero levels of cutting parameters of A, B and C are A_o, B_o and C_o respectively. Further ΔA, ΔB and ΔC denote the intervals of variation in A, B and ‘C’ respectively. In the present research work a quadratic model of function (*f*) has been selected as a fitted model to analyse the cutting tool tip temperature, surface roughness and MRR respectively.

4.4 RESULTS AND DISCUSSIONS

The effect of cutting parameters such as: cutting speed, feed rate and depth of cut on the performance characteristics of proposed PFM and existing CFM is studied with the help of two statistical methods: (1) Relationships among the factors by multiple linear regressions and then by (2) Analysis of Variance. Minitab-18 statistical analysis software has been used to analyse and to develop the quadratic regression models, through which the machining performance characteristics such as: R_a, T and MRR can

be predicted using input data obtained through the RSM experimental design (Table 4.3).

4.4.1 ANOVA outcomes

ANOVA is a statistical analysis method used to examine the design considerations and for establishing the significant input factor which affects the design model (Vasu and Nayaka 2018a). It is useful for understanding the input data and test results in a well-thought-out way from the DoE (Tien et al. 2019; Raneen et al. 2019). In this section the influence of controllable process parameters on output performance characteristics have been studied with the help of ANOVA. It is usually used to find the fitness level of the developed regression models as well as to find the percentage of influence of each cutting parameter on performance responses.

4.4.1.1 ANOVA outcomes for surface roughness (R_a)

Surface roughness values obtained from both CFM and PFM are depicted in Table 4.3 have been further analysed with the help of Minitab -18 interface in order to find the effect of individual input factors on the said performance characteristic R_a. The importance of the cutting parameter is concluded based on its P-value in ANOVA results; if the P-value attained is less than 0.05 then the parameters are consigned to be significant parameters. Table 4.4 and Table 4.5 shows the ANOVA results for surface roughness (R_a) of the work sample in CFM and PFM respectively. The last column of ANOVA table (Table 4.4), displays the percentage influence of each input process parameter on the total variation indicating degree of influence on the performance response R_a for CFM.

The percentage of influence of input factors on output response (R_a) in CFM is as follows: feed rate: 76.58%, cutting speed: 16.36% and depth of cut: 6.22% (Table 4.4). The interaction terms {(*s*f*: 0.00%), (*s*d*: 0.05%) and (*f*d*: 0.00%)} do not have much statistical significance on surface roughness since their P–values for these terms are more than the confidence level of 0.05. Residual error of model: 0.79%.

Table 4.4 ANOVA results for R_a with un-coated cutting tool with CFM

Source	DF	Seq SS	Adj SS	Adj MS	F-Value	P-Value	% of Contribution
Regression	6	0.85170	0.85170	0.14195	420.65	0.000	99.21%
s	1	0.14045	0.01479	0.01479	43.81	0.000	16.36%
f	1	0.65754	0.03151	0.03151	93.38	0.000	76.58%
d	1	0.05336	0.00413	0.00413	12.25	0.002	6.22%
*s*f*	1	0.00003	0.00003	0.00003	0.10	0.757	0.00%
*s*d*	1	0.00041	0.00041	0.00041	1.21	0.284	0.05%
*f*d*	1	0.00003	0.00003	0.00003	0.10	0.757	0.00%
RE	20	0.00675	0.00749	0.00034			0.79%
Total	26	0.85845					100.00%
Model summary: R^2 = 99.21%, R^2 (adj)=98.98%, R^2 (pred)= 98.53%							

Table 4.5 ANOVA results for R_a with un-coated cutting tool with PFM

Source	DF	Seq SS	Adj SS	Adj MS	F-Value	P-Value	% of Contribution
Regression	6	0.62949	0.62949	0.10492	360.11	0.000	99.08%
s	1	0.10889	0.00949	0.00949	32.57	0.000	17.14%
f	1	0.46401	0.04500	0.04500	154.46	0.000	73.04%
d	1	0.04909	0.00133	0.00133	4.56	0.045	7.73.%
*s*f*	1	0.00068	0.00068	0.00068	2.32	0.144	0.11%
*s*d*	1	0.00120	0.00120	0.00120	4.12	0.056	0.19%
*f*d*	1	0.00563	0.00563	0.00563	19.34	0.000	0.89%
RE	20	0.00583	0.00583	0.00583			0.92%
Total	26	0.63532					100.00%
Model summary: R^2 = 99.08%, R^2 (adj)=99.81%, R^2 (pred)= 98.32%							

The percentage influence of input process parameters on output response in PFM is as follows: feed rate: 73.04%, cutting speed: 17.14% and depth of cut: 7.73% (Table 4.5). The interaction terms {(s*f: 0.11%) and (s*d: 0.19%)} do not have much statistical significance on surface roughness. But interaction term (f*d: 0.89% and its value of $P < 0.05$) shows some statistical significance on average surface roughness since its P-value is less than or equal to the confidence level of 0.05. And residual error for this model is: 0.92%.The total variations are explained by the model is R^2 = 99.21% in CFM, whereas R^2 = 99.08% in PFM. R^2 (Adj) is 98.98% with the significant factors (d, s& f) in CFM whereas R^2 (Adj) is 99.81% in PFM with the significant factors (d, s &f). R^2 (Pred) is 98.53%, expected to explain the new data in CFM and it is 98.32% in PFM (Table 4.4

and Table 4.5).

Three-dimensional pie charts have been established for the results obtained through ANOVA analysis in order to represent graphically the effect of each individual cutting process parameter, on the performance characteristics. A three-dimensional pie-chart is a circular statistical graphic in which a circle is divided into a series of sectors. Each sector represents a proportion of the summation of all values in a dataset. These charts are basically used to depict the share of a particular constituent as a part of whole. Figure 4.1 (a) is the 3D pie chart has been established in order to show graphically the percentage influence of cutting parameters on the process response R_a in the existing CFM. Figure 4.1 (b) is the 3D pie chart has been drawn to show the percentage influence of cutting parameters on the surface roughness with the proposed PFM.

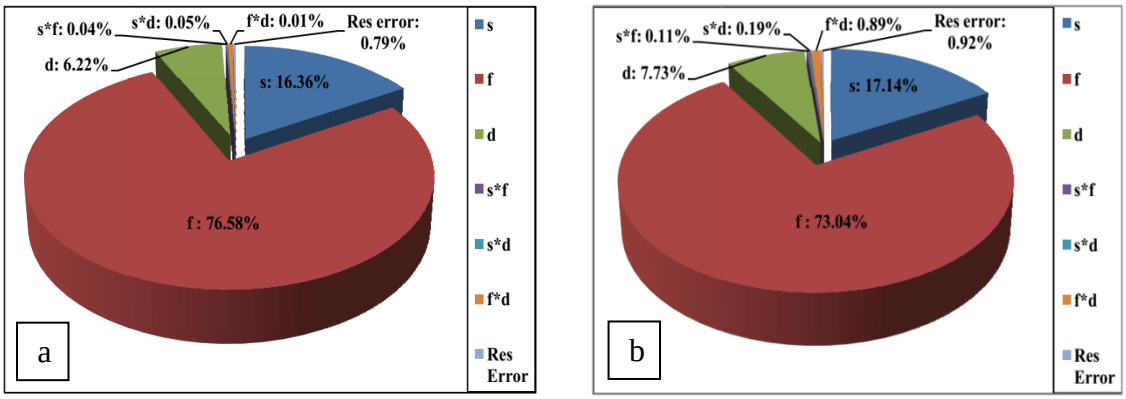

Figure 4.1 Percentage of influence of input machining parameters on R_a with (a) CFM (b) PFM

It is evident that from Table 4.4, Table 4.5, Figure 4.1 (a) and Figure 4.1 (b), ANOVA outcomes reveals that feed rate is the most influencing parameter among the considered process parameters in CFM as well as PFM. It is well accepted that for a given value of cutting tool diameter, nose radius, rake angle, number of cutting edges and flutes of a cutting tool, quality of the surface finish is primarily a function of feed rate.

4.4.1.2 ANOVA outcomes for cutting tool tip temperature (T)

Table 4.6 and Table 4.7 depict the ANOVA results for cutting tool tip temperature with CFM and PFM respectively. The last column of these tables displays percentage contribution of each parameter on the total variation indicating degree of influence of

process control factor on the performance response (T). The percentage of influence of input parameters on the performance response (T) in CFM is as follows: depth of cut: 72.73%, feed rate: 21.36% and cutting speed: 2.75% (Table 4.6). The interaction terms {(*d**s: 0.04%), (*d***f*: 0.00%) and *s***f*: 0.11%)} do not have much statistical significance on cutting tool tip temperature, as P–values for these terms are more than the confidence level of 0.05.

Table 4.6 ANOVA results for T with un-coated cutting tool with CFM

Source	DF	Seq SS	Adj SS	Adj MS	F-Value	P-Value	% of Contribution
Regression	6	3977.54	3977.54	662.924	117.58	0.000	97.24%
d	1	2974.78	128.50	128.496	22.79	0.000	72.73%
s	1	112.50	5.82	5.819	1.03	0.322	2.75%
f	1	873.62	9.47	9.466	1.68	0.210	21.36%
*d***s*	1	1.69	1.69	1.688	0.30	0.590	0.04%
*d***f*	1	10.64	10.64	10.641	1.89	0.185	0.26%
*s***f*	1	4.32	4.32	4.320	0.77	0.392	0.11%
RE	20	112.76	112.76	5.638			2.76%
Total	26	4090.30					100.00%
Model Summary		R^2=97.24%		R^2(adj)=96.42%		R^2(pred)=95.22%	

Table 4.7ANOVA results for T with un-coated cutting tool with PFM

Source	DF	Seq SS	Adj SS	Adj MS	F-Value	P-Value	% of Contribution
Regression	6	3992.03	3992.03	665.338	101.63	0.000	96.82%
d	1	2951.68	117.92	117.924	18.01	0.000	71.59%
s	1	114.50	4.35	4.349	0.66	0.425	2.78%
f	1	908.80	9.35	9.354	1.43	0.246	22.04%
*d***s*	1	0.75	0.75	0.750	0.11	0.739	0.02%
*d***f*	1	11.60	11.60	11.603	1.77	0.198	0.28%
*s***f*	1	4.69	4.69	4.687	0.72	0.407	0.11%
RE	20	130.94	130.94	6.547			3.18%
Total	26	4122.97					100.00%
Model Summary		R^2=96.82%		R^2(adj)=95.87%		R^2(pred)=94.57%	

From Table 4.7 it is clear that, the percentage influence of input parameters on output response in PFM is as follows: depth of cut: 71.59%, feed rate: 22.04%and cutting speed 2.78%. The interaction terms {(*d**s: 0.02%, *d***f*: 0.28% and *s***f*: 0.11%)} do not

have much statistical significance on cutting tool tip temperature, since their P-values are more than the confidence level of 0.05. Residual error of the model developed is 3.18%. ANOVA reveals that depth of cut is the most influencing process parameter among all the input process parameters considered on process response T, in existing CFM as well as proposed PFM. It is well accepted from the literature that, for a given values of tool diameter, nose radius, rake angle, number of cutting edges and flutes of a cutting tool, the value of cutting tool tip temperature is primarily a function of depth of cut. Total variations are explained by the model is R^2 = 97.24% in constant feed machining whereas R^2 = 96.82% in progressive feed machining. R^2 (Adj) is 96.42% with the significant factors (*d, s & f*) in constant feed machining whereas it is 95.87% in progressive feed machining with the significant factors (*d, s, f*). R^2 (Pred) is 95.22% expected to explain the new data in constant feed machining and it is 94.57% in progressive feed machining (Table 4.6 and Table 4.7).

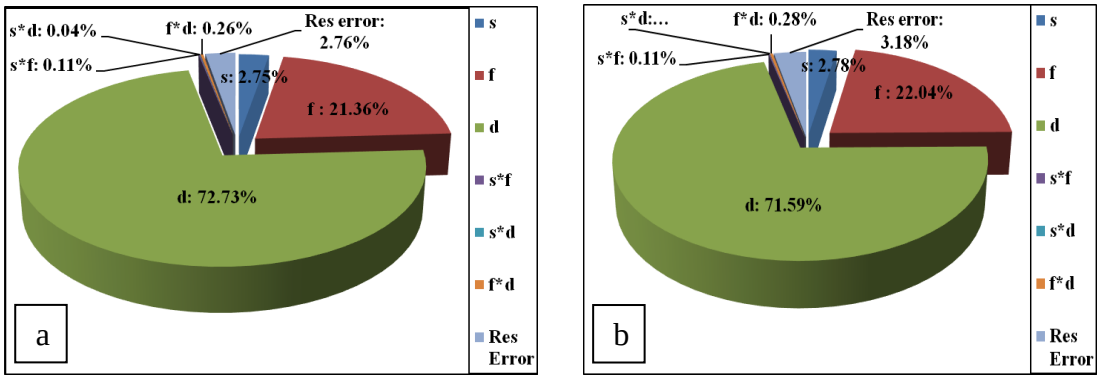

Figure 4.2 Percentage of influence of input machining parameters on T with (a) CFM (b) PFM

Figure 4.2 (a) & (b) are the 3D pie chart has been drawn to show the percentage influence of cutting parameters on the cutting tool tip temperature (T) with the existing CFM and PFM respectively. It is well evident from (Table 4.6 and Table 4.7) and 3D pie charts that, in both the types of machining depth of cut is having predominant effect followed by feed rate on the cutting tool tip temperature (T).

4.4.1.3 ANOVA outcomes for material removal rate (MRR)

ANOVA results for MRR are depicted in Table 4.8 and Table 4.9 obtained in CFM and PFM respectively. The last column of these tables displays percentage contribution of

each input parameter on the total variation, indicating the degree of influence on the process response MRR.

Table 4.8 ANOVA results for MRR with un-coated cutting tool in CFM

Source	DF	Seq SS	Adj SS	Adj MS	F-Value	P-Value	% of Contribution
Regression	6	383804	383804	63967.3	8350.07	0.000	99.96%
s	1	146	0	0.0	0.00	0.994	0.04%
f	1	183988	33	32.8	4.28	0.052	47.92%
d	1	165892	153	153.1	19.98	0.000	43.21%
*s*f*	1	2	2	1.7	0.22	0.643	0.00%
*s*d*	1	13	13	13.0	1.69	0.208	0.00%
*f*d*	1	33764	33764	33763.7	4407.39	0.000	8.79%
Error	20	153	153	7.7			0.04%
Total	26	383957					100.00%
Model Summary		R^2=99.96%		R^2(adj)=99.95%		R^2(pred)=99.92%	

Table 4.9 ANOVA results for MRR with un-coated cutting tool in PFM

Source	DF	Seq SS	Adj SS	Adj MS	F-Value	P-Value	% of Contribution
Regression	6	326039	326039	54339.8	7519.46	0.000	99.96%
s	1	106	0	0.1	0.02	0.892	0.03%
f	1	156177	31	31.1	4.30	0.051	47.88%
d	1	140844	125	124.9	17.28	0.000	43.18%
*s*f*	1	1	1	1.2	0.16	0.690	0.00%
*s*d*	1	7	7	6.6	0.92	0.350	0.00%
*f*d*	1	28903	28903	28903.2	3999.59	0.000	8.86%
Error	20	145	145	7.2			0.04%
Total	26	326183					100.00%
Model Summary		R^2=99.96%		R^2(adj)=99.94%		R^2(pred)=99.91%	

From the Table 4.8 it is evident that, the percentage of influence of input process parameters on the performance response (MRR) in CFM is as follows: feed rate: 47.92%, depth of cut: 43.21% and cutting speed: 0.04%. Feed rate and depth of cut are showing maximum influence, whereas cutting speed is showing least or almost negligible influence on the output response. It is in line with the literature, for a given vale of tool diameter, rake angle, number of flutes and nose radius, MRR is basically a function of feed rate and depth of cut. The interaction terms {(*s*f* = 0.00%), (*s*d* =

0.00%) do not have any statistical influence at all, and P–values for these terms are more than the confidence level of 0.05. But, interaction term (*f***d* =8.79%) do have some statistical significance on MRR and its P-value is less than 0.05. Residual error of the model is only 0.04%. The percentage of influence of input process parameters on output response in PFM is as follows: feed rate: 47.88%, depth of cut: 43.18% and cutting speed: 0.03% (Table 4.9). The interaction terms {(*s***f* =0.00%) and (*s***d* = 0.00%)} do not have any statistical significance on material removal rate, since their P-values are more than the confidence level of 0.05. The interaction term (*f***d*: 8.86%) is showing statistical significance on material removal rate. Residual error of the model is only 0.04%.

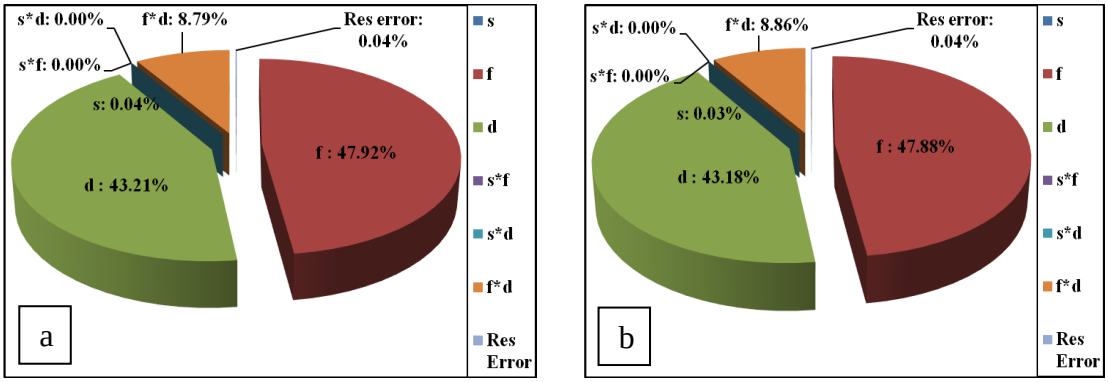

Figure 4.3 Percentage of influence of input machining parameters on MRR with (a) CFM (b) PFM

Figure 4.3 (a) & (b) are the 3D pie charts have been established to show the percentage influence of cutting parameters on the MRR from the existing CFM and PFM. ANOVA reveals that feed rate is the most influencing parameter among all the input process parameters considered in CFM and PFM on the MRR performance characteristic followed by depth of cut. It is in line with the literature, for a given vale of tool diameter, rake angle, number of flutes and nose radius, MRR is basically a function of feed rate and depth of cut. Same trend has been observed in CFM and PFM. Total variations are explained by the model is R^2= 99.96% for both CFM and PFM. R^2 (Adj) is 99.95% with the significant factors {*f*, *d*, and (*f***d*)} in CFM whereas 99.94% in PFM with the same kind of significant factors {*f*, *d* and (*f***d*)} as that of CFM. R^2 (Pred) is 99.92% expected to explain the new data in CFM and it is 99.91% expected in PFM. It is evident from (Table 4.8 and Table 4.9) and corresponding pie charts that, in both the

types of machining feed rate is having predominant effect on material removal rate followed by depth of cut and cutting speed is having least influence and interaction terms (*s*f, s*d*) do not have any influence, whereas interaction term (*f*d*) is having considerable influence after feed rate and depth of cut.

4.4.2 Development of linear regression mathematical models

RSM has been followed to develop regression mathematical models for the prediction of considered process responses. It is a pool of mathematical and statistical techniques those are useful for modelling and analysis of problems in which response of attentiveness is influenced by several input parameters. The most commonly used techniques for investigating the relationship between two quantitative variables are correlation and regression. Correlation quantifies the strength of linear relationship between a pair of variables, whereas regression expresses the relationship in the form of an equation.

4.4.2.1 Regression mathematical models for surface roughness

A second-order polynomial response surface regression mathematical equation was developed for surface roughness (R_a) as a function of machining parameters namely cutting speed, feed rate and DoC. The developed regression model to predict the process output response (R_a) with un-coated cutting tool in existing CFM is shown at equation 4.6, and with un-coated cutting tool in PFM is shown at equation 4.7.

$$R_{acu} = 0.6920 - 0.000107^{*}s + 0.001036^{*}f - 0.0856^{*}d - 0.0020^{*}d^{*}d + 0.000008^{*}s^{*}d - 0.000011^{*}f^{*}d \quad \text{----------} \quad (4.6)$$

$$R_{apu} = 0.5535 - 0.000109^{*}s + 0.000943^{*}f - 0.0400^{*}d - 0.0040^{*}d^{*}d + 0.000013^{*}s^{*}d - 0.000144^{*}f^{*}d \quad \text{----------} \quad (4.7)$$

Experimental values of surface roughness from the performed twenty-seven numbers of experiments as per L_{27} orthogonal array and predicted values of output response (R_a) from these developed regression models are displayed in Table 4.10.

Table 4.10 Experimental vs Predicted values of surface roughness

Trial No	R_a with un-coated cutting tool in CFM				R_a with un-coated cutting tool in PFM			
	Exp values	Pred values	% of error	Abs % of error	Exp values	Pred values	% of error	Abs % of error
1	0.64	0.630	1.56	1.56	0.50	0.494	1.15	1.15
2	0.57	0.573	-0.53	0.53	0.46	0.469	-1.94	1.94
3	0.51	0.514	-0.78	0.78	0.42	0.448	-6.68	6.68
4	0.83	0.836	-0.72	0.72	0.68	0.661	2.76	2.76
5	0.76	0.777	-2.24	2.24	0.62	0.614	0.92	0.92
6	0.71	0.716	-0.85	0.85	0.57	0.572	-0.33	0.33
7	1.01	1.041	-3.07	3.07	0.90	0.828	7.97	7.97
8	0.95	0.981	-3.26	3.26	0.78	0.760	2.60	2.60
9	0.90	0.918	-2.00	2.00	0.71	0.696	2.02	2.02
10	0.51	0.529	-3.73	3.73	0.40	0.395	1.25	1.25
11	0.52	0.478	8.08	8.08	0.42	0.379	9.67	9.67
12	0.43	0.425	1.16	1.16	0.36	0.368	-2.31	2.31
13	0.75	0.735	2.00	2.00	0.59	0.562	4.75	4.75
14	0.67	0.682	-1.79	1.79	0.52	0.525	-0.92	0.92
15	0.60	0.627	-4.50	4.50	0.47	0.492	-4.70	4.70
16	0.92	0.94	-2.17	2.17	0.78	0.729	6.54	6.54
17	0.86	0.886	-3.02	3.02	0.72	0.670	6.92	6.92
18	0.82	0.829	-1.10	1.10	0.64	0.616	3.77	3.77
19	0.41	0.428	-4.39	4.39	0.33	0.296	10.40	10.38
20	0.42	0.383	8.81	8.81	0.34	0.290	14.70	14.74
21	0.34	0.336	1.18	1.18	0.28	0.289	-3.05	3.05
22	0.67	0.634	5.37	5.37	0.53	0.463	12.70	12.69
23	0.58	0.587	-1.21	1.21	0.47	0.435	7.38	7.38
24	0.54	0.538	0.37	0.37	0.42	0.412	1.82	1.82
25	0.83	0.839	-1.08	1.08	0.68	0.630	7.39	7.39
26	0.76	0.791	-4.08	4.08	0.61	0.581	4.80	4.80
27	0.74	0.740	0.00	0.00	0.58	0.536	7.56	7.56
Mean value of absolute % of error				2.56	Mean value of absolute % of error			5.08

The mean absolute percentage error is also known as mean absolute percentage deviation is a measure of prediction accuracy of a forecasting method in statistics. It measures the accuracy of a forecast system in terms of percentage. The mean value of absolute percentage of error is ‘2.56’ with CFM and it is ‘5.08’ with PFM. Hence the developed regression models for surface roughness will work with 95% of confidence level to predict the responses against a given set of input parameters.

4.4.2.2 Regression mathematical models for cutting tool tip temperature

Table 4.11 Experimental vs Predicted values of cutting tool tip temperature

Trial No	Tcu with un coated cutting tool in CFM				Tcu with un coated cutting tool in PFM			
	Exp	Pred	% of error	Abs % of error	Exp	Pred	% of error	Abs % of error
1	42.6	40.460	5.025	5.025	39.50	37.02	6.27	6.27
2	44.3	45.882	-3.570	3.570	41.80	42.47	-1.59	1.59
3	51.8	51.304	0.958	0.959	48.20	47.91	0.60	0.60
4	43.3	42.735	1.306	1.306	39.40	39.14	0.65	0.65
5	49.7	48.757	1.898	1.898	46.70	45.19	3.24	3.24
6	59.2	54.779	7.469	7.469	56.30	51.23	9.00	9.00
7	46.2	45.010	2.577	2.577	42.60	41.26	3.14	3.14
8	52.7	51.632	2.028	2.028	49.10	47.91	2.43	2.43
9	59.4	58.254	1.930	1.930	55.90	54.55	2.41	2.41
10	51.3	52.749	-2.825	2.825	46.70	49.09	-5.13	5.13
11	58.7	59.113	-0.704	0.704	54.80	55.52	-1.32	1.32
12	63.6	65.477	-2.951	2.913	59.70	61.95	-3.77	3.77
13	53.5	54.649	-2.148	2.148	50.30	50.96	-1.32	1.32
14	58.6	61.613	-5.142	5.142	55.00	57.99	-5.44	5.44
15	64.3	68.577	-6.652	6.652	60.70	65.02	-7.12	7.12
16	54.7	56.549	-3.380	3.380	50.80	52.84	-4.01	4.01
17	60.1	64.113	-6.677	6.677	56.90	60.46	-6.26	6.26
18	69.1	71.677	-3.729	3.729	65.70	68.09	-3.64	3.64
19	64.9	65.039	-0.213	0.213	61.20	61.17	0.06	0.06
20	74.5	72.345	2.893	2.893	71.50	68.58	4.09	4.09
21	81.2	79.651	1.908	1.908	77.80	75.99	2.33	2.33
22	66.4	66.564	-0.246	0.246	62.40	62.79	-0.62	0.62
23	75.6	74.470	1.495	1.495	72.60	70.80	2.48	2.48
24	82.3	82.376	-0.092	0.092	78.90	78.81	0.11	0.11
25	69.8	68.089	2.452	2.452	66.10	64.41	2.56	2.56
26	78.7	76.595	2.675	2.675	75.80	73.02	3.67	3.67
27	87.2	85.101	2.408	2.408	83.70	81.63	2.47	2.47
	Mean value of absolute % of error			2.789	Mean value of absolute % of error			3.175

The developed regression models to predict the output response with uncoated cutting tool in traditional CFM and PFM are shown at equation 4.8 and equation 4.9.

$$T_{cu} = 19.59 + 16.13^{*}d + 0.00205^{*}s + 0.0164^{*}f - 0.000500^{*}d^{*}s + 0.00628^{*}d^{*}f + 0.000003^{*}s^{*}f \quad \text{----------} \quad (4.8)$$

$$T_{pu} = 16.95 + 15.45^{*}d + 0.00177^{*}s + 0.0163^{*}f - 0.000333^{*}d^{*}s + 0.00656^{*}d^{*}f + 0.000003^{*}s^{*}f \quad \text{----------} \quad (4.9)$$

Experimental values of cutting tool tip temperature (T) from the performed twenty-seven number of experiments as per L_{27} orthogonal array and predicted values of output response (T) from the developed regression models (equation 4.8 & equation 4.9) are displayed in Table 4.11. In case of cutting tool tip temperature, the mean value of absolute percentage of error is: 2.789 for CFM and it is 3.175 for PFM. Hence the developed model for cutting tool tip temperature will work with more than 95% of confidence level to predict the responses.

4.4.2.3 Regression mathematical models for material removal rate

The developed regression mathematical models to predict output response (MRR) with un-coated cutting tools in existing CFM and PFM are shown at equation 4.10 & 4.11.

$$MRR_{cu} = 11.49 + 0.00002^{*}s - 0.0306^{*}f - 17.60^{*}d + 0.000002^{*}s^{*}f + 0.00139^{*}s^{*}d + 0.35362^{*}f^{*}d \quad \text{----------} \quad (4.10)$$

$$MRR_{pu} = 10.23 + 0.00031^{*}s - 0.0297^{*}f - 15.90^{*}d + 0.000002^{*}s^{*}f + 0.00099^{*}s^{*}d + 0.32718^{*}f^{*}d \quad \text{----------} \quad (4.11)$$

Experimental values of MRR from the twenty-seven numbers of experiments conducted as per L_{27} OA and predicted values of process output response (MRR) from the developed regression models (equation 4.10 and equation 4.11) are displayed in Table 4.12. The mean absolute percentage error also known as mean absolute percentage deviation is a measure of prediction accuracy of a forecasting method in statistics. It measures the accuracy of a forecast system in terms of percentage. The mean value of absolute percentage of error is: 1.80 for constant feed machining where as it is 1.68 for PFM. Therefore, the developed regression model for material removal rate will work with more than 95% of confidence level to predict the MRR response for a given set of input process control parameters.

Table 4.12 Experimental Vs Predicted values of material removal rate

Trial No	MRRcu with un coated cutting tool in CFM				MRRcu with un coated cutting tool in PFM			
	Exp	Pred	% of error	Abs % of error	Exp	Pred	% of error	Abs % of error
1	47.49	47.34	0.31	0.31	43.65	43.55	0.23	0.23
2	92.19	94.26	-2.24	2.24	84.82	86.69	-2.20	2.20
3	145.69	141.18	3.09	3.09	134.22	129.83	3.27	3.27
4	49.75	48.40	2.72	2.72	45.87	44.61	2.76	2.76
5	94.27	95.32	-1.11	1.11	86.87	87.74	-1.00	1.00
6	147.40	142.25	3.50	3.50	135.84	130.88	3.65	3.65
7	50.17	49.46	1.40	1.40	46.19	45.66	1.15	1.15
8	96.72	96.39	0.35	0.35	88.98	88.80	0.21	0.21
9	150.87	143.31	5.01	5.01	138.72	131.93	4.89	4.89
10	93.13	89.27	4.15	4.15	85.63	82.19	4.02	4.02
11	193.13	189.23	2.02	2.02	177.79	174.40	1.91	1.91
12	289.78	289.20	0.20	0.20	265.87	266.62	-0.28	0.28
13	95.41	91.37	4.24	4.24	87.54	83.99	4.06	4.06
14	195.32	191.34	2.04	2.04	178.52	176.20	1.30	1.30
15	292.41	291.30	0.38	0.38	268.42	268.41	0.00	0.00
16	97.98	93.48	4.59	4.59	89.78	85.78	4.45	4.45
17	197.52	193.44	2.07	2.07	181.65	178.00	2.01	2.01
18	294.52	293.41	0.38	0.38	270.25	270.21	0.01	0.01
19	131.27	131.19	0.06	0.06	120.77	120.83	-0.05	0.05
20	282.43	284.20	-0.63	0.63	260.47	262.12	-0.63	0.63
21	441.21	437.21	0.91	0.91	406.98	403.41	0.88	0.88
22	133.52	134.34	-0.61	0.61	123.76	123.36	0.32	0.32
23	289.75	287.35	0.83	0.83	265.32	264.66	0.25	0.25
24	444.62	440.36	0.96	0.96	411.76	405.95	1.41	1.41
25	135.25	137.49	-1.66	1.66	123.84	125.90	-1.67	1.67
26	297.23	290.50	2.27	2.27	272.86	267.20	2.08	2.08
27	447.29	443.51	0.85	0.85	411.63	408.49	0.76	0.76
	Mean value of absolute % of error			1.80	Mean value of absolute % of error			1.68

4.4.3 Correlation and confirmation graphs

It is the most commonly used technique for investigating the relationship between two quantitative variables. Correlation and confirmation plots have been established for

surface roughness, cutting tool tip temperature and material removal rate to find the strength of relation between experimental and predicted values. Correlation quantifies the strength of linear association between a pair of variables.

4.4.3.1 Correlations and confirmations for surface roughness

In the present study, in order to recognize the effect of cutting speed, feed rate, and depth of cut on the process response R_a and to verify the exactness of the developed regression model, correlation and conformation tests were accomplished through Minitab-18software.The correlation graphs between predicted and experimental values of surface roughness in CFM and PFM are established at Figure 4.4 (a) and Figure 4.4 (b) respectively.

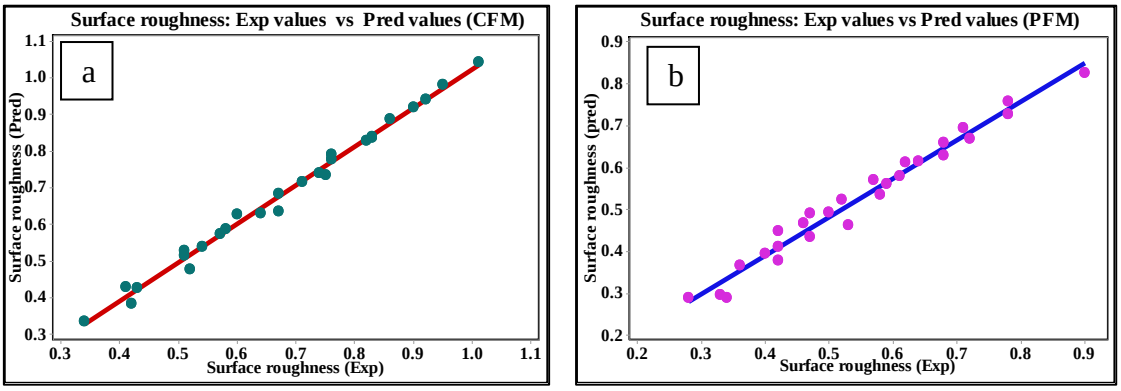

Figure 4.4 Correlation plot for Exp vs Pred values of R_a in (a) CFM and (b) PFM

From the established correlation graphs from Figure 4.4 (a), Figure 4.4 (b) and Table 4.10 it is clear that experimental values of surface roughness are distributed over the range of 0.34 µm to 1.01 µm in constant feed machining and 0.28µm to 0.90µm in case of progressive feed machining respectively. Especially Figure 4.4 (a) and Figure 4.4 (b) clearly reveals the level of fit or level of understanding between predicted and experimental values in both the kinds of machining environments is good. The best value of surface finish noticed among all the experimental values is 0.34 µm in CFM, whereas it is 0.28 µm in PFM. In the same way the worst value of surface roughness noticed is 1.01 µm in constant feed machining and it is 0.90µm in case of progressive feed machining.

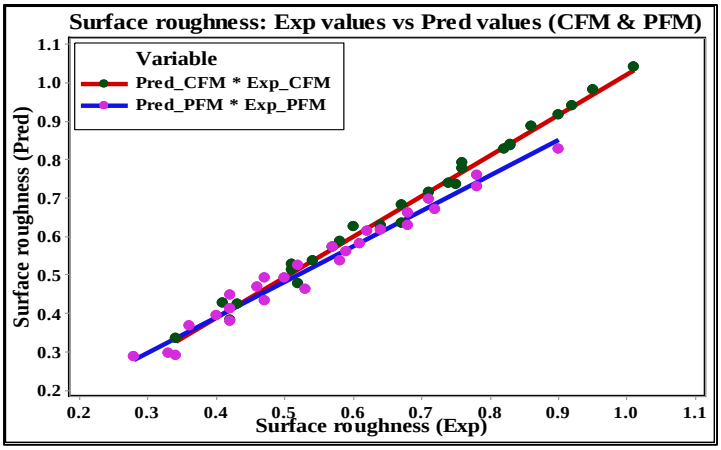

Figure 4.5 Combined correlation plot for Exp vs Pred values of R_a with CFM and PFM

A combined correlation plot between experimental and predicted values of surface roughness has been established on the same scale at Figure 4.5 for both the types of machining in-order to better understand the variation of performance response (R_a). It displays the actual range of variation of performance characteristic (R_a). It also reveals the range of variation of surface roughness in CFM is wider than that of PFM. The mean value of absolute percentage of relative error between experimental and predicted values of surface roughness is only ***2.56*** for constant feed machining and it is ***5.08*** for progressive feed machining (Table 4.10). These errors may be due to machine tool vibration, spindle run-out, chip loads and workpiece material property, etc. The developed regression models for CFM and PFM shows a good correlation between experimental and predicted values of surface roughness with more than 95% confidence level. Therefore, the developed regression models in both the kinds of machining are effective and can be used to find the process response for any given set of input parameters with 95% confidence level.

4.4.3.2 Correlations and confirmations for cutting tool tip temperature

In the present study, in order to identify the effect of cutting speed, feed rate and depth of cut on cutting tool tip temperature and to verify the exactness of developed regression model, correlation and conformation tests have been accomplished through Minitab-18 statistical analysis software. The correlation graphs between predicted and experimental values of cutting tool tip temperature for CFM and proposed PFM are established at Figure 4.6 (a) and Figure 4.6 (b) respectively.

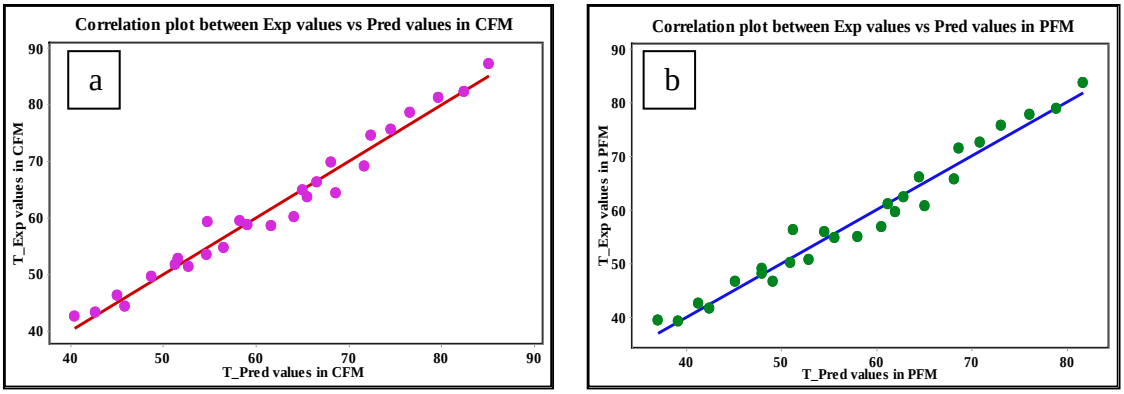

Figure4.6 Correlation plot for Exp vs Pred values of T with (a) CFM and (b) PFM

From the correlation plots of cutting tool tip temperature {Figure 4.6 (a), Figure 4.6 (b) and Table 4.11}, it is clear that experimental values of process output response; cutting tool tip temperature are distributed over the range of 42.60^0C to 87.20^0C in constant feed machining and 39.40^0C to 83.70^0C in case of progressive feed machining. The minimum value of cutting tool tip temperature was noticed among all the experimental values is 42.60^0C with constant feed machining, whereas it is 39.40^0C with proposed progressive feed machining. In the same way the maximum value of cutting tool tip temperature noticed is 87.20^0C in constant feed machining and it is 83.70^0C in case of progressive feed machining.

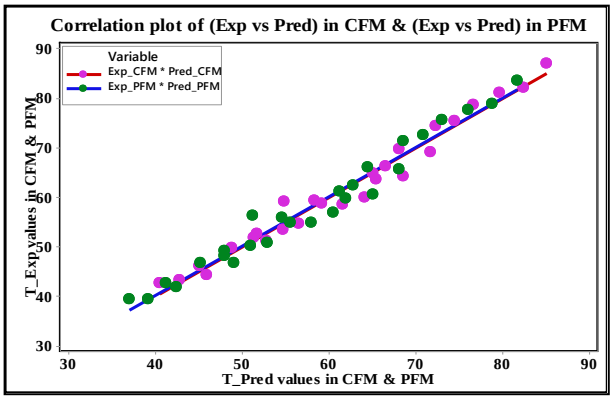

Figure 4.7 Combined correlation plot for Exp vs Pred values of T with CFM and PFM

Particularly, Figure 4.6 (a) and Figure 4.6 (b) clearly reveals that, the level of fit and understanding between predicted and experimental values in existing constant feed machining and proposed progressive feed machining is good.

A combined correlation plot of experimental and predicted values of cutting tool tip temperature with constant feed machining and progressive feed machining has been

established on the same scale at Figure 4.7 for both the types of machining, which depicts the actual range of variation of performance characteristic T. It also reveals the range of variation of cutting tool tip temperature (T) in CFM is wider than that of PFM. The mean value of absolute percentage of relative error between experimental and predicted values of T is only **2.789** for constant feed machining and it is **3.175** with progressive feed machining (Table 4.11). These errors may be due to machine tool vibration, spindle run-out, chip loads and workpiece material property, etc. The developed regression models for CFM and PFM shows a good correlation between the experimental and predicted values of cutting tool tip temperature with more than 95% of confidence level. Hence the developed regression models for both the kinds of machining environments are effective and can be used to find the performance response T; for any given set of input parameters with more than 95% of confidence level.

4.4.3.3 Correlations and confirmations for material removal rate

In the present study, in order to recognize the effect of cutting speed, feed rate, and depth of cut on the material removal rate (MRR) and to verify the exactness of the developed linear regressive models, correlation and conformation tests were accomplished between predicted and experimental values of material removal rate.

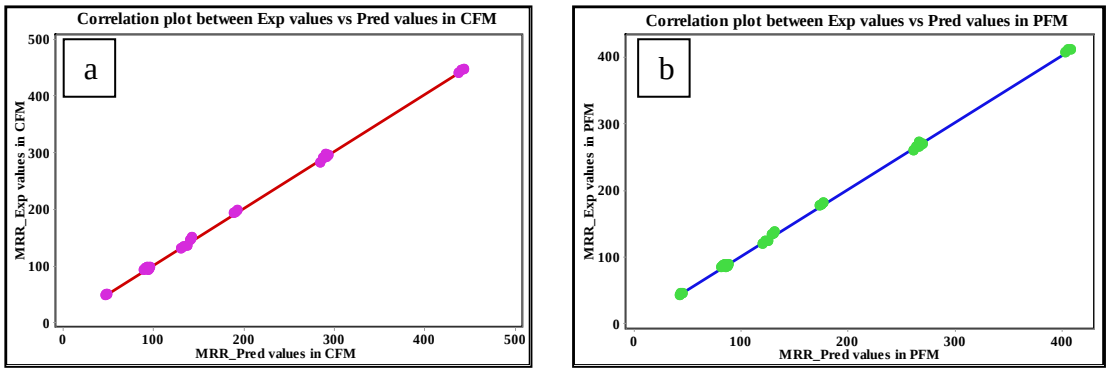

Figure 4.8 Correlation plot for Exp vs Pred values of MRR with (a) CFM and (b) PFM

The correlation graphs between predicted and experimental values of MRR for constant feed machining and progressive feed machining are established at Figure 4.8 (a) and Figure 4.8 (b) respectively. From the correlation graphs {Figure 4.8 (a), Figure 4.8 (b) and Table 4.12} it is clear that experimental value of MRR is distributed over the range of 47.49mm^3/min to 447.29mm^3/min in constant feed machining and 43.65mm^3/min to

411.63mm^3/min in case of progressive feed machining. The highest value of material removal rate was noticed among all the experimental values is 447.29mm^3/min in constant feed machining, whereas it is411.63 mm^3/min in progressive feed machining. In the same way the least value of material removal rate was noticed is 47.49mm^3/min in constant feed machining and it is 43.65mm^3/min in case of progressive feed machining.

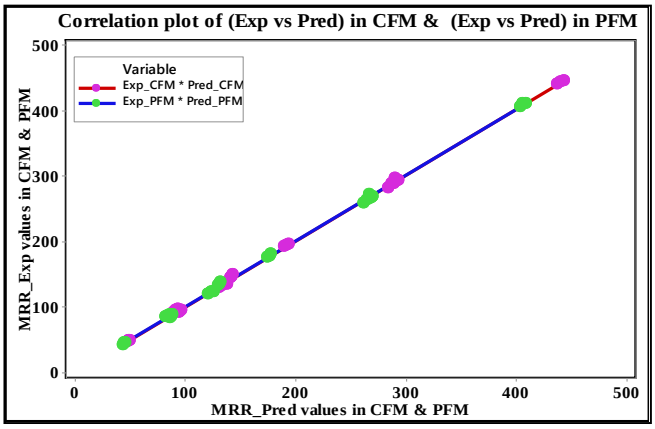

Figure 4.9 Combined correlation plot of Exp vs Pred values of MRR with PFM & CFM

A combined correlation plot between experimental and predicted values has been drawn on the same scale at Figure 4.9 for both the types of machining for better understanding of the response variation. It depicts the actual relative range of variation of performance characteristic (MRR) in constant feed machining w.r.t progressive feed machining. It also reveals the range of variation of MRR in CFM is wider than that of PFM. The mean value of absolute percentage of error between experimental and predicted values of MRR is only **1.80** with constant feed machining and it is **1.68** with progressive feed machining (Table 4.12). These errors may be due to machine tool vibration, spindle run-out, chip loads and workpiece material property, etc. Figure 4.8 (a) and Figure 4.8 (b) clearly reveals that the level of fit or level of understanding between predicted and experimental values in constant feed machining and proposed progressive feed machining is good with more than 95% of confidence level. Therefore, developed regression models in both the types of machining are effective and can be used to find the performance response (MRR) for any given set of input parameters.

4.4.4 Model fitness checks

Model fitness checks through normal probability plots have been done in order to find the validity of the developed regression models. Normal probability plot is a graphical

technique used to assess a specific data set is normally distributed or not? These are the plots will be drawn of raw data obtained from the experimentation, residuals from model fits and estimated parameters. The data sets are plotted against a theoretical normal distribution in such a way that the points should form an approximate straight line.

4.4.4.1 Model fitness check for surface roughness

Residual plots are used to analyse and to investigate the adequacy of developed model. Residual is the differences between experimentally measured value and predicted value from the developed regression models. These are studied using following model fitness plots: Normal probability plots of residual {Figure 4.10(a) and Figure 4.10(b)}, Plots of residuals versus predicted response {Figure 4.11(a) and Figure 4.11(b)} and plot of residual versus order of predicted response {Figure 4.12(a) and Figure 4.12(b)}.

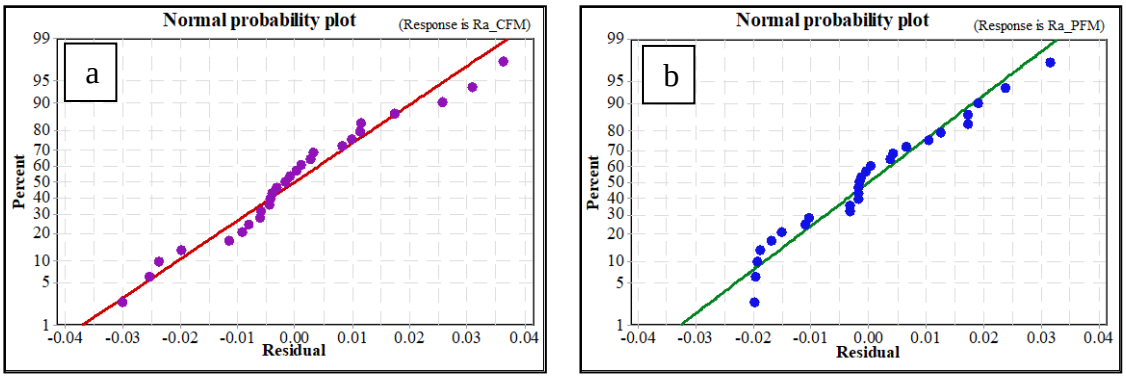

Figure 4.10 Normal probability plot of residual for R_a (a) CFM and (b) PFM

Normal probability plot of residual for surface roughness has been drawn to evaluate the fitness of the developed regression models. Figure 4.10(a) is the normal probability plot drawn for the raw data of surface roughness obtained with constant feed machining experiments and which was depicted in Table 4.3. It reveals that the residual is not in a particular trend. However, the errors are distributed normally. Figure 4.10(b) is the normal probability plot drawn for the raw data of surface roughness obtained with proposed progressive feed machining experiments, which was depicted in Table 4.3. It reveals that the residual is not in a particular trend. However, the errors are distributed normally. A similar trend has been observed in both the types of machining for surface roughness response.

Residual versus fits plot is the most frequently created plot to analyse the residuals. It is a scatter plot of residuals on Y-axis and fitted values on X-axis. These plots are used to

detect the non-linearity, unequal error variances and outliers.

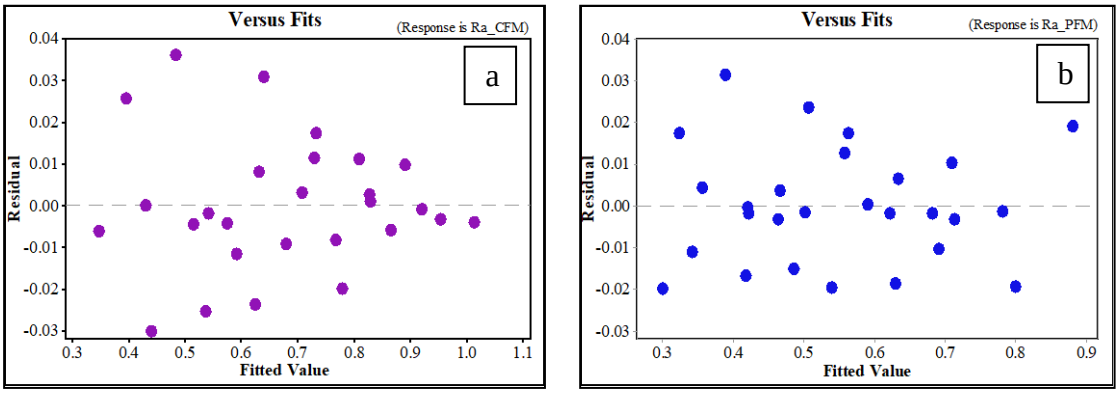

Figure 4.11 Plot of residual vs fitted value of R_a with (a) CFM and (b) PFM

Figure 4.11(a) is the plot of residual versus fitted surface roughness for the raw data obtained with constant feed machining experiments, which was depicted in Table 4.3. It shows that there is no foreseeable trend or planned structure detected.

The first residual is negative and second is positive, whereas third is exactly lying on zero line (i.e it is neither negative nor positive) and fourth is negative and fifth is positive. But, last three residuals are negative and last but fourth (twenty fourth) is positive and last but five (twenty-three) is negative. Hence, the residuals are randomly distributed without any foreseeable trend. This random pattern indicates that a linear model provides a decent fit to the data. Figure 4.11(b) is the plot of residual versus fitted surface roughness for the raw data depicted in Table 4.3, which was obtained with progressive feed machining experiments. It shows that there is no conceivable trend or planned structure noticed.

The first residual is negative and second is positive, whereas third is negative, fourth is positive and fifth is negative. But, last residual (twenty seventh) is positive and last but one (twenty sixth) and last but two (twenty fifth) are negative. Hence, in case of surface roughness with progressive feed machining also, residuals are randomly distributed without any foreseeable trend like in constant feed machining. This random pattern indicates that the linear model provides a decent fit to the data.

Plot of residual versus order of response will be used as a way of detecting a particular form of non-independence of the error terms, namely serial correlation. If the data

obtained is in time or space equate, a residual versus order plot helps to see, is there any correlation between the error terms that are near each other in the sequence.

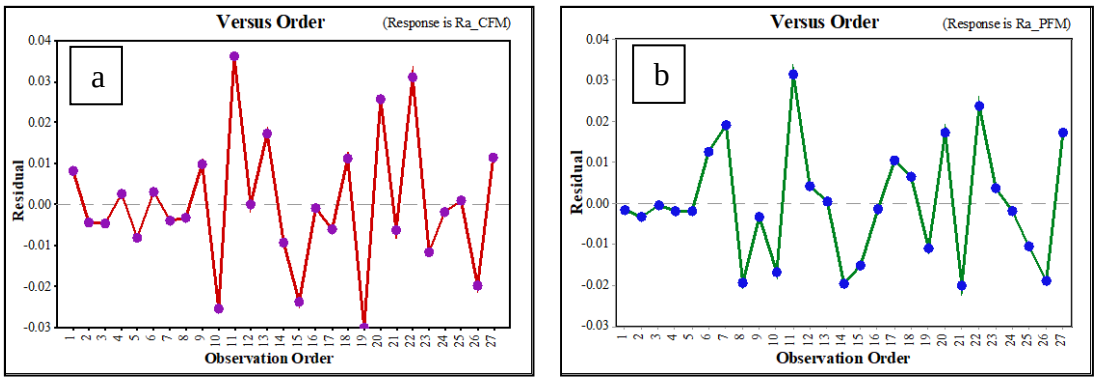

Figure 4.12 Plot of residual Vs Observation order of R_a with (a) CFM and (b) PFM

Figure 4.12(a) is the plot of residual versus order of surface roughness experimental raw data depicted in Table 4.3, which was obtained with CFM experiments. It displays the distribution of residuals against observation order. First residual is positive, second and third are negative whereas fourth one is positive and fifth one is negative. Twenty seventh or last residual is positive, last but one (twenty sixth) is negative and twenty fifth is positive. Hence, it is implicit that, residuals of surface roughness with constant feed machining are randomly distributed against observation order, without any foreseeable trend. Figure 4.12 (b) is the plot of residual versus order of surface roughness raw data obtained from the experimentation depicted in Table 4.3, with progressive feed machining experiments. It displays the distribution of residual against observation order. First five residuals are negative, sixth and seventh are positive. Twenty seventh residual is positive and twenty sixth, twenty fifth and twenty fourth are negative. Hence, it is implicit that, residuals of surface roughness with progressive feed machining are randomly distributed against observation order like in constant feed machining, without any conceivable trend.

4.4.4.2 Model fitness check for cutting tool tip temperature

The residual plots are used to analyse and to investigate the adequacy of the developed regression models. The residual is the differences between experimentally measured value and predicted value through the developed regression models. These are studied using the following model fitness plots: Normal probability plots of residuals {Figure

4.13(a) and Figure 4.13(b)}, plots of residuals versus predicted response {Figure 4.14(a) and Figure 4.14(b)} and plots of residual versus order of predicted response {Figure 4.15(a) and Figure 4.15(b)}.

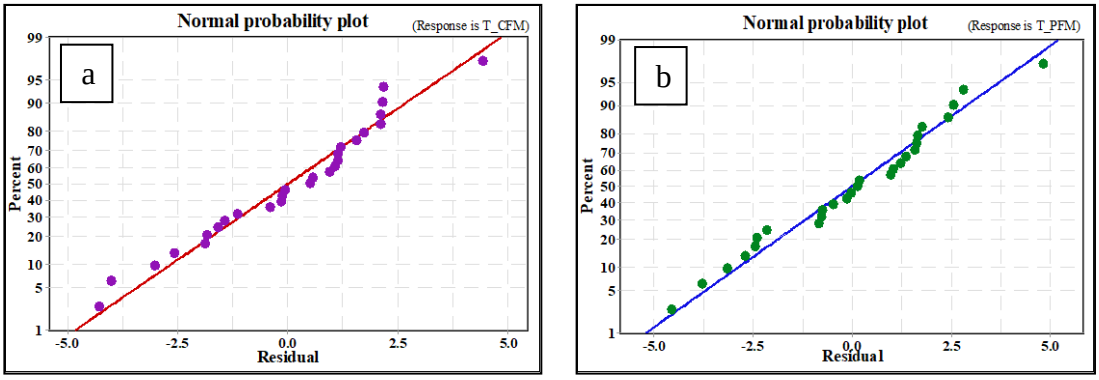

Figure 4.13 Normal probability plot of residual for T with (a) CFM and (b) PFM

Normal probability plot of residual for cutting tool tip temperature has been drawn to evaluate the fitness of the developed regression models. Figure 4.13(a) is the normal probability plot drawn for the raw data of cutting tool tip temperature obtained through constant feed machining experiments, depicted in Table 4.3. It reveals that the residual is not in a particular trend. However, the errors are distributed normally. Figure 4.13(b) is the normal probability plot drawn for the raw data of cutting tool tip temperature obtained through progressive feed machining experiments, which was depicted in Table 4.3.

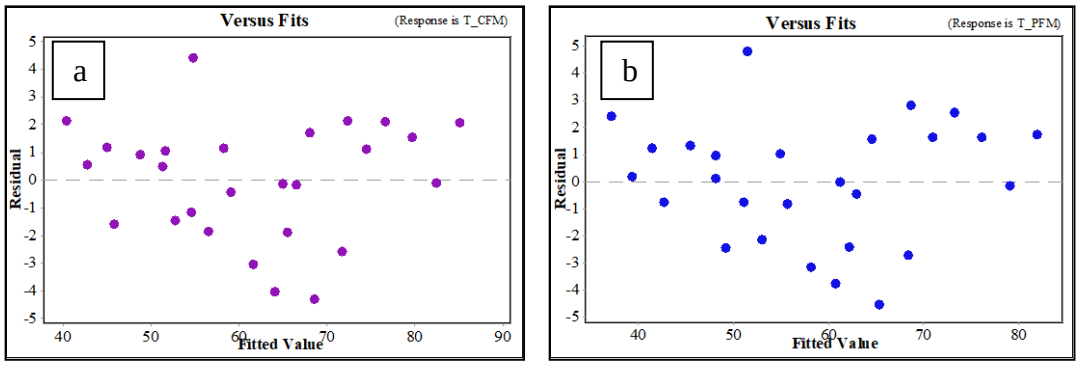

Figure 4.14 Plot of Residual Vs Fitted value of T with (a) CFM (b) PFM

It reveals that the residuals are not in a particular trend. However, the errors are distributed normally. A similar trend was observed in both the types of machining for cutting tool tip temperature. Figure 4.14(a) is the plot of residual versus fitted cutting tool tip temperature for the raw data obtained through constant feed machining

experiments and was depicted in Table 4.3. It shows that there is no foreseeable trend or planned structure noticed. The first three residuals are positive and fourth one is negative, whereas fifth, sixth and seventh are positive. Twenty seventh or last but one residual is positive and twenty sixth or last but one is negative and twenty fifth or last but two is positive. This kind of random pattern indicates that a linear model provides a decent fit to the data. Figure 4.14(b) is the plot of residual versus fitted cutting tool tip temperature (T) for the raw data depicted in Table 4.3, obtained through progressive feed machining experiments. It shows that there is no anticipated trend and planned structure noticed.

First, second and third residuals are positive, but fourth residual is negative. Whereas six, seven and eight are positive. Twenty seventh is positive, twenty sixth is negative but twenty fifth, twenty fourth and twenty third are positive. Hence, in case of cutting tool tip temperature with progressive feed machining also, residuals are randomly distributed without any foreseeable trend like in constant feed machining. This random pattern indicates that the linear model provides a decent fit to the data.

Plot of residual versus order of process response will be used as a way of detecting a particular form of non-independence of the error terms, namely serial correlation. If the data obtained is in time or space equate, a residual versus order plot helps to see, is there any correlation between the error terms that are near each other in the sequence.

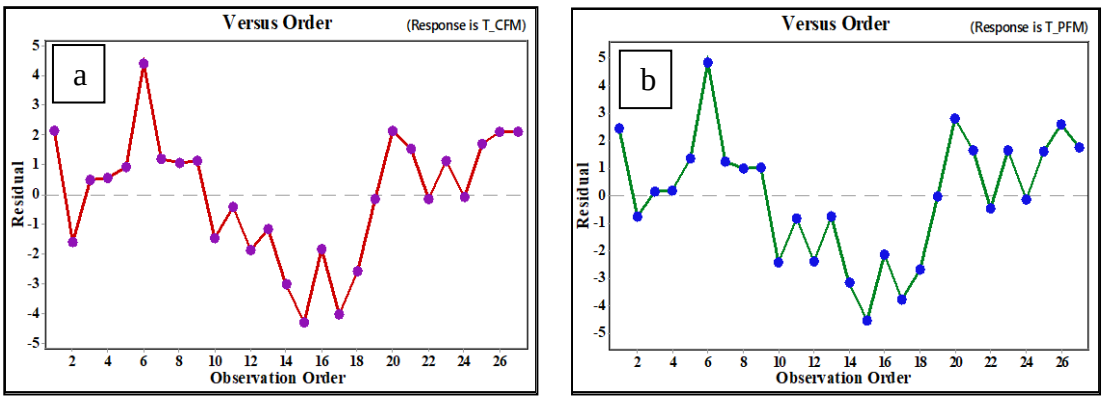

Figure 4.15 Plot of Residual Vs Order of T with (a) CFM and (b) PFM

Figure 4.15(a) is the plot of residual versus order of cutting tool tip temperature data depicted in Table 4.3, which was obtained with constant feed machining. It displays the

distribution of residuals against observation order. First residual is positive, second is negative whereas third, fourth and fifth are positive. Last or twenty seventh, twenty sixth and twenty fifth are positive. But twenty fourth is exactly lying on ZERO line; it is neither positive nor negative. Hence, it is implicit that, residuals of cutting tool tip temperature with constant feed machining are randomly distributed against observation order, without any foreseeable trend. Figure 4.15(b) is the plot of residual versus order of cutting tool tip temperature for the raw data depicted in Table 4.3, obtained with progressive feed machining. It displays the distribution of residual against observation order. First residual is positive, second is negative whereas third to ninth are positive. Twenty seventh, twenty sixth and twenty fifth are positive. But, twenty fourth is exactly lying on just below ZERO line as negative. Hence, it is implicit that, residuals of cutting tool tip temperature in progressive feed machining are also randomly distributed against observation order, without any foreseeable trend.

4.4.4.3 Model fitness check for material removal rate

The residual plots are used to analyse and to investigate the adequacy of the developed model. Residual is the difference between the experimentally measured value and predicted value obtained from the developed regression models. These are studied using the following plots: Normal probability plots of residuals {Figure 4.16(a) and Figure 4.16(b)} plots of residuals versus predicted response {Figure 4.17(a) and Figure 4.17(b)} and residual versus the order of predicted response {Figure 4.18(a) and Figure 4.18(b)}.

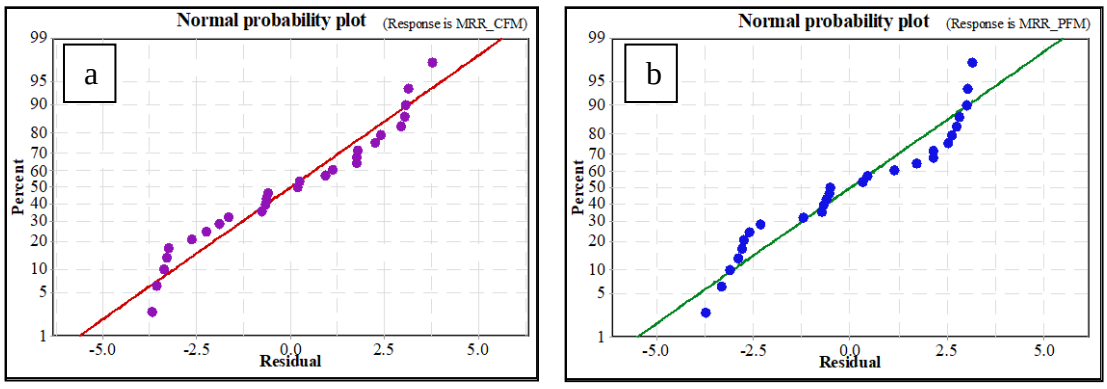

Figure 4.16 Normal probability plot of residual for MRR with (a) CFM and (b) PFM

Normal probability plot of residual for material removal rate have been drawn to

evaluate fitness of the developed regression mathematical models. Figure 4.16(a) is the normal probability plot established for the raw data of material removal rate depicted in Table 4.3, obtained through constant feed machining experiments. It reveals that the residual is not in a particular trend. However, the errors are distributed normally. Figure 4.16 (b) is the normal probability plot drawn for the raw data of material removal rate obtained through progressive feed machining experiments, which was depicted in Table 4.3. It reveals that the residual is not in a particular trend. However, the errors are distributed normally. A similar trend has been observed in both the types of machining for material removal rate.

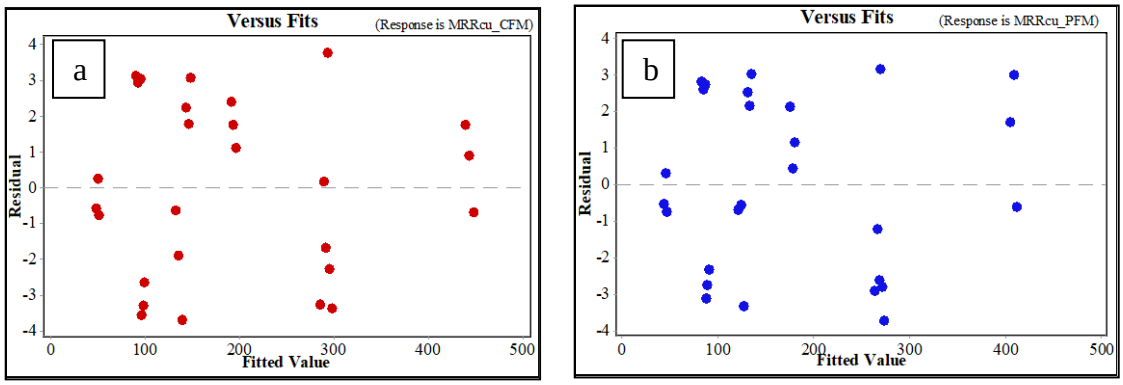

Figure 4.17 Plot of Residual Vs Fitted value of MRR with (a) CFM and (b) PFM

Figure 4.17(a) is the plot of residual versus fitted material removal rate for the raw data depicted in Table 4.3, obtained through constant feed machining experiments. It shows that there is no anticipated trend or planned structure noticed.

The first and second residual are negative, third is positive, but fourth and fifth are positive. Whereas twenty seventh is negative and twenty sixth, twenty fifth are positive. Therefore, the residuals are randomly distributed without any conceivable trend. This random pattern indicates that a linear model provides a decent fit to the data.

Figure 4.17 (b) is the plot of residual versus fitted material removal rate for the raw data depicted in Table 4.3 obtained through progressive feed machining experiments. It shows that there is no predictable trend and random structure. The first residual is negative and next one is positive, third one is negative. Last or twenty seventh residual is negative and last but one (twenty sixth) and last but two (twenty fifth) are positive. Hence, in the case of material removal rate with progressive feed machining also,

residuals are randomly distributed without any foreseeable trend like in constant feed machining. This random pattern indicates that the linear model provides a decent fit to the data.

Plot of residual versus order of response will be used as a way of detecting a particular form of non-independence of the error terms, namely serial correlation. If the data obtained is in time or space equate, a residual versus order plot helps to see, is there any correlation between the error terms that are near each other in the sequence.

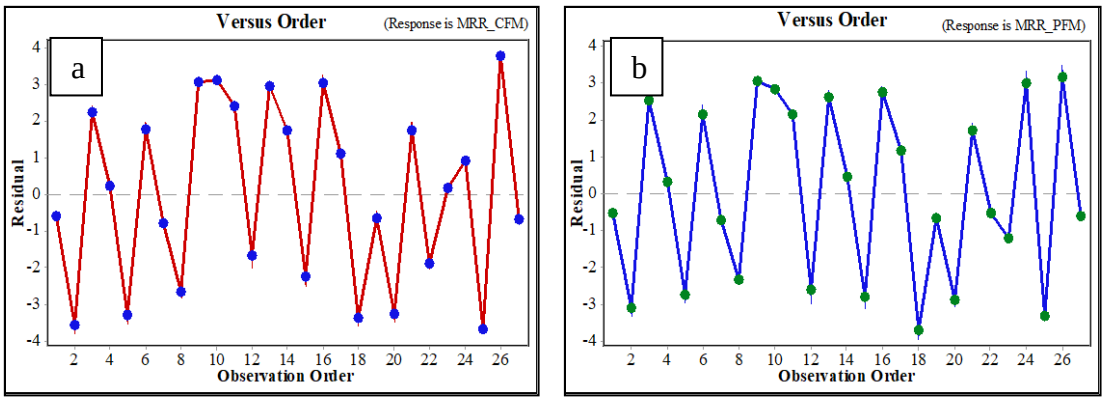

Figure 4.18 Plot of Residual Vs Observed order of MRR with (a) CFM and (b) PFM

Figure 4.18(a) is the plot of residual versus order of cutting tool tip temperature raw data depicted in Table 4.3, which was obtained through constant feed machining experiments. It displays the distribution of residuals against observation order. First and second residuals are negative, third and fourth are positive and fifth are negative. Twenty seventh is negative, twenty sixth is positive and twenty fifth is negative. Therefore, it is implicit that, residuals of cutting tool tip temperature for constant feed machining are randomly distributed against observation order, without any foreseeable trend.

Figure 4.18(b) is the plot of residual versus order of material removal rate, the raw data of response depicted in Table 4.3 obtained through progressive feed machining experiments. It displays the distribution of residual against observation order. First two residuals are negative, third and fourth are positive, whereas fifth is negative. Twenty seventh is negative, twenty sixth is positive and twenty fifth is negative. Hence, it is implicit that, residuals of material removal rate with progressive feed machining are also randomly distributed against observation order, without any predictable trend

4.4.5 Parametric analysis through main effects plots

The main effect is the influence of an independent variable on a dependent variable averaging across the levels of any other independent variables. Main effects plot is a plot of mean response values at each level of a design parameter or process variable. These plots are used to compare the relative strength of the effects of various factors on output response. Slop of plot reveals the level of influence of input process parameter on the process response. There will be the same number of main effects as independent variables.

4.4.5.1 Main effects plot for means of surface roughness

The main effects plot of machining parameters on mean value of surface roughness for constant feed machining and progressive feed machining are shown at Figure 4.19 (a) and Figure 4.19 (b) respectively on the same scale for better understanding of the trend. In both, constant feed machining and progressive feed machining; increase in cutting speed decreases the average surface roughness. But an increase in feed rate drastically increases the output response R_a as shown in Figure 4.19 (a), and an increase in depth of cut causes decrease in R_a.

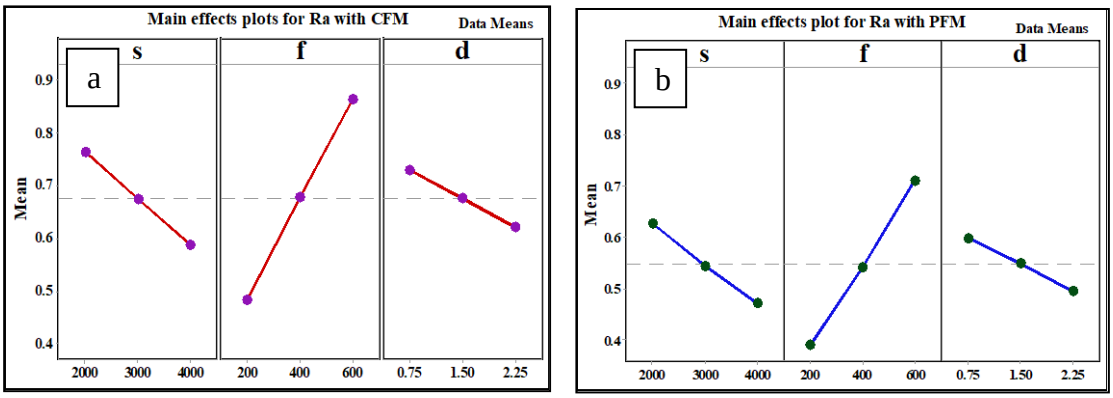

Figure 4.19 Main effect plots for means of R_a with (a) CFM and (b) PFM

Even though a similar trend has been observed in both the types of machining, main effect plots reveal that average surface roughness in PFM is comparatively lesser than that of CFM as shown in Figure4.19 (a) and Figure 4.19 (b). The trend shows that progressive feed machining is giving better surface finish than the constant feed

machining. This is mainly due to avoidance of sudden impact of the cutting tool with the workpiece, reduction in sudden cutting forces and in turn reduction in cutting tool deflections, minimal tool vibration, less chattering and rubbing on workpiece.

4.4.5.2 Main effects plot for means of cutting tool tip temperature

Main effect plots of machining parameters on mean value of cutting tool tip temperature for constant feed machining and progressive feed machining are shown in Figure 4.20 (a) and Figure 4.20 (b) on the same scale for better understanding of the trend. The trend shows that progressive feed machining is giving lesser cutting tool tip temperature than that of constant feed machining. This is mainly due to avoidance of sudden impact of the cutting tool with the workpiece, reduction in sudden cutting forces and in turn reduction in cutting tools deflection, minimal tool vibration, less chattering and mainly less rubbing of tool with workpiece.

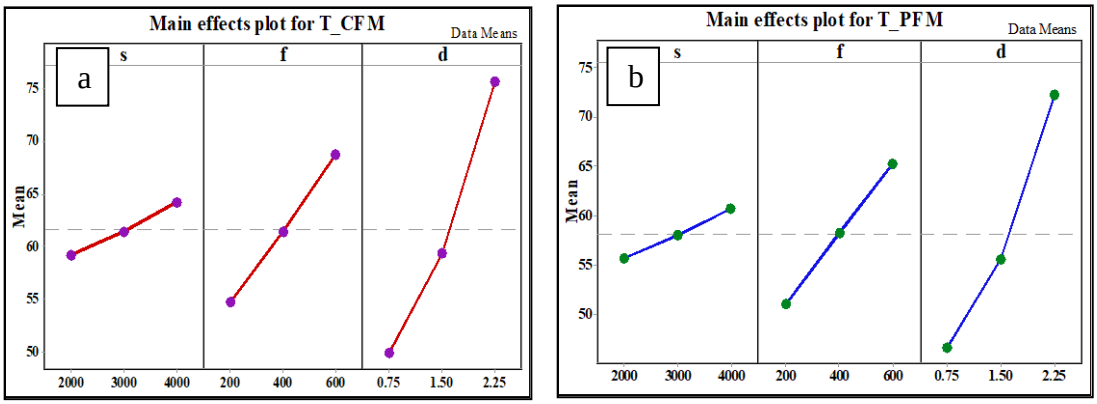

Figure 4.20 Main effect plots for means of T with (a) CFM and (b) PFM

In both, constant feed machining and progressive feed machining; increase in cutting speed, feed rate and depth of cut causes an increase in the mean value of cutting tool tip temperature (T) as shown in Figure 4.20 (a) and Figure4.20 (b) respectively. But an increase in depth of cut causes a drastic increase in the output response T, and an increase in feed rate causes moderate increase in the cutting tool tip temperature (T), and an increase in cutting speed also causes an increase in output response to the extent of minimum. Even though similar trend has been observed in both the kinds of machining, main effects plots reveal that cutting tool tip temperature in progressive feed machining is comparatively lesser than that of constant feed machining as depicted

in Figure 4.20 (a) and Figure 4.20 (b).

4.4.5.3 Main effects plot for means of material removal rate

The main effect plots of machining parameters on mean value of material removal rate for constant feed machining and progressive feed machining are shown in Figure 4.21 (a) and Figure 4.21 (b) on the same scale for better understanding of the trend. The trend shows that progressive feed machining is giving comparatively lesser amount of material removal rate than that of constant feed machining, which is almost negligible. This is mainly due to controlling the drastic increase in feed rate at beginning of each cut through part programming.

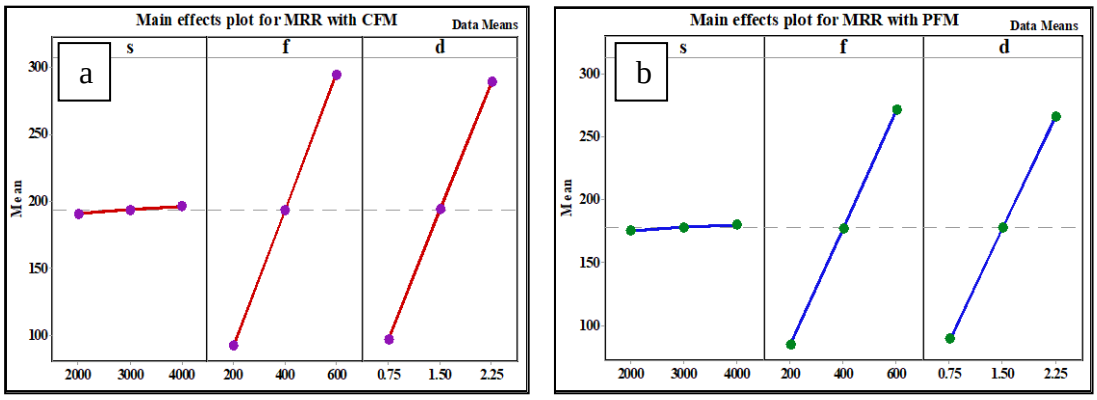

Figure4.21 Main effect plots for means of MRR with (a) CFM and (b) PFM

In both, constant feed machining and progressive feed machining; increase in cutting speed, feed rate and depth of cut as well causing an increase in the mean value of material removal rate. An increase in feed rate causes a drastic increase in the output response MRR. And an increase in depth of cut is causing of an increase in the MRR considerably. Whereas an increase of cutting speed slightly increasing the output response MRR. A similar trend has been observed in both the kinds of machining. Main effect plots reveal that mean value of MRR in PFM is nominally lesser than the CFM as depicted in Figure 4.21 (a) and Figure 4.21 (b).

4.4.6 Parametric analysis through interaction effects plots

An interaction plot displays the levels of one variable on X-axis and has a separate line for the means of each level of the other variable. Y-axis shows the dependent variable

or process response. Interaction plots are most often used to visualize interactions during ANOVA or DoE. In regression, an interaction effect exists when the effect of an independent variable on a dependent variable, based on the values of one or more other independent variables.

4.4.6.1 Interaction effect plots for surface roughness in CFM

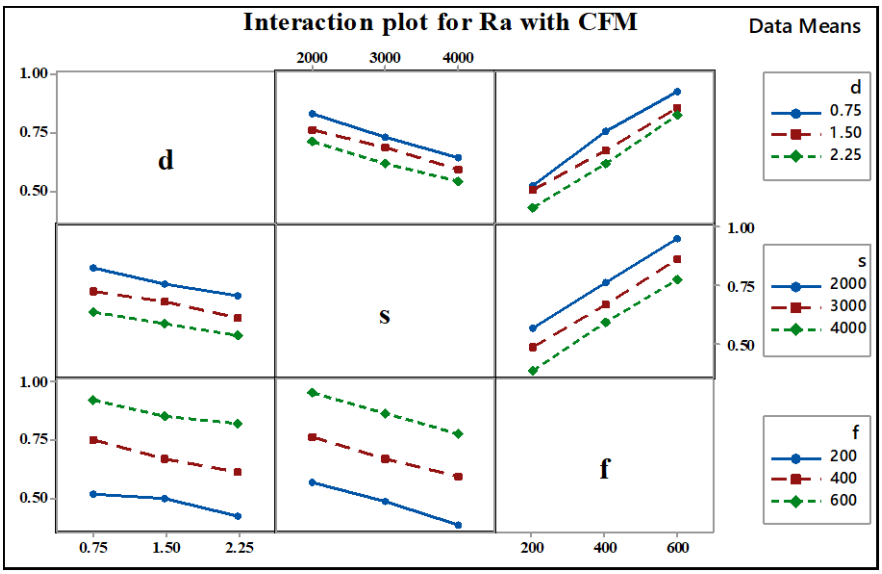

Figure 4.22 (a) Interaction affects plots for average surface roughness with CFM

Interaction plots at Figure 4.22 (a) for mean value of surface roughness obtained through CFM have been established against feed rate, cutting speed and depth of cut keeping other factors constant one at a time.

From the graph of cutting speed verses depth of cut at different values of feed rate (f: 200mm/min, 400mm/min & 600mm/min) with CFM, it is revealed that surface roughness is getting decreasing with the increase of cutting speed. It is maximum at 200mm/min, moderate at 400mm/min and least at 600mm/min of feed rate. From the slope of surface roughness verses depth of cut graphs, it is evident that increase in cutting speed causes a substantial decrease in surface roughness.

Similarly, from the graph of feed rate vs depth of cut at different values of cutting speed (s: 2000mm/min, 3000mm/min and 4000mm/min) with CFM, it is observed that surface roughness is increasing with the increase of feed rate. It is high at 2000rpm,

moderate at 3000rpm and least at 4000rpm of cutting speed. From the slope of feed rate vs depth of cut graphs, it is evident that increase in feed rate causes a considerable increase in surface roughness. And also, there is a satisfactory decrease in surface roughness with the variation of cutting speed from 2000rpm to 400rpm.

From the graph of feed rate vs cutting speed at different values of depth of cut (d: 0.75mm, 1.50mm &2.25mm) with CFM, it is revealed that surface roughness is increasing drastically with the increase of feed rate. It is maximum at 0.75mm, moderate at 1.50mm and least at 2.25mm of depth of cut. From the slope of surface roughness; it is evident that increase in feed rate causes a considerable increase in surface roughness. And also, there is a substantial increase in surface roughness with the variation of depth of cut 2.25mm to 0.75mm.

Similarly, from the graph of cutting speed vs feed rate at different values of depth of cut (d: 0.75mm, 1.5mm & 2.25mm) with CFM, it is observed that surface roughness is decreasing significantly with the increase of cutting speed. It is maximum at 2.525mm, moderate at 1.5mm and least at 0.75mm of depth of cut. From the slope of surface roughness graph, it is evident that increase in cutting speed causes a considerable decrease in surface roughness. And also, there is a huge decrease in surface roughness with the variation of depth of cut from 2.25mm 0.75mm.

From the graph of depth of cut verses feed rate at different values of cutting speed (s: 2000rpm, 3000rpm and 4000rpm) with CFM, it is implicit that there is a decrease in surface roughness with the increase of depth of cut. Value of surface roughness is high at 4000rpm, moderate at 3000rpm and its value is least at 2000rpm. There is a considerable decrease in surface roughness with the variation of cutting speed change from 4000rpm to 2000rpm.

Similarly, from the graph of depth of cut verses cutting speed at different values of feed rate (f: 200mm/min, 400mm/min and 600mm/min) with CFM, it is implicit that there is a decrease in R_a with the increase of cutting speed. Value of surface roughness is high at 0.75mm, moderate at 1.5mm and its value is least at 2.25mm. There is a negligible change in R_a with the variation of depth of cut from 0.75mm to 2.25mm.

4.4.6.2 Interaction effect plots for surface roughness in PFM

Interaction plots at Figure 4.22 (b) for mean value of surface roughness through PFM have been established against feed rate, cutting speed and depth of cut keeping other factors constant one at a time. A similar trend has been observed as that of CFM, with an improvement in the performance responses.

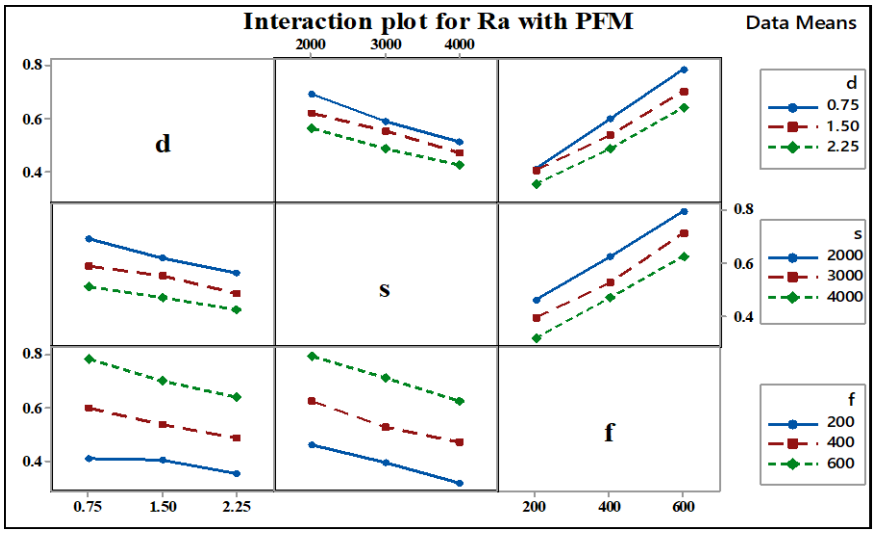

Figure 4.22 (b) Interaction effects plots for average surface roughness with PFM

4.4.6.3 Interaction effect plots for cutting tool tip temperature in CFM

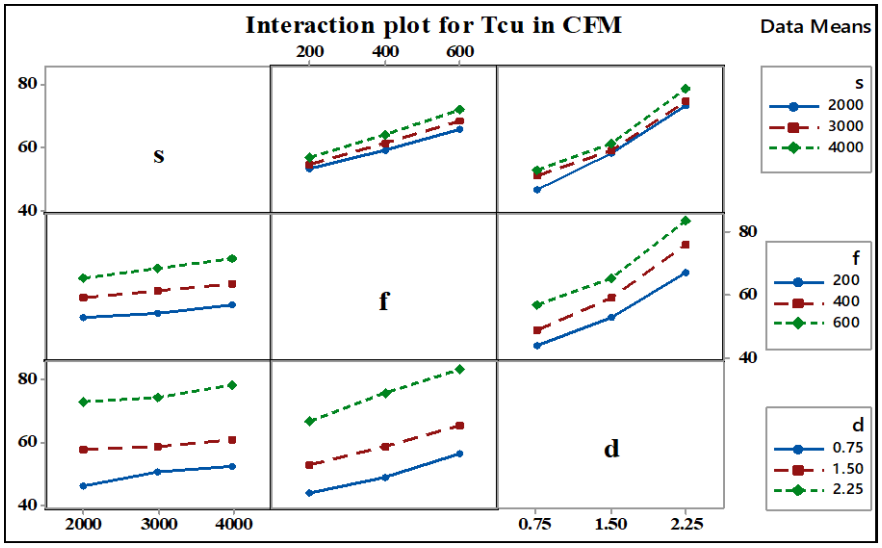

Figure 4.23 (a) Interaction effects plots for temperature on cutting tool tip with CFM

Interaction plots at Figure 4.23 (a) for mean value of cutting tool tip temperature through CFM have been drawn against feed rate, cutting speed and depth of cut keeping

other factors constant one at a time.

4.4.6.4 Interaction effect plots for cutting tool tip temperature in PFM

Interaction plots at Figure 4.23 (b) for mean value of cutting tool tip temperature through PFM have been drawn against feed rate, cutting speed and depth of cut keeping other factors constant one at a time. It is clear that PFM had yielded better results than CFM.

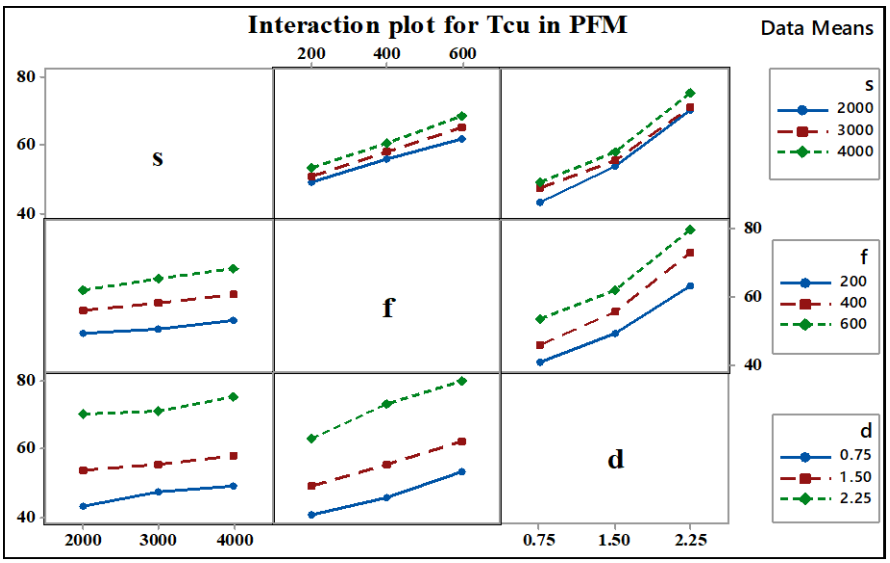

Figure 4.23(b) Interaction affects plots for temperature on cutting tool tip with PFM

4.4.6.5 Interaction effect plots for material removal rate in CFM

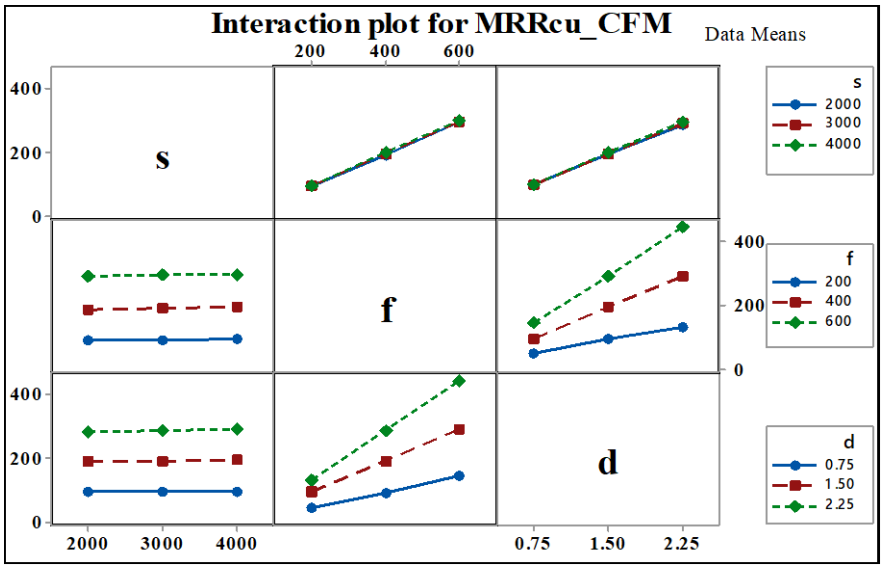

Figure 4.24 (a) Interaction affects plots for MRR with CFM

Interaction plots at Figure 4.24 (a) for mean value of material removal rate through

CFM have been drawn against feed rate, cutting speed and depth of cut keeping other factors constant one at a time.

4.4.6.6 Interaction effect plots for material removal rate in PFM

Interaction plots at Figure 4.24 (b) for mean value of material removal rate through PFM have been drawn against feed rate, cutting speed and depth of cut keeping other factors constant one at a time. PFM is giving little bit lesser MRR compared to CFM.

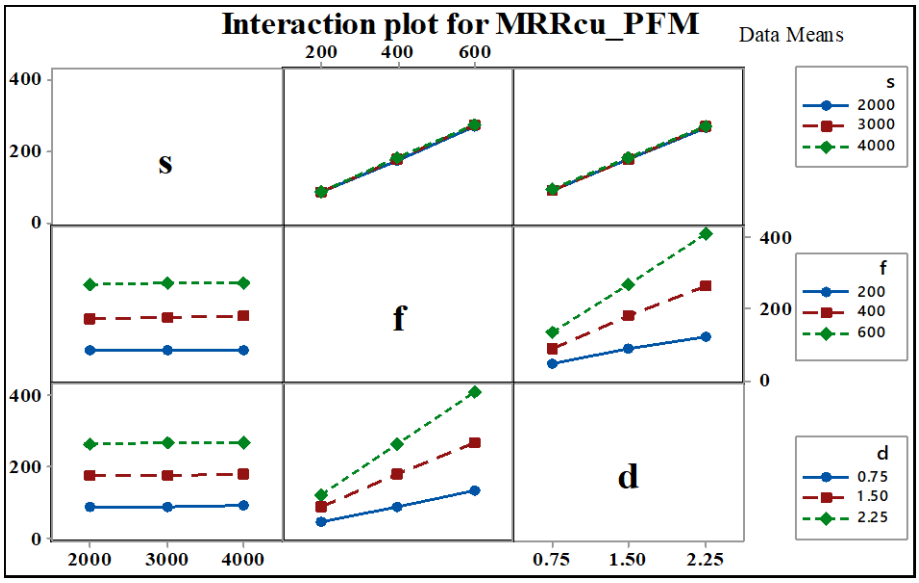

Figure 4.24 (b) Interaction affects plots for MRR with PFM

4.4.7 Parametric analysis through 3D surface plots

Surface plots are diagrams of three-dimensional data. Rather than showing the individual data points, surface plots show a functional relationship between a designated dependent variable (Y) and two independent variables (X and Z) obviously it is a companion to the contour plot.

4.4.7.1 Surface plots for surface roughness with CFM and PFM

The experimental results of surface roughness depicted in Table 4.3 have been further analysed with the help of three-dimensional surface plots. The main objective was to find the effect of input process parameters such as: feed rate, cutting speed and depth of cut on cutting tool tip temperature. Therefore, surface roughness Vs feed rate & cutting

speed, surface roughness vs feed rate & depth of cut and surface roughness vs cutting speed & depth of cut plots have been established for this study in both types of machining environments.

Figure 4.25 (a) and Figure 4.25 (b) represents the effect of feed rate and cutting speed on surface roughness in constant feed machining and progressive feed machining respectively. Better surface finish is attainable at high cutting speed and low feed rate in both the cases of machining. However, PFM has yielded still better average surface roughness over CFM at this combination of high cutting speed and low feed rate.

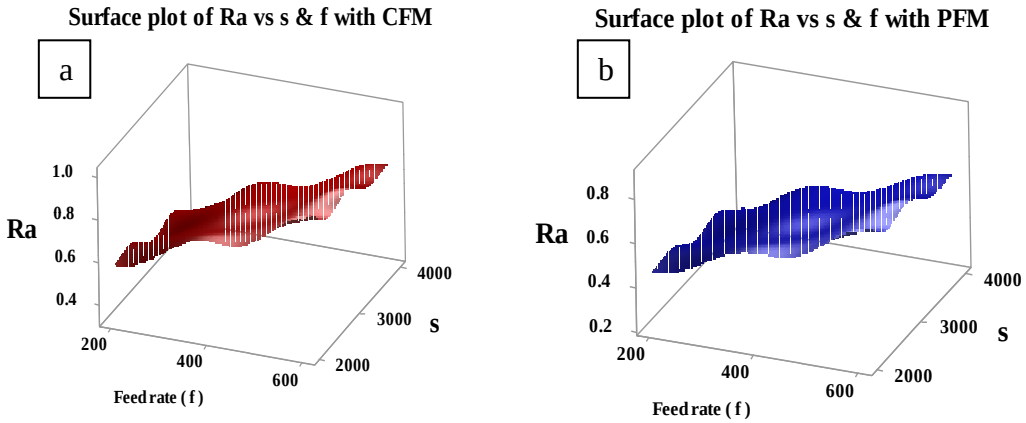

Figure 4.25 Variation of R_a w.r.t Feed rate and Cutting speed with (a) CFM& (b) PFM

Figure 4.26 (a) and Figure 4.26 (b) represents the effect of feed rate and depth of cut on surface roughness in constant feed machining and progressive feed machining respectively. It is clear from these plots that, progressive feed machining yields relatively better surface finish in comparison to constant feed machining. Even though, there is no much influence of DoC on average surface roughness, better surface finish is attainable at low depth of cut and low feed rate in both the cases of machining. However, PFM has yielded still better average surface roughness over CFM at this combination of high depth of cut and low feed rate.

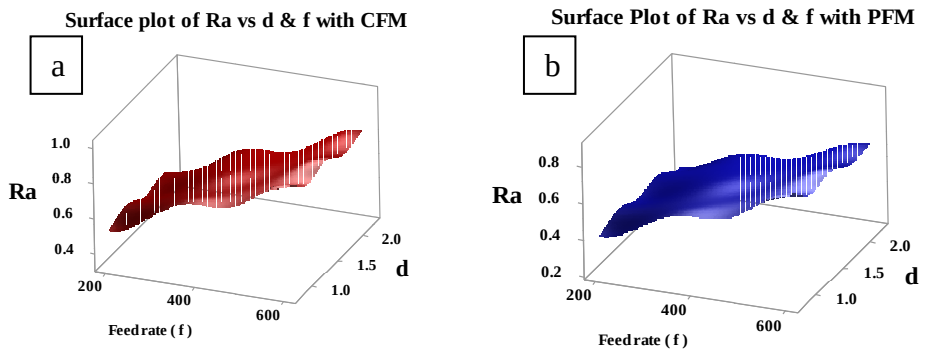

Figure 4.26 Variation of R_a w.r.t Feed rate and Depth of cut with (a) CFM and (b) PFM

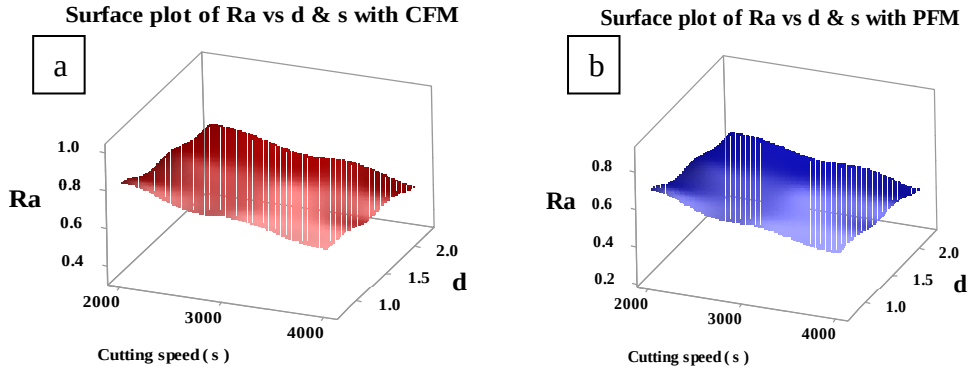

Figure 4.27 Variation of Ra w.r.t Cutting speed and Depth of cut with (a) CFM and (b) PFM

Figure 4.27 (a) and Figure 4.27 (b) represents the effect of cutting speed and depth of cut on surface roughness in constant feed machining and progressive feed machining respectively. It reveals that, progressive feed machining yields relatively better surface finish in comparison to constant feed machining. Even though there is no much influence of DoC on average surface roughness, better surface finish is attainable at low depth of cut and low feed rate in both the cases of machining. However, PFM has yielded still better average surface roughness over CFM at this combination of high depth of cut and low feed rate.

From 3D surface plots it is understood that, feed rate and cutting speed are the most influential cutting parameters on average surface roughness. At higher values of cutting speed and lower value of feed rate better surface finish is possible. However, DoC is not showing much influence on R_a.

4.4.7.2 Surface plots for cutting tool tip temperature with CFM and PFM

The experimental data of cutting tool tip temperature depicted in Table 4.3 has been further analysed with the help of three-dimensional surface plots. The main objective

was to find the effect of input parameters on the performance response: cutting tool tip temperature. Therefore, cutting tool tip temperature vs feed rate & cutting speed, cutting tool tip temperature vs feed rate & depth of cut and cutting tool tip temperature vs cutting speed & depth of cut plots have been established for this study for both types of machining environments.

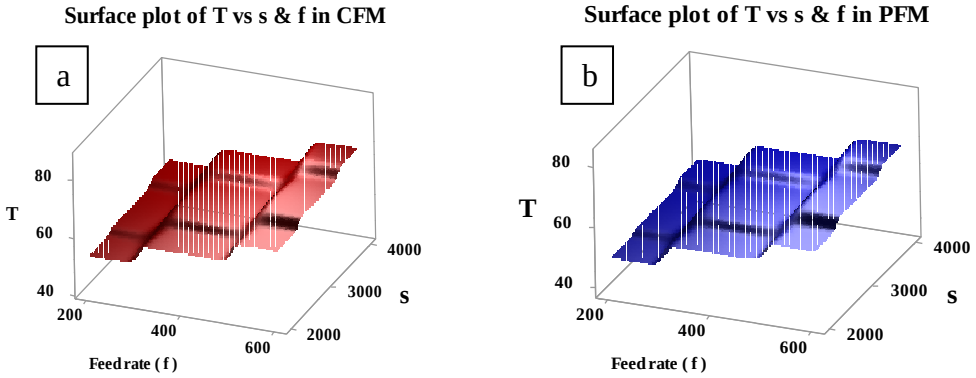

Figure 4.28 Variation of T w.r.t Feed rate and Cutting speed with (a) CFM and (b) PFM

Figure 4.28 (a) and figure 4.28 (b) represents the effect of feed rate and cutting speed on cutting tool tip temperature in constant feed machining and progressive feed machining respectively. Rise in cutting tool tip temperature is low at low value of feed rate and low value of cutting speed. It also reveals that, progressive feed machining produced further lower cutting tool tip temperature over constant feed machining at low level of feed rate and low level of cutting speed.

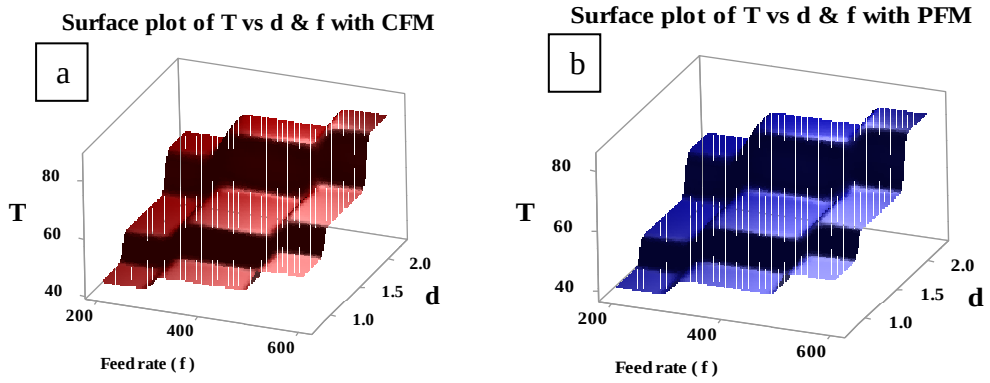

Figure 4.29 Variation of T w.r.t Feed rate and Depth of cut with (a) CFM and (b) PFM

Figure 4.29 (a) and figure 4.29 (b) represents the effect of feed rate and depth of cut on cutting tool tip temperature in constant feed machining and progressive feed machining respectively. It is clear from these plots that in progressive feed machining the rise in

cutting tool tip temperature is less when comparing with constant feed machining. Rise in cutting tool tip temperature is low at low value of feed rate and low value of cutting speed. It also reveals that, progressive feed machining produced further lower cutting tool tip temperature over constant feed machining at low level of feed rate and low level of cutting speed.

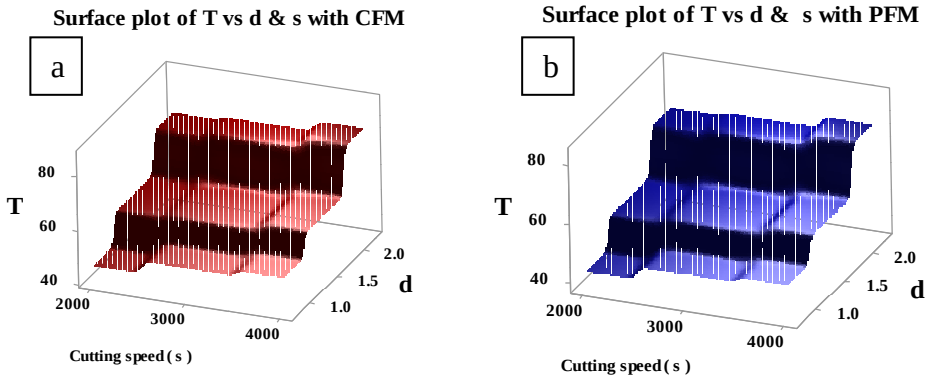

Figure 4.30 Variation of T w.r.t Cutting speed and Depth of cut with (a) CFM and (b) PFM

Figure 4.30 (a) and Figure 4.30 (b) represents the effect of feed rate and depth of cut on cutting tool tip temperature in constant feed and progressive feed machining respectively. It is clear from these plots that in progressive feed machining the rise in cutting tool tip temperature is less when comparing with constant feed machining. Low value of rise in cutting tool tip temperature was observed at low value of cutting speed and low value of depth of cut combination. It also reveals that, PFM has produced further lower of cutting tool tip temperature over CFM at low level of cutting speed and low level of depth of cut.

4.4.7.3 Surface plots for material removal rate with CFM and PFM

The experimental data of MRR depicted in Table 4.3 has been further analysed with the help of three-dimensional surface plots. The main agenda was to find the effect of feed rate, depth of cut and cutting speed on MRR. Figure 4.31 (a) and Figure 4.31 (b) represents the effect of feed rate and cutting speed on material removal rate in constant feed machining and progressive feed machining respectively. MRR is more at higher values of feed rate and it is increasing proportionately wit feed rate. But cutting speed is not showing considerable influence on MRR. It is also understood that in progressive feed machining the material removal rate is marginally less when compared to CFM.

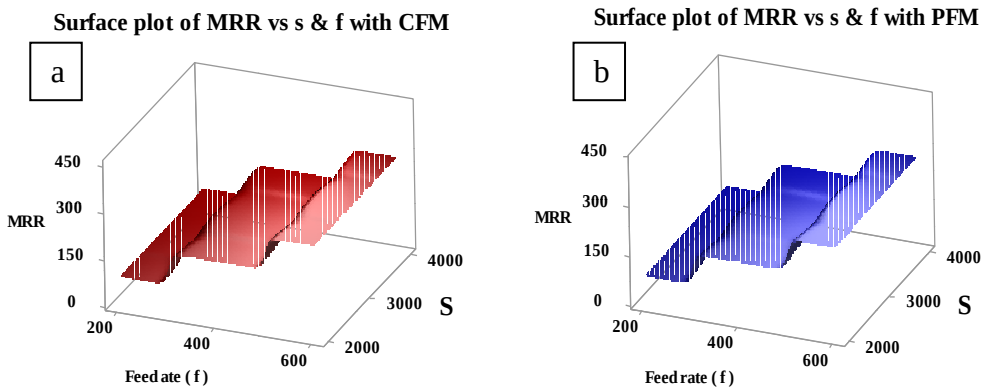

Figure 4.31 Variation of MRR w.r.t Feed rate and Cutting speed with (a) CFM and (b) PFM

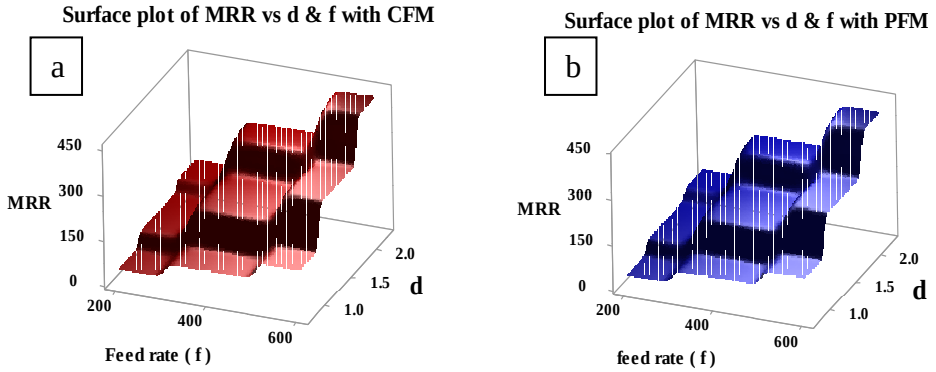

Figure 4.32 Variation of MRR w.r.t Feed rate and Depth of cut with (a) CFM and (b) PFM

Figure 4.32 (a) and Figure 4.32 (b) represents the effect of feed rate and depth of cut on material removal rate in constant feed and progressive feed machining respectively. Depth of cut is showing much influence on MRR. It is clear from the plot that, higher value of MRR is possible at higher value of DoC and higher value of feed rate. However, it is understood from these plots that, in PFM the material removal rate is marginally less when compared to CFM.

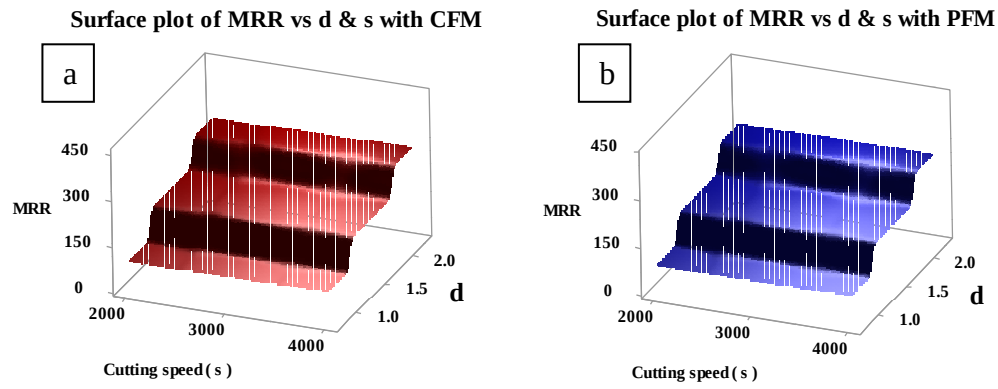

Figure 4.33 Variation of MRR w.r.t Cutting speed and Depth of cut with (a) CFM and (b) PFM

Figure 4.33 (a) and Figure 4.33 (b) represents the effect of Cutting speed and Depth of cut on material removal rate in constant feed and progressive feed machining respectively. It is understood from these plots that, MRR is increasing with the increase of depth of cut. Higher values of MRR are possible at high value of depth of cut and feed rate. But cutting speed is not having much influence on MRR. It also reveals that, progressive feed machining produced little bit lower MRR over constant feed machining. It is mainly duly restricting the feed rate at the start of each cut.

4.4.8 Parametric analysis through contour plots

Contour plots are used to show a three-dimensional surface on a two-dimensional plane. Basically, it shows how a response variable relates to two predictor variables simultaneously. Contour line will connect the points that have the same output response value. Contour colored bands will represent the range of output response values.

4.4.8.1 Contour plots for surface roughness

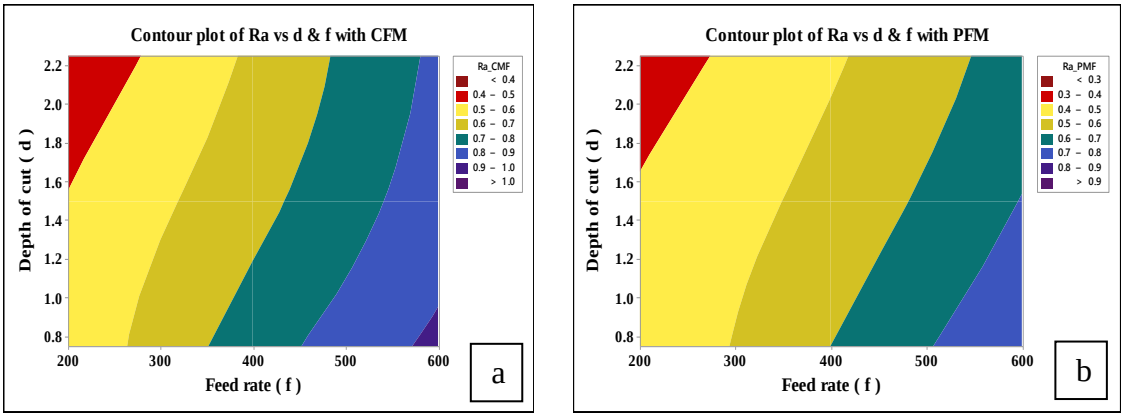

Figure 4.34 Variation of R_a w.r.t Feed rate and DoC with (a) CFM and (b) PFM

Figure 4.34 (a) and Figure 4.34 (b) illustrates the three-dimensional variation of surface roughness on a two-dimensional plane of feed rate vs depth of cut in constant feed machining and progressive feed machining respectively. Almost a similar trend has been observed in both the kind of machining, but PFM yielded better results over CFM. It is clear from these plots that, progressive feed machining yields relatively better surface finish in comparison to constant feed machining.

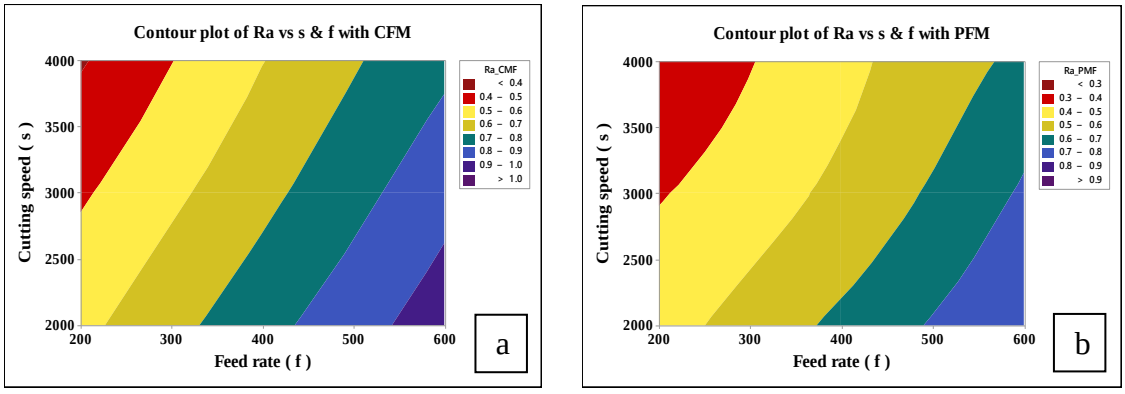

Figure 4.35 Variation of R_a w.r.t Feed rate and Cutting speed with (a) CFM and (b) PFM

Figure 4.35 (a) and Figure 4.35(b) illustrates the three-dimensional variation of surface roughness on a two-dimensional plane of feed rate Vs cutting speed in constant feed machining and progressive feed machining respectively. It is clear from these plots that, progressive feed machining yields relatively better surface finish in comparison to constant feed machining.

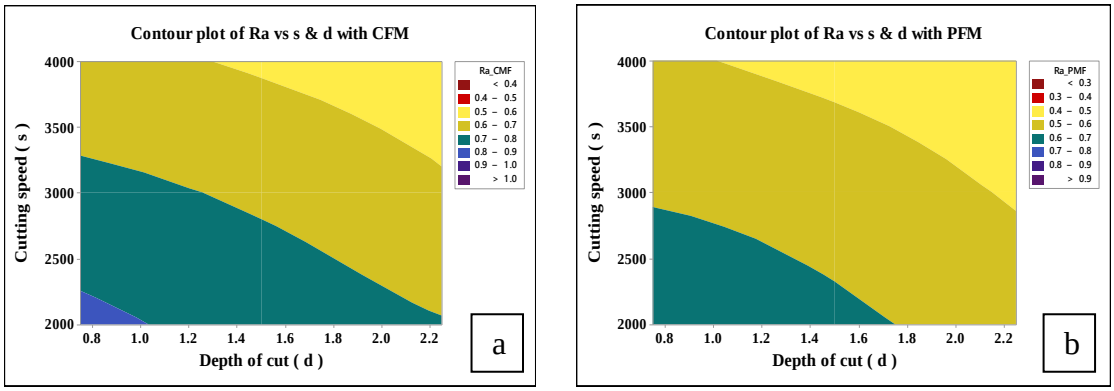

Figure 4.36 Variation of R_a w.r.t DoC and cutting speed with (a) CFM and (b) PFM

Figure 4.36 (a) and Figure 4.36(b) illustrates the three-dimensional variation of surface roughness on a two-dimensional plane of depth of cut Vs cutting speed in constant feed machining and progressive feed machining respectively. It is well understood from the main effects plots, interaction plots, 3D surface plots and contour plots that progressive feed machining is a good solution, for machining the aerospace components, which requires fine surface finishes and also it avoids additional finishing operations like bench work and save the machining time.

4.4.8.2 Contour plots for cutting tool tip temperature

Contour plots are used to show a three-dimensional surface on a two-dimensional

plane. Basically, it shows how a response variable relates to two predictor variables simultaneously. Contour line will connect the points that have the same output response value. Contour coloured bands will represent the range of output response values. Figure 4.37 (a) to figure 4.39 (b) illustrates the three-dimensional variation of cutting tool tip temperature against various combinations of input machining process parameters like: feed rate vs DoC, feed rate vs cutting speed and DoC vs cutting speed.

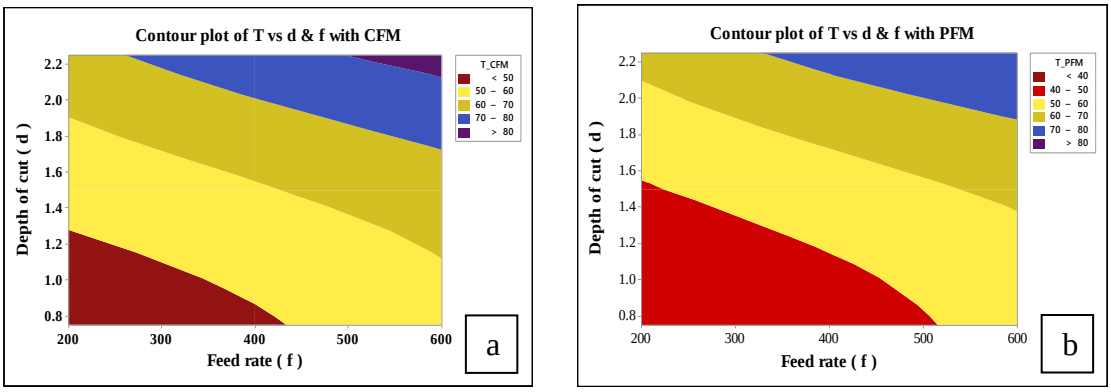

Figure 4.37 Variation of T w.r.t Feed rate and DoC with (a) CFM and (b) PFM

Figure 4.37 (a) and Figure 4.37 (b) illustrates the three-dimensional variation of cutting tool tip temperature on a two-dimensional plane of feed rate verses depth of cut in constant feed machining and progressive feed machining respectively. It is clear from these plots that, progressive feed machining yields relatively better surface finish in comparison to constant feed machining.

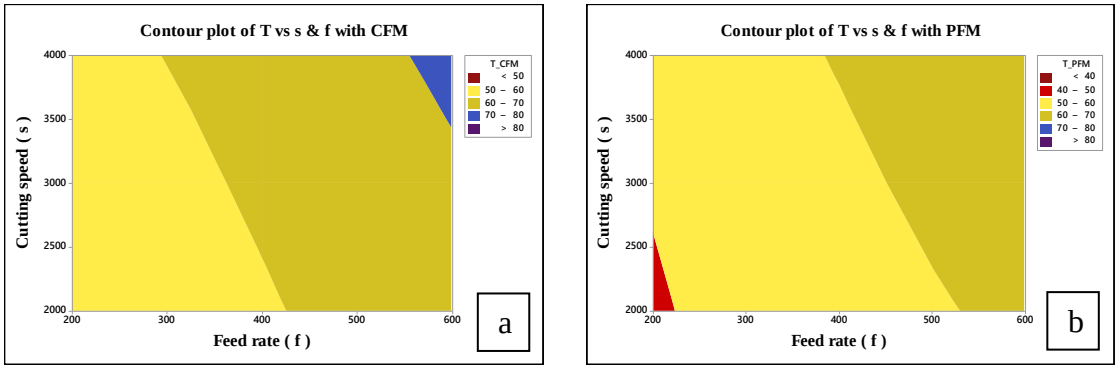

Figure 4.38 Variation of T w.r.t Feed rate and Cutting speed with (a) CFM and (b) PFM

Figure 4.38 (a) and Figure 4.38(b) illustrates the three-dimensional variation of cutting tool tip temperature on a two-dimensional plane of feed rate verses cutting speed in constant feed machining and progressive feed machining respectively. It is clear from

these plots that, progressive feed machining yields relatively better surface finish in comparison to constant feed machining.

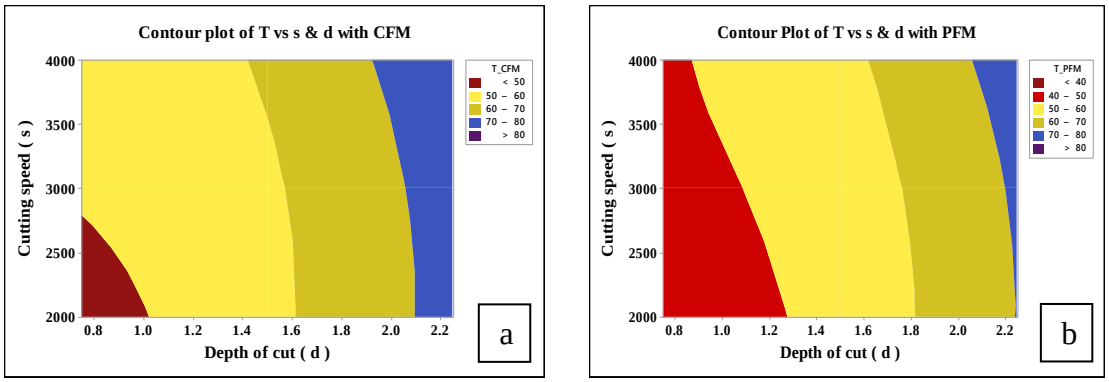

Figure 4.39 Variation of T w.r.t Cutting speed and DoC with (a) CFM and (b) PFM

Figure 4.39 (a) and Figure 4.39 (b) illustrates the three-dimensional variation of cutting tool tip temperature on a two-dimensional plane of depth of cut verses cutting speed in constant feed machining and progressive feed machining respectively.

It is well understood from the main effects plots, interaction plots, 3D surface plots and contour plots that progressive feed machining is a good solution for machining the aerospace components, which requires fine surface. PFM gives lower cutting tool tip temperature and in turn better tool life and better surface topography.

4.4.8.3 Contour plots for material removal rate

Figure 4.40 (a) to Figure 4.42 (b) illustrates the three-dimensional variation of material removal rate against various combinations of input machining parameters like: feed rate vs DoC, feed rate vs cutting speed and DoC vs cutting speed.

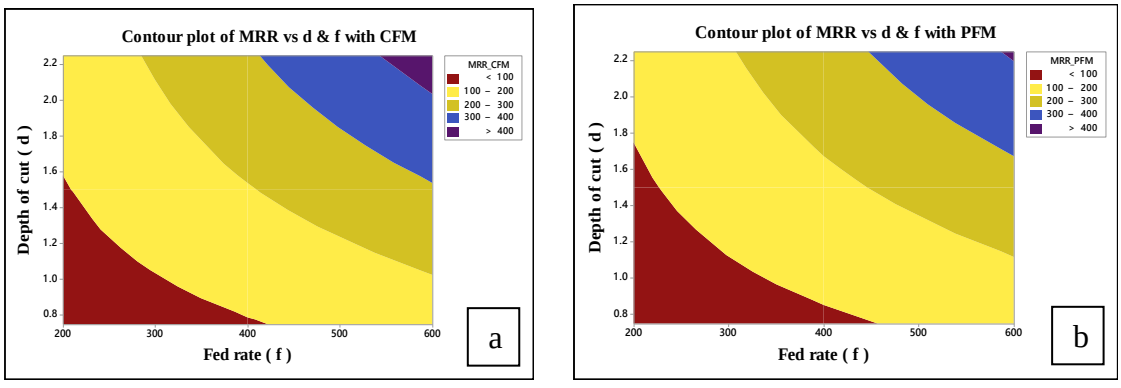

Figure 4.40 Variation of MRR w.r.t Feed rate and DoC with (a) CFM and (b) PFM

Figure 4.40 (a) illustrates the three-dimensional variation of material removal rate on a two-dimensional plane of feed rate verses depth of cut in constant feed machining. Whereas, Figure 4.40 (b) illustrates the three-dimensional variation of material removal rate on a two-dimensional plane of feed rate verses depth of cut in progressive feed machining. Figure 4.41 (a) illustrates the three-dimensional variation of material removal rate on a two-dimensional plane of feed rate Vs cutting speed in constant feed machining. Figure 4.41 (b) illustrates the three-dimensional variation of material removal rate on a two-dimensional plane of feed rate Vs cutting speed in progressive feed machining.

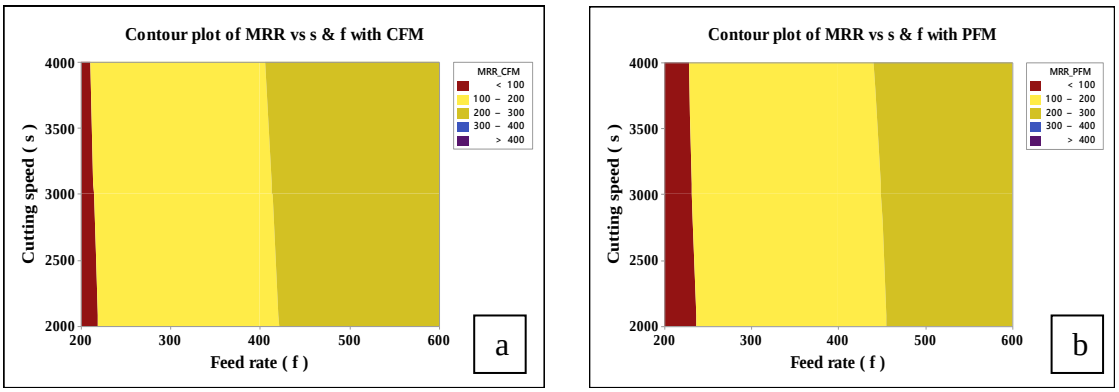

Figure 4.41 Variation of MRR w.r.t Feed rate and Cutting speed with (a) CFM and (b) PFM

Figure 4.42 (a) illustrates the three-dimensional variation of material removal rate on a two-dimensional plane of cutting speed vs depth of cut in constant feed machining. Figure 4.42(b) illustrates the three-dimensional variation of material removal rate on a two-dimensional plane of cutting speed vs depth of cut in constant feed machining.

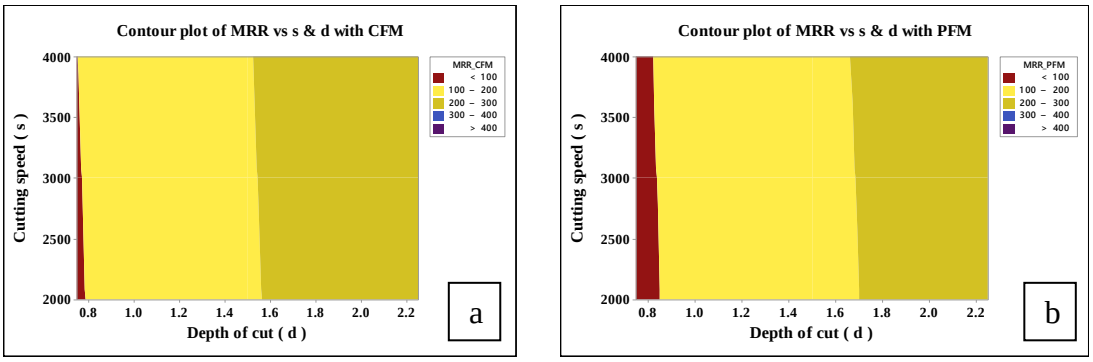

Figure 4.42 (a) Variation of MRR w.r.t Cutting speed and DoC with (a) CFM and (b) PFM

It is well understood from the main effects plots, interaction plots, 3D surface plots and

contour plots that progressive feed machining is a good solution for machining the aerospace components which requires fine surface finish. It also minimises the cutting tooltip temperature and there by increases tool life. But there is a negligible reduction in material removal rate.

4.5 CLOSURE

The effect of cutting process parameters; cutting speed, feed rate and depth of cut on the considered performance responses: surface roughness, cutting tool tip temperature and material removal rate during machining of BS L168 alloy has been analysed through RSM modelling. Experiments were conducted as per the Taguchi's L_{27} factorial method in both the types of machining. Then ANOVA has been carried out in order to find out the most influential cutting parameter on each performance response. This will help in controlling such a significant factor accordingly in achieving the desired quality response. Further, from the experimental results of performance characteristics linear regression mathematical equations were developed by means of RSM technique. These developed regression models will help us in determining or predicting the required combination of input process parameters to achieve desired performance responses. Then correlation and confirmation plots have been established to find out the level of agreement or level of fit between experimental and predicted values. Later model fitness check plots such as: Normal probability plots of residuals, plots of residuals Vs predicted response and plot of residual Vs order of predicted response have been established to check the fitness of developed regression models. Further, parametric analysis through main effects plots, interaction plots, three-dimensional surface plots and contour plots have been carried out to express the effect of input process parameters graphically on the performance characteristics. From the attained results, subsequent conclusions have been derived from this chapter as follows:

- Progressive feed machining with un-coated cutting tools offered considerable reduction in average surface roughness by 19.206%, reduction in cutting tool tip temperature by 5.63% over conventional constant feed machining with same cutting tools (Table 4.3). Progressive feed machining with coated cutting tools offered considerable reduction in average surface roughness by 29.48%, reduction

in cutting tool tip temperature by 12.67% over conventional constant feed machining with same cutting tools (Table 4.3). It is due to reduction in sudden impact of cutting tool with workpiece; reduction in cutting tool deflection, minimal tool vibration, less chattering and avoidance of rubbing in progressive feed machining has contributed to substantial drop in the aforesaid response.

- Progressive feed machining also causes a negligible reduction in material removal rate over conventional constant feed machining (Table 4.3). It is mainly due to controlling the sudden increase of feed rate at start of each cut.

- Predicted values of surface roughness from the developed regression models are in good agreement with the experimental results. Errors, in constant feed machining and progressive feed machining are only 2.56% and 5.08%respectively. Predicted values of cutting tool tip temperature from the developed regression models are in good agreement with the experimental results. Errors, in constant feed and progressive feed machining are only 2.789% and 3.175% respectively. The predicted values of material removal rate from the developed regression models are in good agreement with the experimental results. Errors, in constant feed and progressive feed machining are only 1.80% and 1.68% respectively. These errors are mainly due to uncontrollable variables like: chip loads, chip formation, tool wear and unexpected variations in power supply and rigidity of the machine tool, etc.

- From the ANOVA analysis it is implicit that, feed rate has the fore most influence on surface roughness (R_a) both in constant feed machining as well as in progressive feed machining.

- The normal probability plot of residuals {Figure 4.10 (a) & (b), Figure 4.13 (a) & (b) and Figure 4.16 (a) & (b)} were normally distributed, since the model residuals are following the path of straight line. Main effect plots, Interaction plots and 3D surface plots revealed that the output response (R_a) is drastically increasing with the increase of feed rate in both the types of machining.

- Better surface finish can be attained by incorporating lower feed rate, with higher cutting speed and higher depth of cut for the aforesaid material. This work also emphasizes that proper selection of cutting parameters along with progressive feed machining eliminates the use of secondary finishing operations and hence saves the manufacturing time and cost.

- This work can be aimed to extend with hard-to-machine aerospace materials, such as Titanium, Nimonic alloys, Steel and Composite materials as well in the future study of progressive feed machining. More process responses may be considered for study, such as tool wear, tool vibration, tool deflection, tool tip temperature, cutting force, surface waviness, surface flatness, MRR and power consumption etc.

CHAPTER 5

ONE FACTOR AT A TIME EXPERIMENTAL ANALYSIS

5.1 INTRODUCTION

One factor at a time (OFAT) approach of experimental procedure explains the effect of individual cutting parameters on machining performance characteristics such as: cutting tool tip temperature, surface roughness, material removal rate and surface topography. Sharp edges of a cutting tool may cause breakage of the same while doing machining. In order to avoid this sudden breakage of tool corners, will be rounded off to some radius. This rounding off, of the cutting tool edge forms nose radius (NR), which helps in distributing the cutting force uniformly across the corners, helping to prevent chipping, to reduce tool wear and causes to extend the tool life. But nose radius beyond certain limit will have bad effects on performance responses. Hence, there is a need to find the better value of NR for a particular application in order to obtain good output responses. OFAT approach of experimental design was considered to know the effect of individual process controllable factors on machining performance characteristics in which one factor varies at one time and others were kept constant at their average levels. Many researchers have used OFAT approach of experimental design in their research works (Sharma et al. 2015; Manjaiah et al. 2016; Manna 2013). Table 3.15 shows the format ofL_{15}Orthogonal Array used for OFAT approach of experimentation, indicating *v3*, *f3* and *d3*as the mean levels of cutting velocity (*v*), feed rate (*f*) and depth of cut (*d*) respectively.

5.2 OFAT EXPERIMENTAL PLAN

End milling experiments were performed on BS L168 aluminium alloy test specimen of size 100mmx80mmx20mm on an AMS make three axis vertical CNC milling machining centre. Specimens were cut from a single billet of BS L168 aluminium alloy, in order to get uniform chemical and mechanical properties all over the test coupons.

Table 5.1 Experimental results from the OFAT design of experimentation

Exp run	Controllable process parameters			Nose radius: 0.4mm			Nose radius: 0.8mm			Nose radius: 1.2mm		
	Cutting Speed (*v*)	Feed rate(*f*)	Depth of cut (*d*)	Ra µm	T ^{0}C	MRR mm^3/sec	Ra µm	T ^{0}C	MRR mm^3/sec	Ra µm	T ^{0}C	MRR mm^3/sec
1	*v1*	*f3*	*d3*	1.05	63.4	438.56	0.90	77.3	431.21	0.76	89.1	413.96
2	*v2*	*f3*	*d3*	0.93	66.9	444.12	0.82	77.2	432.78	0.69	91.7	415.47
3	*v3*	*f3*	*d3*	0.861	71.38	454.62	0.74	83.1	434.03	0.62	103.7	419.62
4	*v4*	*f3*	*d3*	0.82	79.8	449.65	0.71	90.4	438.23	0.57	107.8	430.82
5	*v5*	*f3*	*d3*	0.82	82.3	459.87	0.72	93.7	446.41	0.61	110.7	438.95
6	*v3*	*f1*	*d3*	0.39	52.2	159.67	0.34	64.8	138.26	0.31	73.8	125.56
7	*v3*	*f2*	*d3*	0.64	66.4	310.65	0.57	73.6	284.28	0.48	92.7	262.91
8	*v3*	*f3*	*d3*	0.86	71.4	454.617	0.739	83.1	434.027	0.62	103.7	419.62
9	*v3*	*f4*	*d3*	0.99	84.5	591.08	0.80	99.7	550.02	0.72	119.9	511.98
10	*v3*	*f5*	*d3*	1.18	88.6	759.18	0.98	106.8	712.35	0.82	129.8	636.52
11	*v3*	*f3*	*d1*	0.97	47.2	162.79	0.83	55.4	143.07	0.73	66.7	132.35
12	*v3*	*f3*	*d2*	0.89	50.6	323.66	0.76	63.2	291.98	0.64	80.9	270.32
13	*v3*	*f3*	*d3*	0.861	71.38	454.62	0.74	83.1	434.03	0.62	103.7	419.616
14	*v3*	*f3*	*d4*	0.86	86.8	613.87	0.75	101.6	580.32	0.62	124.5	527.21
15	*v3*	*f3*	*d5*	0.87	88.4	795.23	0.77	107.2	731.04	0.67	130.7	694.81

Chemical composition of BS L168Al alloy has been confirmed by means of spectroscopy. One Factor at A Time approach of experimental design was considered here to know the effect of each input process parameter on the output machining performance characteristics. Surface roughness, cutting tool tip temperature, material removal rate and surface topography are the investigative machinability characteristics considered in this chapter. Experimental values of cutting tool tip temperature, average surface roughness and material removal rate have been depicted in the Table 5.1. The selection of range and levels of controllable process parameters considered for conducting experiments were finalized based on the trial runs, tool catalogues and from the literature. Three number of uncoated solid end mills of diameter: 20mm, rake angle of 16^0, with two flutes and nose radii of 0.4mm, 0.8mm and 1.2mm have been considered for this experimentation. Cutting speed varies from 2000rpm (2.09m/sec) to 6000rpm (6.282m/sec), feed rate varies from 200mm/min (0.1mm/rev) to 1000mm/min (0.1667mm/rev) and depth of cut varies from 0.75mm to 3.75mm. All these cutting parameters are increased in five levels from minimum to maximum value in order to obtain smooth and extended form of plots for better understanding.

Cutting tool tip temperature has been measured by taking average of three readings taken on the cutting tool tip from three different directions immediately after completion of each experimental run. An industrial infrared non-contact type digital thermometer has been used for this purpose. Average surface roughness was measured by taking average of three readings measured at three different locations on the machined surface of the test specimen. Then surface topography was observed with the help of optical microscope. Material removal rate was measured after each experimental run by taking the dimensions of milling slot made and feed rate in to consideration and then compared with weight reduction method of material removal rate. Each specimen has been weighted using afore said digital weighing machine before and after each experimental run. MRR has been calculated after each machining run using weight loss method and computed from equation 3.3 (Refer section: 3.7.3 of chapter-3) and then cross verified with equation 5.1. Essae DS-852 model digital weighing scale has been used for measuring weight of the workpieces before and after making each milling slot as shown in Figure 3.13 (Refer section: 3.7.3 of Chapter-3). The material removal rate for end milling operation has been calculated against each experimental run by the equation 5.1(Parida and Maity, 2017).

$$\text{MRR} = \frac{W*D*L}{t} \quad \ldots\ldots\ldots\ldots\ldots\ldots\ldots\ldots \quad (5.1)$$

Where, W is the width of milling slot in mm,

D is the depth of milling slot in mm,

L is the length of milling slot in mm and

't' is the time taken to form the milling slot in sec.

5.3 ANALYSIS OF THE EFFECT OF INPUT PROCESS PARAMETERS ON PERFORMANCE CHARACTERISTICS

One Factor at A Time (OFAT) approach of experimentation and corresponding readings for cutting tool tip temperature; surface roughness and material removal rate are depicted in Table 5.1. The influence of considered input process parameters is analysed with the help of established 2D plots by using MINITAB-18 statistical analysis software.

5.3.1 Effect of input process parameters on cutting tooltip temperature with different nose radii end mills

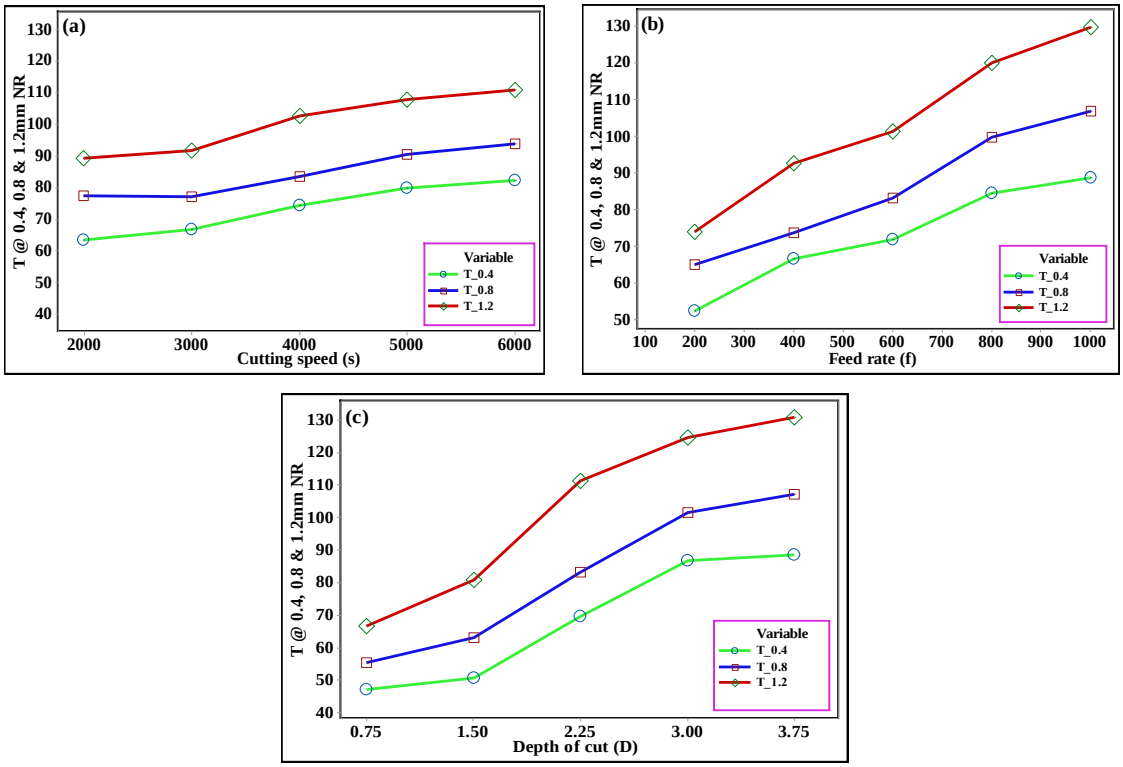

Figure 5.1 Effect of (a) cutting speed (b) feed rate and (c) depth of cut on T with different nose radii by keeping all other factors constant at their respective mean values.

Figure 5.1(a) to Figure 5.1(c) illustrates the influence of input process parameters on

cutting tool tip temperature as a performance characteristic.

5.3.1.1 Effect of cutting speed on cutting tool tip temperature

Figure 5.1(a) represents the cutting tool tip temperature obtained with different nose radii end mills under dry cutting environment with the variation of cutting speed from 2000rpm (2.094m/sec) to 6000rpm (6.282m/sec) in five levels by keeping other process parameters; feed rate and depth of cut constant at their average levels of 600mm/min (0.15mm/rev) and 2.25mm respectively. It is a matter-of-fact that, cutting tool tip temperature increased with the increase of cutting speed for the considered nose radii of the cutting tool. This might be due to, the development of more friction between the tool and workpiece with the increase of cutting speed. The rise in cutting tool tip temperature is comparatively more with 1.2mm nose radius end mill than with 0.8mm and 0.4mm nose radius at any given point of cutting speed within the range of selection. This is due to more contact area in cutting zone in case of 1.2mm nose radii over 0.8mm & 0.4mm nose radii end mills and in turn due to more friction between the tool and workpiece in the cutting zone.

It can be seen from the Figure 5.1 (a) and Table 5.1 that at low level of cutting speed 2000rpm (2.09m/sec) the obtained cutting tool tip temperature is 63.4^0C, 77.3^0C and 89.1^0C with 0.4mm, 0.8mm and 1.2mm nose radius respectively. Similarly, at high level of cutting speed 6000rpm (6.28m/sec) the obtained tool tip temperature is 82.3^0C, 93.7^0C and 110.7^0C with 0.4mm, 0.8mm and 1.2mm nose radii respectively. The percentage increase in cutting tool tip temperature w.r.t increase in cutting speed from 2000rpm (2.09m/sec) to 6000rpm (6.28m/sec) is 29.81%, 21.22%, and 24.24% with the cutting tool nose radius of 0.4mm, 0.8mm and 1.2mm respectively.

5.3.1.2 Effect of feed rate on cutting tool tip temperature

Figure 5.1 (b) represents the cutting tool tip temperature obtained with different nose radii under dry cutting environment with the variation of feed rate from 200mm/min (0.1mm/rev) to 1000mm/min (0.167m/sec) keeping other process parameters depth of cut and cutting speed kept constant at their average levels 2.25mm and 4000rpm (4.188m/sec) respectively. It is pragmatic that, cutting tool tip temperature increased

with the increase of feed rate at the considered nose radii of the cutting tool. This might be due to more relative movement between cutting tool and workpiece in the cutting zone and hence development of more friction between the tool and workpiece with the increase of feed rate and cutting speed. In this case also, the rise in cutting tool tip temperature is relatively more with 1.2mm nose radius end mill compared to 0.8mm and 0.4mm nose radii tools for a given value of cutting speed within the range of selection. This is due to more contact area between the cutting tool and workpiece in the cutting zone in case of 1.2mm nose radius than 0.8mm & 0.4mm nose radii and in turn development of more friction between the tool and workpiece in the cutting zone.

It can be seen from the Figure 5.1 (b) and Table5.1 that at low level of feed rate: 0.1mm/rev (200mm/min) the obtained cutting tool tip temperature is 52.2^0C, 64.8^0C and 73.8^0C with 0.4mm, 0.8mm and 1.2mm nose radii respectively. Similarly, at a high level of feed rate: 0.167mm/rev(1000mm/min) the obtained cutting tool tip temperature is 88.6^0C, 106.8^0C, and 129.8^0C, with 0.4mm, 0.8mm and 1.2mm nose radii respectively. The percentage increase in cutting tool tip temperature w.r.t increase in feed rate from 0.1mm/rev (200mm/min) to 0.167mm/rev (1000mm/min) is 69.16%, 64.82%, and 75.88% with the end mill nose radii of 0.4, 0.8 and 1.2mm respectively.

5.3.1.3 Effect of depth of cut on cutting tool tip temperature

Figure 5.1 (c) represents the cutting tool tip temperature obtained with different nose radii under dry machining environment with the variation of depth of cut from 0.75mm to 3.75mm keeping other process parameters feed rate and cutting speed constant at their average levels 600mm/min(0.15mm/rev) and 4000rpm (4.188m/sec) respectively. It is evident that, cutting tool tip temperature increases with the increase of depth of cut for considered nose radii of the cutting tool. It is due to, with the increase in depth of cut, cutting tool need to maintain more contact area with the workpiece and hence more cutting force is required to remove the material layers from the workpiece. This will develop more frictional force between the tool and workpiece and causes excess heat generation in the cutting zone. Hence, this excess heat generation in machining zone leads to rapid tool tip temperature. In this case also, the rise in cutting tool tip temperature is relatively more with 1.2mm nose radius cutting tool compared to 0.8mm and 0.4mm nose radii tools at a particular value of depth of cut within the range of

selection. This is due to more contact area between the cutting tool and workpiece in the cutting zone in case of 1.2mm nose radius cutting tool than 0.8mm & 0.4mm nose radii and in turn development of more friction between the tool and workpiece in the cutting zone.

It can be seen from the Figure 5.1 (c) and Table 5.1 that at low level of depth of cut (0.75mm) the obtained cutting tool tip temperature is 47.2^0C, 55.4^0C and 66.7^0C with 0.4mm, 0.8mm and 1.2mm respectively. Similarly, at a high level of depth of cut (3.25mm) the obtained cutting tool tip temperature is 88.4^0C, 107.2^0C and 130.7^0C with 0.4mm, 0.8mm and 1.2mm nose radii respectively. The percentage increase in cutting tool tip temperature w.r.t increase in depth of cut from 0.75mm to 3.75mm is 87.29%, 93.50%, and 95.95% with the cutting tool nose radii 0.4mm, 0.8mm and 1.2mm respectively. Hence, from section 3.1.1, 3.1.2 and 3.1.3 of chapter-3, it is implicit that depth of cut is having highest influence on cutting tool tip temperature followed by feed rate with moderate influence and cutting speed is having least influence.

From Figures 5.1 (a) to Figure5.1 (c) it is observed that the cutting tool tip temperature increases with the increase of cutting speed, feed rate and depth of cut as well. Because cutting tool tip temperature has a directly propositional relationship with these controllable process parameters, thus causes increase in T. But the influence of depth of cut is high over cutting tool tip temperature compared to other two factors.

5.3.2 Effect of input process parameters on material removal rate with different nose radii end mills

The influence of considered input process parameters is analysed with the help of established 2D plots by using MINITAB -18 statistical analysis software. From the Figures 5.2 (a) to Figure 5.2(c) it is observed that material removal rate increases with the increase of cutting speed, feed rate and depth of cut as well. Because material removal rate has a directly propositional relationship with these controllable process parameters, thus causes increase in MRR. This effect is observed due to reduction in chip reduction coefficient resulting higher material removal rate (Parida and Maity, 2017). But the effect of cutting speed is almost negligible on MRR.

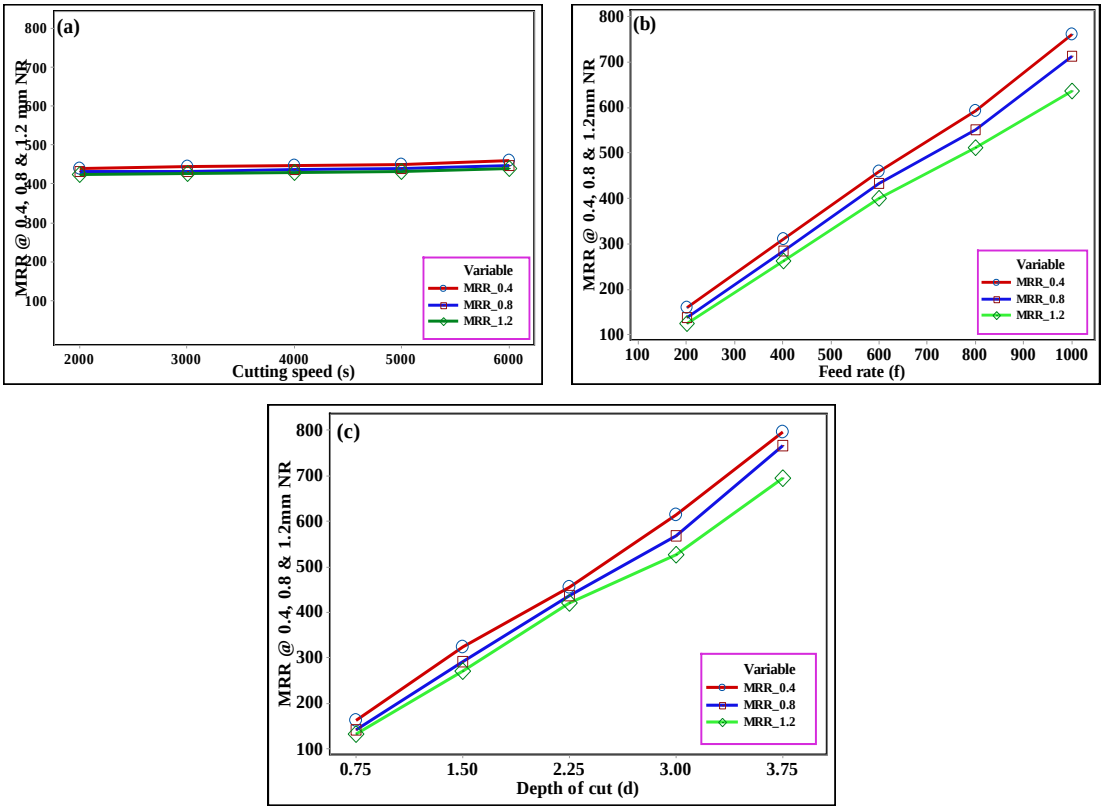

Figure 5.2 Effect of (a) cutting speed (b) feed rate and (c) depth of cut on MRR with different nose radii by keeping all other factors constant at their respective mean values.

5.3.2.1 Effect of cutting speed on material removal rate

Figure 5.2(a) illustrates the material removal rate obtained with different nose radii under dry machining environment with the variation of cutting speed from 2000rpm (2.09m/sec) to 6000rpm (6.28m/sec) keeping other process parameters feed rate and depth of cut constant at their average levels 600mm/min (0.15mm/rev) and 2.25mm respectively. It is observed that, material removal rate increased with the increase of cutting speed within considered nose radii of the end mills. It is obvious that, with the increase of cutting speed cutting tool pushes out more and more material from the cut slot and hence material removal rate increases with cutting speed. It is also observed that, the removal of material is more with 0.4mm nose radius end mill compared to 0.8mm and 1.2mm nose radius tools for a given value of cutting speed. This is matter of fact that, in end milling process as nose radius of the cutting tool increases, it leaves more uncut material at the corners of cut slot and hence the volume of material removal will come down with the increase of nose radius of end mills. Low value nose radius cutting tools obviously forms almost sharp corners at the bottom of the cut slot and

hence leads to removal of more material compared to the high value nose radius cutters.

It can be seen from the figure 5.2 (a) and Table5.1 that at low level of cutting speed 2000rpm (2.09m/sec) the obtained material removal rate is 438.56mm^3/sec, 431.21mm^3/sec and 413.96mm^3/sec with 0.4mm, 0.8mm and 1.2mm nose radius respectively. Similarly, at high level of cutting speed 6000rpm (6.28m/sec) the obtained material removal rate is 459.87mm^3/sec, 446.41mm^3/sec and 438.95mm^3/sec with 0.4mm, 0.8mm and 1.2mm nose radius respectively. The percentage increase in material removal rate w.r.t increase in cutting speed from 2000rpm (2.09m/sec) to 6000rpm (6.28m/sec) is 4.86%, 3.53%, and 3.54% with the cutting tool nose radius 0.4mm, 0.8mm and 1.2mm respectively.

5.3.2.2 Effect of feed rate on material removal rate

Figure 5.2(b) illustrates the material removal rate obtained with different nose radii under dry cutting environment with the variation of feed rate from 0.1mm/rev to 0.167mm/rev keeping other process parameters cutting speed and depth of cut constant at their average levels 4.19m/sec and 2.25mm respectively. It is pragmatic that, material removal rate increases with the increase of feed rate for the considered nose radii of the end mills. This is due to more relative movement of the cutting tool w.r.t workpiece in the cutting zone and hence scoops out more and more material with the increase of feed rate. It is obvious that, with the increase of feed rate cutting tool pushes out more material from the cut slot and hence material removal rate increases with feed rate. In this case also, end mill with 0.4mm nose radius removes comparatively more material than 0.8mm and 1.2mm nose radius end mills by forming sharp corners in the cut slots for a given value of cutting speed.

It can be seen from the Figure 5.2(b) and Table 5.1 that at low level of feed rate 200mm/min (0.1mm/rev) the obtained material removal rate is 159.67mm^3/sec, 138.26mm^3/sec and 125.56mm^3/sec with 0.4mm, 0.8mm and 1.2mm nose radius respectively. Similarly, at high level of feed rate 1000mm/min (0.167mm/rev) the obtained material removal rate is 759.18mm^3/sec, 712.35mm^3/sec and 636.52mm^3/sec with 0.4mm, 0.8mm and 1.2mm nose radius respectively. The percentage increase in material removal rate w.r.t increase in feed rate from 0.1mm/rev to 0.167mm/rev is

375.47%, 415.23%, and 406.95% with the end mill nose radii 0.4mm, 0.8mm and 1.2mm respectively.

5.3.2.3 Effect of depth of cut on material removal rate

Figure 5.2(c) illustrates the material removal rate obtained with different nose radii under dry cutting environment with the variation of depth of cut from 0.75mm to 3.75mm keeping other process parameters cutting speed and feed rate kept constant at their average levels 4.19m/sec and 0.15mm/rev respectively. It is pragmatic that, material removal rate increases with the increase of depth of cut within considered nose radii of the end mills. It is obvious that, with the increase of depth of cut cutting tool pushes out more material from the cut slot and hence material removal rate increases with depth of cut. It is also observed that, the removal of material is more with 0.4mm nose radius tool compared to 0.8mm and 1.2mm nose radius tools for a given value of depth of cut. This is matter of fact that, in end milling process as nose radius of the tool increases, it leaves more material at the corners of cut slot and hence the volume of material removal will come down with the increase of nose radius of end mills. Low value nose radius cutting tools obviously forms almost sharp corners at the bottom of the cut slot and leads to removal of comparatively more material than the high value nose radius tools.

It can be seen from the Figure 5.2(c) and Table 5.1 that at low level of depth of cut 0.75mm the obtained material removal rate is 162.79mm^3/sec, 143.07mm^3/sec and 132.35mm^3/sec with 0.4mm, 0.8mm and 1.2mm nose radius respectively. Similarly, at high level of depth of cut 3.75mm the obtained material removal rate is 795.23 mm^3/sec, 731.04 mm^3/sec and 694.81mm^3/sec with 0.4mm, 0.8mm and 1.2mm nose radius respectively. The percentage increase in material removal rate w.r.t increase in depth of cut from 0.75mm to 3.75mm is 388.50%, 410.96%, and 424.98% with the end mill nose radius 0.4mm, 0.8mm and 1.2mm respectively. Hence, from section 3.2.1, 3.2.2 and 3.2.3 of the chapter-3, we can observe that depth of cut and feed rate are having highest influence and cutting speed is having insignificant influence on material removal rate respectively.

5.3.3 Effect of input process parameters on surface roughness with different nose radii end mills

Figure 5.3(a) to Figure 5.3(c) illustrates the variation of average surface roughness in contradiction of cutting speed, feed rate and depth of cut respectively. From these figures it is observed that the surface roughness decreases with the increase of cutting speed and depth of cut as well. But it is increasing with the increase in feed rate.

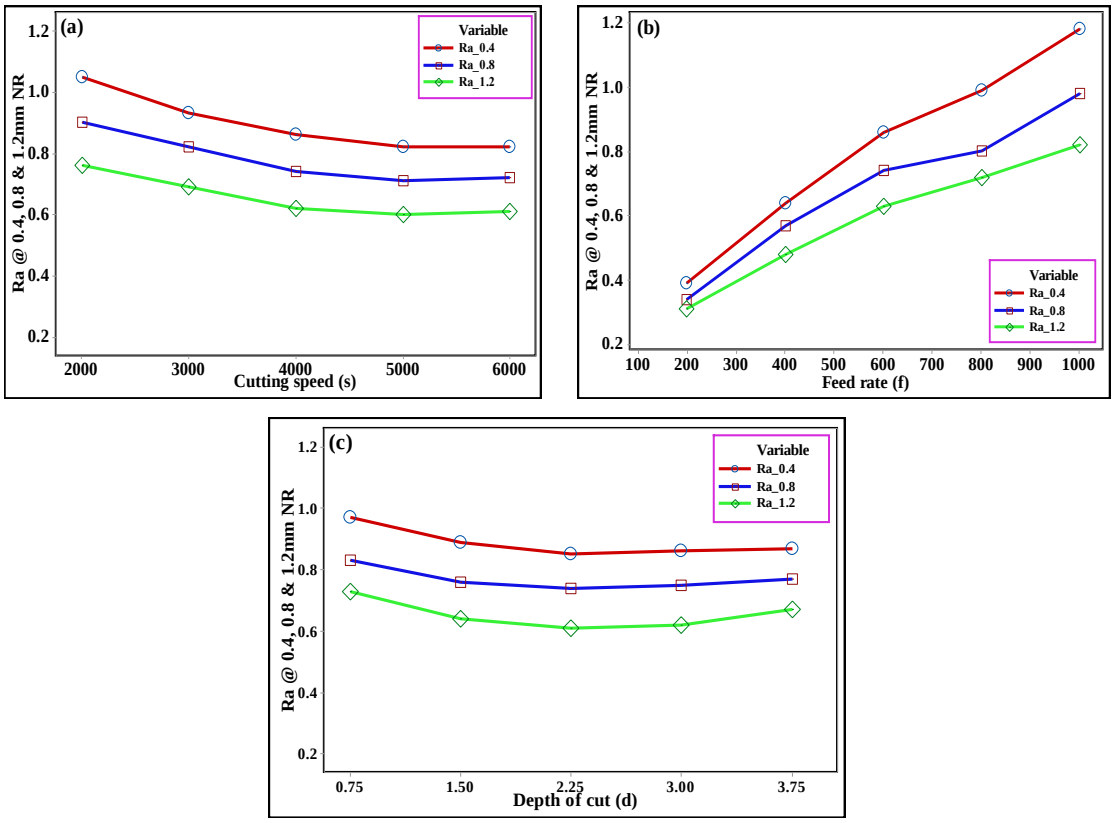

Figure 5.3 Effect of (a) cutting speed (b) feed rate and (c) depth of cut on R_a with different nose radii by keeping all other factors constant at their respective mean values.

5.3.3.1 Effect of variation of cutting speed on surface roughness

Figure 5.3(a) illustrates the surface roughness obtained with different nose radii of cutting tool under dry machining environment with the variation of cutting speed from 2000rpm (2.09m/sec) to 6000rpm (6.28m/sec) keeping other process parameters feed rate and depth of cut constant at their average levels 600mm/min(0.15mm/rev) and 2.25mm respectively. It is pragmatic that, surface roughness decreases with the increase

of cutting speed from 2000rpm to 4000rpm considerably after that, there is a mild decrease and almost become stable at 5000rpm, from that there is a mild increase with further increase in cutting speed in the considered range of nose radii of the end mills. This might be due to the smooth relative movement between cutting tool and workpiece with the increase of cutting speed up to 5000rpm and further increase in cutting speed led to machine tool vibration in turn slight increase in surface roughness. It is observed that surface roughness obtained with 1.2mm nose radius end mill is comparatively less compared to 0.8mm and 0.4mm nose radius end mills for a given value of cutting speed within the selected range. This is due to more stable relative movement between tool and workpiece with increase in nose radius and workpiece and overlapping of one cut over other in cutting zone in case of 1.2mm NR than 0.8mm and 0.4mm NR.

It can be seen from the Figure 5.3(a) and Table 5.1 that at low level of cutting speed of 2000rpm (2.09m/sec) the obtained average surface roughness is 1.05µm, 0.90µm and 0.76µm with 0.4mm, 0.8mm and 1.2mm nose radius respectively. Similarly, at high level of cutting speed 6000rpm (6.28m/sec) the obtained average surface roughness is 0.82µm, 0.72µm and 0.61µm with 0.4mm, 0.8mm and 1.2mm nose radius respectively. The percentage decrease in average surface roughness w.r.t increase in cutting speed from 2000rpm (2.09m/sec) to 6000rpm (6.28m/sec) is 21.91%, 20%, and 19.74% with the cutting tool nose radius 0.4mm, 0.8mm and 1.2mm respectively.

5.3.3.2 Effect of feed rate on surface roughness

Figure 5.3(b) illustrates the surface roughness obtained with different nose radii under dry machining condition with the variation of feed rate from 0.1mm/rev to 0.167mm/rev keeping other process parameters cutting speed and depth of cut constant at their average levels 4.19m/sec and 2.25mm respectively. It is pragmatic that, surface roughness increases with the increase of feed rate for the considered nose radii of the end mills. This might be due to the smooth relative movement between cutting tool and workpiece with the increase of cutting speed. It is observed that surface roughness obtained with 1.2mm NR end mill is comparatively less compared to 0.8mm and 0.4mm NR end mills for a given value of cutting speed within the selected range. This might be, due to more contact area between nose and workpiece and overlapping of one cut over other in cutting zone in case of 1.2mm NR than 0.8mm & 0.4mm NR.

It can be seen from the Figure 5.2(c) and Table5.1 that at low level of feed rate 200mm/min (0.1mm/rev) the obtained average surface roughness 0.39µm, 0.34µm and 0.31µm with 0.4mm, 0.8mm and 1.2mm nose radius respectively. Similarly, at high level of feed rate 1000mm/min (0.167mm/rev) the obtained average surface roughness is 1.18µm, 0.98µm and 0.82µm with 0.4mm, 0.8mm and 1.2mm nose radius respectively. The percentage of reduction in average surface roughness w.r.t increase in feed rate from 200mm/min (0.1mm/rev) to 1000mm/min (0.167mm/rev) is 66.95%, 65.31%, and 62.195 with the end mill nose radius 0.4mm, 0.8mm and 1.2mm respectively.

5.3.3.3 Effect of depth of cut on surface roughness

Figure 5.3(c) illustrates the surface roughness obtained with different nose radii under dry machining environment with the variation of depth of cut from 0.75mm to 3.75mm, keeping other process parameters cutting speed and feed rate constant at their average levels 4000rpm (4.188m/sec) and 600mm/min(0.15mm/rev) respectively. It is matter-of-fact that, surface roughness starts decreasing from 0.75mm to 2.25mm depth of cut and then started a mild increasing from 2.25mm to 3.75mm with 0.8mm and 0.4mm nose radii of the end mill. Whereas with 1.2mm nose radius end mill the increase in surface roughness with the increase of depth of cut from 2.25mm to 3.75mm is little bit considerable than with 0.8mm and 0.4mm nose radius tools. It is obvious that, with the increase of depth of cut (from 0.75 to 2.25mm) cutting tool will have more contact area with the workpiece and smooth relative movement between cutting tool and workpiece may cause for considerable reduction in surface roughness. But further increase in depth of cut (from 2.25mm to 3.75mm) lead to increase in cutting force and friction, which leads to slight vibration in machine tool and in turn increase in surface roughness. In this case also, surface roughness is relatively low with 1.2mm nose radius compared to 0.8mm and 0.4mm nose radii end mill for a given value of depth of cut within the range of selection. This might be, due to smooth relative movement between the cutting tool and workpiece in the cutting zone in case of 1.2mm nose radius than 0.8mm & 0.4mm nose radii.

It can be seen from the Figure 5.3(c) and Table5.1 that at low level of depth of cut 0.75mm the obtained average surface roughness is 0.97µm, 0.83µm and 0.73µm with 0.4mm, 0.8mm and 1.2mm nose radius respectively. Similarly, at high level of depth of

cut 3.75mm the obtained average surface roughness is 0.87µm, 0.77µm and 0.67µm with 0.4mm, 0.8mm and 1.2mm nose radius respectively. The percentage of reduction in average surface roughness w.r.t increase in depth of cut from 0.75mm to 3.75mm is 10.31%, 7.79%, and 8.22% with the end mill nose radii 0.4mm, 0.8mm and 1.2mm respectively. Hence, from section 3.3.1, 3.3.2 and 3.3.3 of the chapter-3, it is understood that cutting speed and depth of cut are showing moderate influence on surface roughness, when compared to the effect of feed rate.

5.4 EFFECT OF NOSE RADIUS ON SURFACE TOPOGRPHY

The detailed description of the surface feature or region is called surface topography. Whereas surface integrity, is the study and control of surface metallurgy as well as surface topography. Both of these quality features influence the quality of machined surface and subsurface of the machined component. Hence, they become very much significant while designing and manufacturing the fighter aircrafts structural components that have to withstand high level of static and dynamic stresses. It is a known fact that, when dynamic loading is a major factor in a design, useful strength is usually limited by fatigue characteristics of the materials. The fatigue failures almost always nucleate near the surface of the machined component. Therefore, nature of the surface from both topological and metallurgical point of view is very important in the design and manufacturing of critical structural component of an aircraft fuselage.

Author considered three case studies of surface topography samples, obtained by varying the nose radius from 0.4mm to 1.2mm in three steps by keeping other process controlling factors (cutting speed, feed rate and depth of cut) constant at their mean levels. The rake angle of the chosen end mills is kept constant at 16^0.In the present work, microscopic examination has been carried out on the machined surface formed with different nose radii end mills. Optical microscope machine has been used for making microscopic images and a personal computer has been used for capturing the surface topography images with the help of data acquisition system.

5.4.1 Effect of 0.4mm nose radius on surface topography

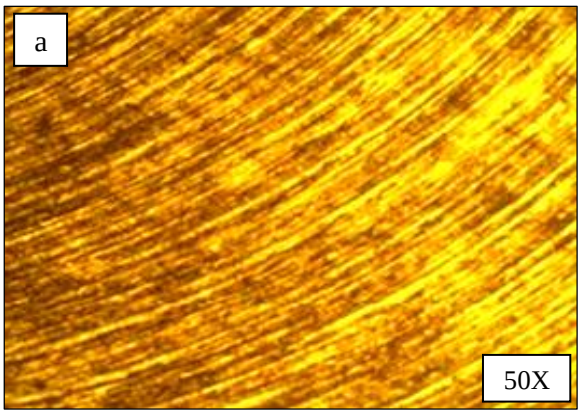

Fig. 5.4 (a) Surface topography at NR: 0.4mm, rake angle: 16^0, cutting speed of 4.188m/sec, feed rate of 0.15mm/rev and depth of cut 2.25mm

Figure 5.4 (a) shows the surface topography of an end milled surface of BS L168 test specimen with a cutting tool having nose radius of 0.4mm, at a cutting speed of 4.188m/sec, feed rate of 0.15mm/rev, axial depth of cut 2.25mm and with a radial rake angle of 16^0. Due to sharp nose radius, cutting tool marks were occurred on the machined surface forming deep crests. Due to which the average surface roughness obtained is about 0.861µm. Uneven chip flow patterns caused formation of 'ears' on the chip and cut surface on the machined surface. Considerable amount of cutting tool feed marks and collar formation has been observed on the machined surface.

5.4.2 Effect of 0.8mm nose radius surface topography

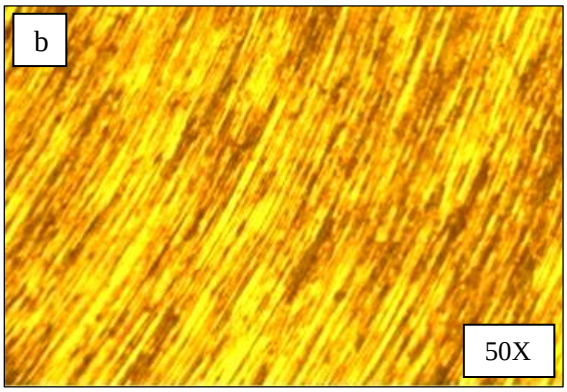

Fig. 5.4(b) Surface topography at NR: 0.8mm, rake angle: 16^0, cutting speed of 4.188m/sec, feed rate of 0.15mm/rev and depth of cut 2.25mm

Figure 5.4 (b) shows the surface topography of an end milled surface of BS L168 test specimen with a cutting tool having nose radius of 0.8mm, at a cutting speed of 4.188m/sec, feed rate of 0.15mm/rev, axial depth of cut 2.25mm and with a radial rake angle of 16^0. There are some small amounts of cutting tool feed marks and average

amount of collar formation was noticed on the machined surface. The average surface roughness obtained in this particular combination of input parameters is 0.74µm.

5.4.3 Effect of 1.2mm nose radius surface topography

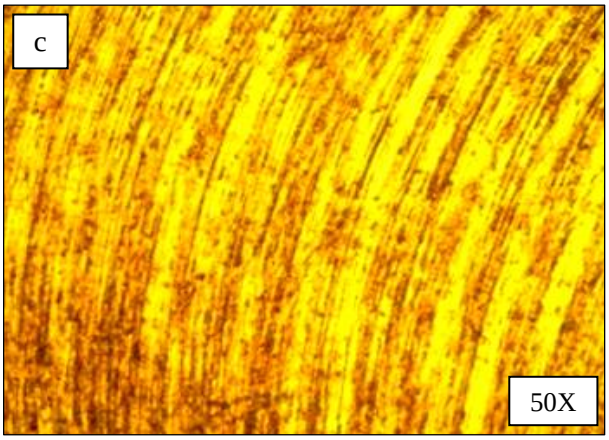

Fig. 5.4 (c) Surface topography at NR: 1.2mm, rake angle: 16^0, cutting speed of 4.188m/sec, feed rate of 0.15mm/rev and depth of cut 2.25mm.

Figure 5.4(c) shows the surface topography of an end milled surface of BSL168 test specimen with a cutting tool having nose radius of 1.2mm, at a cutting speed of 4.188m/sec, feed rate of 0.15mm/rev, axial depth of cut 2.25mm and with a radial rake angle of 16^0.It shows comparatively smoother surface when compared to previous two cases of experimental runs. It is observed that, a well-defined feed marks running almost perpendicular to feed direction. Nose radius marks occurred comparatively less due to wiping effect in this case. Better surface finish noticed due to minimum number of tool marks or crests with an average surface roughness of 0.62µm.

5.5 CLOSURE

In this chapter, experimentation has been carried out based on the One Factor at A Time (OFAT) approach of experimental methodology on BS L168 aluminium alloy test specimens. The effect of end milling process parameters and nose radius have been analysed on afore discussed performance characteristics such as: cutting tool tip temperature, surface roughness, and material removal rate with the help of established 2D plots. Further, microscopic examination has been carried out on the machined surface formed with different nose radii end mills. Optical microscope machine has been used for making microscopic images. A personal computer was used for capturing the surface topography images with the help of data acquisition system.

CHAPTER 6

OPTIMISATION OF END MILLING PROCESS

6.1 INTRODUCTION

This chapter talk about the optimisation of cutting circumstances through single-objective optimisation and multi-response optimisation techniques, with the existing CFM and proposed PFM. Taguchi's technique is one of the powerful single response optimisation techniques available and it has been used for single-response optimisation of end milling machining parameters. There after ANOVA technique was employed to find the most influencing input process parameter as well as to find the percentage of influence of each individual input process parameter on the output performance characteristics. Taguchi based GRA and Taguchi coupled TOPSIS optimisation techniques have been employed for multi-objective optimisation. Finally, the best suitable multi-objective optimisation technique for the present study has been carefully chosen in the course of the confirmation experiments.

From the literature review it was experiential and understood that no individual optimisation technique alone is sufficient for determining the optimum machining conditions for multi-response optimisation of a particular type of machining process. However, the best way is to apply more than one multi-objective optimisation technique for a particular process and to select the best one among those. Therefore, here two types of multi-objective optimisation techniques have been applied namely: T-GRA and T-TOPSIS to find out the optimum cutting condition for both CFM as well as proposed PFM.

6.2 EXPERIMENTAL PLAN

Taguchi's L_9 orthogonal array (OA) was considered to conduct required experiments and to determine the optimum cutting conditions for single-objective and multi-response optimisations with the existing CFM and proposed PFM. List of input machining parameters and their range of levels considered are listed in Table 6.1, percentage of starting feed rate and feed rate steps considered for PFM are listed in

Table 6.2. The machining performance characteristics taken into consideration are cutting tool tip temperature, surface roughness and material removal rate.

Table 6.1 Control factors and their levels

Cutting Parameters	Unit	Level 1	Level 2	Level 3
Cutting speed (s)	rpm	2000	3000	4000
Depth of cut (d)	mm	0.75	1.5	2.25
Feed rate (f)	mm/min	200	400	600
Starting % of (f) in PF machining (X)	mm/min	30%(60)	25%(100)	20%(120)

Table 6.2 Feed rate steps for progressive feed machining

Levels	Feed rate mm/min					
	Starting % of feed mm/min	Step 1	Step 2	Step 3	Step 4	Beyond Steps
1	30% of 200	60	95	130	165	200
2	25% of 400	100	175	250	325	400
3	20% of 600	120	240	360	480	600

6.3 TAGUCHI SINGLE OBJECTIVE OPTIMIZATION

S/N ratio is defined as the ratio of mean to standard deviation. Taguchi's method (Taguchi 1987) uses a loss function to find the difference between experimental and predicted values. This loss function is further converted to S/N ratio (Lin and Lin2002). Taguchi used terms like 'signal' and 'noise' which represent 'mean' and 'standard deviation' for the responses respectively. The term 'signal' means required value (mean) and 'noise' means un-wanted value (standard deviation) for the responses. Therefore, S/N ratio gives the dispersion in the region of required value (Shi et al. 2015). Based on the requirement of responses, Taguchi divided S/N ratio quality characteristics into three categories namely: 'Larger-the-better', 'Nominal-the-better' and 'Smaller-the-better'.

Table 6.3 Experimental results and their calculated S/N ratios for constant feed machining

Exp run No	Depth of cut	Cutting speed	Feed rate	Constant feed machining (CFM)											
	mm	rpm	mm/ min	Uncoated tool			S/N ratio of results with Un-coated tool			Coated tool			S/N ratio of results with Coated tool		
	d	*s*	*f*	T_{CU} ^{o}C	R_{acu} µm	MRR_{cu} mm^3/sec	T_{CC} (dB)	R_{acc} (dB)	MRR_{cc} (dB)	T_{CC} ^{o}C	R_{acc} µm	MRR_{cc} mm^3/sec	T_{CC} (dB)	R_{acc} (dB)	MRR_{cc} (dB)
1	0.75	2000	200	42.6	0.64	47.486	-32.5882	3.8764	33.5313	38.1	0.57	47.481	-31.6185	4.8825	33.5304
2	1.5	2000	400	58.7	0.76	193.126	-35.3728	2.3837	45.7168	53.8	0.66	192.987	-34.6156	3.6091	45.7106
3	2.25	2000	600	81.2	0.90	441.211	-38.1911	0.9151	52.8929	77.3	0.78	441.524	-37.7636	2.1581	52.8991
4	1.5	3000	200	53.5	0.52	95.414	-34.5671	5.6799	39.5922	48.5	0.47	95.278	-33.7148	6.5580	39.5799
5	2.25	3000	400	75.6	0.60	289.752	-37.5704	4.4370	49.2405	70.7	0.51	289.435	-36.9884	5.8486	49.2310
6	0.75	3000	600	59.2	0.92	147.404	-35.4464	0.7242	43.3702	54.1	0.83	147.627	-34.6639	1.6184	43.3833
7	2.25	4000	200	69.8	0.34	135.246	-36.8771	9.3704	42.6225	64.8	0.31	135.718	-36.2315	10.1728	42.6528
8	0.75	4000	400	52.7	0.67	96.723	-34.4362	3.4785	39.7106	48.2	0.56	96.571	-33.6609	5.0362	39.6969
9	1.5	4000	600	69.1	0.76	294.524	-36.7896	2.3837	49.3824	63.2	0.67	294.175	-36.0143	3.4785	49.3721

Table 6.4 Experimental results and their calculated S/N ratios for progressive feed machining

Exp run No	Depth of cut	Cutting speed	Feed rate	Progressive feed machining (PFM)											
	mm	rpm	mm/ min	Uncoated tool			S/N ratio of results with Un-coated tool			Coated tool			S/N ratio of results with Coated tool		
	d	*s*	*f*	T_{PU} ^{O}C	R_{apu} µm	MRR_{pu} mm3/sec	T_{PU} (dB)	R_{apu} (dB)	MRR_{pu} (dB)	T_{PC} ^{O}C	R_{apc} µm	MRR_{pc} mm3/sec	T_{PC} (dB)	R_{apc} (dB)	MRR_{pc} (dB)
1	0.75	2000	200	39.5	0.50	43.651	-31.9319	6.0206	32.7999	35.2	0.43	44.641	-30.9309	7.3306	32.9947
2	1.5	2000	400	54.8	0.62	177.792	-34.7756	4.1522	44.9982	51.2	0.53	178.454	-34.1854	5.5145	45.0305
3	2.25	2000	600	77.8	0.71	406.986	-37.8196	2.9748	52.1916	73.3	0.63	407.897	-37.3021	4.0132	52.2110
4	1.5	3000	200	50.3	0.42	87.542	-34.0314	7.5350	38.8443	46.5	0.34	88.613	-33.3491	9.3704	38.9499
5	2.25	3000	400	72.6	0.47	265.327	-37.2187	6.5580	48.4756	68.2	0.43	267.976	-36.6757	7.3306	48.5619
6	0.75	3000	600	56.3	0.78	135.843	-35.0102	2.1581	42.6607	50.8	0.66	136.401	-34.1173	3.6091	42.6964
7	2.25	4000	200	66.1	0.28	123.841	-36.4040	11.0568	41.8573	61.3	0.25	124.547	-35.7492	12.0412	41.9067
8	0.75	4000	400	49.1	0.53	88.983	-33.8216	5.5145	38.9861	45.1	0.45	89.242	-33.0835	6.9357	39.0114
9	1.5	4000	600	65.7	0.61	270.258	-36.3513	4.2934	48.6356	61.2	0.54	272.489	-35.7350	5.3521	48.7070

The aim of present work is to minimize both surface roughness as well as cutting tool tip temperature, and at the same time to maximise the MRR in order to enhance the machinability, and also to improve the machining performance. Hence, out of three quality characteristics (larger-the-better, nominal-the-better and smaller-the-better); 'smaller-the-better' quality characteristic was chosen for both cutting tool tip temperature and surface roughness. And 'larger-the-better' quality characteristic was chosen for material removal rate.

$$\text{S/N ratio for 'smaller-the-better': } \eta = -10 \log_{10} \frac{1}{n} \sum_{i=1}^{n} R^2 \ldots\ldots\ldots \quad (6.1)$$

$$\text{S/N ratio for 'larger-the-better': } \eta = -10 \log_{10} \frac{1}{n} \sum_{i=1}^{n} \frac{1}{R^2} \ldots\ldots\ldots\ldots \quad (6.2)$$

Where, n = Number of observations made
R = Observed data against each response

Experimental results of surface roughness, cutting tool tip temperature and material removal rate and their corresponding S/N ratio values against all experimental runs have been calculated using equation 6.1 and equation 6.2 in dB for both the types of machining with coated (TiAlN) and un-coated cutting tools and are depicted in Table 6.3 and Table 6.4 respectively. Taguchi analysis was performed using Minitab-18 statistical analysis software; ANOVA results and means of S/N ratio plots were obtained and presented in the forthcoming sections of this chapter.

6.3.1 Selection of optimum cutting conditions for better output responses

6.3.1.1 Optimum cutting conditions for cutting tool tip temperature with CFM

The effect of input parameters on cutting tool tip temperature in CFM and proposed PFM with coated (TiAlN) and un-coated carbide end mills are analysed using S/N ratios and are presented in 'Response table for means of S/N ratios' from Table 6.5 to Table 6.8. The superior value of 'Δ' for a particular control factor indicates its substantial influence on output response. The minimum value of cutting tool tip temperature can be calculated from total mean value of the experimental results. The highest value of S/N ratio will be used as a decisive factor to decide the best level for

each of the control factor.

Table 6.5 Response table for means of S/N ratios of T in CFM with un-coated tools

Level	Mean S/N ratio		
	Depth of cut, d	**Spindle speed, s**	**Feed rate, f**
1	-34.1569	-35.3840	-34.6775
2	-35.5765	-35.8613	-35.7931
3	-37.5462	-36.0343	-36.8090
Delta(Δ)	3.3893	0.6503	2.1316
Rank	1	3	2

Table 6.6 Response table for means of S/N ratios of T in CFM with coated tools

Level	Mean S/N ratio		
	Depth of cut, d	**Spindle speed, s**	**Feed rate, f**
1	-33.3145	-34.6659	-33.8549
2	-34.7816	-35.1224	-35.0883
3	-36.9945	-35.3023	-36.1473
Delta(Δ)	3.6800	0.6363	2.2923
Rank	1	3	2

In constant feed machining with un-coated cutting tool (Table 6.5), the value of delta for depth of cut (Δ=3.3893) is maximum, followed by feed rate (Δ=2.1316), for cutting speed (Δ=0.6503) it is least. Whereas with coated (TiAlN) cutting tool (Table 6.6), value of delta for depth of cut (Δ=3.6800) is maximum, for feed rate (Δ=2.2923) it is moderate and for cutting speed (Δ=0.6363) it is low. Based on the values of 'Δ' from Table 6.5 and Table 6.6, it is evident that in both the cases of constant feed machining with uncoated and coated (TiAlN) cutting tools, depth of cut is showing maximum influence on the output response T, followed by feed rate with moderate influence and cutting speed is showing least effect.

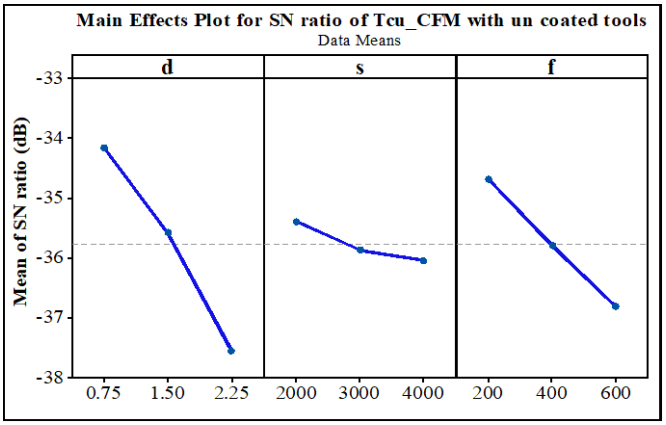

Figure6.1 Main effect plots for mean of S/N ratio of T in CFM with Un-coated tools

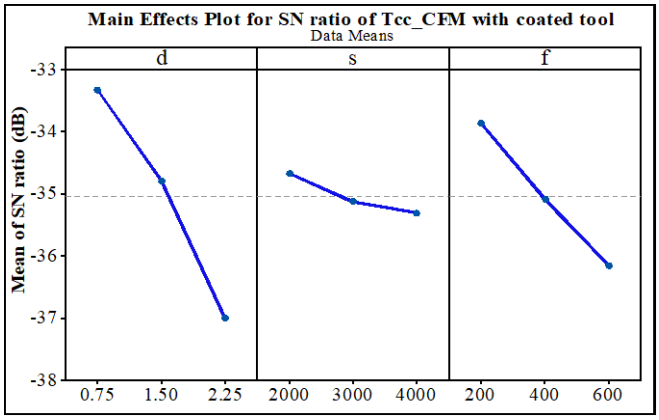

Figure 6.2 Main effect plots for mean of S/N ratio of T in CFM with Coated tools

Main effects plots (Figure 6.1 and Figure 6.2) are the graphical illustrations for the means of S/N ratio of cutting tool tip temperature values depicted in Table 6.3 obtained from CFM with un-coated and coated (TiAlN) cutting tools respectively. Best level of control parameter to minimize the value of T, can be determined from the main effect plots established for existing CFM with coated (TiAlN) and un-coated cutting tools. A higher value of S/N ratio indicates the least variation difference between desirable output and calculated output.

These main effect plots reveal that DoC is viewing utmost slope followed by feed rate and spindle speed is having least slope. Hence the influence of DoC is highest while feed rate is having moderate influence and spindle speed is having least influence on cutting tool tip temperature response and it is in line with response table for S/N ratios analysis. From main effects plots (Figure 6.1 and Figure 6.2) it is also evident that, the highest mean value of S/N ratio obtained for cutting tool tip temperature are at depth of

cut 0.75mm, cutting speed 2000 rpm, and feed rate 200mm/min respectively. So, the predicted optimum cutting parameters combination to obtain better (low) value of cutting tool tip temperature using Taguchi' single-objective optimisation method was found at *d*=0.75mm, *s* = 2000rpm, *f*=200mm/rev. Therefore, the predicted optimum combination of cutting process parameters for cutting tool tip temperature is ***d1-s1-f1*.**

6.3.1.2 Optimum cutting conditions for cutting tool tip temperature with PFM

In progressive feed machining with uncoated cutting tool (Table 6.7), the value of delta for depth of cut (Δ=3.5595) is maximum, followed by feed rate (Δ= 2.2712), for cutting speed (Δ=0.6833) it is least. Whereas with coated cutting tool (Table 6.8), the value of delta for depth of cut (Δ=3.8651) is maximum, for feed rate (Δ=2.3751) it is moderate and for cutting speed (Δ=0.7165) it is least.

Table 6.7 Response table for means of S/N ratios of T in PFM with un-coated tools

Level	**Mean S/N ratio**		
	Depth of cut, d	**Spindle speed, s**	**Feed rate, f**
1	-33.5879	-34.8424	-34.1224
2	-35.0528	-35.4201	-35.2720
3	-37.1475	-35.5257	-36.3937
Delta(Δ)	3.5595	0.6833	2.2712
Rank	1	3	2

Table 6.8 Response table for means of S/N ratios of T in PFM with coated tools

Level	**Mean S/N ratio**		
	Depth of cut, d	**Spindle speed, s**	**Feed rate, f**
1	-32.7106	-34.1394	-33.3430
2	-34.4232	-34.7140	-34.6482
3	-36.5757	-34.8559	-35.7181
Delta(Δ)	3.8651	0.7165	2.3751
Rank	1	3	2

Based on the values of 'Δ' from Table 6.7 and Table 6.8, it is evident that in both the

cases of progressive feed machining with uncoated and coated (TiAlN) cutting tools, depth of cut is showing maximum influence on output response T, followed by feed rate and spindle speed is showing least effect.

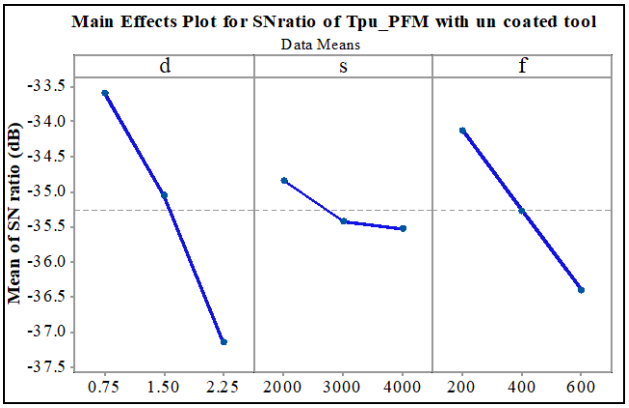

Figure6.3 Main effect plots for mean of S/N ratios of T in PFM with Un-coated tools

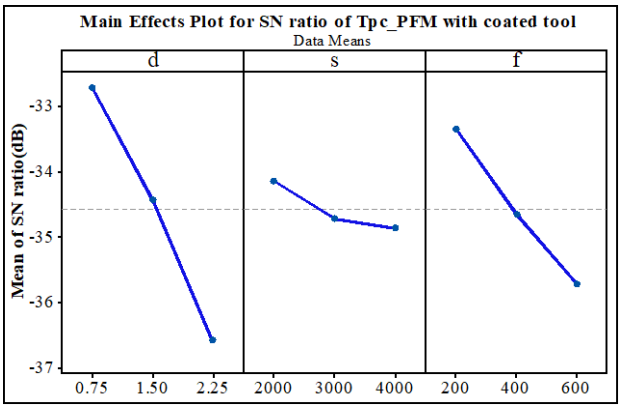

Figure 6.4 Main effect plots for mean of S/N ratios of T in PFM with Coated tools

Main effects plots (Figure 6.3 and Figure 6.4) are the graphical illustrations for the means of S/N ratios of cutting tool tip temperature values depicted in Table 6.4 obtained from proposed progressive feed machining with un-coated and coated (TiAlN) cutting tools respectively. Best level of control factors for minimizing the cutting tool tip temperature can be determined from the main effect plots established for proposed progressive feed machining with coated (TiAlN) and un-coated cutting tools. Higher value of S/N ratio indicates minimum variation difference between the wanted output and calculated output. These main effect plots reveal that DoC of cut is viewing highest slope, followed by feed rate and spindle speed is showing least slope. Hence the influence of depth of cut is highest while feed rate is having moderate influence and

cutting speed is having low influence on cutting tool tip temperature response, and it is in line with 'response table for S/N ratios' analysis result.

From main effects plots (Figure 6.3 and Figure 6.4) it is also evident that the highest value of mean S/N ratio obtained for cutting tool tip temperature are at DoC 0.75mm, spindle speed 2000rpm, and feed rate 200mm/min respectively. Hence, the predicted optimum control factors to attain the better (low) value of cutting tool tip temperature using Taguchi' single objective optimisation method were found at d=0.75mm, s = 2000rpm, f =200mm/rev. Hence, the predicted optimum combination of process parameters for cutting tool tip temperature is ***d1-s1-f1*.**

6.3.1.3 Optimum cutting conditions for surface roughness with CFM

Table 6.9 Response table for means of S/N ratio of Ra in CFM with un-coated tools

Level	**Mean S/N ratio**		
	Depth of cut, d	**Spindle speed, s**	**Feed rate, f**
1	2.6930	2.3918	6.3089
2	3.4825	3.6137	3.4331
3	4.9075	5.0776	1.3410
Delta(Δ)	2.2145	2.6858	**4.9679**
Rank	3	2	1

Table 6.10 Response table for means of S/N ratio of Ra in CFM with coated tools

Level	**Mean S/N ratio**		
	Depth of cut, d	**Spindle speed, s**	**Feed rate, f**
1	3.8457	3.5499	7.2044
2	4.5486	4.6750	4.8313
3	6.0598	6.2292	2.4184
Delta(Δ)	2.2141	2.6793	**4.7861**
Rank	3	2	1

The influence of input process parameters on surface roughness in CFM and in proposed PFM with coated (TiAlN) and un-coated carbide end mills are analysed using

S/N ratio and are presented in 'Response table for means of S/N ratio' (Table 6.9 to Table 6.12). The minimum value of surface roughness can be computed from total mean values of the experimental results. The highest S/N ratio value will be used as a criterion to determine the best level of input process controllable factor in the machining.

For the case of surface roughness, in constant feed machining with un-coated cutting tool (Table 6.9), the value of delta for feed rate (Δ= 4.9679) is maximum, followed by cutting speed(Δ=2.6858), and for depth of cut (Δ=2.2145) it is least. Whereas with coated cutting tool (Table 6.10), value of delta for feed rate (Δ=4.7861) is maximum, for cutting speed (Δ=2.6793) it is moderate and for depth of cut (Δ=2.2141) it is least. Based on the values of 'Δ' from Table 6.9 and Table 6.10, it is evident that in case of proposed progressive feed machining with un-coated and coated (TiAlN) cutting tools, feed rate is showing maximum effect on surface roughness, followed by spindle speed and DoC of cut is having least influence.

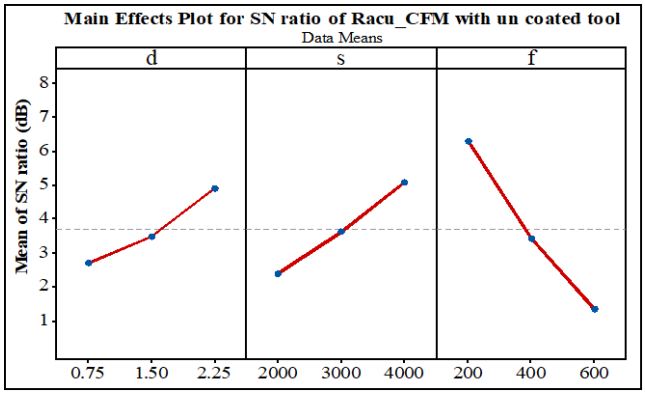

Figure 6.5 Main effect plots for mean of S/N ratio of Ra in CFM with Un-coated tools

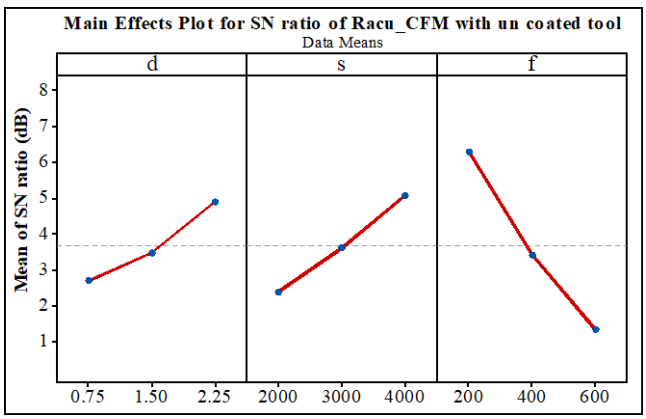

Figure 6.6 Main effect plots for mean of S/N ratio of Ra in CFM with Coated tools

Main effects plots (Figure 6.5 and Figure 6.6), are the graphical illustrations for the means of S/N ratio values against surface roughness values depicted in Table 6.3 obtained from constant feed machining with uncoated and coated (TiAlN) cutting tools respectively. Best level of process parameters to minimize the surface roughness can be determined from the main effect plots established for existing constant feed machining with coated (TiAlN) and uncoated cutting tools.

Main effect plots (Figure 6.5 and Figure 6.6), reveals that feed rate is viewing highest slope followed by cutting speed, and DoC is showing least slope. Hence the effect of feed rate is highest while cutting speed is having moderate influence and DoC is having least influence on output response R_a, and it is in line with 'response table for S/N ratios' analysis result. From main effects plots (Figure 6.5 and Figure 6.6), it is also evident that the highest mean value of S/N ratio were obtained for surface roughness are at depth of cut: 2.25mm, cutting speed: 4000rpm, and feed rate: 200mm/min respectively.

Thus, the predicted optimum machining process parameters to obtain low value of surface roughness using Taguchi' single-objective optimisation method were found at *d*=2.25mm, *s*=4000rpm, *f*=200mm/min. Hence, the predicted optimum combination of process parameters for response R_a is ***d3-s3-f1*.**

6.3.1.4 Optimum cutting conditions for surface roughness with PFM

In case of proposed progressive feed machining with un-coated cutting tools (Table 6.11), the value of delta for feed rate (Δ=5.0620) is maximum, followed by spindle speed (Δ= 2.5724), and for DoC (Δ=2.2988) it is least. But, with the coated cutting tools (Table 6.12), the value of delta for feed rate (Δ=5.2559) is maximum, for cutting speed (Δ=2.4903) it is moderate and for depth of cut (Δ=1.8365) it is least.

Based on the values of 'Δ' from Tables 6.11 and Table 6.12, it is evident that in the case of proposed progressive feed machining with uncoated and coated (TiAlN)cutting tools, feed rate is showing maximum effect on the response R_a, followed by spindle speed and DoC is having least influence.

Table 6.11 Response table for S/N ratio of Ra in PFM with un-coated tools

Level	Mean S/N ratio		
	Depth of cut, d	**Spindle speed, s**	**Feed rate, f**
1	4.5644	4.3825	8.2042
2	5.3269	5.4171	5.4082
3	6.8632	6.9549	3.1421
Delta(Δ)	2.2988	2.5724	5.0620
Rank	3	2	1

Table 6.12 Response table for S/N ratio of Ra in PFM with coated tools

Level	Mean S/N ratio		
	Depth of cut, d	**Spindle speed, s**	**Feed rate, f**
1	5.9585	5.6194	9.5808
2	6.7457	6.7701	6.5936
3	7.7950	8.1097	4.3248
Delta(Δ)	1.8365	2.4903	5.2559
Rank	3	2	1

Main effect plots (Figure 6.7 and Figure 6.8), revealed that feed rate is viewing highest slope, followed by cutting speed and DoC is showing least slope. Hence the influence of feed rate is maximum while cutting speed is having moderate influence and DoC is showing least influence on surface roughness response. Main effect plots (Figure 6.7 and Figure 6.8), reveals that feed rate is viewing highest slope followed by cutting speed and DoC is showing least slope. Hence the influence of feed rate is highest while cutting speed is moderate and depth of cut is having least influence on surface roughness response, and it is in line with 'response table for S/N ratios' analysis result.

From the main effects plots (Figure 6.5 and Figure 6.8), it is observed that, highest mean value of S/N ratio obtained for surface roughness are at : depth of cut 2.25mm, cutting speed at 4000 rpm, feed rate 200mm/rev respectively. Hence, the predicted optimum process parameters to obtain low value of R_a using Taguchi's single objective optimisation method were found at d = 2.25mm, v = 2000rpm, f =200mm/rev. Hence, the predicted optimum combination of process parameters for surface roughness

response is: ***d3-s3-f1.***

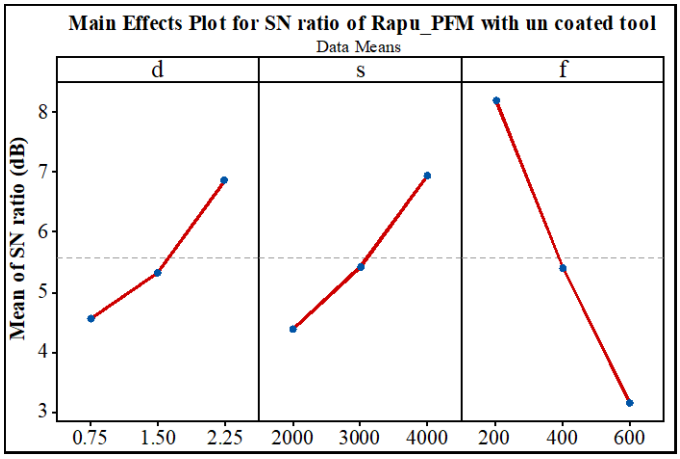

Figure 6.7 Main effect plots for mean of S/N ratio of R_a at PFM with uncoated tools

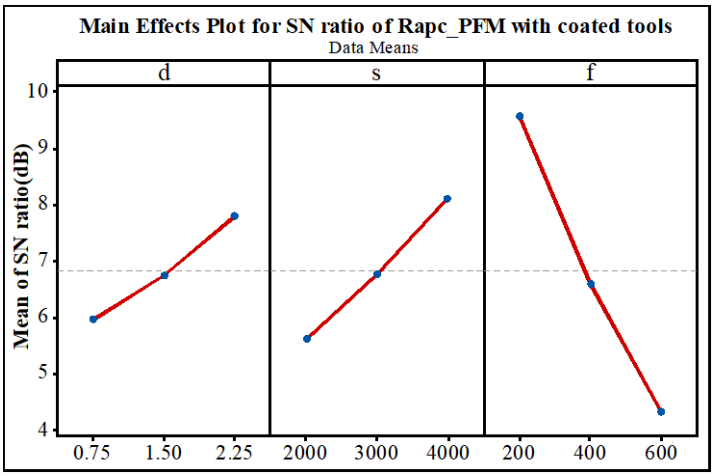

Figure 6.8 Main effect plots for mean of S/N ratio of Ra in PFM with coated tools

6.3.1.5 Optimum cutting conditions for material removal rate with CFM

The effect of input process parameters on material removal rate in CFM and proposed PFM with coated (TiAlN) and un-coated solid carbide end mills are analysed using S/N ratio and are presented in 'Response table for S/N ratios' (Table 6.13 to Table6.16). The maximum value of material removal rate can be calculated from total mean values of the experimental results. The topmost value of S/N ratio will be used as a decisive factor to find the best level of each of the control factor.

Table 6.13 Response table for S/N ratio of MRR in CFM with uncoated tools

Level	Mean S/N ratio		
	Depth of cut, d	Spindle speed, s	Feed rate, f
1	38.8707	44.0470	38.5820
2	44.8972	44.0677	44.8893
3	48.2520	43.9052	48.5485
Delta(Δ)	9.3813	0.1625	9.9665
Rank	2	3	1

Table 6.14 Response table for S/N ratio of MRR in CFM with coated tools

Level	Mean S/N ratio		
	Depth of cut, d	Spindle speed, s	Feed rate, f
1	38.8702	44.0467	38.5877
2	44.8875	44.0647	44.8795
3	48.2610	43.9073	48.5515
Delta(Δ)	9.3907	0.1575	9.9638
Rank	2	3	1

In constant feed machining with uncoated cutting tool (Table 6.13), the value of delta for feed rate (Δ=9.9665) is maximum, followed by DoC (Δ=9.3813), and for spindle speed (Δ=0.1625) it is least. Whereas with coated cutting tool (Table 6.14), value of delta for feed rate (Δ=9.9638) is maximum, for depth of cut (Δ=9.3907) it is moderate and for cutting speed (Δ=0.1575) it is least. Based on the values of 'Δ' from Table 6.13 to Table 6.14, it is evident that in the case of constant feed machining with uncoated and coated (TiAlN) cutting tools, feed rate is showing maximum influence on material removal rate, followed by DoC and spindle speed is having least influence.

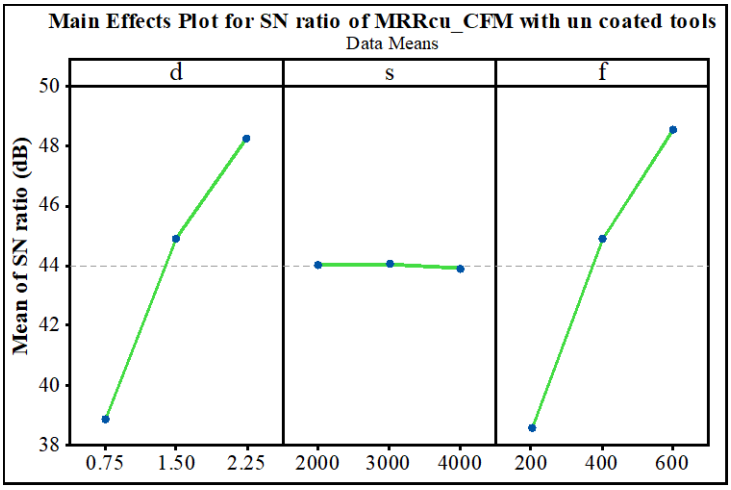

Figure 6.9 Main effect plots for mean of S/N ratio of MRR in CFM with uncoated tools

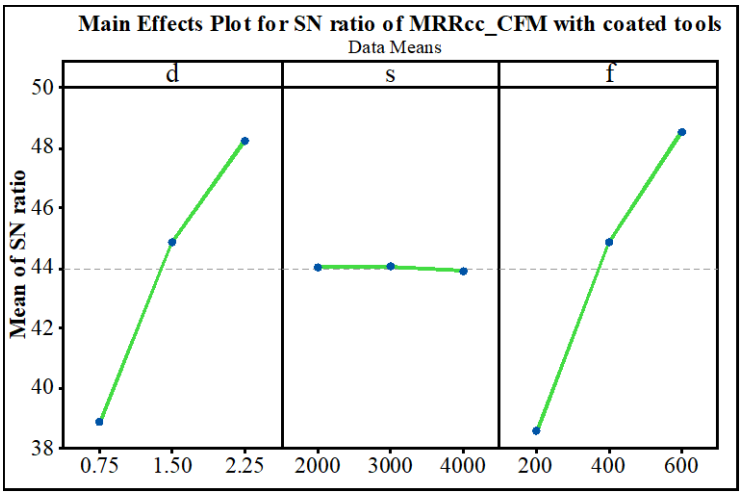

Figure 6.10 Main effect plots for mean of S/N ratio of MRR in CFM with coated tools.

Main effects plots (Figure 6.9 and Figure 6.10), are the graphical illustrations for the means of S/N ratio of material removal rate values depicted in Table 6.3 obtained from constant feed machining with uncoated and coated (TiAlN) cutting tools respectively. Best level of control factors for maximising the material removal rate can be determined from the main effect plots established for existing constant feed machining with coated (TiAlN) and uncoated cutting tools.

Main effect plots (Figure 6.9 and Figure 6.10), also reveals that feed rate is viewing highest slope followed by DoC of cut and spindle speed is having least slope. Hence the influence of feed rate is highest while DoC is moderate and spindle speed is showing least influence on MRR and it is in line with 'response table for S/N ratios' analysis

result. From main effects plots (Figure 6.9 and Figure 6.10) it is also evident that, the highest mean S/N ratio values obtained for material removal rate are at DoC: 2.25mm, spindle speed: 2000rpm, and feed rate: 600mm/min respectively. Hence, the predicted optimum cutting parameters to obtain the higher value of material removal rate using Taguchi' single objective optimisation methods were found at: *d*=2.25mm, *s*= 2000rpm, *f*=600mm/min. Therefore, the predicted optimum combination of process parameters for MRR response is: ***d3-s1-f3*.**

6.3.1.6 Optimum cutting conditions for material removal rate with PFM

Table 6.15 Response table for S/N ratio of MRR in PFM with uncoated tools

Level	Mean S/N ratio		
	Depth of cut, d	Spindle speed, s	Feed rate, f
1	38.1489	43.3299	37.8338
2	44.1594	43.3269	44.1533
3	47.5082	43.1597	47.8293
Delta(Δ)	9.3592	0.1702	9.9955
Rank	2	3	1

Table 6.16 Response table for S/N ratio of MRR in PFM with coated tools

Level	Mean S/N ratio		
	Depth of cut, d	Spindle speed, s	Feed rate, f
1	38.2341	43.4121	37.9504
2	44.2292	43.4027	44.2013
3	47.5599	43.2083	47.8714
Delta(Δ)	9.3257	0.2037	9.9210
Rank	2	3	1

In case of progressive feed machining with uncoated cutting tool (Table 6.15), the value of delta for feed rate (Δ=9.9955) is maximum, followed by DoC (Δ= 9.3592), and for spindle speed (Δ=0.1702) it is least. Whereas with coated cutting tool (Table 6.16), the value of delta for feed rate (Δ=9.9210) is maximum, for depth of cut (Δ=9.3257) it is

moderate and for cutting speed (Δ=0.2037) it is least. Based on the values of 'Δ' from Table 15 to Table 16, it is obvious that in case of proposed PFM with uncoated and coated (TiAlN) cutting tools, feed rate is showing maximum influence on material removal rate, followed by DoC and spindle speed is having least effect.

Main effects plots (Figure 6.11 and Figure 6.12) are the graphical illustrations for the means of S/N ratio of MRR values depicted in Table 6.4 obtained from proposed progressive feed machining with uncoated and coated (TiAlN) cutting tools respectively. Best level of control factors for maximising the material removal rate can be determined from the main effect plots established for proposed progressive feed machining with coated (TiAlN) and uncoated cutting tools.

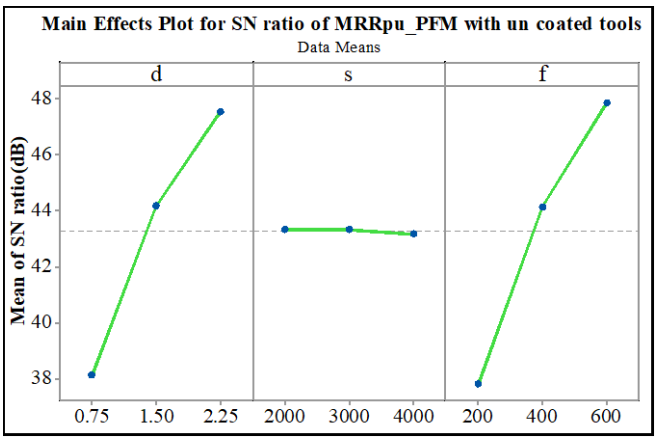

Figure 6.11 Main effect plot for mean of S/N ratio of MRR in PFM with uncoated tools

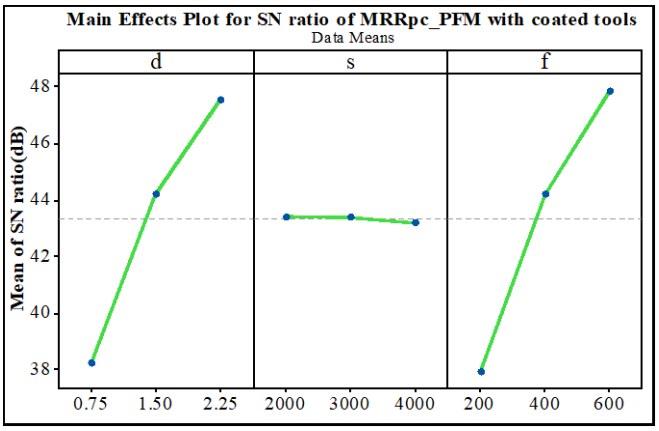

Figure 6.12 Main effect plot for mean of S/N ratio of MRR in PFM with coated tools

Main effect plots (Figure 6.11 and Figure 6.12), it is observed that feed rate is viewing highest slope followed by DoC and spindle speed is having least slope. Hence the

influence of feed rate is showing highest while DoC is having moderate influence and spindle speed is showing least impact on MRR response, and it is in line with 'response table for S/N ratios analysis result. From main effects plots (Figure 6.11 and Figure 6.12) it is also evident that, the highest mean S/N ratio values obtained for material removal rate are at depth of cut: 2.25mm, cutting speed: 2000rpm, and feed rate: 600mm/min respectively. For that reason, the predicted optimum cutting parameters for obtaining the high value of material removal rate using Taguchi' single objective optimisation method were found at d = 2.25mm, s = 2000rpm, f = 600mm/min. Therefore, the predicted optimum combination of process parameters for material removal rate response is: ***d3-s1-f3.***

6.3.2 Confirmation tests for Taguchi's single objective optimisation

For validating the predicted optimum cutting process parameter combinations by Taguchi's single objective optimisation method, confirmation tests have been performed. The predicted S/N ratio $(\varepsilon_{predicted})$will be to predict and to verify the response at the predicted optimum cutting conditions. And it was calculated by using equation 6.3.

$$\varepsilon_{predicted} = \varepsilon_m + \sum_{i=1}^{n}(\varepsilon_0 - \varepsilon_{m)} \ldots\ldots\ldots\ldots\ldots\ldots(6.3)$$

Where, ε_m is the total mean S/N ratio,

ε_o is the mean S/N ratio at optimal level

n is the number of input process parameters considered (Three).

Predicted optimum cutting conditions by means of Taguchi's optimisation technique, and then confirmation experiments were conducted and the results were depicted in Table 6.17, Table 6.18 and Table 6.19, for cutting tool tip temperature, surface roughness and MRR respectively. It is observed that, the predicted optimum cutting conditions for cutting tool tip temperature, surface roughness and MRR gave an enhancement in the performance characteristics. From these results, it was also noticed that S/N ratios of predicted and optimum cutting conditions are close to each other for all the responses.

6.3.2.1 Confirmation test results of cutting tool tip temperature

The improvement found in S/N ratio at the optimal cutting conditions for cutting tool tip temperature is 2.77dB over initial cutting parameter settings (*d2-s2-f2*) as shown in Table 6.17. From the confirmation experiments it was understood that, predicted optimum cutting conditions obtained by means of Taguchi's single-objective optimisation technique gave a favourable cutting tool tip temperature over the initial cutting parametric settings (*d2-s2-f2*). The cutting tool tip temperature value obtained by confirmation experiments at optimum machining parameters is considerably reduced. The predicted cutting tool tip temperature (T) was decreased from 58.60^0C to 40.46^0C at Taguchi's optimal cutting parameters. It is found to be a decrease of 30.96% in cutting tool tip temperature has been observed when compared to initial cutting process parameter settings. And conformation experiments have given a value of 42.60^0C.

Table 6.17 Confirmation test results for cutting tool tip temperature

	Initial machining parameters	**Optimal machining parameters**	
		Predicted	**Experimental**
Setting Level	*d2-s2-f2*	*d1-s1-f1*	*d1-s1-f1*
Cutting tool tip temp rise (T)	58.60^0C	40.46^0C	42.60^0C
S/N ratio (dB)	-35.3580		-32.5882
Improvement in S/N ratio (dB)	2.7698		
Percentage reduction of T	30.96%		

6.3.2.2 Confirmation test results of surface roughness

Table 6.18 Confirmation test results for surface roughness

	Initial machining parameters	**Optimal machining parameters**	
		Predicted	**Experimental**
Setting Level	*d2-s2-f2*	*d3-s3-f1*	*d3-s3-f1*
Surface roughness (Ra)	0.67	0.336	0.34
S/N ratio (dB)	3.4785		9.3704
Improvement in S/N ratio (dB)	5.8919		
Percentage reduction of Ra	49.851%		

The improvement found in S/N ratio value at the optimum cutting condition for R_a is 5.8919dB, over initial parameter settings (*d2-s2-f2*) as depicted in Table 6.18. From the confirmation experiments it was also understood that, the predicted value of response at optimum cutting conditions obtained by means of Taguchi's single objective optimisation gave a favourable surface finish value over the same obtained at initial cutting process parameter settings. As per Taguchi's optimum cutting conditions the predicted value of surface roughness (R_a) has decreased from 0.67µm to 0.336µm. It is found to be a decrease of 49.851% in an average surface roughness when compared to initial cutting process parametric settings. Conformation experimental run has given a value of 0.34µm. It is noticed that, experimental value of surface roughness is considerably reduced by Taguchi's single objective optimisation method.

6.3.2.3 Confirmation test results of material removal rate

The improvement found in S/N ratio at the optimal cutting condition for material removal rate is 7.0781dB over initial parameter settings (*d2-s2-f2*) as depicted in Table 6.19. The experimental value of material removal rate has been increased from 195.32 mm^3/min to 441.21mm^3/min at Taguchi's optimum cutting conditions. It is found to be an increase of 127.042% in material removal rate has been observed when compared to initial cutting process conditions. It is notice that the experimental value of MRR is considerably increased by Taguchi's single objective optimisation method.

Table 6.19 Confirmation test results for material removal rate

	Initial machining parameters	**Optimal machining parameters**	
		Predicted	**Experimental**
Setting Level	*d2-s2-f2*	*d3-s1-f3*	*d3-s1-f3*
Material removal rate (MRR)	195.32	443.4586	441.21
S/N ratio (dB)	45.8148		52.8929
Improvement in S/N ratio (dB)	7.0781		
Percentage improvement of MRR	127.042%		

Therefore, from the brief analysis of above three cases of surface roughness, cutting tool tip temperature and MRR, Taguchi predicted optimum cutting process conditions

were considered to obtain the better performance characteristics in machining of BS L168. From all the above discussed results, it was understood that Taguchi's single objective optimisation method significantly improved the machinability characteristics of considered work material under the considered process parameters.

6.3.3 ANOVA outcomes for S/N ratio of output responses

ANOVA is useful to infer the input data and to test the output results in a structured way by DoE. It is a powerful computational technique used to analyze the significance of developed model and to determine the impact of each individual control factor on the observed responses (Sivarao et al. 2014). In the present study, ANOVA is used to examine the effects of control factors on surface roughness, cutting tool tip temperature and material removal rate. The outcome of ANOVA for CFM and PFM are analyzed for un-coated as well as coated end mills in the forthcoming chapters in detail at 95% accuracy level. The F-factor for each of the input process parameters is compared. PCR column of the tables shows the percentage contribution ratio for each of the process controlling factor on output response. The PCR can be calculated by using the following equation 6.4.

$$\text{PRC} = \frac{SSn - Ve.Vn}{SSt} \text{ x } 100 \quad \ldots\ldots\ldots\ldots\ldots\ldots \quad (6.4)$$

Where, *SSn* is sum of square for parameter N,
Ve is variance of error
Vn is the degree of freedom for parameter N and
SSt is total sum of squares.

6.3.3.1 ANOVA for S/N ratio of cutting tool tip temperature with CFM

In case of cutting tool tip temperature in constant feed machining with uncoated cutting tool the PCR for DoC is 68.98%, it is the peak among all the values (Table 6.20). Therefore, it indicates that DoC is the most influencing factor followed by feed rate (PCR=27.28%) and cutting speed (PCR=2.54%) is showing least influence. In case of PFM (Table 6.21) the DoC is the most important process parameter followed by feed rate (PCR=26.93%) and cutting speed (PCR=2.08%) is having least influence on cutting tool tip temperature.

Table 6.20 ANOVA for S/N ratio of T obtained in CFM with uncoated tools

Source	DF	Seq SS	PCR	Adj SS	Adj MS	F-Value	P-Value
Regression	6	24.8815	99.61%	24.8815	4.14691	84.12	0.012
d	1	17.2308	68.98%	0.1318	0.1318	2.67	0.244
s	1	0.6343	2.54%	0.1311	0.13105	2.66	0.245
f	1	6.8154	27.28%	0.7473	0.74725	15.16	0.060
d*s	1	0.0005	0.00%	0.0031	0.00314	0.06	0.824
d*f	1	0.1465	0.59%	0.017	0.01702	0.35	0.616
s*f	1	0.054	0.22%	0.054	0.05396	1.09	0.405
Error	2	0.0986	0.39%	0.0986	0.0493		
Total	8	24.9801	100.00%				

Table 6.21 ANOVA for S/N ratios of T obtained in CFM with coated tools

Source	DF	Seq SS	PCR	Adj SS	Adj MS	F-Value	P-Value
Regression	6	29.1132	99.47%	29.1132	4.8522	62.56	0..016
d	1	20.3139	69.41%	0.1349	0.13488	1.74	0.318
s	1	0.6074	2.08%	0.2642	0.26424	3.41	0.206
f	1	7.8823	26.93%	1.0049	1.00489	12.96	0.069
d*s	1	0.0074	0.03%	0.0024	0.0024	0.03	0.877
d*f	1	0.1791	0.61%	0.0066	0.00664	0.09	0.797
s*f	1	0.1231	0.42%	0.1231	0.1231	1.59	0.335
Error	2	0.1551	0.53%	0.1551	0.07756		
Total	8	29.2683	100.00%				

6.3.3.2 ANOVA for S/N ratio of cutting tool tip temperature with PFM

In case of cutting tool tip temperature in progressive feed machining with uncoated cutting tools, the PCR for DoC is 68.27%, it is the peak value among all (Table 6.22). It means that DoC is the most influencing factor followed by feed rate (PCR=27.79%) and cutting speed (PCR=2.52%) is having least influence on cutting tool tip temperature. Whereas with coated cutting tool the highest PCR value is arrived for DoC is 70.15% (Table 6.23). It indicates that DoC is the most significant parameter followed by feed rate (PCR = 26.49%) and cutting speed (PCR =2.41%) is having least impact on output response. Therefore, ANOVA results in all the above discussed cases of machining are complimenting the results attained through S/N ratio analysis and depth of cut is the most influencing factor for T.

Table 6.22 ANOVA for S/N ratio of T obtained in PFM with uncoated tool

Source	DF	Seq SS	PCR	Adj SS	AdjMS	F-Value	P-Value
Regression	6	27.6684	99.39%	27.6684	4.6114	53.96	0.018
d	1	19.0055	68.27%	0.147	0.14704	1.72	0.32
s	1	0.7003	2.52%	0.1153	0.11529	1.35	0.365
f	1	7.7378	27.79%	0.8303	0.83026	9.71	0.089
d*s	1	0.0041	0.01%	0.0051	0.0051	0.06	0.83
d*f	1	0.1698	0.61%	0.0246	0.02457	0.29	0.646
s*f	1	0.0509	0.18%	0.0509	0.05088	0.6	0.521
Error	2	0.1709	0.61%	0.1709	0.08547		
Total	8	27.8393	100.00%				

Table 6.23 ANOVA for S/N ratio of T obtained in PFM with coated tool

Source	DF	Seq SS	PCR	Adj SS	AdjMS	F-Value	P-Value
Regression	6	31.8413	99.63%	31.8413	5.30689	104.84	0.009
d	1	22.4086	70.15%	0.3303	0.33033	6.53	0.125
s	1	0.77	2.41%	0.165	0.16502	3.26	0.213
f	1	8.4616	26.49%	0.6838	0.68377	13.51	0.067
d*s	1	0.0082	0.03%	0.0131	0.0131	0.26	0.661
d*f	1	0.1807	0.57%	0.059	0.05896	1.16	0.393
s*f	1	0.0123	0.04%	0.0123	0.01233	0.24	0.671
Error	2	0.1012	0.32%	0.1012	0.05062		
Total	8	31.9426	100.00%				

In case of cutting tool tip temperature in progressive feed machining with uncoated cutting tools, the PCR for DoC is 68.27%, it is the peak value among all (Table 6.22). It means that DoC is the most influencing factor followed by feed rate (PCR=27.79%) and cutting speed (PCR=2.52%) is having least influence on cutting tool tip temperature. Whereas with coated cutting tool the highest PCR value is arrived for DoC is 70.15% (Table 6.23). It indicates that DoC is the most significant parameter followed by feed rate (PCR = 26.49%) and cutting speed (PCR =2.41%) is having least impact on output response. Therefore, ANOVA results in all the above discussed cases of

machining are complimenting the results attained through S/N ratio analysis and depth of cut is the most influencing factor for T.

6.3.3.3 ANOVA for S/N ratio of surface roughness with CFM

Table 6.24 ANOVA for S/N ratios of R_a obtained in CFM with uncoated tools

Source	DF	Seq SS	PCR	Adj SS	Adj MS	F-Value	P-Value
Regression	6	56.7566	99.97%	56.7566	9.45944	1193.28	0.001
d	1	7.3558	12.96%	0.2031	0.2031	25.62	0.037
s	1	10.8202	19.06%	0.3747	0.37465	47.26	0.021
f	1	37.0197	65.21%	0.011	0.01102	1.39	0.36
d*s	1	0.7855	1.38%	0.8933	0.89334	112.69	0.009
d*f	1	0.2427	0.43%	0.0143	0.01426	1.8	0.312
s*f	1	0.5327	0.94%	0.5327	0.53272	67.2	0.015
Error	2	0.0159	0.03%	0.0159	0.00793		
Total	8	56.7725	100.00%				

Table 6.25 ANOVA for S/N ratios of R_a obtained in CFM with coated tools

Source	DF	Seq SS	PCR	Adj SS	Adj MS	F-Value	P-Value
Regression	6	53.092	99.45%	53.0918	8.8464	60.77	0.016
d	1	7.3533	13.77%	0.0503	0.05033	0.35	0.616
s	1	10.768	20.17%	0.7217	0.72172	4.96	0.156
f	1	34.36	64.36%	0.1247	0.1247	0.86	0.452
d*s	1	0.1859	0.35%	0.3364	0.3364	2.31	0.263
d*f	1	0.1003	0.19%	0.0207	0.02.067	0.14	0.743
s*f	1	0.3247	0.61%	0.3247	0.32466	2.23	0.274
Error	2	0.2912	0.55%	0.2912	0.1456		
Total	8	53.383	100.00%				

In case of constant feed machining with uncoated cutting tool the highest PCR value arrived for feed rate is 65.21% (Table 6.24). It means that feed rate is the most influencing factor followed by cutting speed with PCR=19.06% and depth of cut with PCR=12.96% showing least impact. Whereas with coated cutting tool the highest PCR value arrived for feed rate was found to be 64.36% (Table 6.25). Therefore, feed rate is the most influencing parameter followed by cutting speed with PCR=20.17% and depth of cut with PCR=13.77% is showing least influence on the response (R_a).

6.3.3.4 ANOVA for S/N ratio of surface roughness with PFM

Table 6.26 ANOVA for S/N ratio of R_a obtained in PFM with uncoated tool

Source	DF	Seq SS	PCR	Adj SS	Adj MS	F-Value	P-Value
Regression	6	57.0964	99.88%	57.0964	9.51606	285.97	0.003
d	1	7.927	13.87%	0.2657	0.26567	7.89	0.106
s	1	9.9257	17.36%	0.4359	0.43587	13.1	0.069
f	1	38.4363	67.24%	0.2646	0.26458	7.95	0.106
d*s	1	0.3961	0.69%	0.7478	0.7478	22.47	0.042
d*f	1	0.0007	0.00%	0.1992	0.19916	5.98	0.134
s*f	1	0.4106	0.72%	0.4106	0.41064	12.34	0.072
Error	2	0.0666	0.12%	0.0666	0.03328		
Total	8	57.1629	100.00%				

Table 6.27 ANOVA for S/N ratio of Ra obtained in PFM with coated tool

Source	DF	Seq SS	PCR	Adj SS	Adj MS	F-Value	P-Value
Regression	6	56.2788	99.88%	56.2788	9.37981	279.81	0.004
d	1	5.0591	8.98%	0.0615	0.06154	1.84	0.308
s	1	9.3021	16.51%	0.7091	0.70911	21.15	0.044
f	1	41.4373	73.54%	0.2725	0.27247	8.13	0.104
d*s	1	0.1162	0.21%	0.278	0.27799	8.29	0.102
d*f	1	0.0602	0.11%	0.0341	0.0341	1.02	0.419
s*f	1	0.3039	0.54%	0.3039	0.30391	9.07	0.095
Error	2	0.067	0.12%	0.067	0.03352		
Total	8	56.3459	100.00%				

In case of surface roughness in progressive feed machining with uncoated cutting tools, the PCR value for feed rate (67.24%) is the highest (Table 6.26). Therefore, it is the most influencing factor followed by cutting speed with PCR=17.36% and depth of cut with PCR=13.87% is having least influence. Whereas with coated cutting tool the highest PCR value arrived for feed rate is 73.54% (Table 6.27). Therefore, feed rate is the most influencing parameter, cutting speed is showing moderate influence with PCR=16.51% and depth of cut is having least influence with PCR=8.98% on the output

response R_a. ANOVA results in all the cases of machining are in line with S/N ratio results and feed rate is the most influencing factor on R_a.

6.3.3.5 ANOVA for S/N ratio of material removal rate with CFM

Table 6.28 ANOVA for S/N ratio of MRR obtained in CFM with uncoated tools

Source	DF	Seq SS	PCR	Adj SS	Adj MS	F-Value	P-Value
Regression	6	286.639	99.47%	286.639	47.7732	62.03	0.016
d	1	132.013	45.81%	10.187	10.1867	13.23	0.068
s	1	0.03	0.01%	0.245	0.2453	0.32	0.629
f	1	148.997	51.70%	0.201	0.2007	0.26	0.66
d*s	1	0.9	0.31%	4.67	4.6705	6.06	0.133
d*f	1	0.069	0.02%	2.659	2.6592	3.45	0.204
s*f	1	4.631	1.61%	4.631	4.6309	6.01	0.134
Error	2	1.54	0.53%	1.54	0.7701		
Total	8	288.18	100.00%				

Table 6.29 ANOVA for S/N ratio of MRR obtained in CFM with coated tools

Source	DF	Seq SS	PCR	Adj SS	Adj MS	F-Value	P-Value
Regression	6	286.666	99.47%	286.666	47.7777	62.11	0.016
d	1	132.279	45.90%	10.037	10.0369	13.05	0.069
s	1	0.029	0.01%	0.242	0.2418	0.31	0.631
f	1	148.917	51.67%	0.233	0.2329	0.3	0.637
d*s	1	0.861	0.30%	4.543	4.5426	5.91	0.136
d*f	1	0.077	0.03%	2.63	2.6299	3.42	0.206
s*f	1	4.503	1.56%	4.503	4.5028	5.85	0.137
Error	2	1.539	0.53%	1.539	0.7693		
Total	8	288.205	100.00%				

In case of material removal rate in constant feed machining with uncoated cutting tool the highest PCR value arrived for feed rate is 51.70% (Table 6.28). Therefore, feed rate is the most influencing factor, depth of cut with PCR=45.81% showing next higher impact and cutting speed (PCR=0.01%) showing almost zero influence. CFM with coated cutting tools also showed a similar trend with different percentage of PCR values (Table 6.29). ANOVA results in all the cases of machining are in line with S/N ratio results and feed rate is the most influencing factor on MRR.

6.3.3.6 ANOVA for S/N ratio of material removal rate with PFM

Table 6.30 ANOVA for S/N ratio of MRR obtained in PFM with uncoated tool

Source	DF	Seq SS	PCR	Adj SS	Adj MS	F-Value	P-Value
Regression	6	286.836	99.46%	286.836	47.806	61.17	0.016
d	1	131.396	45.56%	10.123	10.1228	12.95	0.069
s	1	0.044	0.02%	0.226	0.2265	0.29	0.644
f	1	149.863	51.96%	0.227	0.2265	0.29	0.644
d*s	1	0.933	0.32%	4.662	4.6621	5.97	0.135
d*f	1	0.074	0.03%	2.626	2.6264	3.36	0.208
s*f	1	4.527	1.57%	4.527	4.5272	5.79	0.138
Error	2	1.563	0.54%	1.563	0.7815		
Total	8	288.399	100.00%				

Table 6.31 ANOVA for S/N ratio of MRR obtained in PFM with coated tool

Source	DF	Seq SS	PCR	Adj SS	Adj MS	F-Value	P-Value
Regression	6	283.693	99.50%	283.693	47.2822	65.79	0.015
d	1	130.45	45.75%	9.879	9.8789	13.75	0.066
s	1	0.062	0.02%	0.311	0.3113	0.43	0.578
f	1	147.645	51.78%	0.158	0.1581	0.22	0.685
d*s	1	0.829	0.29%	4.495	4.4947	6.25	0.13
d*f	1	0.037	0.01%	2.509	2.5094	3.49	0.203
s*f	1	4.67	1.64%	4.67	4.6703	6.5	0.126
Error	2	1.437	0.50%	1.437	0.7187		
Total	8	285.131	100.00%				

In case of material removal rate in progressive feed machining with uncoated cutting tools the maximum value of PCR was obtained is for feed rate: 51.96% (Table 6.30). Therefore, feed rate is the most influencing factor, depth of cut is moderately influencing with PCR=45.56% and cutting speed (PCR=0.02%) is showing almost zero influence on output response. A similar trend has been observed with coated tools also (Table 6.31). It is observed that ANOVA results are in line with from S/N ratio analysis results.

6.4 MULTI-RESPONSE OPTIMISATION OF MACHINING PROCESS

Multi-objective optimization will give an overall improved machining and therefore it has been chosen for optimizing the end milling process. Cutting tool tip temperature, average surface roughness and MRR values obtained through the experimentation with CFM and PFM are depicted in Table 6.3 and Table 6.4. These experimental values are further analysed by means of multi-objective optimisation techniques such as: T-GRA and T-TOPSIS for both conventional CFM and proposed PFM respectively.

6.4.1 Taguchi based Grey Relational Analysis (T-GRA)

In multi-objective optimisation problem, the relationships between various parameters are multifaceted and not clear. This condition of data is termed as grey, which means that it is uncertain and poor information. GRA studies this complex uncertainty among multi-objectives and optimizes it with the help of GRG. Then, a multi-objective optimization problem will be reduced to a single-response optimization problem known as single relational grade. The scope of present research work is to identify the optimal combination of machining parameters that simultaneously minimizes the cutting tool tip temperature, surface roughness and maximizes the MRR.

6.4.1.1Steps involved in Grey Relational Analysis (Lin & Lin 2005)

This consists of the following major steps to be followed.

i) Identifying, the process parameters of end milling and the output performance characteristics to be assessed.
ii) Finding input process parameters levels.
iii) Choosing the suitable OA and assigning the machining parameters to OAs.
iv) To perform the experiments according to the preparations of the orthogonal array (OA) considered.
v) Normalizing the results obtained from the experiments conducted in the previous step for: cutting tool tip temperature, surface roughness and MRR.
vi) To carry out the grey relational generation and calculating the grey relational coefficient.

vii) Calculating the GRGs by averaging the grey relational coefficients.

viii) Then, analyzing the experimental values using GRG and ANOVA.

ix) Choosing the optimal levels of input process parameters for end milling.

x) Finally, verifying the obtained optimal process parameters through the confirmation experiments.

Following flowchart (Figure 6.13) illustrates the step-by-step procedure to be followed for multi-objective optimization of process parameters by means of T-GRA.

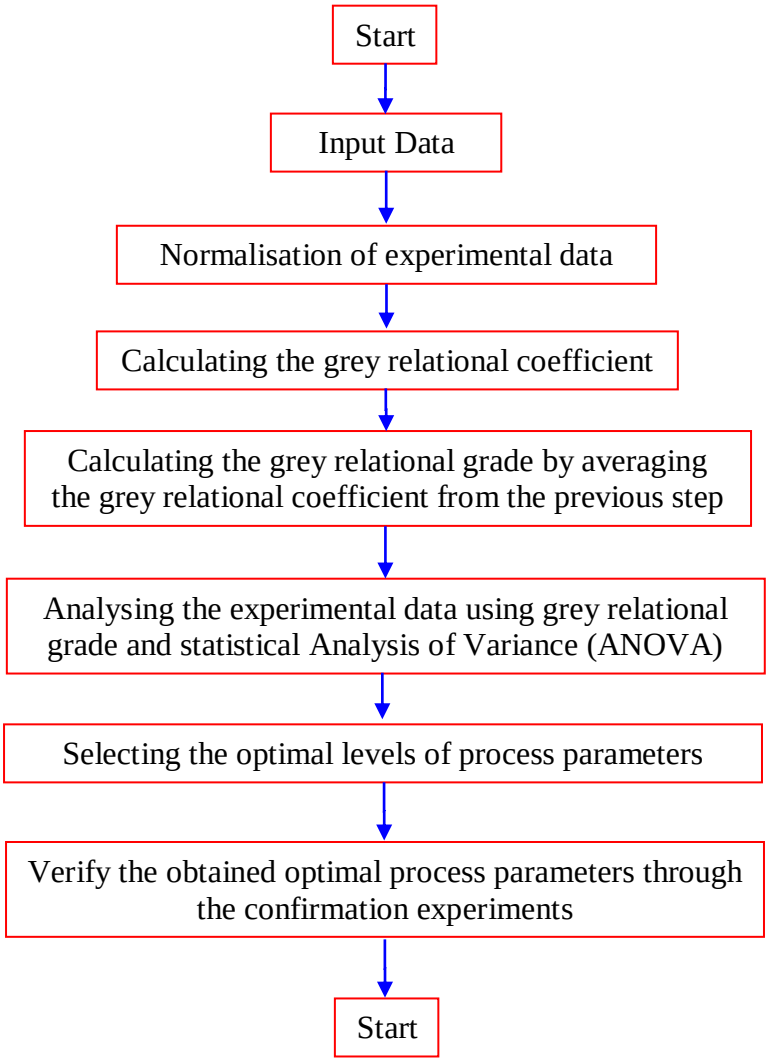

Figure 6.13 Optimisation procedures for the present study.

6.4.1.2 Data Processing

In grey relational analysis, different sequences will be used. The sequence is nothing but an arrangement of data in an experiment. And the reference sequence is not

anything, but the order, which needs to be used for reference. Minimum R_a, minimum T and maximum MRR are set to be the reference sequences. Generally, the reference sequence is taken as 1.

Step 1: Grey relational generation

Optimum condition of various cutting factors is determined by deploying grey relational analysis to obtain the best quality characteristics (Gupta and Kumar 2013; Wang et al. 2013; Ramanujam et al. 2011; Senthilkumar et al. 2014). First step involved in GRA is normalizing the experimental data to reduce the variability according to the type of performance response to avoid different kinds of units. A suitable value is derived from the original value to make the array between '0'and '1', and this procedure is termed as data processing. It is a procedure of converting the original data in to a comparable data. If the response is to be minimized, smaller-the-better quality characteristic is envisioned for normalization, to scale it into an acceptable range. In the present work, the surface roughness and cutting tool tip temperature are the responses needs to be minimized for betterment, therefore 'Smaller-the-better' (SB) is the form we obtained as the original sequence, then this original sequence can be normalized as follows (Rao et al. 2018) using equation 6.5.

$$x_i^*(k) = \frac{\max(x_i^o(k)) - (x_i^o(k))}{\max(x_i^o(k)) - \min(x_i^o(k))} \quad \ldots\ldots\ldots\ldots\ldots\ldots (6.5)$$

If the target value of actual sequences is infinite, such as material removal rate which needs to be maximised for better performance, it has the 'higher-the-better' (HB) characteristic and the normalization of actual sequence can be performed as follows (Rao et al. 2018) using equation 6.6.

$$x_i^*(k) = \frac{x_i^o(k) - \min(x_i^o(k))}{\max(x_i^o(k)) - \min(x_i^o(k))} \quad \ldots\ldots\ldots\ldots\ldots\ldots (6.6)$$

Where, i=1,….,m; k=1,….,n., and 'm' is the number of experimental data and 'n' is the number of responses,$x_i^o(k)$ denotes the original sequence,$x_i^*(k)$denotes the sequence after data processing, $max\left(x_i^0(k)\right)$denotes the largest value of $x_i^0(k)$, $min\left(x_i^o(k)\right)$ denotes the smallest value of $x_i^o(k)$, and $x$is the desired value (Tosun and Pihtili 2010).

If a defined target value for OA exists, the normalization of actual sequence can be performed using equation 6.7 as follows:

$$x_i^*(k) = 1 - \frac{|x_i^0(k) - OA|}{max\left[max\left(x_i^0(k)\right) - OA,\ OA - min\left(x_i^0(k)\right)\right]} \ldots\ldots\ldots\ldots \quad (6.7)$$

Where, $x_i^*(k)$ is the value after grey relational generation (normalized value), $max(x_i^0(k))$ and $min(x_i^0(k))$ are the largest and smallest values of $x_i^0(k)$ for the k^{th} response respectively, $k$is being 1 for surface roughness, 2 for cutting tool tip temperature and 3 for material removal rate.

6.4.1.3 Grey Relational Coefficient and Grey Relational Grade

After carrying out data processing, a grey relational coefficient is calculated to express the association between best and actual normalised experimental results.

Step 2: Grey relational coefficient (GRC)

The correlation between the best and actual normalised experimental results is denoted by grey relational coefficients (GRC). The formulae to calculate the grey relational coefficient $(\zeta_i(k))$ is given at equation 6.8 below, and its value lies between ZERO and ONE as per equation 6.9.

$$\zeta_i(k) = \frac{\Delta_{min} + \zeta\Delta_{max}}{\Delta_{0i}(k) + \zeta\Delta_{max}} \ldots\ldots\ldots\ldots\ldots\ldots \quad (6.8)$$

$$\text{And } 0 < \zeta_i(k) \leq 1 \quad \ldots\ldots\ldots\ldots\ldots\ldots \quad (6.9)$$

Where,$\Delta_{0i}(k)$ is the deviation sequence (equation 6.10) of the reference sequence $x_0^*(k)$and comparability sequence$x_i^*(k)$, its minimum and maximum values will be obtained by equation 6.11 and equation 6.12 respectively.

$$\Delta_{0i}(k) = \left\|x_0(k) - x_{ij}\right\| \ldots\ldots\ldots\ldots\ldots\ldots \quad (6.10)$$

$$\Delta_{min} = \min\left\|x_0(k) - x_{ij}\right\| \quad \ldots\ldots\ldots\ldots \quad (6.11)$$

$$\Delta_{max} = \max\left\|x_0(k) - x_{ij}\right\| \ldots\ldots\ldots\ldots\ldots \quad (6.12)$$

Where, ζ is the distinctive coefficient (ζ ∈[0, 1]) and it is used to regulate the difference of the relational coefficient. In this work ζ value was chosen as 0.5 and the grey relational coefficients are calculated using equation 6.8 against each experimental run and are depicted in Table 6.32.

Step 3: Grey relational grade (GRG)

The grey relational grade is computed by finding the average of the grey relational coefficient corresponding to each performance characteristic. This degree is being estimated using following equation 6.13.

$$\alpha_i = \frac{1}{n} \sum_{k=1}^{n} \zeta_i(k) \ldots\ldots\ldots\ldots\ldots\ldots\ldots\ldots \quad (6.13)$$

Where, α_i is the required grey relational grade for i^{th} experiment and 'n' is number of performance characteristics. If the grey relational grade is having a greater value, it shows that the concerned parameter combination is closer to the optimum value. GRG depicts the overall quality index, transformed to single response. The values of GRG determine the ranking of experimental runs and to obtain near-optimal set of variables.

Step 4: Grey relational ordering

Grey relational grades were calculated using equation 13, and the calculated grey relational order was figured out in Table 6.32 using L_9 orthogonal array (OA). An order of '1' is allotted to greatest grey relational grade. From Table 6.32, we can see that the control parameter's setting of seventh experiment had the greatest grey relational grade and this indicates that, seventh experiment has the optimal end milling parameters combination to obtain minimum surface roughness, minimum cutting tool tip temperature and maximum material removal rate simultaneously among the conducted nine experimental runs as per L_9 orthogonal array (OA). Here, higher the grey relational grade better is the product quality. Therefore, on the basis of grey relational grade, the factor effect can be estimated and the optimal level for each controllable factor can be determined.

Table 6.32 Normalized values, grey relational coefficients and grey relational grades of responses

Normalized values of responses			Deviation Sequence			Grey Relational Coefficients			GRG	Rank
Ra µm	**T °C**	**MRR mm^3/sec**	**Ra µm**	**T °C**	**MRR mm^3/sec**	**Ra µm**	**T °C**	**MRR mm^3/sec**	**GRG**	**Grade**
0.483	1.000	0.000	0.517	0.000	1.000	0.492	1.000	0.333	0.608	2
0.276	0.583	0.411	0.724	0.417	0.589	0.408	0.545	0.459	0.471	8
0.034	0.000	1.000	0.966	1.000	0.000	0.341	0.333	1.000	0.558	3
0.690	0.718	0.166	0.310	0.282	0.834	0.617	0.639	0.375	0.544	4
0.552	0.145	0.761	0.448	0.855	0.239	0.527	0.369	0.676	0.524	5
0.000	0.570	0.305	1.000	0.430	0.695	0.333	0.538	0.418	0.430	9
1.000	0.295	0.348	0.000	0.705	0.652	1.000	0.415	0.434	0.616	**1**
0.431	0.738	0.184	0.569	0.262	0.816	0.468	0.656	0.380	0.501	7
0.276	0.313	0.805	0.724	0.687	0.195	0.408	0.421	0.719	0.516	6

6.4.1.4 Analysis of Results using 'Response Tables' and 'Response Graphs'

Since the experimental design was orthogonal, it is possible to separate the effect of each machining parameter on the grey relational grade at different levels. For example, the mean of grey relational grade for cutting speed at level ONE, TWO and THREE could be calculated by averaging the grey relational grade for experiments 1 to 3, 4 to 6 and 7 to 9 respectively. The mean of grey relational grade for each level of parameter is summarized and were shown in Table 6.33. In addition to that, the total mean of grey relational grade (0.5156) for all the nine experiments has been calculated and it is listed in the Table 6.33. If larger the grey relational grade, better is the multiple performance characteristics. However, the relative importance among cutting parameters for multi-performance characteristics will still need to be identified, so that the optimal combinations of process parameter levels can be determined more accurately (Ramanujam and Muthukrishnan 2011). Bigger delta reverence demonstrates higher centrality of parameter in controlling the response. In the response table (Table 6.33) it can be seen that feed rate has been assigned with a rank ONE which means it is the

most significant parameter in controlling the responses followed by cutting speed with rank TWO and depth of cut with rank THREE.

Table 6.33 Response table for means of GRG

Levels and Parameters	**Level-1**	**Level-2**	**Level-3**	**Delta (max-min)**	**Rank**
A. Cutting speed (s)	0.5440*	0.4836	0.5219	0.0604	2
B. Feed rate (f)	0.5834*	0.4829	0.4833	0.1005	**1**
C. Depth of cut (d)	0.5094	0.4909	0.5492*	0.0583	3
Total mean value of the Grey Relational Grade = 0.5165					
* Indicates optimum levels					

Figure 6.14 illustrates the main effects plot for grey relational grade for various levels of process control parameters considered. The peak value at each level of the Figure 6.14 represents the optimal result for GRG i.e. A1 (cutting speed at 2000 rpm), B1 (feed rate at 200mm/min) and C3 (depth of cut at 2.25mm), and the same was observed from the response table for grey relational grades as displayed in Table 6.33. To achieve simultaneously minimum surface roughness, minimum cutting tool tip temperature and maximum material removal rate this combination of process controlling factors were used. Hence, the optimum combination of input process parameters is: ***A1-B1-C3 (s1-f1-d3)***.

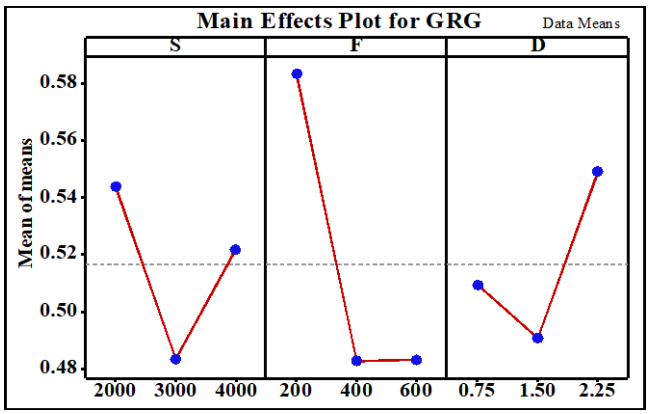

Figure 6.14 Main effects plot for Grey Relational Grade

In the interaction plots, non-parallelism of lines denotes significant interaction (Mukhopadhyay et al. 2016). From Figure 6.15, it can be seen that the combinations of

cutting speed &feed rate, cutting speed & depth of cut and depth of cut & feed rate have significant interaction effects compared to other combinations.

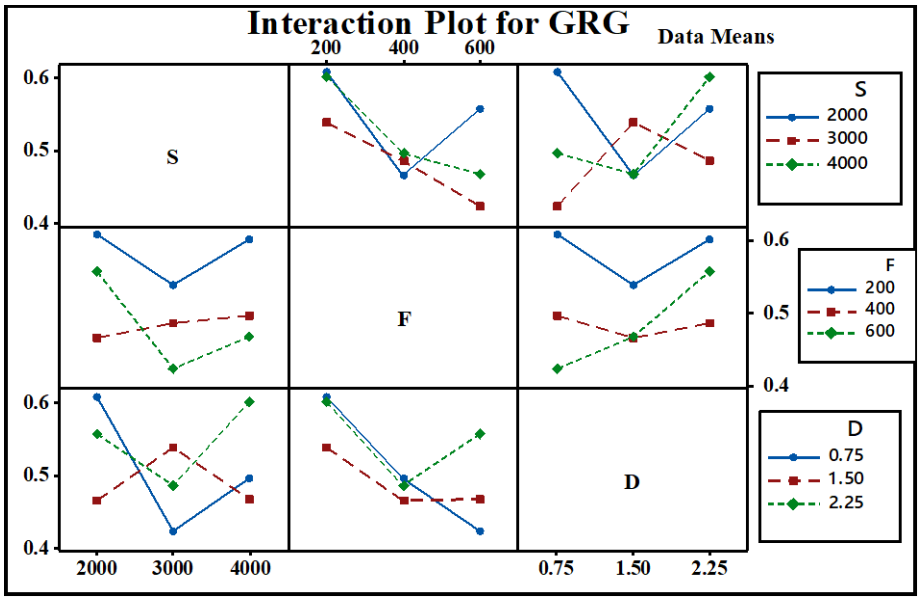

Figure 6.15 Interaction plots for Grey Relational Grade

Analysis of surface roughness

The measured experimental values of surface roughness, cutting tool tip temperature and material removal rate are listed in Table 6.3. Highest value of surface roughness (0.92µm) was obtained in the sixth experimental run (i.e at *s*: 3000rpm, *f*: 600mm/min and *d*: 0.75mm) and least value (0.34µm) of the same was found at seventh experimental run (i.e at *s*: 4000rpm, *f*: 200mm/min and *d*: 2.25mm).

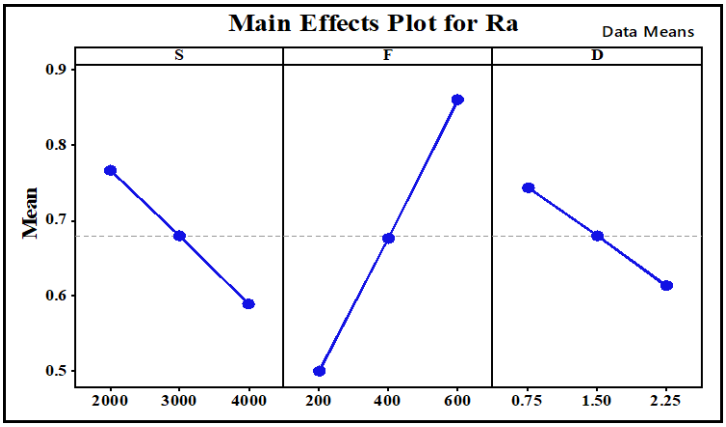

Figure 6.16 Main effects plot for average surface roughness

From the main effects plot (Figure 6.16) it is implicit that, surface roughness is decreasing with the increase of cutting speed and depth of cut as well, whereas it is increasing considerably with the increase of feed rate.

Analysis of cutting tool tip temperature

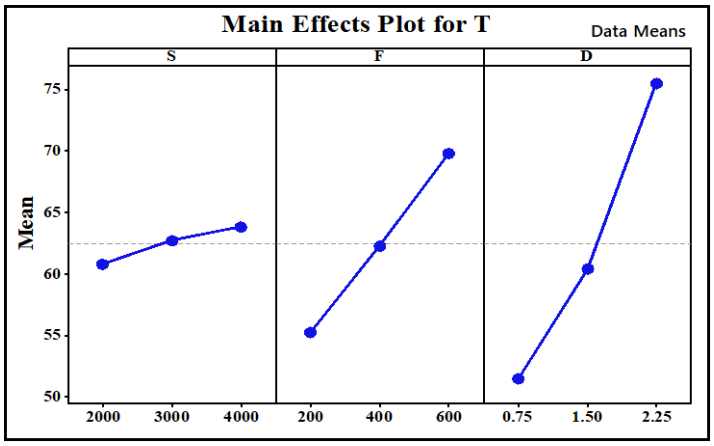

Figure 6.17 Main effects plot for cutting tool tip temperature

From the results (Table 6.3), it is implicit that, highest value of cutting tool tip temperature (81.2^{o}C) was found at the combination of input process parameters (*s*: 2000rpm, *f*: 600mm/min and *d*: 2.25mm). Whereas least value of cutting tool tip temperature (42.6^{o}C) was attained at the combination (*s*: 2000rpm, *f*: 200mm/min and *d*: 0.75mm). From the main effects plot (Figure 6.17) it is perceived that cutting tool tip temperature is increasing with the increase of cutting speed, feed rate and depth of cut as well. But the rate of increase of cutting tool tip temperature is sluggish w.r.t cutting speed, intermediate w.r.t feed rate and it is drastic w.r.t depth of cut.

Analysis of material removal rate

From the results (Table 6.3), it is implicit that, the highest value of material removal rate (441.211mm^3/min)) was found at the combination of controllable process parameters (*s*: 2000rpm, *f*: 600mm/min and *d*: 2.25mm). Whereas least value of material removal rate (47.486mm^3/min) was achieved at the input parameters combination of (*s*: 2000rpm, *f*: 200mm/min and *d*: 0.75mm). From the main effects plot (Figure 6.18) it is observed that the material removal rate is drastically increasing with

the increase of feed rate and also with the increase of depth of cut as well. But it is decreasing sharply with the increase of cutting speed from 2000rpm to 3000rpm and there after it is slowly decreasing with the increase of cutting speed from 3000rpm to 4000rpm.

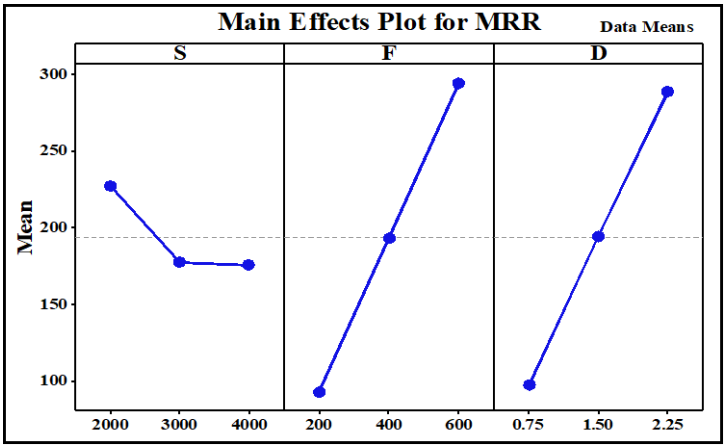

Figure 6.18 Main effects plot for material removal rate

6.4.1.5 ANOVA outcomes for GRG

Basically, larger the grey relational grade better is the multi performance characteristics. However, the relative importance among the machining parameters for a multi-performance characteristic is still need to know, so that the optimal combinations of machining levels can be determined more accurately.

The purpose of ANOVA is to investigate, which machining parameter is significantly affecting the performance characteristics. This is consummated by separating the total variability of the grey relational grades, which is measured by the sum of squared deviations from the total mean of grey relational grade, into contributions by each machining parameter and the error (Lin and Lin 2002). The total sum of squared deviations SS_T from the total mean of grey relational grade γ_m is calculated by equation 6.14.

$$SS_T = \sum_{j=1}^{P}(\gamma_j - \gamma_m)^2 \ldots\ldots\ldots\ldots\ldots\ldots \quad (6.14)$$

Where, p is the number of experiments conducted through the selected orthogonal array (OA), and γ_j is the mean grey relational grade for j^{th} experiment.

The total sum of squared deviations (SS_T) is disintegrated in to two sources: the sum of squared deviations (SS_d) due to each machining parameter and the sum of squared error (SS_e). The percentage contribution of each of the machining parameter in the total sum of squared deviations (SS_T) can be used to evaluate the importance of machining parameter change on the performance characteristics. In addition, the Fisher's F-test can also be used to determine which machining parameter has a significant effect on the performance characteristic. Usually, the change of machining parameters has a significant effect on the performance characteristics when F-value is large.

Table 6.34 ANOVA for grey relational grade (Multiple response characteristics)

Source	**DF**	**Seq SS**	**Contribution**	**Adj SS**	**Adj MS**	**F-Value**	**P-Value**
Regression	6	0.032514	98.91%	0.032514	0.005419	30.22	0.032
s	1	0.000727	2.21%	0.001111	0.001111	6.20	0.131
f	1	0.015025	45.71%	0.000165	0.000165	0.92	0.439
d	1	0.002369	7.21%	0.011065	0.011065	61.71	0.016
s*f	1	0.000247	0.75%	0.008648	0.008648	48.23	0.020
s*d	1	0.000124	0.38%	0.007613	0.007613	42.46	0.023
f*d	1	0.014021	42.65%	0.014021	0.014021	78.19	0.013
Error	2	0.000359	1.09%	0.000359	0.000179		
Total	8	0.032872	100.00%				

Percentage contribution of each machining parameter on multi-objective optimization was assessed using ANOVA. Results of ANOVA for grey relational grade (GRG) depicted in Table 6.34, indicates that feed rate is the machining parameter showing substantial influence on multi-performance characteristics with 45.71% followed by depth of cut with 7.21% and cutting speed is showing least influence with 2.21%. Then, coming to interaction effect of process control factors feed rate multiplied by depth of cut (*f*d*) is having significant influence with 42.65%on multi-performance characteristics. Whereas, cutting speed multiplied by feed rate (*s*f*) and cutting speed multiplied by depth of cut (*s*d*) are having almost negligible influence with 0.75% and 0.38% respectively.

6.4.1.6 Confirmation experiments for T-GRA

By grey relational analysis, the optimal combination of the process parameters is identified to improve the milling characteristics. The final stage of grey relational analysis is to verify the obtained optimum condition for multi-objective quality characteristics through conformation experiments. The equation for confirmation experiments can be expressed as follows (Shi et al. 2015) at equation 6.15.

$$\gamma_{predicted} = \gamma_m + \sum_{i=1}^{n}(\gamma_i - \gamma_{m)} \ldots\ldots\ldots\ldots \quad (6.15)$$

Where,

$\gamma_{predicted}$: Is the grey relational grade to predict the optimal end milling process parameters.

γ_m: Is the total mean of the grey relational grade,

γ_i: Is the mean of grey relational grade at optimum level of significant factors *s*, *f* and *d*.

n: Is the number of significant milling parameters (*s*, *f* and *d*) affect the quality characteristics.

Table 6.35 Confirmation test results for T-GRA optimisation

Levels	**Initial Machining Parameters**	**Optimal Machining Parameters**	
		Predicted	**Experimental**
Setting Level	***d2-s2-f2***	***d3-s1-f1***	***d3-s1-f1***
Surface roughness (μm)	0.67	0.514	0.51
Cutting tool tip temperature (^{0}C)	58.6	65.04	64.9
Material removal rate (mm3/sec)	195.32		131.27
Grey relational grade	0.6080	**0.6436**	0.7156
Improvement in grey relational grade = 0.1017			

Calculation of grey relational grade for predicting the optimal end milling process parameters is as follows:

$$\gamma_{predicted} = \gamma_m + \sum_{i=1}^{3}(\gamma_i - \gamma_{m)}$$

= 0.5165+ (0.5440-0.5165) + (0.5834-0.5165) + (0.5492-0.5165) = **0.6436**

The optimum combination for input control parameters is ***s1-f1-d3*** and calculated grey relational grade by equation 6.15 is 0.6436.

Based on the equation 6.15, the estimated grey relational grade using the optimal machining parameters can then be obtained. Table 6.35 shows the results of confirmation experiment using optimal machining parameters. The surface finish is improved from 0.67µm to 0.51µm, cutting tool tip temperatures lightly increased from 58.6^{0}C to 64.9^{0}Cand material removal rate is greatly increased from 47.486mm^3/sec to 195.32mm^3/sec and it is very much required for quick machining. It can be noted that the experimental value of surface roughness and material removal rate are considerably enhanced by Taguchi based Grey Relational Analysis (T-GRA).

6.4.2 Taguchi coupled 'Technique for Order Preference by Similarity to Ideal Solution' (TOPSIS) analysis

Technique for Order Preference by Similarity to Ideal Solution (TOPSIS) is another technique similar to T-GRA, most frequently used for multi-objective optimization solution in the manufacturing field in order to acquire optimum cutting process conditions. It was introduced by Hwang and Yoon (Hwang and Yoon 1981). It is used to identify the best alternatives which have the shortest separation from the positive ideal solution and farthest separation from the negative ideal solution (Sivaiah and Chakradhar 2019). This method selects the best alternative answer which is close to the ideal solution. A detailed step by step procedure to be followed according to Taguchi coupled TOPSIS technique to convert a multi response optimization problem in to a single response optimization problem (Sivaiah and Chakradhar 2019) has been explained in detail in this section. It is a perfect ranking method, which compares the performance characteristics by eliminating the unit differences among the data by normalization process.

6.4.2.1 Conversion of multi responses into a single response using TOPSIS methodology

Step 1: The first step of this technique is to build the experimental decision matrix (DM_{ij}) in which each row (***i***) represents the experimental run number (alternative combinations) and (***j***) represents the performance characteristics (performance attributes).

$$DM_{ij} = \begin{bmatrix} X_{11} & X_{12} & X_{1j} & X_{1m} \\ X_{21} & X_{22} & X_{2j} & X_{2m} \\ X_{i1} & X_{i2} & X_{ij} & X_{im} \\ X_{n1} & X_{n2} & X_{nj} & X_{nm} \end{bmatrix} \ldots\ldots\ldots\ldots\ldots\ldots\ldots\ldots \quad (6.16)$$

Where,

i= is the number of experimental runs (i = 1, 2, 3, …….,*n*), and in the present case '*n*' is equal to '9'.

j=is the number of performance responses or attributes considered for the study (j =1, 2,……..,*m*), and in this study *m* is equal to '3' (T, R_a and MRR).

The experimental values obtained by conducting experiments according to Taguchi's L_9 orthogonal array (OA) are depicted in Table 6.3 were considered for decision matrix DM_{ij} elements as mentioned in equation 6.16. All the calculations made are rounded up to five fractions accuracy after the decimal.

Step 2: In this step, the performance characteristics are normalized in order to bring them to a common scale and to eliminate the variation of their measuring units. These normalized values vary between '0' and '1'. Equation 6.17 has been used to obtain the normalized matrix and computed normalized values were depicted in Table 6.36.

$$NM_{ij} = \frac{X_{ij}}{\sqrt{\sum_{j=1}^{n} X_{ij}^2}} \ldots\ldots\ldots\ldots\ldots\ldots\ldots \quad (6.17)$$

Where,

NM_{ij} = Normalised performance matrix

X_{ij} = Normalised value of i^{th} experimental run allied with j^{th} response

n= Number of experimental runs conducted (l = 1, 2, 3, ……..……, 9)

m = Number of performance responses considered for study (m = 1, 2, 3)

Table 6.36 Normalized data and weighted normalized data

Exp run	Normalized values			Weighted normalized values		
	Ra	T	MRR	Ra	T	MRR
1	0.30455	0.22341	0.06976	0.10152	0.07447	0.02325
2	0.36165	0.30784	0.28370	0.12055	0.10261	0.09457
3	0.42828	0.42584	0.64814	0.14276	0.14195	0.21605
4	0.24745	0.28057	0.14016	0.08248	0.09352	0.04672
5	0.28552	0.39647	0.42565	0.09517	0.13216	0.14188
6	0.43779	0.31046	0.21654	0.14593	0.10349	0.07218
7	0.16179	0.36605	0.19868	0.05393	0.12202	0.06623
8	0.31883	0.27637	0.14209	0.10628	0.09212	0.04736
9	0.36165	0.36238	0.43266	0.12055	0.12079	0.14422

Step 3: In this step, the weighted normalised matrix (WM_{ij}) was built by multiplying each normalised element of this matrix by assigned weight of their respective response (w_j). Decision maker importance was given to surface roughness, cutting tool tip temperature and material removal rate in such a way that, the sum of weights is equal to 1.

$$WM_{ij} = [w_j N\ M_{ij}] \quad \text{……..} \quad (6.18)$$

Where, w_j= Relative importance given to the j^{th}response (j = 1,2,3).

Here, all the three performance characteristics (responses) are given equal importance and hence the relative weight of 1/3 is assigned to each response. Then, using these relative weights, the weighted normalised matrix (WM_{ij})was obtained by multiplying each element by their relative weight as per the equation 6.18. The obtained weighted normalised values were depicted in Table 6.36, as a weighted normalised matrix (WM_{ij}).

Step 4: In this step of TOPSIS analysis, ideal positive (P^+)and ideal negative (P^-) alternative of the performance characteristic is obtained using close to the ideal solution of each performance attribute (response) using equation 6.19 and equation 6.20. In the

present study both surface roughness (R_a) and cutting tool tip temperature (T) are the responses to be minimized, whereas material removal rate is the response to be maximized for performance enhancement.

$$P^+ = \left\{\sum_i^{max} WM_{ij}\,/j \in L\,,\ \sum_i^{min} WM_{ij}\,/j \in L'\,/i, i = 1,\ 2,\ \ldots\ldots,9\right\}$$

$$= \{P_1^+\,, P_2^+,\ P_3^+,\ \ldots\ldots P_m^+\}\ldots\ldots\ldots\ldots\ldots\ldots\ldots\ldots(6.19)$$

$$P^- = \left\{\sum_i^{max} P_{lm}\,/m \in L\,,\ \sum_l^{min} P_{lm}\,/m \in L'\,/l\ \ l = 1,\ 2,\ \ldots\ldots,9\right\}$$

$$= \{P_1^-\,, P_2^-,\ P_3^-,\ \ldots\ldots P_m^-\}\ldots\ldots\ldots\ldots\ldots\ldots\ldots\ldots\ (6.20)$$

Where,

L *= (l =1, 2,……..…..,9)/l* is related with beneficial attributes.

L' = (*l =1, 2,……, 9)/l* is related with non-beneficial attributes.

In the present case, the value of

P^+ = ideal best solution = {0.05393} and

P^- = ideal worst solution = {0.14593} for surface roughness,

P^+ = ideal best solution = {0.07447} and

P^- = ideal worst solution = {0.14195} for cutting tool tip temperature,

P^+ = ideal best solution = {0.21605} and

P^- = ideal worst solution = {0.02325} for material removal rate.

Step 5: In this step, separation measure was calculated for the best alternative (Q^+) and worst alternative (Q^-) to know the separation of each alternative to the ideal alternative which is given by Euclidean distance. Equation 6.21 and equation 6.22 were used to compute the Euclidean distances ($Q^+$and Q^-) and corresponding results were shown in Table 6.37.

$$Q^{+}= \sqrt{\sum_{i=1}^{9}(WP_{ij} - P_m^{+})^2}(l = 1, 2, \ldots\ldots,9) \quad \ldots\ldots\ldots \quad (6.21)$$

$$Q^{-}= \sqrt{\sum_{i=1}^{9}(WP_{ij} - P_m^{-})^2}(l = 1, 2, \ldots\ldots,9) \quad \ldots\ldots\ldots \quad (6.22)$$

Step 6: In this step, closeness coefficient (RCL_i) was calculated using equation 6.23 for each alternative. It indicates the closeness distance of each alternative to the ideal solution. Table 6.37 shows the respective closeness coefficient (RCL_i) values for each alternative in L_9 orthogonal array (OA) design.

$$RCL_i = \frac{Q^{-}}{Q^{+}+Q^{-}} \quad \ldots\ldots\ldots\ldots\ldots\ldots\ldots \quad (6.23)$$

Where, i = 1, 2, ……., 9

Then through this step, multiple responses (R_a, T and MRR) were merged into a single response in the name of closeness coefficient (RCL_i). Now, this closeness coefficient (RCL_i) will be treated as a single response for further analysis. The higher value of closeness coefficient (RCL_i)indicates thelevel of nearness to the ideal solution. Because of this reason closeness coefficient (RCL_i) is treated as the 'higher-the-better' characteristic for better performance.

6.4.2.2 Determination of optimum cutting parameters

After converting multiple responses (R_a, T and MRR) into a single response (in the form of closeness coefficient), Taguchi's single objective optimization method was used to optimize this single response closeness coefficient (RCL_i). Minitab-2018 has been used to calculate the S/N ratios of the closeness coefficients depicted in Table 6.37. The larger value of closeness coefficient indicates least distance from the ideal solution. Hence, by considering 'higher-the-better' maximization of closeness coefficient(RCL_i)was considered to determine the S/N ratio through Taguchi's single objective optimisation technique. Figure 6.19 is the main effects plot for the mean of S/N ratios of the respective cutting parameter levels of closeness coefficient(RCL_i). Levels of the cutting parameters corresponding to maximum means of the S/N ratios are taken as the optimum setting of input parameters as per Taguchi's approach.

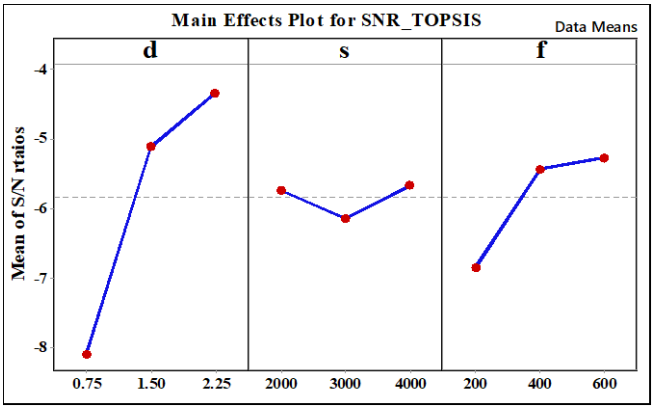

Figure 6.19 Main effects plot for S/N ratio of closeness coefficient

Table 6.37 Separation measures, closeness coefficient and signal to noise ratios

Exp run	Separation measures		Closeness coefficient	S/N Ratio	Rank
	Q+	Q-	RCLi	SNR	R
1	0.12246	0.08078	0.39748	-8.0136356	8
2	0.06861	0.08531	0.55426	-5.1257264	4
3	0.11552	0.19282	0.62535	-4.0775839	3
4	0.09934	0.08320	0.45577	-6.8250544	6
5	0.05911	0.12941	0.68644	-3.2679715	1
6	0.10029	0.06224	0.38293	-8.3375245	9
7	0.09570	0.10348	0.51952	-5.6878808	5
8	0.10129	0.06809	0.40200	-7.9153964	7
9	0.05996	0.12540	0.67652	-3.3944112	2

According to Figure 6.19, the highest mean of respective process parameters of closeness coefficient (RCL_i) was taken as Taguchi's predicted optimum process parameter settings. Thus, the Taguchi predicted optimum settings were identified from the main effects plot and from Table 6.38, they are: d = 2.25mm, s = 4000RPM, f = 600mm/min respectively (***d3-s3- f3***).

Table 6.38 Response table for S/N ratio of closeness coefficient

Symbol	Process Parameter	Closeness Coefficient				
		Level 1	Level 2	Level 3	Delta	Rank
s	Cutting speed (RPM)	-5.739	-6.1435	-5.6659	0.47762*	3
f	Feed rate (mm/min)	-6.8422	-5.4364	-5.2698	1.57235*	2
d	Depth of cut (mm)	-8.0889	-5.1151	-4.3445	3.74437*	1

6.4.2.3 Confirmation tests for TOPSIS

Using following equation 6.24, predicted closeness coefficient value ($\psi_{predicted}$) at Taguchi predicted optimum parameter settings was computed.

$$\psi_{predicted} = \psi_{predicted} + \sum_{l}^{m} \psi_o - \psi_l \quad \text{.....} \quad (6.24)$$

Where, ψ_l = Total mean of S/N ratio

ψ_o = Mean of S/N ratio at optimal level

m = number of input process parameters = 3 (*f, s and d*)

As per Taguchi's predicted optimum parameter settings confirmation tests have been conducted and the results (Table 6.39) were compared with the results obtained through initial parameter settings (***s2-f2-d2***).

From the confirmation results obtained at Taguchi optimum cutting parameters, it was observed that, surface roughness is 0.74µm, cutting tool tip temperature is 87.2°C and material removal rate is 447.291mm^3/min (**Table 6.39**).

Table 6.39 Confirmation test results for TOPSIS optimization

Levels	**Initial Machining Parameters**	**Optimal Machining Parameters**	
		Predicted	**Experimental**
Setting Level	*(d2-s2-f2)*	*(d3-s3-f3)*	*(d3-s3-f3*
Surface roughness (µm)	0.67	0.734	0.74
Cutting tool tip temperature (°C)	58.2	87.24	87.2
Material removal rate (mm^3/min)	195.32		447.291

6.5 COMPARISSION BETWEEN 'T-GRA'AND 'T-TOPSIS'

The summarised confirmation results at optimum cutting conditions determined through T-GRA and T-TOPSIS have depicted in Table 6.40 for better understanding.

Table 6.40 Comparison of confirmation test results from T-GRA and T-TOPSIS

Levels	**Initial machining parameters**	**Optimal machining parameters**		**Change in terms of percentage**	
Setting level	***(d2-s2-f2)***	GRA	TOPSIS	GRA	TOPSIS
		d3-s1-f1	***d3-s3-f3***	***d3-s1-f1***	***d3-s3-f3***
Surface roughness (µm)	0.67	**0.51**	0.74	**23.88% Reduction**	10.45% Increase
Cutting tool tip temperature (^{o}C)	58.6	64.9	87.2	10.75% Increase	48.81% Increase
Material removal rate (mm^3/min)	195.32	131.27	**447.29**	32.79% Reduction	**129.01% Increase**

6.5.1 Taguchi based Grey Relational Analysis

From the Table 6.40, it is evident that T-GRA optimisation methodology gave an overall better solution compared to TOPSIS optimisation technique. There is a considerable betterment in the most critical response (R_a) at T-GRA optimal machining parameters over the initial machining parameters. There is an improvement of 23.8806% in surface finish, this effect owing to the **softening** of the area near to the chip-tool interface at higher temperatures. This would cause removal of surface discontinuities and flaws at the cutting zone (Pawadeet al.2007). But there is a slight increase in cutting tool tip temperatureof10.75%and 32.79% of reduction in material removal rate which were negligible.

6.5.2 Taguchi coupled TOPSIS

From Table 6.40, it is evident that all the responses with Taguchi coupled TOPSIS optimal machining parameters (***d3-s3-f3***) got increased compared to initial machining parameters (***d2-s2-f2***). Surface roughness got increased by 10.45% and there is a considerable increase in cutting tool tip temperature by 48.81%, which is not recommended. But there is a substantial increase in material removal rate by 129.01%. Hence, TOPSIS optimal machining conditions are more suitable when we need to complete the machining process very quickly. But we have to compromise quality of surface roughness and increase in cutting tool tip temperature, which may not be

possible in all the situations. From Table 6.40 T-GRA is giving the low level of surface roughness and low value of cutting tool tip temperature over TOPSIS. But a considerable decrease of MRR was found with T-GRA over T-TOPSIS.

Since an equal importance was given to all three responses in the present research work. T-GRA multi-objective optimisation technique positively improved the most critical response (Ra), whereas Taguchi coupled TOPSIS technique had showed an improvement in trivial response (MRR) which is not an important facet in the product quality point of view. In any manufacturing process, surface finish of the machined component significantly improves the life of the product. Similarly, cutting tool tip temperature directly affects the tool life. However, from both the results of Taguchi based GRA and Taguchi coupled TOPSIS we can choose any one, based on the relative importance of quality of the product required or quickness of the process to be completed. But, T-GRA is giving overall better solution over TOPSIS in the present research work. Hence, T-GRA is more suitable multi-objective optimisation technique within a given range of process parameters of end milling.

6.6 CLOSURE

Taguchi's single objective optimisation has been employed and optimum values of each performance characteristic found separately. Further to obtain high-quality machining, multi-response decision models have been developed by considering cutting speed, feed rate and depth of cut as process parameters and cutting tool tip temperature, surface roughness and material removal rate are the performance characteristics chosen for evaluation. Two types of multi-objective optimisation techniques such as: Taguchi based grey relational analysis (T-GRA) and Taguchi coupled TOPSIS are employed for multi-objective process optimization.

1. Grey relational analysis of the experimental results for surface roughness, cutting tool tip temperature and material removal rate can convert optimization of multiple performance characteristics into optimization of a single performance characteristic called grey relational grade.

2. The optimal machining parameters combination by employing Taguchi's single objective optimisation for cutting tool tip temperature is ***d1-s1-f1***. Cutting tool tip

temperature has decreased from 58.60^{0}C to 42.6^{0}0C with this combination of optimal machining parameters over the initial machining parameters considered: ***d2-s2-f2***.

3. The optimal machining parameters combination by employing Taguchi's single objective optimisation for average surface roughness is ***d3-s3-f1***. Average surface roughness has decreased from 0.67 μmto 0.34 μmwith this combination of optimal machining parameters over the initial machining parameters considered: ***d2-s2-f2***.

4. The optimal machining parameters combination by employing Taguchi's single objective optimisation for material removal rate is ***d3-s1-f3***. Material removal rate has increased 195.32mm^3/min to 441.21mm^3/min with this combination of optimal machining parameters over the initial machining parameters considered: ***d2-s2-f2***.

5. Through T-GRA, the optimal machining parameters combination obtained is: ***d3-s1-f1.*** Whereas by means of Taguchi coupled TOPSIS, the optimal machining parameters combination obtained is: ***d3-s3-f3.*** T-GRA is giving 23.88% of decrease in most critical performance characteristic, whereas TOPSIS gave an increase of 10.45% of the same over initial machining parameters combination: *d2-s2-f2*. This encourages applying the Taguchi based grey relational analysis (T-GRA) concept for optimizing multi-response processing with multiple input cutting process factors is more appropriate over Taguchi coupled TOPSIS.

CHAPTER 7

CONCLUSIONS AND FUTURE SCOPE

7.1 CONCLUSIONS

A new approach of controlling the machining feed rate called progressive feed machining (PFM) has been adopted, studied and analysed experimentally over the traditional constant feed machining (CFM) by mainly focusing on measurement, prediction and analysis of output performance responses such as: surface roughness (R_a), cutting tool tip temperature (T), material removal rate (MRR), surface topography through end milling experiments on BS L168 aluminium alloy work material. Response surface methodology (RSM) has been used for predictive modelling and to analyse the process responses. ANOVA was used to further analyse and to find the level of model fitness, percentage of influence of each process parameter along with most influenced process parameter on the performance responses. Further analysis has been carried out to find the effect of nose radius on performance characteristics with the help of One-Factor-at-A-Time approach of experimentation and then graphical analysis was done by establishing 2D plots. Later on, Taguchi's method was employed for single response optimization, ANOVA and S/N ratio tools were employed to find most influenced process parameter on each output response. Taguchi based Grey Relational Analysis (T-GRA) and Taguchi coupled Technique of Order Preference Similarity to the Ideal Solution (T-TOPSIS) optimization techniques have been employed for multi-response optimization. To validate the results from these optimization techniques confirmation tests were conducted. Through comparative analysis, best multi-objective optimization tool which suits for the current study has been selected between T-GRA and T-TOPSIS. The following are the conclusions drawn from the experimental and analytical results obtained from the present research work.

1. Reduction in sudden impact of cutting tool with workpiece, in turn reduction in tool deflection, minimal tool vibration, less chattering and rubbing in PFM with coated and uncoated cutting tools has been observed over CFM. These things contributed to a substantial change in the process responses: R_a, T, Surface topography in PFM

over CFM.

- Overall, PFM attained positive results in terms of R_a, T and Surface topography but there is a mild decrease in MRR.

2. PFM with coated cutting tools combination has yielded better results over CFM with coated & un-coated cutting tools combination.

   - PFM with coated and uncoated cutting tools presented a considerable reduction in surface roughness (R_a) about **29.48**% and **19.01%**over CFM with un-coated cutting tools respectively.
   - PFM with coated and uncoated cutting tools presented a considerable reduction in cutting tool tip temperature (T) about **12.67**% and **5.63%** over CFM with un-coated cutting tools respectively.
   - PFM with coated and uncoated cutting tools offered negligible drop in MRR about **8.01**% &**7.56**% over CFM with uncoated cutting tools. It is mainly due to controlling the feed rate at the beginning and where there is a change in cut direction.

3. RSM analysis revealed that, predicted values of R_a, T and MRR from the developed regression models are in good agreement with the experimental results.

   - The mean value of absolute percentage of errors for surface roughness (**R_a)** in CFM and PFM are **2.56**% and **5.08**% respectively. For cutting tool tip temperature (**T)** these errors are only **2.78**% and **3.18**% in CFM and PFM respectively. While, for **MRR** these errors in CFM and PFM are only **1.80**% and **1.68**% respectively.
   - These errors are mainly due to uncontrollable variables like: chip loads, type of chip formation, tool wear and unexpected fluctuations in power supply, variation in air flow rate, variation in room temperature etc.
   - ANOVA results for R_a, T and MRR reveals that accuracy of more than 95% with un-coated & coated cutting tools is expected in both CFM & PFM.
   - Therefore, the developed models are adequate with more than 95% of confidence level and appropriate for predicting R_a, T and MRR for any given set of input parameters.

4. From the established 3D surface plots it is clear that,

- Combination of low levels of feed rate, cutting speed and DoC is giving low value of cutting tool tip temperature (T).
- Combination of low feed rate, high cutting speed and high depth of cut is yielding better surface finish.
- Combination of high feed rate and high depth of cut yielding higher MRR, and cutting speed does not showing much influence on MRR.

5. From OFAT approach of experimental analysis, it is understood that,

- Nose radius (NR) of end mill cutter is having significant influence on the output performance characteristics other than MRR.
- Cutting tool tip temperature (T) is increasing with the increase of NR of the end mills.
- Whereas, average R_a and MRR are getting decreasing with the increase of nose radius.
- But the variation in MRR is very mild w.r.t variation of NR of the end mills.

6. From the surface topography analysis carried out with help of optical microscope, it is understood that,

- As the NR of the end mill increases from 0.4mm to 1.2mm, surface roughness (R_a) is getting reduced from 0.86µm to 0.62µm at constant values of rake angle: 16^0, cutting speed of 4.188m/sec, feed rate of 0.15mm/rev and depth of cut 2.25mm.

7. Taguchi's single objective optimisation gave 30.96% of reduction in cutting tool tip temperature (T), 49.85% reduction in surface roughness (R_a) and 127.04% of improvement in MRR individually with *s1-f1-d1*, *s3-f1-d3* and *s1-f3-d3*combinations of input process parameters respectively (Table 6.4 to Table 6.6) over initial combination of process parameters *s2-f2-d2*.

8. Improved end milling performance responses were found with T-GRA over T-TOPSIS.

- Therefore, for the present work, T-GRA is more suitable for solving the multi response optimization problem within the given range of process parameters under both the machining environments.
- The optimal cutting parameters obtained through T-GRA for machining process is: *s1-f1-d3*. Whereas, the optimal cutting parameters obtained through T-TOPSIS for machining process is: *s3-f3-d3*.

9. This work also emphasizes that proper selection of cutting parameters along with PFM eliminates the use of secondary finishing operations and therefore saves the manufacturing time and cost.

FUTURE SCOPE OF WORK

- Proposed concept of PFM can be extended to the following areas of research for better results through machining. Can be aimed to extend with hard-to-machine aerospace materials, such as Titanium, Monel, Inconel, Tungsten, Al904L, Al6XN, Nimonic, Steel and different types of composites.

- More process responses can be considered, such as tool wear, chatter, cutting tool vibration, machine tool vibration, cutting force, surface waviness, surface flatness, white layer thickness and power consumption by the machine tool etc.

- Metallurgical aspects of different materials for machining can be taken up study. A combined regression model to address multiple cutting tools can be developed. Comparative FEM analysis between CFM and PFM can be done.

- Progressive feed with different combinations of work materials and tool materials can be tried to assess the effectiveness of the same.

REFERENCES

Aggarwal, A., Singh, H., Kumar, P. and Singh, M. (2008). "Optimization of multiple quality characteristics for CNC turning under cryogenic cutting environment using desirability function." *Journal of Materials Processing Technology*, 205 (1), 42-50. https://api.semanticscholar.org/CorpusID:135501874

Ajith, A. D. S., Pugazhenthi, K. R. and Vijayananth, S. (2019). "Multi objective prediction and optimization of control parameters in the milling of aluminium hybrid metal matrix composites using ANN and Taguchi-grey relational analysis." *Defense Technology*, 15, 545-556. https://doi.org/10.1016/j.dt.2019.01.001

Badrinadhan, K. S. and Karunamoorthy, L. (2014a). "Study of the effect of Progressive Feed Rate on the Cutting Force in CNC End milling of AISI 1045 Steel." *International Journal of Engineering and Technology*, 5(6), 4741 – 4751. http://www.enggjournals.com/ijet/docs/IJET13-05-06-231.pdf

Badrinathan, K. S. and Karunamoorthy, L. (2014b). "Reducing Tool Wear in CNC End Milling Operation Using Progressive Feed Rate." *Applied Mechanics and Materials*, (592-594), 716-723. https://doi.org/10.4028/www.scientific.net/AMM.592-594.716

Baptista, A., Silva, F. J. G., Porteiro, J., Míguez, J. L. and Pinto, G. (2018a). "Sputtering physical vapour deposition (PVD) coatings: A critical review on process improvement and market trend demands." *Coatings*, 8, 402 - 412. https://doi.org/10.3390/coatings8110402

Baptista, A., Silva, F. J. G., Porteiro, J., Míguez, J. L., Pinto, G. and Fernandes, L. (2018b). "On the Physical Vapour Deposition (PVD): Evolution of Magnetron Sputtering Processes for Industrial Applications." *Procedia Manufacturing*, 17, 746 - 757. https://doi.org/10.1016/j.promfg.2018.10.125

Barathiraja, S. and Basker, N. (2012). "Application of Particle Swarm Optimization Technique for Achieving Desired Milled Surface Roughness in Minimum Machining

Time.” *International Journal of Expert Systems with Applications*, 39, 5982 - 5989.

Baskar, N., Asokan, P. and Prabaharan, G. (2005). “Optimization of machining parameters for milling operations using non-conventional methods.” *The International Journal of Advanced Manufacturing Technology*, 25 (11-12), 1078 - 1088.

Bhirud, N. L. and Gawande, R. R. (2017). “Measurement and prediction of cutting temperatures during dry milling: review and discussions.” *Journal of Brazilian Society for Mechanical Science and Engineering*, 39, 5135 - 5158. https://doi.org/10.1007/s40430-017-0869-7

Caliskan, H., Panjan, P. and Kurbanoglu, C. (2017). “Hard Coatings on Cutting Tools and Surface Finish.” *Comprehensive Materials Finishing*, 3, 230 - 242. https://doi.org/10.1016/B978-0-12-803581-8.09178-5

Campatelli, G., Lorenzini, L. and Scippa, A. (2014). “Optimization of process parameters using a Response Surface Method for minimizing power consumption in the milling of carbon steel.” *Journal of Cleaner Production*, 66, 309 - 316.

Chockalingam, P. (2012). “Surface Roughness and Tool Wear Study on Milling of AISI304 Stainless Steel Using Different Cooling Conditions.” *International Journal of Engineering and Technology*, 2, 1386-1391.

Daniyan, I. A., Tlhabadira, I., Mpofu, K., Adeodu, A.O. (2021). “Process Design and Optimization for the Milling Operation of Aluminum Alloy (AA6063 T6).” *Materials Today: Proceedings,* 38, 536–543.

Deng, Qi., Rong, Mo., Zezhong, C. C. and Zhiyong, C. (2020). “An Analytical Approach to Cutter Edge Temperature Prediction in Milling and Its Application to Trochoidal Milling.” *Applied Science*, 10, 1746. https://doi.org/10.3390/app10051746

Deshpande, Y., Andhare, A. and Sahu, N. K. (2017). “Estimation of surface roughness using cutting parameters, force, sound, and vibration in turning of Inconel 718.” *Journal of the Brazilian Society of Mechanical Sciences and Engineering*, 1, 1-10.

Durga, P. K. G., Prasad, M. V. and Venkata, S. K. (2015). “Optimization of process parameters in CNC end milling of glass-fibre reinforced plastic.” *International Journal for Research in Emerging Science and Technology*, 2(6), 60 - 67.

Dutta, S., Kanwat, A., Pal, S. K. and Sen, R. (2013). “Correlation study of tool flank wear with machined surface texture in end milling.” *Measurement,* 46, 4249 - 4260.

Emel, K. and Ozcelik, B. (2013). “Multi-objective optimization using Taguchi based grey relational analysis for micro-milling of Al 7075 material with ball nose end mill.” *Measurement*, 46 (6), 1849–1864.

Fernández-Abia, A.I., Barreiro, J., Fernández-Larrinoa, J., Lacalle, L. N. L., Fernández-Valdivielso, A. and Pereira, O. M. (2013). Behaviour of PVD Coatings in the Turning of Austenitic Stainless Steels.” *Procedia Engineering*, 63, 133 - 141. https://doi.org/10.1016/j.proeng.2013.08.241

Fukuo, H., Rahul, G. C., Shreyes, N. and Melkote. (2016). “Characteristics and Performance of Surfaces Created by Various Finishing Methods (Invited Paper).” *Procedia CIRP*, 45, 1- 6.

Ghosh,T., Wang, Y.i., K. and Martinsen, K. W. (2020). “A surrogate-assisted optimization approach for multi-response end milling of aluminium alloy AA3105.” *International Journal of Advanced Manufacturing Technology*, 111(9-10), 2419- 2439.

Gilberth., W. W. (1950). “Economics of machining, machining theory and practice.” *American Society of Metals*, 465 - 485.

Gopal, P. M. and Soorya, P. K. (2018). “Minimization of cutting force, temperature and surface roughness through GRA TOPSIS and Taguchi techniques in end milling of Mg hybrid MMC.” *Measurement*, 116, 178 - 192.

Gupta, M. and Kumar, S. (2013). “Multi-objective optimization of cutting parameters in turning using grey relational analysis.” *International Journal of Industrial Engineering Computations*, 4, 547 - 58.

Gürcan, S. (2016). “Optimization of Cutting Parameters Using Taguchi Method During the Face Milling of AISI 1040 with Coated and Uncoated Inserts.” *Düzce University Journal of Science & Technology,* 4 (1), 278 - 292.

Harne, M. S. and Ravikumar, L. S. (2015). “Optimization of End Milling Parameters on Surface Roughness of Die Steel HCHCr by Taguchi Method.” 4, 6699 - 2702.

Hwang, C. L. and Yoon, K. (1981). “*Multiple Attribute Decision Making Methods and Applications*.” Springer. New York.

Kadirgama, K., Noor, M. M., Rahman, M. M., Harun, W. S. W. and Haron, C. H. C. (2009). “Finite element analysis and statistical method to determine temperature distribution on cutting tool in end milling.” *European Journal of Scientific Research*, 30(3), 451 - 463.

Kai, Y., Ying-chun, L., Kang-ning, Z., Qing-shun, B.and Wan-qun, C. (2011). “Tool edge radius effect on cutting temperature in micro-end-milling process.” *International Journal of Advanced Manufacturing Technology,* 52, 905 - 912.

Kant, G., Rao, V. V. and Sangwan, K. S. (2013). “Predictive modelling of turning operations using response surface methodology.” *Applied Mechanics and Materials*, 307, 170 - 173.

Kant, G. and Sangwan, K. S. (2014). “Prediction and optimization of machining parameters for minimizing power consumption and surface roughness in machining.” *Journal of Cleaner Production,* 83, 151 - 164.

Kannan, S., Baskar, N., Varatharajulu, M. and Suresh K. B. (2015a). “Modelling and optimization of face milling parameters on brass component using response surface methodology and genetic algorithm.” *International Journal of Applied Engineering Research,* 10 (76), 219 - 224.

Kannan, S., Baskar, N., Suresh, K. B. and Varatharajulu, M. (2015b). “Investigation on optimum cutting condition in face milling of copper with HSS cutter using response

surface methodology and genetic algorithm." *International Journal of Applied Engineering Research*, 10 (57), 243 - 247.

Kannan, S., Suresh, K. B. and Baskar, N. (2014). "Selection of machining parameters in face milling operations for copper workpiece material using response surface methodology and genetic algorithm."*5th International & 26th All India Manufacturing Technology, Design and Research Conference (AIMTDR 2014).* 137, 1- 6.

Kumar, Y. and Singh, H. (2014). "Multi-response optimization in dry turning process using Taguchi's approach and utility concept." *Procedia Materials Science*, 5, 2142 - 2151.

Landau, L.D. and Lifschitz, E.M. (1966). "*Fluid Mechanics Pergamon Press*: *New York.*" New York, USA, 157 - 191.

Lande, A. R., Patil, S. B. and Gaidhani, Y. B. (2016). "Experimental Investigation of AL-6351 by using Gray Taguchi Methodology." *International Journal of innovation and research*, 2, 371 - 380.

Liao, Y. S. and Lin, H. M. (2007). "Mechanism of minimum quantity lubrication in high-speed milling of hardened steel." *International Journal of Machine Tools and Manufacturing*, 47 (11), 1660 - 1666.

Liu, N., Wang, S.B., Zhang, Y.F. and Lu, W. F. (2016). "A novel approach to predicting surface roughness based on specific cutting energy consumption when slot milling Al-7075.*" International Journal of Mechanical Sciences*, 118, 13 - 20.

Lin, J. L. and Lin, C.L. (2002). "The use of the orthogonal array with grey relational analysis to optimize the electrical discharge machining process with multiple performance characteristics." *International Journal of Machine Tools and Manufacture*, 42, 237 - 244.

Lin, J.L. and Lin. C.L. (2005). "The use of grey-fuzzy logic for the optimization of the manufacturing processes." *Journal of Materials Processing Technology*, 160, 9 - 14.

Li, C., Xiao, Q., Tang, Y. and Li, L.i. (2016). “A method integrating Taguchi, RSM and MOPSO to CNC machining parameters optimization for energy saving.” *Journal of Cleaner Production*, 135, 263 - 275.

Li, W.Y.B. and Guo, Y. B. (2014). “Effect Tool Wear during End Milling on the Surface Integrity and Fatigue Life of Inconel 718.” *International Conference on High Performance Cutting*, HCP2014, 546 - 551.

Mahesh, G. (2020). “Optimization of machining parameters on temperature rise in CNC turning process of aluminum 6061 using RSM and Genetic algorithm.” *International Journal of Modern Manufacturing Technologies,* XII (1): 36 - 43.
ISSN 2067–3604, Vol.XII, No. 1 / 2020

Majumder, H. and Maity, K. (2018). “Prediction and optimization of surface roughness and micro hardness using grnn and MOORA-fuzzy-a MCDM approach for nitinol in WEDM.” *Measurement*, 118, 1- 13.

Manjaiah, M., Narendranath, S. and Basavarajappa, S. (2016). “Wire Electro Discharge Machining Performance of TiNiCu Shape Memory Alloy.” *Silicon*, 8 (3), 467 - 475.

Manna, A. (2013). “Multi-response optimization of machining parameters during drilling LM6Mg15SiC-Al-MMC based on Grey relational analysis”. *International Journal of Machining and Machinability of Materials*, 14(3), 275 - 294.

Masmiati, N., Ahmed, A.D. S. (2015). “Optimizing cutting parameters in inclined end milling for minimum surface residual stress -Taguchi approach.” *Measurement,* 60, 267 - 275.

Masooth, P. H. S., Vijayarangam, J. and Bharathiraja, G. (2020). “Experimental investigation on surface roughness in CNC end milling process by uncoated and TiAlNcoated carbide end mill under dry conditions.” *Materials Today Proceedings,* 22(3), 726 - 736. https://doi.org/10.1016/j.matpr.2019.10.036

Mia, Mozammel. (2018). “Mathematical modelling and optimization of MQL assisted

end milling characteristics based on RSM and Taguchi method." *Measurement,* 121: 249 - 260. https://doi.org/10.1016/j.measurement.2018.02.017

Mithilesh, K. D., Asit, B. P. and Atanu, M. (2014). "Experimental Study of Cutting Forces in Ball End Milling of Al2014-T6 Using Response Surface Methodology." *Procedia Materials Science*, 6, 612 - 622.

Mohamad, A. S. T. (2014). "Prediction of Tool Wear for Ball End Nose in Milling Inconel 718 Using a Feed Forward Back Propagation Neural Network." *Australian Journal of Basic and Applied Sciences,* 8, 383 - 390.

Montgomery, D.C. (1987). "*Design and analysis of experiments.*" Second edition". Quality and Reliability Engineering International, 3(3), 212 - 212.

Montgomery, D. C. (2017). "*Design and analysis of experiments.*" John wiley & sons. Eight edition.

Muhammad, R. M. and Adesta Y. E. T. (2016). "Investigation of Cutting Temperature for AISI H13 in High-Speed End Milling." *International Journal of Engineering Materials and Manufacture,* 1(1), 27 - 34.
https://doi.org/10.26776/ijemm.01.01.2016.06

Mukhopadhyay, A. S., Duari, T.K., Barman, P. and Sahoo. (2016). "Wear behaviour of electroless Ni-PW coating under lubricated condition-a Taguchi based approach, IOP Conf. Series." *Materials Science and Engineering*, 149, 012004.
https://doi.org/10.1088/1757- 899X/149/1/012004.

Murthy K.S. and Rajendran, I. (2012). "Optimization of end milling parameters under minimum quantity lubrication using principal component analysis and grey relational analysis." *Journal of Brazilian Society of Mechanical Sciences and Engineering,* 34(3), 253 - 261.

Myers, R. H., Montgomery, D. C., Christine, M. and Anderson-Cook, C. M. (2016). "Response surface methodology: process and product optimization using designed

experiments." *John Wiley & Sons*. Fourth edition, ISBN: 978-1-118-91601-8

Naresh, N. and Rajasekhar, K. (2016), "Multi-response optimization for milling AISI 304Stainless steels using GRA and DFA." *Advanced Materials Research,* 5(2), 67 - 80.

Natarajan, U., Periyanan, P. R. and Yang, S. H. (2011). "Multiple-response optimization for micro-end milling process using response surface methodology." *The International Journal of Advanced Manufacturing Technology*, 56(1), 177 - 185.

Noor, B., Zeelan, B., Vellimalai, S., Bella, R. and Senthil, K. (2018). "An integrated approach of RSM and MOGA for the prediction of temperature rise and surface roughness in the end milling of Al6061-T6." *TRANSACTIONS OF FAMENA,* XLII (3): 115 - 128.

Norouzifard, V. and Hamedi, M. (2014). "A three-dimensional heat conduction inverse procedure to investigate tool-chip thermal interaction in machining process." *International Journal of Advanced Manufacturing Technology*, 74, 1637 - 1648. https://doi.org/10.1007/s00170-014-6119-6

Nurhaniza, M., Ariffin, M. and Mustapha, F. (2016). "Analysing the effect of machining parameters setting to the surface roughness during end milling of CFRP aluminium composite laminates." *International Journal of Manufacturing Engineering*, 2016, 1- 9. https://doi.org/10.1155/2016/4680380.

Ojolo, S. J., Money, O. D. and Ismail, O. S. (2015). "Experimental investigation of cutting parameters on surface roughness prediction during end milling of aluminium 6061 under mql (minimum quantity lubrication)." *Journal of Mechanical Engineering and Automation,* 5 (1), 1 - 13.

Pandey, A., Goyal, A. and Meghvanshi, R. (2017). "Experimental investigation and optimization of machining parameters of aerospace material using Taguchi's DOE approach." *Materials Today: Proceedings,* 4(8), 7246 - 51.

Parida A.K. and Maity. K. (2017). “Effect of nose radius on forces, and process parameters in hot machining of Inconel 718 using finite element analysis.” *Engineering Science and Technology, an International Journal*, 20(2), 687 - 693. https://doi.org/10.1016/j.jestch.2016.10.006.

Parthiban, K., Duraiselvam, M. and Manivannan, R. (2018). “TOPSIS based parametric optimization of laser micro-drilling of TBC coated nickel based super alloy.” *Optics and Laser Technology,* 102, 32 - 39.

Patel, S. B. and Hiren. P. (2012). “Optimization of Machining Parameters for Surface Roughness in Milling Operation.” *International Journal of Applied Engineering Research,* 7-11.

Pawade, R.S., Joshi, S.S., Brahmankar, P.K. and Rahman, M. (2007). “An investigation of cutting forces and surface damage in high-speed turning of Inconel 718.” *Journal of Materials Processing Technology,* 192,139-146.

Ramanujam, R., Muthukrishnan, N. and Raju, R. (2011). “Optimization of cutting parameters for turning Al-Sic (10p) MMC using ANOVA and grey relational analysis”. *International Journal of Precision Engineering and Manufacturing,* 12(44), 651–656.

Ramesh, S., Karunamoorthy, L. and Palanikumar, K. (2012). “Measurement and analysis of surface roughness in turning of aerospace titanium alloy (gr5).” *Measurement,* 45, 1266–1276.

Raneen, A. A., Mozammel, M., Aqib, M. K., Wenliang, C., Munish, K. G. and Catalin, I. P. (2019). “Multi-Response Optimization of Face Milling Performance Considering Tool Path Strategies in Machining of Al-2024.” *Materials*, 12(7), 3 - 19. http://dx.doi.org/10.3390/ma12071013

Rajender, K., Puneet, K., Kamal, K. and Neeraj, S. (2022). “Investigating machining characteristics and degradation rate of biodegradable ZM21 magnesium alloy in end milling process.” *International Journal of Lightweight Materials and Manufacture*, 5, 102-112. https://doi.org/10.1016/j.ijlmm.2021.11.002

Rao, P.U., Raju, D. R., Suman, K.N.S. and Sankar, B. R. (2018). “Multi objective optimization of Process parameters for hard turning of AISI 52100 steel using Hybrid GRA-PCA.” *Procedia Computer Science,* 133, 703 - 10.

Rao, R.V. and Kalyankar, V. D. (2014). “Optimization of modern machining processes using advanced optimization techniques: a review.” *International Journal of Advanced Manufacturing Technology,* 73(5–8), 1159–1188.https://doi.org/10.1007/s00170-014-5894-4.

Rathod, G. R., Sapkal, S. U. and Chanmanwar, R. M. (2017). “Multi-Objective Optimization of Photochemical Machining by Using GRA.” *Materials Today: Proceedings,* 4 (10), 10830 - 10835.

Reddy, S. (2013). “Optimization of Surface Roughness and Delamination Damage of GFRP Composite Material in End Milling using Taguchi Design Method and Artificial Neural Network.” *Procedia Engineering,* 64, 785 - 794.

Rodygina A. E. (2014). “Application of FEA Metal Cutting Model for Determining Surface Roughness.” *International Journal of Engineering and Technology*, l5, 5207 - 5219.

Sarkar, S. and Datta, S. (2021). “Machining performance of inconel 718 under dry, MQL, and nano fluid MQL conditions: application of coconut oil (base fluid) and multi walled carbon nanotubes as additives.” *Arabian Journal of Science and Engineering*, 46 (3), 2371 -2395. https://doi.org/10.1007/s13369-020-05058-5.

Satish, K., Pankaj, C. and Gian, B. (2020). “Prediction and optimization of work-piece temperature during 2.5-D milling of Inconel 625 using regression and Genetic Algorithm.” *Cogent Engineering*, 7, 1731199.

Savkovic, B., Kovac, P., Rodic, D., Strbac, B. and Klancnik, S. (2020). “Comparison of artificial neural network, fuzzy logic and genetic algorithm for cutting temperature and surface roughness prediction during the face milling process.” *Advances in Production Engineering and Management*, 15, 137 - 150.

https://doi.org/10.14743/apem2020.2.354

Selaimia, A. A., Yallese, M. A. and Bensouilah, H. (2017). "Modelling and optimization in dry face milling of X2CrNi18-9 austenitic stainless steel using RMS and desirability approach." *Measurement*, 107, 53 - 67.

Senthilkumar, N., Tamizharasan, T. and Anandakrishnan, V. (2014). "An hybrid Taguchi-grey relational technique and cuckoo search algorithm for multi-criteria optimization in hard turning of AISI D3 Steel." *Journal of Advanced Engineering and Research,* 1 (1), 16 - 31.

Singh, A., Datta, S., Mahapatra, S. S., Singha, T. and Majumdar, G. (2013). "Optimization of bead geometry of submerged arc weld using fuzzy based desirability function approach." *Journal of Intelligent Manufacturing*, 24(1), 35 - 44.

Singh, R., Shadab, M. and Rai, R.N. (2019). "Optimization and prediction of cutting parameters in the end milling process for cast aluminium B4C based composite." *Journal of scientific & industrial research,* 78(3), 166 - 172.

Sivaiah, P. and Chakradhar, D. (2019). "Performance improvement of cryogenic turning process during machining of 17–4 PH stainless steel using multi objective optimization techniques". *Measurement,* 136, 326 - 336.

Sivarao, S., Milkey, K. R., Samsudin, A. R., Dubey, A.K. and Kidd, P. (2014). *"*Comparison between Taguchi method and response surface." *Jordan Journal of Mechanical and Industrial Engineering,* 8(1), 35 - 42.

Siva, K. K., Bathina and Sreenivasulu. (2015). "Optimization and Process Parameters of CNC End Milling for Aluminum Alloy 6082*." International Journal of Innovations in Engineering Research and Technology*, 2 (1), 1- 6.

Sivasakthivel, P. S. and Sudhakaran, R. (2013). "Optimization of machining parameters on temperature rise in end milling of Al 6063 using response surface methodology and

genetic algorithm." *International Journal of Advanced Manufacturing Technology*, 67(9), 2313 - 2323. https://doi.org/10.1007/s00170-012-4652-8

Sharma, P., Chakradhar, D. and Narendranath, S. (2015). "Evaluation of WEDM performance characteristics of Inconel 706 for turbine disk application." *Materials and Design*, 88, 558 - 566.

Sharma, R. C., Dabra, V., Singh, G., Kumar, R., Singh, R.P. and Sharma, S. (2021). "Multi-response optimization while machining of stainless steel 316L using intelligent approach of grey theory and grey-TLBO." *World Journal of Engineering*, 19(3), 329 - 339. https://doi.org/10.1108/WJE-06-2020-0226.

Shaw, M. C. (1984). "*Metal Cutting Principles*". Clarendon Oxford, London, 1984.

Shi, K., Zhang, D. and Ren, J. (2015). "Optimization of process parameters for surface roughness and micro hardness in dry milling of magnesium alloy using Taguchi with grey relational analysis." *International Journal of Advanced Manufacturing Technology*, 81, 645 -51.

Shihab, S.K. and Mohamed, M. M. E. (2016). "Evaluation of surface roughness and material removal rate in end milling of complex shape." *University Journal of Mechaniacl Engineering*., 4(3), 69 - 73.

Shrivastava, Y. and Singh, B. (2018a). "Assessment of stable cutting zone in CNC turning based on empirical mode decomposition and genetic algorithm approach." *Proceedings of the Institution of Mechanical Engineers, Part C: Journal of Mechanical Engineering Science*, 232(20), 3573 - 94. https://doi.org/10.1177/0954406217740163.

Shrivastava, Y. and Singh, B. (2018b). "Stable cutting zone prediction in CNC turning using adaptive signal processing technique merged with artificial neural network and multi-objective genetic algorithm." *European Journal of Mechanics - A / Solids*, 70, 238 - 48. https://doi.org/10.1016/j.euromechsol.2018.03.009.

Skordaris, G., Bouzakis, K. D., Kotsanis, T., Charalampous, P., Bouzakis, E., Lemmer, O. and Bolz, S. (2016). "Film thickness effect on mechanical properties and milling performance of nano-structured multilayer PVD coated tools." *Surface Coating Technology*, 307, 452 - 460. https://doi.org/10.1016/j.surfcoat.2016.09.026

Sourabh, K. S. (2015). "Optimization of Milling Process Parameter for Surface Roughnessof Inconel718 by Using Taguchi Method." *International Journal for Scientific Research & Development,* 2 (2015), 57 - 63.

Subramanian, M., Sakthivel, M., Sooryaprakash, K. and Sudhakaran, R. (2013). "Optimization of end mill tool geometry parameters for Al7075-T6 machining operations based on vibration amplitude by response surface methodology." *Measurement,* 46 (10), 4005 - 4022.

Sukumar, M. S., Venkata Ramaiah, P. and Nagarjuna, A. (2014). "Optimization and Prediction of Parameters in Face Milling of Al-6061 Using Taguchi and ANN Approach." *Procedia Engineering*, 97, 365 - 371.

Suresh, K. B. and Baskar. N. (2012). "Integration of fuzzy logic with response surface methodology for thrust force and surface roughness modelling of drilling on titanium alloy." *International journal of advanced manufacturing technology*, 65, 1501- 1514.

Swain, N., Venkatesh, V., Kumar, P., Srinivas, G., Ravishankar, S. and Barshilia, H. C. (2017). "An experimental investigation on the machining characteristics of Nimonic 75 using uncoated and TiAlN coated tungsten carbide micro-end mills." *CIRP Journal of Manicuring Science and Technology*, 16, 34 - 42.
https://doi.org/10.1016/j.cirpj.2016.07.005

Taguchi, G. (1987). "*System of experimental design: engineering methods to optimize quality and minimize costs.*" UNIPUB/Kraus International Publications.

Tosun N, H. and Pihtili. (2010). "Gray relational analysis of performance characteristics in MQL milling of 7075 Al alloy." *International Journal of Advanced Manufacturing Technology*, 46 (5-8), 509 - 515.

Tsao, C. C. (2009). “Grey-Taguchi method to optimize the milling parameters of aluminium alloy.” *International Journal of Advanced Manufacturing Technology,* 40 (1-2), 41 - 48. https://doi.org/10.1007/s00170-007-1314-3

Tien, D. H., Nhu-Tung, N., Duc, Q. T. and Van, T. N. (2019). “Cutting Forces and Surface Roughness in Face-Milling of SKD61 Hard Steel.” *Journal of Mechanical Engineering*, 65(6), 375 - 385. http://dx.doi.org/10.5545/sv-jme.2019.6057

Umamaheswar rao, P., Raju, D. R., Suman, K. N. S. and Sankar, B. R. (2018). “Multi objective optimization of Process parameters for hard turning of AISI 52100 steel using Hybrid GRA-PCA.” *Procedia Computer Science,* 133, 703 - 710.

Uma, M. R., Yesu, R. P. and Suresh, K. R. N. (2016). “Measurement and analysis of surface roughness in WS_2 solid lubricant assisted minimum quantity lubrication (MQL) turning of Inconel.” *Procedia CIRP*., 40, 138 - 143.

Vasu, M. and Nayaka, H. S. (2018a). “Comparative Study of Coated and Uncoated Tool Inserts with Dry Machining of EN47 Steel Using Taguchi L_9 Optimization Technique. Advances in Mechanical Design.” *Materials and Manufacture. AIP Conference Proceedings 1943*, 020063, 1-10. http://doi.org/10.1063/1.5029639

Vasu, M. and Shivananda, N. H. (2018b), “Turning process on EN47 spring steel with different tool nose radii using OFAT approach.” *Advances in Modelling and Analysis A.*, 55 (2), 43-46. https://doi.org/10.18280/ama_a.550201

Vasu, M., Shivananda, N. H., Pradeep, V. B. and Vinyas, M. (2019) Machinability studies on EN47 spring steel by optimization technique during dry and wet condition.” *International Journal of Modern Manufacturing Technologies,* XI (2): 57-65. ISSN 2067–3604, 2 /2019

Wang, P. M., Zhai, J.Y. and Zhu, Z.Q. (2013). “A hybrid method using experiment design and grey relational analysis for multiple criteria decision-making problems.” *Knowledge-. Based Systems,* 53, 100 - 107.

https://doi.org/10.1016/j.knosys.2013.08.025

Yinfei, Y., Lu, J., Jinpeng, Z., Jinxing, K. and Liang, Li. (2020). “Study on Cutting Force, Cutting Temperature and Machining Residual Stress in Precision Turning of Pure Iron with Different Grain Sizes.” *Chinese Journal of Mechanical Engineering*, 33(53), 1- 9.

Yuan, G., James, B., Mann, S. C., Ronglei, S. and Jürgen, L. (2017) Modelling of tool temperature in modulation-assisted machining.” *Procedia CIRP*, 58: 204 - 209. https://doi.org/10.1016/j.procir.2017.03.210.

List of Publications based on PhD Research work:

Sl. No.	Name of Authers	Title of paper	Name of the Journal/Conference	Date of publication	Category
1	B. Srinivasa Rao Dr. Shivananda Nayaka H Dr. Ch. KannaBabu	Study and Experimental Investigation of the Effect of Progressive Feed Rate on Surface Roughness in CNC End Milling Process Using RSM	Journal Europeen des Systems Automatises. https://doi.org/10.18280/jesa.550503 **IIETA Publications**	Oct-2022 (Published) [Scopus]	1
2	B.Srinivasa Rao Dr. Shivananda Nayaka H Dr. Ch. Kanna Babu	Multi-Response Optimization of End Milling Process Parameters	Journal of Mines, Metals and Fuels DOI: 10.18311/jmmf/2023/33352 Publisher/s: Informatics Publishing Limited and Books & Journals Private Ltd.	Jan-2023) (Published) [Scopus]	1
3	B. Srinivasa Rao Dr. Shivananda Nayaka H Dr. Ch. Kanna Babu	A novel approach to reduce the temperature rise on cutting tool tip in end milling process	Academic Journal of Manufacturing Engineering, VOL. 21, ISSUE 1/2023 **Publisher: Editura Politehnica**	Mar-2023 (Published) [Scopus]	1
4	B. Srinivasa Rao Dr. Shivananda Nayaka H Dr. Ch. Kanna Babu	Experimental analysis of End milling process on BS L168 alloy with different nose radii end mills using OFAT approach	Proceedings of the Institution of Mechanical Engineers, Part B: Journal of Engineering Manufacturing. SAGE Publications.	Comments received, under review [SCI]	1
5	B. Srinivasa Rao Dr. Shivananda Nayaka H Dr. Ch. Kanna Babu	Multi-response optimization of machining parameters for end milling process on BSL168 Aluminium alloy using Taguchi based grey relational analysis	First International Conference on Computations in Materials and Applied Engineering (CMAE-2021) held during 26-27th June 2021	June-2021	4

Category 1: Journal paper, full paper reviewed

2: Journal paper, Abstract reviewed

3: Conference/Symposium paper, full paper reviewed

4: Conference / Symposium paper, abstract reviewed

BIO-DATA

1	Name	B. SRINIVASA RAO
2	Father's Name	B. VENKATESWARLU
3	Date of Birth	14.07.1977
4	Nationality	INDIAN
5	Permanent Address	H.No: 06, BSR Residential Township, Opp to JAMES English school, Virgonagar PO, AVALAHALLI, Bangalore - 560049. Karnataka, India.
6	Mobile Number	7892241458, 9900231091
7	E Mail Id	bsreducation@gmail.com

8 **Educational Qualification**

Sl. No.	Qualification	University	College	Year of passing	Performance
1	**PhD**	National institute of Karnataka	National institute of Karnataka	2024	9.0 CGPA
2	**M.Tech (Machine Design)**	JNTU, Kakinada	JNTUCE, Kakinada	2006	78.38%
3	**B.E Mechanical**	Andhra University	S.R.K.R Engineering College,	2000	70.54%
4	**D.M.E**	S.B.T.E.T, Andhra Pradesh	Narsipatnam Govt. Polytechnique College,Narsipatnam, Andhra Pradesh.	1995	74.90%

9 **Work Experience**

Name of the Organization	**Duration**	**Position**
Narasaraopeta Enginering College, Narsaraopet, Guntur (Dt), AP.	Dec 2000-Jun 2007	Assistant Professor
LCA Tejas Division, Hindustan Aeronautics Ltd, Bangalore.	July 2007-Till date	Sr. Manager

I declare that above information is true and correct to the best of my knowledge

(Srinivasa Rao Bommisetty)